# **Final Report**

# Reservoir Characterization of Bridgeport and Cypress Sandstones in Lawrence Field Illinois to Improve Petroleum Recovery by Alkaline-Surfactant-Polymer Flood

# DOE Project DE-NT0005664

PIs: Beverly Seyler and John P. Grube

Co PI: Bryan G. Huff

Staff Geologists: Nathan D. Webb, James R. Damico, Curt S. Blakley, Vineeth Madhavan, and Philip M. Johanek

**Petroleum Engineer: Scott Frailey** 

University of Illinois
Illinois State Geological Survey
615 E. Peabody Dr. Champaign, IL 61820

Report period: September 21, 2008 – December 21, 2012

# **Program**

This project was selected in response to DOE's Oil Exploration and Production solicitation DOE Project DE-NT0005664

### Disclaimer

This report was prepared as an account of work sponsored by an agency of the United States Government. Neither the United States Government nor any agency thereof, nor any of their employees, makes any warranty, express or implied, or assumes any legal liability or responsibility for the accuracy, completeness, or usefulness of any information, apparatus, product, or process disclosed, or represents that its use would not infringe privately owned rights. Reference herein to any specific commercial product, process, or service by trade name, trademark, manufacturer, or otherwise does not necessarily constitute or imply its endorsement, recommendation, or favoring by the United States Government or any agency thereof. The views and opinions of authors expressed herein do not necessarily state or reflect those of the United States Government or any agency thereof.

# Contents

Abstract	v
Lawrence Field Background	1
Alkaline-Surfactant-Polymer (ASP) Technology Overview	2
Summary of Alkaline-Surfactant-Polymer Flood Technology	2
Summary of Existing Industry Alkaline-Surfactant-Polymer Field Applications	5
Previous Enhanced Oil Recovery Maraflood Projects in Lawrence Field	5
Lawrence Field Production History and ASP Potential	7
Structure Maps	8
Pennsylvanian Age Reservoirs in Lawrence Field	9
Stratigraphy and Structure	9
Paleogeography and Evolution of Lower-Middle Pennsylvanian Reservoirs	10
Reservoir Characterization of Pennsylvanian Bridgeport Sandstones	10
Buchanan Sandstone Overview	11
Bridgeport A Sandstone Overview	12
Bridgeport B Sandstones Overview	12
Bridgeport C Sandstone Overview	13
Bridgeport D Sandstone Overview	13
Sequence Stratigraphic Techniques for the Regional Mapping of the Bridgeport Reservoir	s . 13
Coal Palynology	15
Depositional Environments Bridgeport B Sandstone Reservoirs	17
Fine-grained tidally influenced Bridgeport B	17
Post Bridgeport B Channel Fill Reservoir Sandstone	18
Review of Bridgeport B Interval Deposition	19
Petrographic Analysis – Pennsylvanian Bridgeport B Interval Reservoirs	20
X ray diffraction analyses	20
Thin section analysis post Bridgeport B Channel fill Section 5	21
Petrography Bridgeport B fine grained sandstone facies	22
Petrographic Analysis Bridgeport B Sandstones	24
Summary EOR Targets in Bridgeport B Sandstones Lawrence Field	24
Cypress Sandstone Reservoir Overview of Lawrence Field	26

Stratigraphy Cypress Sandstone	26
Cypress Sandstone Paleogeography	27
Cypress Sandstone Reservoirs in ASP Middagh Pilot near the Griggs Lease	27
Reservoir Characterization of Cypress Sandstones in Expanded Region	29
Cypress Sandstone Reservoirs in Expanded Area of Lawrence Field	29
Petrographic Analysis Cypress Sandstone Reservoirs	31
Conclusions	33
Geocellular Modeling	35
Data Selection and Normalization	35
Grid and Discretization	36
Geostatistical Analysis and Simulation	37
Model Property Transformation	37
Validation and Post-Processing.	38
Bridgeport Channel Fill Reservoir Model	38
Reservoir Simulation Modeling	39
Relative Permeability	39
Fluid Properties	40
Well locations	40
Well Configuration	40
Simulation Settings	40
Modeling Scenarios	40
Field Operations	42
Assessment of ASP EOR Potential in Sandstone Petroleum Reservoirs in the Illinois Basin .	43
Assessment of Pennsylvanian Sandstone Reservoirs	43
Assessment of Chesterian and Cypress Sandstone Reservoirs	44
Tamaroa Field	45
Richview Field	46
Assessment of ASP Technology for Petroleum Reservoirs in U. S.	49
Sandstone Reservoirs in Non-Interior Cratonic Basins	50
Compilation of United States Oil Producing Basins	54
Appalachian Basin	56

	Bend Arch – Fort Worth Basin	56
	Big Horn Basin	56
	Cherokee Platform	57
	Forest City Basin	57
	Gulf Coast Basins	58
	Illinois Basin	59
	Laramie Basin	59
	Los Angeles Basin	59
	Marathon Thrust Belt	59
	Nemaha Uplift	60
	North-Central Montana Basin	60
	Powder River Basin	60
	San Joaquin Basin	61
	San Juan Basin	61
	Southern Oklahoma Basin	61
	Ventura Basin	62
Tecl	hnology Transfer	63
Pı	ublication	63
A	bstracts for Poster Presentations	63
Pı	resentations	64
Sun	nmary	65
Con	clusions	68
Ack	nowledgments	72
Refe	erences	73
Figu	ıres	83
Ann	nendix A	214

### **Abstract**

Within the Illinois Basin, most of the oilfields are mature and have been extensively water-flooded with water cuts that range up to 99% in many of the larger fields. In order to maximize production of significant remaining mobile oil from these fields, new recovery techniques need to be researched and applied. The purpose of this project was to conduct reservoir characterization studies supporting Alkaline-Surfactant-Polymer Floods in two distinct sandstone reservoirs in Lawrence Field, Lawrence County, Illinois. A project using alkaline-surfactant-polymer (ASP) has been established in the century old Lawrence Field in southeastern Illinois where original oil in place (OOIP) is estimated at over a billion barrels and 400 million barrels have been recovered leaving more than 600 million barrels as an EOR target. Radial core flood analysis using core from the field demonstrated recoveries greater than 20% of OOIP. While the lab results are likely optimistic to actual field performance, the ASP tests indicate that substantial reserves could be recovered even if the field results are 5 to 10% of OOIP.

Reservoir characterization is a key factor in the success of any EOR application. Reservoirs within the Illinois Basin are frequently characterized as being highly compartmentalized resulting in multiple flow unit configurations. The research conducted on Lawrence Field focused on characteristics that define reservoir compartmentalization in order to delineate preferred target areas so that the chemical flood can be designed and implemented for the greatest recovery potential. Along with traditional facies mapping, core analyses and petrographic analyses, conceptual geological models were constructed and used to develop 3D geocellular models, a valuable tool for visualizing reservoir architecture and also a prerequisite for reservoir simulation modeling.

Cores were described and potential permeability barriers were correlated using geophysical logs. Petrographic analyses were used to better understand porosity and permeability trends in the region and to characterize barriers and define flow units. Diagenetic alterations that impact porosity and permeability include development of quartz overgrowths, sutured quartz grains, dissolution of feldspar grains, formation of clay mineral coatings on grains, and calcite cementation. Many of these alterations are controlled by facies.

Mapping efforts identified distinct flow units in the northern part of the field showing that the Pennsylvanian Bridgeport consists of a series of thick incised channel fill sequences. The sandstones are about 75-150 feet thick and typically consist of medium grained and poorly sorted fluvial to distributary channel fill deposits at the base. The sandstones become indistinctly bedded distributary channel deposits in the main part of the reservoir before fining upwards and becoming more tidally influenced near their top. These channel deposits have core permeabilities ranging from 20 md to well over 1000 md. The tidally influenced deposits are more compartmentalized compared to the thicker and more continuous basal fluvial deposits. Fine grained sandstones that are laterally equivalent to the thicker channel type deposits have permeabilities rarely reaching above 250 md.

Most of the unrecovered oil in Lawrence Field is contained in Pennsylvanian Age Bridgeport sandstones and Mississippian Age Cypress sandstones. These reservoirs are highly complex and compartmentalized. Detailed reservoir characterization including the development of 3-D geologic and geocellular models of target areas in the field were completed to identify areas with

the best potential to recover remaining reserves including unswept and by-passed oil. This project consisted of tasks designed to compile, interpret, and analyze the data required to conduct reservoir characterization for the Bridgeport and Cypress sandstones in pilot areas in anticipation of expanded implementation of ASP flooding in Lawrence Field. Geologic and geocellular modeling needed for reservoir characterization and reservoir simulation were completed as prerequisites for design of efficient ASP flood patterns. Characterizing the complex reservoir geology that identifies the geologic conditions that will optimize oil recoveries for expansion of the ASP pilots in the Bridgeport and Cypress sandstones to other areas of Lawrence Field is the primary objective of this project. It will permit evaluation of efficiency of oil recovery from Bridgeport and Cypress sandstone reservoirs using ASP technology. Additionally evaluation of similar Pennsylvanian and Chesterian reservoirs shows that it is likely that ASP flood technology can be successfully applied to similar reservoirs in the Illinois Basin as well as to other U.S. reservoirs.

Chemical flooding was introduced in stages with the first flood initiated in 2010 and a second offset pilot project initiated during 2011. Rex Energy Corporation is reporting a positive response on its ASP Middagh pilot project in the Pennsylvanian Bridgeport B reservoir, Lawrence Field. Oil response in the 15 acre flood has continued to show an increase in oil cut from 1% to 12%. Total pattern production increased from 16 BOPD and stabilized at a range of 65-75 BOPD in the last three months of 2011. Peak production rose to 100 + BOPD. Oil cut in the pilot increased for 1.0% to ~ 12.0% with an individual well showing oil cuts greater than 20%. A second, 58 acre pilot (Perkins-Smith) adjacent to and likely in communication with the Middagh pilot has been initiated. Preliminary brine injection has been implemented and ASP injection was initiated in mid-2012. Response is expected by mid-2013 with peak recovery expected by late 2013. Rex Energy is projecting full scale expansion with the next step of development being a 351 acre project scheduled to begin in mid-2013. Preliminary development has been initiated in this Delta Unit area located in the south half of section 32, T4N, R12W.

# **Lawrence Field Background**

Lawrence Field was discovered in 1906 and encompasses approximately 62.5 square miles in Lawrence County, Illinois (Figures 1 and 2). The Middle Mississippian Cypress Formation, the most prolific oil producing horizon in Illinois and the Lower Pennsylvanian Bridgeport sandstones have yielded most of the 410 million barrels of oil produced from the field. Because most wells commingle production, it is generally believed that the Cypress and Bridgeport sandstones have produced an equivalent amount of oil.

Oil is trapped by anticlinal closure located on the southerly plunging axis of the La Salle Anticlinorium, a major structural feature in the Illinois Basin. Facies changes play an important role in oil recovery from the combined structural-stratigraphic trap. These shallow, thin, low drive energy, compartmentalized reservoirs have yielded up to 40% of original oil in place (OOIP) through long-term, extensive, secondary water-flooding and infill development drilling. Well spacing of less than five acres is common throughout the field.

This "giant" field is approaching its abandonment phase with an average oil cut of less than 2%. Enhanced oil recovery (EOR) technology has been investigated by several previous pilot projects within the field. Although the Kimmel and the Robins Maraflood projects in the 1970s and 1980s succeeded in recovering a significant percentage of the residual oil, the economics apparently did not warrant further development. Advances in the technology that improve efficiency and a stabilizing of higher oil prices have resulted in renewed interest in the EOR approach at Lawrence Field. The ASP flood technology has been successfully implemented in the Griggs-Middaugh lease area in Section 32 T3N R12W in Lawrence Field.

# Alkaline-Surfactant-Polymer (ASP) Technology Overview

The alkaline-surfactant-polymer technology recovers incremental oil by co-injecting interfacial tension reduction agents (alkali and surfactant) with a mobility control agent that improves flood sweep efficiency (polymer). Alkali (NaOH or NA<sub>2</sub>CO<sub>3</sub>) and surfactant alters the relative permeability curve through three primary mechanisms: interfacial tension reduction, solubilization of oil, and wettability alteration. Adding alkali converts acids in oil to soaps and makes more favorable conditions for surfactants. Interfacial tension reductions in excess of 10,000 fold have been observed when alkali and surfactant are blended while either agent alone had at best a 10 to 20 fold interfacial tension reduction. Alkali will reduce surfactant and polymer adsorption when co-injected. Polymer and surfactant affect each other's adsorption as well as interacting on a fluid-fluid basis.

Reservoir characterization for successful application of EOR techniques including alkaline-surfactant-polymer (ASP) floods is well established and requires an understanding of reservoir continuity, flow units, fluid interactions and mineralogy. The bulk of this project involves reservoir characterization focused on application of ASP flood technology.

Most oils in the Illinois Basin are relatively light with API gravities of 34° or greater and have associated brine salinities in excess of 40,000 ppm and calcium in excess of 200 ppm. Most of the fields are mature and have been waterflooded for several decades resulting in oil cuts of less than 2% thereby classifying most wells in the stripper category. Additionally, reservoirs are commonly highly compartmentalized. These circumstances suggest that ASP flooding may be a viable strategy to economically extract from 6.25% to 25% of the original oil in place (OOIP) (Wyatt, K. et. al 2008).

# Summary of Alkaline-Surfactant-Polymer Flood Technology

A summary of the ASP technology will aid in understanding the importance of this enhanced oil recovery technique and how it is applied in this project. The alkaline-surfactant-polymer technology has been developing and applied for more than 20 years. Worldwide, extensive research has been conducted on this technology supported by combined efforts of governments, universities and industry. Research into the alkaline-surfactant-polymer flooding of the Lawrence Field project was initially conducted by Surtek, a company with widespread chemical flood research experience, including the Illinois and Appalachian basins (Wyatt et al., 2002). Surtek researched light oil reservoirs under a PRDA for the Department of Energy (Pitts, 1995), performed detailed laboratory, engineering, and numerical simulation analysis of the West Kiehl Field, Wyoming alkaline-surfactant-polymer project for another Department of Energy investigation (Pitts et al., 1994; Pitts and Surkalo, 1995). The company has researched the Cambridge Minnelusa Field, Wyoming flood, (Clark et al., 1993; Meyers et al., 1992), the Poison Spider Wyoming project and Kentucky's Big Sinking Field project (Miller et al., 2004), and researched pilots and floods in Canada (Pitts et al., 2004), China, and Venezuela (Hernandez et al., 2003).

Universities, including the University of Texas at Austin and the University of Houston have made significant contributions to further understanding ASP technology. Chemical flooding of carbonates and naturally fractured reservoirs that focus on modification of wettability of oil-wet

reservoirs to mixed-wet and water-wet have been investigated by members of both universities (Najafabasi et al., 2008; Steethepalli et al., 2004; Wyatt et al., 2004; Zhang et al., 2008) While ASP technology has tended to focus on the recovery of the more common light crude oils, the University of Texas at Austin investigated methods to recover oils that are difficult to recover due to their high carbon number, high asphaltene, paraffin and/or wax content and in some cases, high viscosity. By using internal olefin sulfonates (IOS) and screening techniques, then using phase behavior experiments in core floods, it was shown that these difficult oils can be economically recovered (Zhao et al., 2008). Further research at the University of Texas, Austin, with screening techniques using a systematic laboratory approach, shows that costs of the complex process of designing a chemical flood can be reduced (Adam et al., 2008). While researching this methodology, it was found that ASP flooding can be applied economically to reservoirs containing very hard, saline brines.

The alkaline-surfactant-polymer technology is a flooding technique in which an interactive fluid is injected either in a secondary or a tertiary mode. The interactive fluid improves oil recovery over a non-interactive fluid such as water by alterations of relative permeability, rock wettability, and viscosity of the displacing phase. Incremental oil recovery has been demonstrated in the laboratory and in a number of field applications (Clark et al., 1993; French et al., 1998; Gao et al., 1996; Gu et al., 1998; Meyers et al., 1992; Qu et al., 1998; Vargo et al., 1999 Wang, C., et al. 1997; Wang, D., et al., 1997; Wang D., et al., 1998; Wu et al., 2008).

The alkaline-surfactant-polymer technology recovers incremental oil by co-injecting interfacial tension reduction agents (alkali and surfactant) with a mobility control agent (polymer) (Pitts, 1995). Alkali and surfactant are combined to change the relative permeability characteristics to maximize pore to pore displacement efficiency. Alkali and surfactant alters the relative permeability curve through three primary mechanisms: interfacial tension reduction, solubilization of oil, and wettability alteration. Decreasing the interfacial tension between the crude oil and the aqueous fluid is the primary mechanism through which low concentration surfactant plus alkali flooding produces incremental oil. Lowering of interfacial tension improves oil recovery either by increasing the viscosity of the injected fluid, increasing the Darcy velocity of the injected fluid, or by decreasing the interfacial tension between the injected fluid and the crude oil. In a petroleum reservoir, only the interfacial tension can be altered sufficiently to change the capillary number to produce incremental oil. According to a number of studies an alteration of at least 100 fold and up to 10,000 fold is required to mobilize incremental oil from a waterflood residual (Abrams, 1988; Tabor, 1988).

The lowering of the oil saturation increases the effective permeability to water as dictated by the relative permeability curve. This increase in turn increases the mobility ratio. Adding an interfacial reducing agent to the injected water stream therefore has the potential to increase viscous fingering which will reduce the reservoir contact efficiency, decreasing the volumetric contact efficiency factor, and potentially eliminating the benefit of reduced oil saturation.

Polymer is typically added to the injected fluid to improve mobility ratio (Pitts et al., 1995). Adding polymer or a mobility control agent to a solution containing interfacial tension reducing agents such as alkali and surfactant as in a mobility control flood will mitigate a potential reduced reservoir contact efficiency. Mobility control polymer flooding is an improved waterflooding process, which involves the addition of a high molecular weight polymer to the

injection water. Incremental oil is produced through: improved reservoir contact efficiency by improving displacement efficiency as a result of increasing the viscosity of the injected fluid, reduction of viscous fingering, and fluid diversion due to the reduction of the effective permeability to water.

Co-injecting an interfacial tension agent with a mobility control agent is a technological idea which originally started with micellar-polymer flooding. (Poettmann, 1983) demonstrated the need to couple the two mechanisms when he stated "mobility control is the most important element in the design of microemulsion-polymer flooding systems."

The synergistic nature of oil recovery by the co-injection of an interfacial tension reducing agent and a mobility control agent began with the co-injection of alkali and polymer. Burk (1987) reported that injection of alkali (interfacial tension reducing agent) without polymer produced 6 to 17% of the waterflood residual oil while simultaneous injection of alkali plus polymer (interfacial tension reducing agent plus mobility control agent) produced 73 to 95% of the waterflood residual oil. Polymer produced 10 to 18% of the waterflood residual oil. Other researchers have demonstrated similar synergistic oil recovery with simultaneous injection of alkali and polymer (Ball and Pitts, 1984; Mihcakan and Van Kirk, 1986).

The alkaline-polymer research ultimately resulted in the implementation of two field projects in the David (Manji and Stasiuk, 1988) and Cessford (Edinga et al., 1980) pools in Canada. Like the alkaline-surfactant-polymer projects, these projects co-injected an interfacial tension reducing agent with a mobility control agent. The David pool investigated the co-injection of alkali plus polymer in reservoir core. In these core floods, waterflood followed by alkali plus polymer recovered 73% of the initial oil saturation with a chemical residual oil saturation of 17% pore volume (PV). Waterflood oil recovery was 50 % of the initial oil saturation with a waterflood residual oil saturation of 33% PV. The Cessford laboratory studies showed similar results.

The synergistic reduction of the interfacial tension when alkali and surfactant are blended was initially patented by Burdyn et al. (1975) and has been demonstrated on a variety of crude oils by a number of researchers (French et al., 1989; Hawkin et al., 1991; Krumrine and Falcone, 1983; Nelson et al., 1984; Olsen et al., 2004; Saleem and Herandex, 1989). Interfacial tension reductions in excess of 10,000 fold have been observed when alkali and surfactant are blended while either agent alone had at best a 10 to 20 fold interfacial tension reduction.

Nelson et al. (1984), Martin et al. (1995), and Martin and Oxley (1985) applied the principles of optimal salinity to explain and maximize the interfacial tension reduction synergism. In this manner, Nelson treated the mixing of alkali plus surfactant as a special case of surfactant flooding and used the optimal salinity design philosophy to determine the appropriate concentration of alkali and added surfactant which would provide the optimal phase behavior.

Adding a mobility control agent to the alkali plus surfactant mixture has been demonstrated to improve oil recovery significantly over injection of polymer alone, alkali plus surfactant without polymer, and alkali plus polymer in a number of laboratory studies (Martin et al., 1995; Martin and Oxley, 1985; Mihcakan and Van Kirk, 1986; Zhao et al., 2008). For reservoirs having crude oil with no interfacial tension reducing activity with alkali, the combination of alkali and

surfactant is essential to produce ultra-low interfacial tension values required to produce incremental oil. Co-injection of the alkali plus surfactant plus polymer improved oil recovery from as little as 10% to as much as 37% of the initial oil saturation above polymer and alkalipolymer.

Research done by Surtek on the mechanisms of alkaline-surfactant-polymer flooding light oil reservoirs concluded the following (Pitts 1995): 1) Mobility control is essential to producing incremental oil. Without adequate mobility control, the best designed alkaline-surfactant solution will result in little or no incremental oil. 2) Loss of surfactant from the alkaline-surfactant-polymer solution either by adsorption or by reduction of injected mass significantly lowered incremental oil recovery. 3) A variety of surfactant types, polymer types, and alkali types can be blended to achieve ultra-low interfacial tension values. Each component will alter the interfacial tension, so how the different components are blended in an alkaline-surfactant-polymer solution can be critical. 4) Interaction of the injected chemical with the rock will have a dominant effect on incremental oil production. Ultra low interfacial tension values do not necessarily correlate with incremental oil production. 5) Alkali will reduce surfactant and polymer adsorption when co-injected. Polymer and surfactant affect each other's adsorption as well as interacting on a fluid-fluid basis.

# **Summary of Existing Industry Alkaline-Surfactant-Polymer Field Applications**

There are many examples of ASP flooding increasing production from petroleum reservoirs. Field applications of combining interfacial tension reducing agents and mobility control agents have been implemented at West Kiehl (Pitts et al., 1994; Pitts and Surkalo, 1995), Cambridge (Vargo et al., 1999; Vargo et al., 2000), Sho-Vel-Tum (French et al., 1998), Daqing – Seartu (Gao et al., 1996; Wang D. et al., 1997), Daqing – Xingshugang (Wang D. et al., 1997), Shengli - Gudong, (Qu Zhijan et al., 1998; Wang C. et al., 1997), and Karamay (Gu, H. et al., 1998). The alkaline-polymer flood publications are David (Manji and Stasiuk 1988; Pitts and Surkalo 2004) and Cessford (Edinga et al., 1980). At least two other ASP floods which have been implemented including Driscoll Creek, Wyoming and Wardlaw, Texas. Both were designed by Surtek. Actual incremental oil production attributed to these ASP floods at the time of reporting ranges from 13% to 28% of the OOIP.

# Previous Enhanced Oil Recovery Maraflood Projects in Lawrence Field

The Maraflood process predates the inception of the alkaline-surfactant-polymer technology and was implemented in three pilots in Lawrence Field in the 1970s and 1980s. The Maraflood process is simply defined as the injection of a micellar solution into an oil reservoir to improve displacement efficiency. The micellar solution also known as a micro emulsion was the basis of a 1962 patent filed by Gogarty and Olson describing the use of micro emulsions in a new miscible type oil recovery process known as MARAFLOOD<sup>TM</sup>. These micro emulsions contain surfactant, hydrocarbon and water. Co-surfactants also may be added to provide some viscosity control to maintain mobility control with the displaced oil. While effective, the micro emulsion displaces essentially all of the oil it contacts. Since this slug is expensive it is displaced by a mobility buffer, a less expensive fluid. After sufficient injection of the mobility buffer, water is injected.

There were three enhanced oil recovery Maraflood projects initiated by the Marathon Oil Company in Lawrence Field in the 1970s and 1980s. The first project was the Kimmel 118-K Maraflood surfactant flood implemented during the 1970s. The second project was the Robins 102-B Maraflood surfactant flood initiated in the 1980s. This was a 25 acre Bridgeport sandstone pilot project. The third project was the Robins 202-B Maraflood surfactant flood. This was a 2.5 acre Bridgeport sandstone reservoir pilot project that was terminated in 1986 due to low oil prices.

Production results are available for two of the Maraflood projects completed in a Cypress Sandstone and a Bridgeport Sandstone reservoir. These projects, the Kimmel 118-K a Cypress sandstone reservoir pilot and the Robins 102-B a Bridgeport sandstone reservoir pilot, are located approximately one mile from the Middaugh ASP pilot site (Figure 3). The detailed results of these two Maraflood projects have not been published, however production curves are available. The production curve for the Robins 102B Bridgeport Maraflood shows an increase in oil cut from 1% to 20% (Figure 4). The 25 acre Bridgeport B channel sandstone pilot project in the SE quarter of Section 5, T3N R12W achieved recovery of an additional 34 percent (15% pore volume) of the residual oil saturation (SOR) recovery beyond what was achieved during primary and waterflood production. Over 450,000 barrels of oil were produced during the surfactant polymer flood from the 25 acre pilot. The Kimmel project was a 2.5 acre Cypress sandstone reservoir pilot project that achieved 30% SOR recovery (10% pore volume) (Figure 5). These Marafloods were scientific successes in substantially increasing oil production but were not expanded presumably due the fact that oil prices were not high enough to offset the costs of polymer and surfactant.

An ASP flood combines three chemicals: an alkali (NaOH or  $Na_2CO_3$ ), a surfactant, and a polymer. The alkali at a concentration of 1 to 2% washes residual oil from the reservoir mainly by reducing interfacial tension between the oil and the water. The surfactant at concentrations of 0.1 to 0.4% enhances the ability of the alkaline to lower interfacial tension. A small amount of polymer in the range of 800 to 1400 ppm is added to improve sweep efficiency.

The ASP chemical slug is injected first at approximately 30% of pore volume. Past surfactant floods only injected polymer following the surfactant. The polymer slug is then injected to push the ASP solution and to maintain mobility control (~ 25% pore volume). Water is then injected to continue pushing the ASP and polymer slugs to economic limit.

The goal of an ASP flood is to duplicate the oil recovery performance of the old surfactant floods at a lower cost. Oil recovery performance is accomplished by optimizing the synergistic performance of the three chemicals. Costs are lowered by being able to inject chemicals at lower concentrations.

# **Lawrence Field Production History and ASP Potential**

Lawrence Field was discovered in 1906. Early production was primarily from shallow wells in Pennsylvanian age sandstone reservoirs. Lawrence Field is one of the oldest fields in the Illinois Basin and has produced in excess of 410 million bbl of oil primarily from Pennsylvanian age Bridgeport sandstone reservoirs and Mississippian age Cypress sandstone reservoirs (Figure 6). Current production is at a rate of less than 2% oil cut and it is estimated that recovery thus far is less than 40% of original oil in place. There has been excellent success with waterflooding and most of the field has been waterflooded for several decades. A substantial increase in production is attributed to secondary recovery involving extensive waterflooding programs in most of the field.

The petroleum trapping mechanism is a combination of structural closure co-incident with Pennsylvanian and Mississippian age porous and permeable sandstone bodies. Deeper Middle Mississippian through Ordovician carbonates were targeted after initial development of shallower reservoirs. Lawrence Field had an extensive period of production starting in 1906 (Figure 7). The earliest phases of primary production were focused on shallow Pennsylvanian sandstones at depths of a 1000 feet or less. Later the deeper Cypress Sandstone, a middle Mississippian Chesterian unit, was targeted. Deeper carbonates became targets during the modern era of production.

Much of the field has been extensively waterflooded and some areas near the ASP pilot were also the sites of earlier Maraflood polymer projects. Remaining oil saturation is believed to be variable throughout the field and is dependent on the effectiveness of waterflooding and proximity to polymer flood pilots. Production history (Figure 7) at Lawrence field shows that waterflooding from the early 1950s through the mid-1970s added substantially to primary production in the field. A second production increase occurred from the mid-1980s through the mid-1990s with the development of secondary producing horizons, additional waterflooding and the advent of tertiary recovery projects.

Several surfactant polymer pilot floods (Maraflood) were initiated in the 1970s and early 1980s. These enhanced oil recovery pilots were conducted in reservoirs subjected to long term waterflooding and were successful in substantially increasing oil production but were abandoned for economic reasons. The graph in figure 7 shows projected field wide oil recovery potential with the widespread application of ASP technology. Plains Illinois Corporation, the field operator in 2002, projected positive economics on 10% incremental recovery of produced oil of approximately 42 million barrels of oil at \$30 per barrel. Rex Energy Corporation, the present operator, projects similar potential recovery from 13,000 net acres.

An ASP Chemical flooding EOR project was introduced in stages with the first flood initiated in 2010 and a second offset pilot project initiated during 2011. Rex Energy Corporation is reporting a positive response on its ASP Middagh pilot project in the Pennsylvanian Bridgeport B sandstone reservoir at Lawrence Field. Oil response in the 15 acre 18 well flood has continued to show an increase in oil cut from 1% to 12% with an individual well showing oil cuts greater than 20%.

Total pattern production increased from 16 BOPD and stabilized at a range of 65-75 BOPD in the last three months of 2011. Peak production rose to 100 + BOPD. A second, 58 acre pilot (Perkins-Smith) adjacent to and likely in communication with the Middagh pilot has been initiated. Preliminary brine injection has been implemented. ASP injection commenced in June 2012. Response is expected by mid-2013 with peak recovery expected by late 2013. Rex Energy is projecting full scale expansion with the next step of development being a 351 acre project scheduled to begin in mid-2013. Drilling and injection tie-in has been completed in the Delta Unit area located in the south half of section 32, T4N, R12W. ASP injection in this project is scheduled to begin during the fourth quarter of 2013.

Site selection and the recovery process for the Middagh ASP pilot in Section 32 T4N R12W in Lawrence Field Illinois were described by Sharma et al., 2012. The 15 acre pilot was positioned in the middle of a confined sandstone body in the Bridgeport B interval to ensure that injection for the pilot was located above the oil/water contact and to ensure that injection fluid loss off pattern would be minimized. The pilot was located near Rex Energy Corporation's existing mix and pump facilities. Sharma et al. 2012 concluded that the pilot ASP flood was successful in displacing residual oil saturation. An observation well located in the pilot showed the formation of an oil bank.

### **Structure Maps**

Lawrence Field is located in the LaSalle Anticlinorium on the eastern portion of the Illinois Basin in Lawrence County, Illinois. The LaSalle Anticlinorium is composed of a series of anticlines oriented parallel to one another that are generally offset to the west as the regional anticlinal features extend from their southernmost extent and expressed in the subsurface in Lawrence County to their northern most extent in LaSalle County where bedrock anticlinal features can be observed in outcrops. There are two major anticlinal features mapped in the subsurface at Lawrence Field (Figure 2). The northern anticline where the ASP pilots are located has the most pronounced structural closure. The southern anticline in the Lawrence Field has less structural closure, most of the production from the field is from reservoir sandstones located in the northern anticline but it is not limited to the crest of the structure.

A number of key field-wide marker beds were picked to provide reliable datums for picking tops on reservoir sand bodies. Field wide structure maps were completed for the following horizons: Base Barlow Limestone (Figure 8), Base Glen Dean Limestone (Figure 9) (both are Middle Mississippian Chesterian strata), Base Alpha Shale, Base Beta Shale, Base Carrier Mills Shale, and Colchester (#2) Coal, (Figures 10, 11, 12, and 13). The stratigraphic relationships of selected mapping horizons are shown in the stratigraphic column and electric log from the the Griggs 106 well in figure 14. The two contoured structure maps on the Mississippian Glen Dean Limestone and the base of the Beech Creek (Barlow) Limestone (Figures 8 and 9) show similar structural closure on the major anticline in the northern portion of the field. The Glen Dean map (Figure 9) shows an area in Sec. 8 T3N R12W where this marker horizon has been eroded. These maps show that the most productive areas of the field do not always coincide with the most pronounced structural closure. The trapping mechanism in the field has a strong stratigraphic component. With such a complete collection of structure maps, a more refined model of structural activity contemporaneous with Pennsylvanian deposition is apparent.

# Pennsylvanian Age Reservoirs in Lawrence Field

# **Stratigraphy and Structure**

In 1906, wildcat drilling in the area south of the Main Consolidated Field led to the discovery of Pennsylvanian Subsystem sandstone reservoirs capable of commercial petroleum production. Development of Lawrence Field began in earnest in 1907–08 (Blatchley, 1913). The field was particularly attractive to operators as early drilling indicated several different sandstone pay zones, including at least three lenses of "Bridgeport" sandstone. Bridgeport is thus an informal drillers' term applied to Pennsylvanian aged sandstone bodies of the Tradewater and upper Caseyville Formations in Lawrence Field (Figure 14). The Caseyville Formation unconformably overlies the sedimentary succession of the Chesterian Series (Upper Mississippian Subsystem). Within the Chesterian, sandstones and shales are interspersed with regionally extensive limestone units that are widely traceable and relatively easy to correlate. Above the Tradewater Formation lie the cyclical successions of sedimentary rock of the classic Pennsylvanian Cyclothems (Weller, 1930; Wanless and Weller, 1932) that make up the Carbondale Formation. These cyclothems are punctuated with coal beds such as the Herrin, Springfield, Colchester and Seelyville that, like the Chesterian Limestones, are widely traceable marker beds that are essential for regional correlation.

Unlike the underlying and overlying formations, the Caseyville and Tradewater Formations are mostly made up of sandstones, siltstones, and shales and generally lack any regionally extensive limestones or coals to act as marker beds for correlation. In fact, the boundary between the two formations is difficult to identify on a lithologic basis due of the lack of variety in the rocks that make up the formations. Caseyville Formation sandstones are typically thickly bedded, medium-coarse grained, and often contain quartz granules and pebbles (Seiver, 1951; Willman et al., 1975; Nelson et al., 1991). Tradewater sandstones are generally more lenticular and lack the quartz granules and pebbles indicative of the Caseville Formation. In some instances, widespread, lenticular sandstone bodies are juxtaposed against exceedingly thick and more linear sandstone bodies. In both cases, the discontinuous and commonly stacked sandstones are usually interbedded with grey to black shale and siltstone with occasional localized limestones or coals.

The pre-Pennsylvanian surface was deeply eroded following deposition of Mississippian upper Chesterian deposits. Lower Pennsylvanian sediments of the Caseyville Formation were deposited onto the surface and in some instances fill or partially fill valleys that were incised deeply into upper Mississippian strata. The infill of these paleovalleys contributed to the highly complex and somewhat chaotic relationship of sandstone bodies in the lower Pennsylvanian Caseyville and Tradewater Formations.

The reservoir horizons in Lawrence Field are draped over the southern reaches of the LaSalle Anticlinorium. The field is broken into two portions based on the two structural elements that form it. To the north is the NNW-SSE trending Bridgeport Anticline. The structurally enclosed area is about 16 km (10 mi) long and 3 km (2 mi) wide with structural closure on the Barlow Limestone measuring 67 m (220 ft). To the south is the more circularly shaped Lawrenceville Dome that exhibits far less closure. The two structures are separated by a NNE-SSW trending saddle. Oil accumulation in the field is controlled mainly by structure; however stratigraphy has a significant effect on recovery (Oltz, 1994).

# Paleogeography and Evolution of Lower-Middle Pennsylvanian Reservoirs

Siliciclastic rock dominates Lower-Middle Pennsylvanian strata in Lawrence Field. Deposition occurred unconformably over older Mississippian strata in an area of active uplift along the southern reaches of the LaSalle Anticlinorium. Contemporaneous tectonic movement in the area influenced both the deposition of the Bridgeport sandstones and environments of deposition and reservoir characteristics.

The Mississippian-Pennsylvanian contact has long been recognized as a major unconformity in the Illinois Basin (Lowenstam, 1951; Siever, 1951; Etheredge, 1953; Wanless, 1955; Clegg, 1959; Potter and Desborough, 1965; Bristol and Howard, 1971; Droste and Keller, 1989; Lumm, 1998). During late Chesterian (latest Mississippian) time the sea that had covered most of Illinois, southwestern Indiana, and western Kentucky began to recede to the south and southwest. As sea level fell, an anastomosing drainage pattern became deeply incised across much of the emergent Illinois Basin. Regional mapping of the surface, known as the Sub-Absaroka unconformity (Sloss, 1963), shows the complex paleodrainage network that represents the erosion of hundreds of feet of older units, especially over paleohighlands such as the LaSalle Anticlinorium (Bristol and Howard, 1971; Howard, 1979). A paleogeologic map of the sub-Pennsylvanian surface in the Illinois Basin is shown in Figure 15. The location of Lawrence Field shown on that map illustrates that valleys were locally incised into the late Mississippian Chesterian age Glen Dean through Barlow Limestones. Pre-Pennsylvanian erosion removed older strata as river systems scoured deep channels into the bedrock, creating a high-relief surface that affected early Pennsylvanian sedimentation by focusing sedimentation into these paleovalleys. Pennsylvanian strata deposited later in the Carbondale Formation strata are characteristically cyclic with widespread coal deposits where channel fill deposits are thinner and much less common due in part to infilling of the high relief surface of the Sub-Absaroka unconformity with Caseyville and Tradewater strata.

Other factors influencing deposition of Pennsylvanian Bridgeport reservoir sandstones include the migration of delta systems and the shoreline through time (Figure 16; Willman et al., 1975; Jacobsen, 2000). Shoreline shifts occurred partly because of eustatic sea level changes, but also because of variations in the amount of sediment influx and local changes in basin subsidence rates or uplift along the LaSalle Anticlinorium resulting in a predominant and complex sequence stratigraphic overprint on Pennsylvanian strata. Lawrence Field occupies a location in the basin that was subject to sedimentation along this shifting shoreline, causing depositional conditions to alternate between marine and non-marine, producing a high degree of lithologic variety in Pennsylvanian rocks. The gentle slope of the basin allowed small changes in sea level to cause large shifts in the coastline which likely exacerbated the lithologic changes recorded by Pennsylvanian strata. Additionally, these eustatic sea level changes resulted in the development of incised valleys and later valley infill within the Pennsylvanian succession on a smaller scale than what is observed at the Sub-Absaroka unconformity. These smaller events play a major role in the juxtaposition of a variety of reservoir types within the Bridgeport interval.

# Reservoir Characterization of Pennsylvanian Bridgeport Sandstones

Detailed characterization of the Pennsylvanian Bridgeport sandstone reservoirs at Lawrence Field has delineated flow units and permeability barriers that identify target zones for the

application of ASP flood technology. Mapping of the subsurface geometry of Bridgeport sandstone reservoirs, as well as examination of petrophysical characteristics of the rock, are critical to the success of an ASP type flood. Thousands of geophysical logs of various vintages were used to map the Bridgeport reservoirs and have revealed that throughout the northern part of the field, a cyclical succession of lenticular sandstone bodies, typically around 30 feet thick, interdigitate with non-reservoir siltstones and shales to create confined reservoirs ideal for the successful application of the ASP EOR technique. Those lenticular reservoirs are further subdivided into compartmentalized flow units that are bounded by thin shaley intervals that may or may not permit communication between compartments. Elsewhere, these more lenticular reservoirs appear to be eroded and replaced with younger, much thicker channel fill deposits of clean sandstones in some areas and fine grained low-energy sediments in others.

Examination of nearly 4,000 feet of core has revealed sedimentological features of both the lenticular sandstone bodies and the channel fill facies. Petrographic analysis further illuminates reservoir characteristics by showing the importance of the diagenetic overprint and areas where high permeabilities create potential thief zones. Finally, recasting the Bridgeport strata in a sequence stratigraphic framework by defining regionally extensive sequence stratigraphic surfaces (sequence boundaries, flooding surfaces, etc.) is helping to clarify how the Bridgeport reservoirs relate to one another and in which environment they were deposited. The successful application of an ASP flood in Lawrence Field would encourage similar EOR projects in comparable fields throughout the Illinois Basin.

The Bridgeport sandstone has been subdivided into the A, B, C, and D intervals with the Bridgeport A the oldest in the succession followed by the Bridgeport B, C and D (Figure 14). These four reservoir zones have been identified as having potential for ASP recovery. In addition, there is production from basal Pennsylvanian sandstone reservoirs in the Caseyville Formation in Lawrence and Crawford Counties that also show EOR potential (Howard and Whitaker, 1988). The JT Griggs #60 type log shows the typical succession of Pennsylvanian rocks in the field (Figure 14).

### **Buchanan Sandstone Overview**

Buchanan is an informal driller's term applied to sandstone found below the Bridgeport reservoirs. The Buchanan sandstone is the lowermost Pennsylvanian sandstone found in Lawrence Field and locally unconformably overlies the older Chesterian strata. The sandstone is typically ~ 30 m (100 ft) thick, but can thin considerably, and in some places, is altogether absent. Most of our information about the lithologic characteristics of the Buchanan sandstone comes from driller's descriptions of the unit, but it was observed in a few cores.

One core (Swail #33) studied not far from the Buchanan type area in Section 16, T3N, R12W, contains what is believed to be a thin Buchanan sandstone. In this core, the Buchanan sandstone is ~5 m (17 ft) thick. The base of the sandstone sits at the Sub-Absaroka Unconformity. The contact of the Buchanan sandstone with the underlying Tar Springs sandstone is sharp. The basal sandstone is highly fractures and is medium grained, indistinctly bedded, and dark brown, with what appears to be grains cemented by siderite. The sandstone then coarsens upward from medium grained to coarse and some very coarse grained sandstone. Some quartz granules were noted, a feature characteristic of basal Pennsylvanian Caseyville Formation sandstones (Seiver,

1951). Rounded quartz granules, chert pebbles, and siderite nodules and clay rip-up clasts make the sandstone conglomeritic in places. The top 1 m (3 ft) is conglomeritic, contains siderite nodules and accumulated calcite cementation. The calcite cementation along with some pedogenic alteration indicates that the top of the sandstone was likely subaerially exposed, thus allowing paleosol development.

# **Bridgeport A Sandstone Overview**

The Bridgeport A is the lowermost of the Bridgeport reservoir sandstones identified in this study. Sandstone bodies within the Bridgeport A sandstone interval show a defined north-south trend. The most common and productive reservoir facies observed in the Bridgeport A is a medium-to high-angle tabular cross-bedded sandstone that is found in the basal, blocky portions of the interval (Figure 17). Bridgeport A sandstones are generally fine-grained with some medium- and minor coarse-grained sandstones in the higher energy deposits. Permeability can be very high in the blocky sands, ranging up to 1.8 darcy. Pyrite cement is very common in the Bridgeport A sandstones, particularly in the basal cross-bedded facies, and occurs as banding and nodules in these beds. The pyrite reduces permeability and interferes with fluid flow in both the horizontal and vertical dimensions. The channel facies scoured into a peat bog at its base (Figure 17). The banded oil staining in the core shows the influence of graded bedding on reservoir quality. The sedimentary structures observed and geometries of the sandstones in the lower units of the Bridgeport A are characteristic of fluvial to distributary channel deposits in a tidally influenced deltaic environment. The Bridgeport A sandstone within the study area is a productive reservoir, although it is less extensive and appears to have cementation and flow unit drawbacks.

### **Bridgeport B Sandstones Overview**

The Bridgeport B sandstone is the most productive and widespread of the Pennsylvanian reservoirs in Lawrence field. Field scale mapping of the target Bridgeport B reservoir was aided by the identification of sequence stratigraphic surfaces. The Bridgeport B stratigraphic interval includes both a near shore tidally influenced facies and a thick, channel-fill facies juxtaposed against one another in different parts of the field. This interval is the current target for ASP flooding and appears to be the most promising target reservoir in the Bridgeport section. An isopach map of the Bridgeport B and stratigraphically correlative beds (Figure 18) is a composite of two depositional facies. The gross interval Bridgeport channel-fill sandstones are mapped in bright colors and tidally influenced, fluvio-deltaic Bridgeport B are mapped in paler colors using a normalized spontaneous potential (SP) 50% clean sandstone cutoff. The base map is a contoured structure map on the base of the Mississippian Barlow Limestone with a contour interval of 25 feet.

The Bridgeport B sandstone typically occurs on the crest of the Bridgeport Anticline, the northern structure in the field, and is most easily defined where it is found in association with the underlying, informally named Beta Shale and an overlying unnamed coal (Figure 19). Evidence from core and geophysical logs indicate that this is the normal succession of rocks in the Bridgeport B interval. In Section 32, T4N, R12W, Bridgeport B sandstones average approximately 25 feet thick and trend more or less east-west over the anticline and are shown in pastel colors on the map (Figure 18).

Two stratigraphically correlative thick sandstone intervals up to approximately 200 feet thick enter Section 5 T3N R12W, one from the northeast and one from the northwest, straddling the anticline and converging toward the south. The thick Bridgeport sandstones are mapped in bright colors (Figure 18). These typical channel-fill reservoirs are found in the Bridgeport B stratigraphic interval in Section 5 T3N, R12W.

Most of the Maraflood and ASP pilots undertaken in Lawrence Field have targeted reservoirs in the Bridgeport B interval; both in the tidally influenced facies and the channel-fill facies. The current ASP pilot in the Middagh lease in Section 32 T4N R12W is targeting the thinner non-channel fluvio-deltaic sandstones. The Robins 102-B Marafood pilot targeted the thick channel fill sandstones in Section 5, T3N, R12W. Therefore it is important to understand the depositional setting of the two very different reservoir types in the Bridgeport B interval.

# **Bridgeport C Sandstone Overview**

The Bridgeport C sandstone occurs far less frequently than any of the other Bridgeport reservoirs in the field. Where it does occur, the Bridgeport C can reach thicknesses up to about 20 feet. The sandstone was studied in a few cores where it was observed to be typically fine grained with common flaser beds throughout as well as thick zones of lenticular bedded sandstone. The amount and apparent lateral continuity of these shaly zones implies a great deal of compartmentalization with the Bridgeport C reservoirs. This combined with the fact that these reservoirs are often thin and not laterally extensive make them unlikely targets for a large scale ASP program.

### **Bridgeport D Sandstone Overview**

The Bridgeport D sandstone is somewhat more continuous that the Bridgeport C, but mapping of the unit shows no distinct trends. The unit averages up to 25 feet thick where it occurs. From a few core, the Bridgeport D was observed to be somewhat similar in character to the Bridgeport C. The base of the Bridgeport D typically sits atop an unnamed coal. Thick intervals of lenticular and flaser bedded sediments are common. Some generally structureless, fine grained, clean sandstone occurs within the Bridgeport D, but it is rarely more than a few feet thick. Much like the Bridgeport C, the reservoir characteristics of the Bridgeport D make it an unlikely target for ASP flooding.

# Sequence Stratigraphic Techniques for the Regional Mapping of the Bridgeport Reservoirs

Regional mapping of the Pennsylvanian Bridgeport B interval became necessary when it was discovered that there were several episodes of sandstone deposition resulting in different reservoir facies with varying architectures in the same stratigraphic interval in Lawrence Field. Placing these reservoirs in a sequence stratigraphic framework also became essential to understanding the variety of observed reservoir characteristics within short distances. Regional marker beds were identified above and below the Bridgeport B in the form of the informally named Gamma and Alpha shales, respectively (Figure 14). Both are interpreted from geophysical logs to be shales of similar character to the Beta shale that underlies the Bridgeport B. One core, the Johnson #32 in Section 32 penetrates the Alpha shale and shows approximately

2 feet of dark grey – black shale with red siderite bands (Figure 19). Correlating these two shales across the field has helped to constrain the Bridgeport B interval. Additionally, these shale units have lateral continuity to a greater extent than that of the Beta Shale. Where the Beta Shale is eroded along the western flank of the field, the Alpha and Gamma Shales persist and help subdivide a multistory succession of thick sandstone bodies.

Sequence stratigraphy is the study of rock relationships within a chronostratigraphic framework of repetitive, genetically related strata bounded by surfaces of erosion or nondeposition, or their correlative conformities (VanWagoner et al., 1989). The sequence stratigraphic method can be particularly useful in reservoir characterization as it can be applied across different scales and different depositional environments. Sequence stratigraphy makes use of directly observable criteria from the geologic record including vertical lithofacies associations, stacking patterns, stratal geometries, and stratal terminations (Abreu, et al., 2010). A sequence stratigraphic framework includes genetic units that result from the interplay of accommodation and sedimentation, which are bounded by sequence stratigraphic surfaces (Catuneanu et al., 2009).

Cyclic sedimentation patterns have long been recognized in the Illinois Basin (Udden, 1912; Weller, 1930; Wanless and Weller, 1932) especially in the form of the cyclothems of Middle Pennsylvanian strata. The sequence stratigraphic technique has been successfully applied to Pennsylvanian rocks younger than the Bridgeport North of Lawrence Field (Weibel, 1996) and to Mississippian rocks older than the Bridgeport in southern Illinois (Nelson, et al., 2002). In Lawrence Field, the application of sequence stratigraphic principals has been particularly useful in differentiating the Bridgeport reservoirs, as thick, channel facies sandstones are juxtaposed against thinner, coastally deposited sandstones in the same stratigraphic interval.

The lower Pennsylvanian rocks that make up the Bridgeport reservoirs in Lawrence Field are difficult to correlate over a large area. This interval is made up of the Caseyville and Tradewater Formations. Caseyville Formation sandstones are typically coarser grained with common quartz granules and are made up of generally thicker sandstone bodies whereas the Tradewater Formation Sandstones lack quartz granules and are characterized by a number of thinner sandstone lenses. Both formations are dominated by thick successions of sandstone and shale, with limestones and coals, strata typically used for regional correlation, largely absent. Cyclic sedimentation persisted through this time period, but the lack or key marker beds and the presence of thick sandstones can make the identification of these patterns difficult. Because of the lack of regionally extensive marker beds in these lower Pennsylvanian strata, the sandstone bodies are difficult to correlate at the scale of Lawrence Field and can be nearly impossible to correlate out of the field and into the Illinois Basin.

Sequence stratigraphy can help to overcome some of the difficulty in correlation by helping to identify genetically related strata. Parasequences are identified on logs between flooding surfaces, and systems tracts are then identified in well logs based on the stacking patterns of those parasequences. Recognizing these parasequence stacking patterns leads to the identification of significant stratigraphic marker horizons including the Maximum Flooding Surface (MFS), the Transgressive Surface (TS) and the Sequence Boundary. Gamma ray logs are often the most effective in displaying strata stacking patters, but due to their relative scarcity in Lawrence Field, stratal boundaries picked on gamma ray logs have to be carefully propagated to nearby electric logs.

Using the sequence stratigraphic method, the Lower-Middle Pennsylvanian strata, from the basal unconformity up through the Curlew Limestone, appear to be made up of at least five cycles of sedimentation. A map showing the locations of cross sections referenced in the discussion to follow is provided (Figure 20). The three well, north-south cross section in Figure 21 shows the basic sequence stratigraphic framework of the Bridgeport reservoirs used in Lawrence Field. The cross section includes wells penetrating both the Bridgeport B in Section 32 as well as the channel facies sandstone in eastern section 5. Sequence 1 is bounded at the base by the sub-Absaroka unconformity. The Buchanan sandstone comprises the lowstand systems tract (LST) and locally overlies Mississipian Glen Dean Limestone and, in places, Tar Springs Sandstone (Lumm, 1998). The maximum flooding surface (MFS) within Sequence 1 occurs at an unnamed Caseyville Fm. shale. The Pounds Sandstone forms the LST of Sequence 2, overlying the highstand systems tract (HST) deposits of Sequence 1. The Alpha Shale forms the MFS for Sequence 2.

Sequence 3 marks the start of the Bridgeport reservoirs with the Bridgeport A comprising the LST. In cross section A-A', the Bridgeport A interval is composed mainly of silty to sandy material, likely the overbank facies of the Bridgeport A sandstone found elsewhere in Section 32. The Beta Shale constitutes the MFS of Sequence 3. The Bridgeport B is the LST of Sequence 4 as it overlies the Beta Shale across much of Lawrence Field. The Bridgeport B is seen only in the Griggs #60 well on cross section A-A' as the entirety of Sequence 4 has been truncated by Sequence 5. The MFS for sequence 4 occurs at the Gamma Shale.

Sequence 5 begins at the base of the Bridgeport C as seen in the Griggs #60 well. The lower sequence boundary occasionally scours down and removes all of the material in the underlying Sequence 4. Such an event likely resulted from a lack of accommodation, as would be expected in a low-relief cratonic basin. The removal of an entire sequence by erosion is not an uncommon occurrence across Lawrence Field. Examination of the stratigraphy along the western flank of the Bridgeport Anticline indicates that there are places where more than one sequence may have been removed by erosion where blocky sandstone deposits can be up to several hundred feet thick.

Through the application of the sequence stratigraphic technique, we can see that the thick channel facies sandstone in Section 5 is actually a younger unit that the Bridgeport B. Further validation is provided below in the discussion of the dating of pollen found in coal, as well as by the distribution of coal in in the stratigraphic succession with respect to the sequence stratigraphic surfaces (Bohacs and Suter, 1997).

# **Coal Palynology**

The Bridgeport B sandstones have been classified as being members of, alternatively, the Caseyville or Tradewater formations in various studies. Marathon conducted a reservoir study (Palmer, 1984) in the 1980s to support their Maraflood program. They concluded that the Bridgeport B sandstone was classified as lower Tradewater Fm. while the thick channel sandstone in Section 5 was classified as middle Tradewater Fm. This classification was based on a comparison of sandstone bulk mineralogy against an earlier petrographic study of Pennsylvanian sediments (Potter and Glass, 1958). In a later Ph. D. dissertation, Lumm (1998)

classified the same Bridgeport B interval as part of the uppermost Caseyville Formation., based on sandstone body geometries, and the amount of mica present in the studied samples.

This project was able to use palynology because it was possible to sample a variety of pertinent coal seams from several cored wells. Palynology can provide chronostratigraphic correlations of coal units across the Illinois Basin (Peppers, 1996; Elbe at al., 2001). The amount of core coverage across Lawrence Field has provided a number of cores containing in place, bedded coals that can be biostratigraphically correlated to other parts of the Illinois Basin. Four such coals were sampled from four different cores in Lawrence Field. Based on correlations in geophysical logs, each of these coals is a different coal unit. Such correlation provided an important stratigraphic anchor to resolve the historical disagreement of unit placement within the Bridgeport units, and to tie the stratigraphy in Lawrence Field into a more basin-wide framework (Figure 22).

Cross section B-B' (Figure 23) shows the four wells where coals were sampled for palynological study. The Curlew Limestone is used as the datum. The difficulty of correctly correlating the Bridgeport B reservoir when channel fill sandstones occupy the same stratigraphic position is apparent. Core measured permeability is plotted in red on the right side of each log with a scale of 0-1000 millidarcies. Average core measured permeability in the Section 5 sandstone is 63% higher averaging 314 millidarcies versus an average of 113 millidarcies in the sandstone in Section 32. Bridgeport B sandstones in Section 32 commonly show a stacking of up to three lenses while the sandstones in Section 5 are characteristically thick and blocky. Coal palynology has clarified the correlation of reservoir sandstone bodies by providing evidence that thick channel fill deposits in the same stratigraphic position as the Bridgeport B are actually later events and have probably removed the Bridgeport B sediments. The channel fill sandstone reservoirs in Section 5 are in the Tradewater Formation while the Bridgeport B reservoirs in the Griggs lease and the Johnson 32 wells in Section 32 are in the Caseyville Formation.

An Isopach map showing the Bridgeport B sandstone on top of the Bridgeport Anticline in the northern part of Lawrence Field is shown in Figure 24. Thick channel fill deposits truncate the Bridgeport B to the west and southeast. Data density drops off significantly to the east. Structure contours are on the base of the Barlow Limestone. From this small scale overview of the northern part of Lawrence Field, it is demonstrated that the Bridgeport B is compartmentalized into discreet sandstone bodies that are separated from one another by stretches of non-reservoir rock. The North-South cross section C-C' in Figure 25 shows small scale compartmentalization of the Bridgeport B reservoir. East-west trending sandstone bodies are bounded by non-reservoir siltstones.

Figure 24 shows the location of ASP flood areas in Bridgeport B sandstone reservoirs. The 15 acre Middagh flood was reaching peak production at the end of 2011. Pre-flood production was 16 BOPD; peak ASP flood production was 100+ BOPD. The Perkins-Smith 58 acre flood was initiated in late 2011. No results have been reported to date. The Delta unit 350 acre expansion is under development with flood initiation expected in mid-2013.

# **Depositional Environments Bridgeport B Sandstone Reservoirs**

# Fine-grained tidally influenced Bridgeport B

The thinner sandstone reservoirs in the Bridgeport B interval of Section 32 T4N, R12W could have formed as a tidally-influenced, deltaic deposit in an estuarine environment (Figure 26). These sandstones are finer grained, more compacted, and are therefore less porous and permeable than the channel fill reservoir sandstones in Section 5 T3N, R12W and were deposited before the channel fill sandstones. Tidal flat, intertidal flat, tidal sand bars and tidal estuarine deposits are located in Section 32. Tidal indicators in the sandstone in Section 32 include ripple bedding, flaser and lenticular bedding, tidal rhythmites and tidal couplets. Some burrowing trace fossils can also be observed. The complexity of this depositional system illustrates the need for detailed mapping of individual sandstone reservoirs and also explains the high degree of variability in reservoir characteristics and geometries over a small area (Figure 25). The geophysical log from the Johnson # 32 well shows the relationship of the Bridgeport B sandstone lenses with the underlying Beta Shale and the overlying coal (Figure 27)

The thin fine-grained facies of the Bridgeport B in Section 32 T4N R12W was informally divided into three subunits; the B1, B2, and B3 from the base to the top of the unit (Figure 28). The lower Bridgeport B sandstone unit (B1) is more consistent, widespread, and thicker, up to 20 feet, than the upper two sandstones units. Isopach flow unit maps of the 50 percent net sandstone of the Bridgeport B1 and B2 subunits in Section 32 Sandstone were mapped using a 2 foot contour interval with the warmer colors representing thicker sandstone (Figure 28). Reservoir sandstone in the northern half of Section 32 trends east-west whereas in the southern half of the section, the sandstone takes on a triangular shape and occupies the region between the two thick channel fill sandstone bodies that trend into Section 5 from the northeast and northwest. Bridgeport B1 and B2 sandstones in Section 32 develop predominantly in the same area. The B1 sandstone is thicker and better developed than the B2 sandstone (Figure 29).

Much of the lowermost reservoir sandstone in the Bridgeport B1 along the crest of the Bridgeport Anticline is composed of fine-grained, tabular cross bedded and sub-horizontal bedded sandstones that show some tidal couplets. Porosity and permeability are greater than the overlying ripple-bedded sandstone facies. A sharp contact between these two facies types with a several inch thick zone of non-reservoir, shaly-to lenticular bedded sandstone that is often burrowed is common and indicative of a rapid change in the depositional setting. An isopach map shows the gross thickness of the cross bedded sandstone facies within the NE-SW trending Bridgeport B reservoir in the northern portion of Section 32 (Figure 30). Bridgeport B sandstones are near shore to deltaic coastal deposits that occupy the lowstand systems tract. Sandstones can typically be broken into a lower cross bedded facies showing many scoured and reactivated surfaces, and an upper, more tidally influenced ripple bedded facies. The Bridgeport B is subdivided into facies to better understand and to more easily trace flow units within the reservoir. The cross section D-D' (Figure 31) is an example where the cross bedded facies has been identified in the lower part of the Bridgeport B. This facies tends to manifest itself on logs by having a more blocky appearance and has better porosity and permeability than the overlying ripple bedded facies. Shaly, lenticular bedded intervals vertically baffle or compartmentalize the Bridgeport B reservoir (Figure 28) while the discontinuous nature of the sandstone lenses tends to horizontally compartmentalize these reservoirs. The Bridgeport B interval has a sharp contact

with the underlying widespread Beta shale unit that was deposited during a maximum marine transgression and separates the Bridgeport A interval from the Bridgeport B interval. That sharp contact defines a sequence boundary at the base of the Bridgeport B sandstone. Isopach mapping of this unit shows a distinctive east-west trend to all three (B1, B2, B3) Bridgeport B intervals in sections 29 and 23, T4N, R12W. These sandstones are interpreted to be tidally influenced near-shore to deltaic deposits based on geometry, orientation and sedimentary structures observed in core.

A typical core from the Johnson 32 well shows sedimentary features representative of the Bridgeport B reservoir in Section 32 (Figure 19). The reservoir sandstone is typically fine to very fine grained and fines upwards. The basal contact of the reservoir sandstone with underlying shale is sharp. Tabular cross beds with small clay rip up clasts are common in the B1 sandstone. The reservoir sandstone is punctuated with calcite cemented zones and intervals of lenticular to flaser bedded sandstone that range in thickness from a few inches to around a foot. Flaser and lenticular bedded zones, and to a lesser extent the calcite cemented zones, may create vertical baffles between porous and nonporous intervals locally, but also extend laterally over a wide area. It is likely that some baffles, especially calcite cemented zones, fade away over distance and some vertical communication between the subunits of the reservoir are established. Ripple bedded sandstone and tidal rhythmites are common in the B2 and B3 sandstone subunits, indicating a tidal influence on deposition.

### Post Bridgeport B Channel Fill Reservoir Sandstone

Flanking the crest of the Bridgeport Anticlinal structure are 50 to 150 foot thick channel sandstone units that appear stratigraphically correlative to the above described intervals (Figure 18). The sandstone reservoirs in Bridgeport B interval of Section 5 T3N R12W formed as stacked braided river deposits in the transitional fluvial-deltaic environment (Figure 32). These channels are interpreted to be younger than the Bridgeport B sequence interval, based on careful correlation of key marker beds and palynological evidence from coals associated with the two sandstones as described in previous sections. These channel sandstones are likely related to the overlying Bridgeport C sequence, and have incised and removed the sediments that make up the Bridgeport B section. The porosity of these sandstones ranges from 18 to 23%, while permeability can reach over 1000 md, up to 5 times the average of the sandstones along the crest. Average permeability in Section 5 sandstone is 2.8 times greater (314 md) compared to 113 md in Section 32. These wells are about 1 ¼ mile apart but this rapid change commonly occurs over just a few hundred feet. Cross section E-E' (Figure 33) shows the stark contrast in reservoir quality of the Bridgeport B fine-grained sandstone and the post Bridgeport B channel fill sandstone reservoirs. The thin stacked sandstone lenses that comprise The Bridgeport B subunits B1, B2 and B3 are much more compartmentalized with much lower permeability and porosity values than the thick blocky post Bridgeport B channel fill sandstone in the Robins #MG 8 well. A regional cross section (Figure 34) shows the regional relationship of the Bridgeport B sandstones and the post Bridgeport B channel fill sandstones in Lawrence Field. The locations of cross section E-E' and F-F' are shown on Figure 20. The Robins 102-B Marafood pilot targeted these channel sandstones in Section 5, T3N, R12W.

Core showing the typical facies of the Bridgeport Channel reservoirs is from the Robins MG-8 well (Figure 35). The core shows sedimentary features common in the thick sandstone in eastern

Section 5 and is indicative of channel fill deposits with rapid deposition followed by limited compaction. The basal contact of sandstone with the underlying shale is typically erosive and chaotic, exhibiting lag gravel, clay rip-up clasts, and zones of iron-carbonate cementation. Sandstone in this lower chaotic zone is coarse but fines upward to medium sand through most of the reservoir. Above the chaotic basal zone, alternating zones of tabular cross bedded sandstone and structureless sandstone are common. Sandstone is generally continuous throughout the reservoir without the baffles seen in the Bridgeport B sandstone in Section 32. Slumping features are common. The sandstone becomes finer grained and more tidally influenced near top of the interval where flaser and lenticular bedding as well as tidal rhythmites are common.

### **Review of Bridgeport B Interval Deposition**

Prior to deposition of the Bridgeport B sandstone, the widespread marine Beta Shale marker bed was deposited during a period of sea level highstand. The highstand was followed by deposition of tidally influenced coastal sediments that prograded across the Lawrence Field region, filling available accommodation as channels aggraded, leading to the vertically stacked and laterally discontinuous patterns found in the Bridgeport B (Figure 18). Depositional energies moderated as reflected in the B2 and B3 intervals where ripple bedded sandstones punctuated by several inch thick shaly, lenticular bedded intervals predominate. These shaly, lenticular bedded intervals act as vertical boundaries to fluid flow, effectively compartmentalizing the Bridgeport B reservoirs. Eventually a sea level still stand took place and the surface of the sand was scoured (Clifton, 1982). East-West trending channels were cut across Section 32 T4N R12W and were filled with very fine grained sandstone to siltstone of non-reservoir quality. A coal swamp capped the succession in the area as indicated by the thin bedded coal at the top of the Bridgeport B. A significant transgression marks the end of the Bridgeport B cycle and the emplacement of another marine shale as the next cycle of sedimentation begins for the Bridgeport C interval. Channel fill episodes are observed in Bridgeport units in the area of interest; especially in Section 5 T3N R12W where channel fill sandstones are found (Figure 18). Tectonic activity likely influenced the deposition of Bridgeport B sediments. Although subsidence of the Illinois Basin continued throughout the Pennsylvanian, subtle uplift along the La Salle Anticlinorium appears to have resulted in low accommodation space and thin successions of sediment along the crest of the anticline. The complexity of this depositional system illustrates the need for detailed mapping of individual sandstone reservoirs and also explains the high degree of variability in reservoir characteristics and geometries over a small area. Understanding this complexity is necessary for successful EOR development.

The lowermost portion of the channel fill facies in Section 5 T3N R12W has a sharp scoured contact with rip-up and conglomerate lag that transitions into medium grained tabular crossbedded sandstone that were initially deposited in a fluvial channel, continuous transgression lead to a change in environment to tide influenced coastal and estuarine. Thick sandstones in Section 5 were initially deposited in an incised channel with the lower erosive contact, tabular cross bedding and indistinct zones being part of the fluvial facies (Figure 35). Sea level transgression occurred during sedimentation within the incised channel resulting in a change in facies from fluvial to tidally influenced coastal -estuarine sandstone deposition. The thick sandstone body in Section 5 becomes more ripple bedded with flaser and lenticular bedding near the top indicating the transition from fluvial facies to tidally influenced coastal/estuarine facies (Dalrymple & Choi, 2007). The abundance of replaced plant material and spores in the lower fluvial facies of the Section 5 sandstone may indicate that the muddy area surrounding the estuary was likely a

lycopod swamp. As sea level continued to rise, the incised channel widened upwards until the estuary finally overran the banks of the channel and embayed the entire area of interest.

The schematic diagram (Figure 36) shows an incised valley fill model. The entire sedimentary sequence is transgressive in character with the basal fluvial deposits overlain by estuarine deposits and capped with shallow marine deposits as progradation continued. This incised valley fill model is analogous to sedimentary structures observed in core in Section 5 3N, 12W, from Dalrymple and Choi, 2007.

Another schematic diagram (Figure 37) illustrates cyclical deposition under conditions where sea level drops and valleys are incised followed by sea level rise with periods of stillstand. Stillstand units are transgressive in character and are relatively tabular or flat-lying. They can begin from channels incised into the previous unit. Basal deposition within the incised channels can be fluvial with associated sediments overlain by intertidal to supratidal units. The sedimentary structures observed in core and depositional characteristics in Section 5 are, in general, analogous to the incised valley models shown in Figures 36 and 37 estuarine fill complex deposited under continuously rising sea level. The stillstand units are relatively tabular and extend from channels cut in the previous unit to the upper intertidal to supratidal units, from Clifton, 1982. This model may represent the complex channel fill cycles and tidally dominated estuarine sequences observed in the Bridgeport interval in Section 32 T4N R12W and Section 5 T3N R12W.

# Petrographic Analysis – Pennsylvanian Bridgeport B Interval Reservoirs

A PIMA (Portable Infrared Mineral Analysis) device was used on core samples to identify potentially different mineralogical zones within reservoir sandstones. All together approximately 280 PIMA analyses were completed on samples from 16 core (Baltzell QS-25; Cooper 108; Robbins MG-8, MG-12, MG-16, MF-9, ME-10, OB-2, OB-4; Griggs 106, 107, 110, 109, 108, 112 and the Johnson 32). Results are returned in the form of spectra traces, similar in appearance to XRD diffractograms, with peaks and trends in the traces representing the presence of certain minerals, water, oil staining, and certain elements.

The PIMA allows for quick, qualitative assessment of the mineralogy of reservoir sandstones so that the units can be sampled for XRD clay mineralogy and bulk mineralogy more expeditiously. PIMA results and core measured porosity and permeability analyses were used to select 88 samples for XRD clay mineralogy and bulk mineralogy analysis from eight different cores in the Lower Pennsylvanian reservoirs in Section 5 T3N R12W. An additional 50 samples from seven cored wells were analyzed from the Bridgeport B fine grained sandstone facies in Section 32 T4N R12W.

### X ray diffraction analyses

X-ray diffraction analyses of bulk mineralogy and clay mineral fraction were completed on core samples from several wells in the channel fill reservoir sandstones in Section 5 T3N R12W. Bulk mineralogy analyses identified the relative abundance of clay minerals, quartz, K-feldspar, plagioclase-feldspar, calcite, dolomite, siderite, and pyrite/marcasite. Over eighty samples from core in the channel fill reservoir sandstones in Section 5 were analyzed. The results from the

Robins MG-10 well (API 1201012871800) are shown in a bar graph in Figure 38. The results for this well show that none of these analyzed samples contains enough quartz to be classified as a quartz arenite because all of the samples have less than 90 percent quartz. Pyrite/marcasite is common in a few samples usually located near the base of the channel fill sequence. However none of the samples tested in the Robins ME-10 well contained significant amounts of pyrite/marcasite. Carbonates are the second most commonly occurring minerals in channel fill sandstones. Carbonates found in these samples include calcite, dolomite and siderite with siderite (FeCO<sub>3</sub>) being the most abundant. Siderite is the only carbonate found in analyzed samples in the Robins MG-10 well. The amount of siderite ranges from 3 percent to 35 percent and is over 10 percent in most samples. Thin section analysis shows that siderite has replaced most of the organic plant material in these sandstones. Feldspar content is relatively low at less than 10 percent in all samples when K-feldspar and P-feldspar are combined. Some feldspar has degraded to clay minerals.

The clay mineral suite in this well consists of kaolinite, chlorite, illite and mixed-layered illite/smectite. Bulk mineral analyses show that total clay mineral content is usually less than 5 percent, thin section analyses show that clay minerals are commonly located in pore spaces where they are most likely to come into contact with and react with fluids in the reservoir. A bar graph showing the relative abundance of clay mineral types in the clay sized fraction of samples analyzed with XRD is shown in Figure 39. The most common clay mineral in most samples in the Robins ME-10 well is kaolinite which comprises 50 percent or more of the clay mineral fraction, illite is the second most common clay mineral and usually makes up approximately 30 percent of the clay mineral fraction. Chlorite and mixed-layered illite/smectite are the least common clay minerals and together usually make up less than 12 percent of the clay mineral fraction.

# Thin section analysis post Bridgeport B Channel fill Section 5

Thin section analysis of some of the samples analyzed with XRD show that quartz sand grains are the most abundant component of most reservoir rock. Sandstones are most commonly cemented by quartz overgrowths with some samples being cemented by plant material such as spores replaced by siderite. A thin section (Figure 40) from the Robins ME-10 well (API 121012871800) at a depth of 905.5 ft., 2.5X magnification and under white transmitted light has horizontal permeability of 221md, vertical permeability of 37.6 md and porosity of 20.6%. This thin section is taken from a sample near the top of the channel fill sequence and contains indicators of deposition in a tidally influenced environment. This sample has less permeability than many in the lower portion of the channel fill sequence. The thin section shows clay rich laminae that have been subjected to compaction. These features are uncommon in the lower portions of the channel fill.

A thin section photomicrograph from the Robins ME-10 well is shown in figure 41. This sample is medium grained sandstone at a depth of 914.5 feet with 23% porosity and 1050md of horizontal permeability. Organic material, such as spores replaced by siderite (FeCO<sub>3</sub>), are common in some channel fill intervals. There is also little evidence of compaction resulting in preservation of a large amount of primary intergranular porosity as is indicated by the large core measured permeability values. The lack of compaction in most intervals of channel fill sandstone has resulted in excellent reservoir qualities of high porosity and permeability. In contrast, many reservoir samples from reservoirs in the Griggs lease in Section 32 T4N R12W show evidence of

compaction after deposition resulting in less porosity and permeability. A thin section photomicrograph from the Robins ME-10 well (figure 42) shows medium grained sandstone at a depth of 923.5 feet. This sample has core measured porosity of 22.5% and a horizontal permeability of 710md. There is a large amount of organic material including numerous spores replaced by siderite located between quartz sand grains. A thin section from a depth of 933.5 feet (Figure 43) also has very good porosity and permeability and numerous spores replaced by siderite. The least porous and permeable sample in the channel fill sequence is shown in figure 44. This sample is from a depth of 946.5 and has a horizontal permeability of 80md and porosity of 17.5 percent. The quartz grains in this thin section are sutured and there is a noticeable decrease in the amount of preserved primary intergranular porosity.

Another thin section photomicrograph (Figure 45) from the Robins ME-10 well at a depth of 953.4 feet, has 22.3% porosity and 557md permeability. This higher magnification photomicrograph shows a small plant with roots with a high level of detail preserved in the replacement of original organic material by mica. The replacement of plant stems, roots and cones by mica and or siderite is found in many thin sections from channel fill samples. Other thin sections in the channel fill sequence showing large amounts of porosity and permeability as well as an abundance of spores replaced by siderite are shown in figures 46 - 48. A thin section micrograph from the Robins ME-10 well (Figure 49) shows a close-up from a depth of 985.5 feet. The image shows a spore replaced by siderite and that exhibits the rhombohedral shape of siderite crystals. This thin section is from a sample with a core measured porosity of 19.3% and 39md of permeability. The relatively low porosity and permeability in figures 49 and 50 in this sample is attributed the very great abundance of spores replaced by siderite. The abundance of siderite cement has significantly reduced permeability in this sample. XRD analysis shows that the siderite comprises approximately 35 percent of the bulk mineralogy. This is the largest amount of siderite in samples analyzed in this well.

### **Petrography Bridgeport B fine grained sandstone facies**

XRD analyses of bulk mineralogy are available from fifty samples taken from six cored wells in the fine-grained sandstone facies of the Bridgeport B in Section 32 T3N R12W. Most samples have 90 percent or greater quartz, siderite is most commonly a minor component in these samples at less than five percent, however there are four samples with 30 percent or greater siderite, the clay mineral fraction most commonly ranges from 3 to 10 percent, plagioclase and potassium feldspar combined are usually less than 4 percent, pyrite/marcasite are not present in these samples. Calcite and dolomite are rarely present in samples from the fine-grained sandstone facies. Siderite is the most common carbonate present.

X-ray diffraction analyses of the bulk mineralogy of core samples from the Bridgeport B reservoir in the Griggs 109 well located in Section 32 T4N R12W is shown in figure 51. The sandstone is fine to very fine grained has been interpreted as deltaic. The average porosity and permeability of the Bridgeport B in this well are 19% and ~150 md respectively. Quartz is the most abundant mineral and ranges between 75-95% in sandstone reservoir samples. Siderite and diagenetic clay minerals are the next most abundant minerals, siderite ranges between 2-15%, clay minerals range between 3-15%. Potassium and plagioclase feldspars are minor components in all samples. One sample at 906.5feet is calcite rich with 8% calcite, this sample is entirely cemented by calcite with no porosity and permeabiliity. The X-ray diffraction analyses of

samples from the Bridgeport B in the Griggs 109 well are typical of the fine to very fine grained sandstone of the Bridgeport B1, B2 and B3.

X-ray diffraction analysis of the clay mineral fraction (Figure 52) of samples from the Griggs 109 well shows that kaolinite is usually the most abundant clay mineral and illite is the second most abundant clay mineral. There are a few examples in shale rich samples where illite is the most abundant clay mineral. Chlorite and mixed layered illite/smectite are the least common clay minerals

X-ray diffraction analyses of bulk mineralogy (Figure 53) from core samples in the Johnson #32 well in Section 32 T4N R12W located in the delta triangle south of the Bridgeport B1, B2, B3 mapped units show that quartz is the most abundant mineral comprising between 78-93% of most reservoir samples. Two samples at 867 ft. and 883 ft. contain very large amount of siderite. Siderite (FeCO3) is a minor component in all other samples. Diagenetic clay minerals comprise 2-8% of samples. Although clay minerals are a minor component they play a major role in preserving porosity by coating many quartz grains, thereby limiting the development of quartz overgrowths. Potassium and plagioclase feldspar are minor components. The average porosity and permeability of these samples is also 19% and ~150 md respectively. The bulk mineralogy of the Bridgeport B sandstones in the Johnson 32 well is very similar to that of the Griggs wells. XRD analysis of the clay sized fractions of the fine grained facies of Pennsylvanian Bridgeport B and Cypress sandstones in the Griggs lease area of Section 32 T3N R12W shows that the Pennsylvanian strata are contrasted from the Cypress materials by containing more illite and significantly less chlorite. Further, the chlorite in the Bridgeport suites appears to contain less iron and relatively more magnesium. The kaolinite in all the samples from sandstones is diagenetic, but some of the claystones or shales in the Bridgeport strata contain fireclay-type kaolinite. The shale samples are too few to draw strong conclusions, but in general they contain higher illite and less kaolinite than the sandstones and are similar to other shales of the Paleozoic. They also contain chlorite with typical Fe:Mg ratios that are much different from Cypress chlorites.

Two different types of kaolinite occur in these strata. Diagenetic kaolinite has sharp XRD peaks and the ratio of 001 to 002 XRD peaks is typically between 2:1 and 3:2. The second type of kaolinite is mixed-layered kaolinite/smectite, or as we suggested kaolinite/expandables (K/S or K/E), which occurs in Pennsylvanian paleosols or what are often described as shales or claystones. This variety of kaolinite has been called fireclay kaolinite (Hughes, DeMaris, and White 1992), and the occurrence and origin of this mineral has been described in Hughes, Moore, and Reynolds (1993). The 001:002 ratio of XRD peaks for fireclay kaolinite is near 1:1, with the 002 sometimes stronger than the 001. These two types of kaolinite have distinctly different PIMA spectra, which are discussed in the PIMA section of this report.

Three types of diagenetic kaolinite are recognized, and all are well crystallized in terms of their XRD and PIMA spectra. The first is typical of the Cypress Sandstone and occurs as vermicular or book-like stacks of plates that are strongly bonded or cemented together. The diagenetic kaolinite in Pennsylvanian reservoirs may be at least in part smaller, plate-like individual hexagonal particles that can be easily disaggregated and mobilized. The third variety of kaolinite also occurs in Pennsylvanian strata as tightly cemented flint clay. This variety develops in soils

that are reducing, which seems unlikely to occur in these sequences. However, siderite and pyrite are commonly associated with flint clays, and they are abundant in parts of these strata.

### **Petrographic Analysis Bridgeport B Sandstones**

Thin section photomicrograph from the Bridgeport B3 in the Griggs #107 (Figure 54) well shows fine grained sandstone at 929.5 feet depth. Porosity is 19.1% porosity and permeability is 66md. These are common values for this facies. Some fracturing of the sandstone is apparent. Much of the porosity is occluded in this sample by suturing of quartz grains and compaction of ductile grains.

Thin section photomicrograph from the Griggs #107 well shows fine grained sandstone at 932.5 feet depth. This sample (Figure 55) has good porosity at 20.3% and good permeability at 171md. There is some compaction and a high degree of quartz cementation. Some pores have been enlarged due to dissolution of feldspar grains. The greater the amount of feldspar the greater the opportunity for the development of secondarily enhanced porosity caused by dissolution of feldspar framework grains.

Thin section photomicrograph from the Griggs #107 well is also fine grained sandstone at 942.8 feet depth with very good porosity at 20.1% porosity and good permeability at 206md. This example (Figure 56) shows a close-up of quartz overgrowths cementing sand grains. Degraded feldspar grains replaced by kaolinite are also prominent in this thin section and are common features in this facies. The greater the amount of quartz overgrowth development the more primary intergranular porosity is filled resulting in the reduction of porosity and permeability.

Scanning photomicrographs (Figure 57) of the Bridgeport A sandstone from the Griggs 107 well at a depth of 1005.7 feet show a highly porous sandstone cemented by quartz overgrowths. Enlarged pores caused by dissolution of feldspar grains are evident in the top two photographs of the series. The sharp euhedral crystals formed by quartz overgrowths as well as a closeup of vermiform kaolinite booklets are evident in the middle photographs of the series in figure 57. The last three photographs (Figure 57) show kaolinite at various magnifications and illustrate the location of the clay mineral in pore throats.

Scanning electron micrographs from the B2 interval of the Griggs #107 well at 942.8 feet depth show diagenetic features typical of Bridgeport B sandstones. The SEM micrograph (Figure 58) illustrates a three dimensional view of quartz overgrowths, enlarged pores due to the dissolution of feldspar grains, and pore filling and bridging diagenetic clay minerals similar to those illustrated in figure 57 from the Bridgeport A sandstone. The SEM micrograph (Figure 59) shows a closeup of booklets of the most commonly occurring diagenetic clay mineral kaolinite.

### **Summary EOR Targets in Bridgeport B Sandstones Lawrence Field**

The Bridgeport B sandstones in Section 32 at the present time is likely a better EOR target than the channel fill facies reservoirs in Section 5 The Bridgeport B reservoirs in this area have not been as effectively produced as the channel facies reservoirs in Section 5 because of their more compartmentalized characteristics. Yet because these target reservoirs are more confined, flow units and their geometries tend to be more mappable, and as a result the chemical flood can be designed and implemented for the greatest recovery potential. A better understanding of

reservoir characteristics allows for better cost control which increases the economic feasibility of EOR projects. The thick sandstones in the eastern portion of Section 5 are along the flank of the structure with a portion of the sandstone dropping below the original oil-water contact. Loss of expensive EOR chemicals into the water zone becomes a factor. Additionally, oil saturations have been lowered due to primary and secondary production and implementation of the Maraflood Project. While highly porous and permeable reservoirs are generally very good targets for EOR application, there is less remaining oil to recover using ASP technology due to a previously implemented EOR pilot in the reservoir. It is difficult to correlate preferential flow units within the channel facies reservoirs with standard mapping techniques using the older style SP- electric logs that are principally available throughout Lawrence Field. Recent porosity logs and core information have greatly enhanced the ability to delineate reservoir characteristics that are necessary to increase the likelihood for successful ASP- EOR applications.

#### **Conclusions**

Reservoir characterization is important for implementation of Enhanced Oil Recovery programs because the economic success of an EOR project is dependent on the design and implementation of the project being aligned with the unique geologic characteristics of each reservoir. Successful implementation of EOR programs in mature Pennsylvanian reservoirs will have broad application in the Illinois Basin and elsewhere. The potential for channelized flow in more permeable portions of the channel fill facies in Section 5 and the more marine influenced facies in Section 32 versus intervals with low permeability has added to the difficulty of implementing EOR techniques in these reservoirs. The more permeable intervals have less residual oil as primary production and secondary waterflooding have selectively recovered more oil from these intervals while leaving more recoverable oil in the less porous and permeable intervals. Thus, techniques to reduce channelized flow must be designed and implemented. Compartments can be most effectively drained where they are geologically well defined and reservoir management practices are coordinated through unified, compartment-wide, development programs. The overprint of diagenetic alteration has added to the high degree of variability in these reservoirs taking place over a geologic time frame resulting in areas of both enhanced and diminished porosity and permeability. Compaction of grains, particularly in some ripple-bedded intervals has greatly reduced porosity and permeability, diminishing reservoir quality. Other facies, such as the cross bedded facies have increased porosity and permeability due to the lack of compaction in channel fill deposits Thin section and X-ray diffraction analysis shows that the identified clay mineral suite in reservoir intervals should be considered because they are primarily located in pores where interaction with existing or injected fluids is likely. These data are important for determining the suitability of various EOR techniques. Depositional environments of the Pennsylvanian Bridgeport sandstone reservoirs are complex and are characterized by sea level drop resulting in regressive incisement, followed by transgressive infill packages that commonly show tidal influence in the upper sediments of the cycle. Understanding the depositional setting is necessary to unravel the complexity of the reservoir facies and their individual characteristics that are fundamental components for the design and implementation of successful ASP-EOR projects

# **Cypress Sandstone Reservoir Overview of Lawrence Field**

Cumulative production from the Mississippian Cypress sandstone reservoirs in the Illinois Basin is over one billion barrels of oil, the highest of all producing horizons. Approximately 200 million barrels of oil have been produced from the Cypress sandstones at Lawrence Field. An estimated 39.5% of OOIP (Udegbunam and Grube, 1993) has been recovered due in part, to infill drilling on less than 5 acre spacing, extensive waterflooding and development since the early 1900s. The bypassed volume of oil within the Cypress reservoirs at Lawrence Field is therefore greater than 60% which is a significant target.

Examination of Cypress cores and detailed geological mapping using geophysical log data show that sandstone body geometries and trends are consistent with deposition in tidally dominated coastal to shallow marine settings in Lawrence Field. The Cypress sandstone can be divided vertically into five distinct intervals separated by thin impermeable shales or shaly sandstones. This package of sandstones can attain a thickness of 60 feet with the thickness of individual intervals averaging 10 feet. The upper four sandstones appear to be tidally derived, each showing an elongated sheet geometry with ridges that trend northeast-southwest. Oil production is predominantly from the middle three sandstones. Also, tightly cemented calcareous intervals, typically less than one foot thick, develop within the sandstones that act as barriers to fluid flow.

The shale to shaly sandstone and calcareous, impermeable barriers form horizontal reservoir compartments within most of the study area. Compartmentalization is also present at a smaller scale where abundant, discontinuous shale layers, one to several laminations thick, form oil trapping compartments that are a fraction of an inch thick. Recognition of these compartments is essential to properly evaluate the recovery potential of the reservoir and to design a reservoir development and management program to effectively drain the compartments.

# **Stratigraphy Cypress Sandstone**

The Cypress Sandstone is a part of the Pope Group in the Chesterian Series that is composed of cycles of mostly siliciclastics punctuated by widespread thin limestones that separate cycles. The Cypress Sandstone is underlain by the Ridenhower Limestone, a widespread limestone that can be correlated across much of the Illinois Basin. The Cypress is directly overlain by the Beech Creek Limestone "Barlow limestone", a thin limestone marker horizon that is a prominent basin wide strata commonly used for constructing contoured structure .maps. The stratigraphic relationships of the Cypress Sandstone with underlying and overlying stata are shown in figure 60. The Cypress Sandstone is a Lower Chesterian strata located above the transition from the Middle Mississippian Valmeyeran carbonates. The Cypress Sandstone on this log shows a typical lower, thick, in part shaly, sandstone, separated from thin upper sandstones by a shale interval. The Beech Creek "Barlow limestone" is easily recognized on geophysical logs and is used in regional mapping. There are approximately ten cycles of siliciclastics alternating with widespread thin limestones in the Chester Series (Figure 61). In total these cycles have a maximum thickness of approximately 1400 feet and are bounded at the base by the Valmeyeran carbonate Series and truncated at the top by the Pennsylvanian System (sub-Absaroka unconformity).. Each cycle is usually less than 100 feet thick and represents between 500,000 and 1 million years of deposition if each cycle is approximately equal.

The siliciclastic intervals of Chesterian cycles are commonly sandstone rich and when structural and stratigraphic conditions are appropriate host petroleum reservoirs. Reservoirs in these sandstones have produced over 60 per cent of the petroleum produced to date in the Illinois Basin (Howard 1991). The Cypress Sandstone is the most widespread and thickest Chesterian age sandstone and has produced over a billion barrels of oil from reservoirs distributed across the Illinois Basin.

# **Cypress Sandstone Paleogeography**

The Chesterian sedimentary section records a complex and cyclical depositional sequence (Figure 61). These ten cycles are made up of sandstone beds bounded by shale and capped by limestone. Locally, thicker sandstones can fill most of the cycle and immediately overlie or truncate an underlying limestone. The cycles are generally less than 100 feet thick although in some areas and in particular cycles, the sandstones alone can exceed a thickness of 100 feet.

The rock record deposited during the Chesterian Series indicates that the Illinois Basin had a low gradient sea floor and a low subsidence rate relative to rates of sedimentation (Figure 62). Water depths were probably quite shallow. Widespread tidal features observed within the sediments indicate that tidal currents had a significant influence on sediment movement within the Basin. The embayed geometry of the entire Basin combined with regional embayments resulting from the dynamics of prograding delta systems may have induced a high tidal range in some regions or possibly across the entire Basin. The thin accommodation space, combined with shallow water depths and active currents (including tidal and storm) caused prograding sediments to be actively reworked and spread laterally rather than vertically. Thin, widespread, discontinuous, and stacked deposits are characteristics of this setting. Relative sea level changes also had a significant effect on the distribution of sediments and the geometry and architecture of sandbodies within the Basin. Northeast to southwest prograding deltas concentrated sands, greater than 100 feet thick, along fairways and into the heart of the Basin as sea level dropped. Incisement and subsequent valley fill during sea level rise complicated the preexisting distribution and geometry of the prograded, regressive sediments.

The paleogeologic map (Figure 62) illustrates an environment where siliciclastics were deposited by a tidally dominated river system. Tidal currents reworked sediments in near shore environments usually orienting sand bodies in a direction perpendicular to the shoreline. Placement of the shoreline shifted through the deposition of Middle Mississippian Chesterian deposits as well as during the Pennsylvanian.

# Cypress Sandstone Reservoirs in ASP Middagh Pilot near the Griggs Lease

The Cypress Sandstone in much of Lawrence Field can be subdivided into as many as five separate, stacked sandstone lenses with a basal shale unit that is commonly overlain by a siltstone interval. The sandstone intervals are designated with letters A, B, C, D, and E. The Cypress is comprised of a series of stacked, depositionally similar primarily siliciclastic units (Figure 63). Sandstone lenses are commonly separated from other sandstone lenses by impermeable intervals composed of shaly sandstones, thinly interbedded shale and sandstone, and in some cases, shale beds. The Cypress Sandstone in this area is a composite of stacked compartments, each compartment being generally 10 feet thick or less. The Griggs 107 contains four sandstone intervals separated by thin intervals of very low permeability siltstones, shales or

interbedded siltstone and shale (Figure 63). The sandstone intervals can be highly porous and permeable with permeabilities exceeding 500 md. The centers of the sandstone lenses contain some of the highest porosity and permeability values. The intervals between sandstone lenses contain very low porosity and permeability values (Figure 63). These low permeability intervals form barriers between reservoir quality sandstones that tend to compartmentalize the sandstone.

A detailed series of cross sections was constructed using Geographix software and were used to correlate the reservoir intervals in the Cypress Sandstone first using over 150 logs in the Middagh pilot area and later in an enlarged region surrounding the pilot in Section 32 T4N R12W (Figure 64). Reservoir modeled isopach maps of Cypress sandstone intervals B, C, D, and E define elongate northeast-southwest oriented sandstone bodies.

Three different but depositionally related reservoir facies have been identified in Cypress sandstone reservoirs in the Griggs lease area as well as other areas of Lawrence Field. The different reservoir facies were observed in core of the middle Cypress Sandstone in the pilot area (Figures 65-68). The three reservoir facies observed in core are 1. a mottled/obscured bedding facies possessing excellent porosity and permeability (Figure 65), consisting of fine grained, poorly sorted sandstone composed of 94% or greater of quartz grains and small amounts of diagenetic clay minerals and feldspar grains; 2. parallel laminated tidal rhythmites (Figures 66 and 67) possessing excellent to good porosity and permeability, consisting of fine grained, well sorted sandstone composed of 90% or greater quartz grains and small amounts of feldspar grains and diagenetic clay minerals; 3. ripple bedded/herringbone facies (Figure 68) possessing good to poor porosity and permeability, consisting of well sorted very fine- fine grained sandstone with laminae of ductile clay sized particles and composed of 85% or greater quartz grains, feldspar grains and laminae of clay sized particles. The most common reservoir facies is composed of ripple bedded, fine-grained sandstone with wispy shale laminations. This facies has been identified in all available core in the Griggs lease and expansion area. Figure 68 is an example of the ripple bedded facies from the Cypress E Interval in the Griggs lease in the pilot area. This example shows the dark wispy, wavy clay laminations that are ubiquitous within this facies. This is the predominant reservoir facies within all the Cypress intervals in this and in the expanded area of study. Herringbone micro cross-bedding such as that observed in the Griggs 106 well at 1416 feet (Figure 68) is also associated with the ripple-bedded facies. An important nonreservoir facies consists of very fine grained sandstone and shale that transition from flaser tolenticular to- wavy bedding (Figure 69). The shale component in this facies reduces porosity and permeability to nearly zero. This transition from wavy through flaser bedding along with cycles of rippled bedding and herringbone bedding are indicators of tidal deposition and these sediments are interpreted as tidal shoal or bar deposits (Grube and Frankie, 1999).

Non-reservoirs facies are commonly observed separating intervals of reservoir quality sandstone. Intervals of calcite cemented sandstone a few inches thick are observed in many reservoir quality Cypress sandstone lenses (Figure 70). The example shown in Figure 70 is typical and lacks porosity and permeability, if these thin intervals are laterally extensive, they may form permeability barriers and cause compartmentalization within Cypress sandstone reservoirs. Another non-reservoir facies representing potential permeability barriers are shown in the flaser interbedded shale and siltstones at the base of the core in Figure 69, and in the siltstone with ripup clast intervals. Tidal couplets observed in the non-reservoir facies of these units are additional diagnostic characteristics of tidal deposition. Another non-reservoir facies include calcite

cemented intervals color coded blue and flaser bedded facies color coded purple. The composite core photograph (Figure 71) shows the possible vertical relationship of these facies in a typical Cypress Sandstone reservoir.

# Reservoir Characterization of Cypress Sandstones in Expanded Region

This project was enlarged from characterization of Cypress Sandstone reservoirs in the Middagh pilot and Griggs lease area in Sec. 32-T4N-R12W to include detailed mapping of individual sandstone lenses in a five square mile area surrounding the Griggs lease Figure 64. Description and facies interpretation of 14 cores and available core measured porosity and permeability data in the expansion area were completed and compared to the type Griggs 107 well in the pilot area. Five square miles immediately adjacent to Sec. 32 T4N R12W in Sec. 5 T3N R12W, Sec. 6 T3N R12W, Sec. 30 T4N R12W, and Sec. 31 T4N R12W were incorporated in the regional study area because expansion to areas near the initial pilot ASP floods would make the best economic use of the established infrastructure. The addition of 790 wells greatly expands the area for reservoir characterization and detailed mapping from one square mile to five square miles. Fourteen additional cores encompassing 750 feet from Cypress Sandstone reservoirs were described, photographed and integrated into facies interpretations.

# **Cypress Sandstone Reservoirs in Expanded Area of Lawrence Field**

Sandstone reservoirs in the Cypress Sandstone in the pilot area are similar to those observed in core in the expansion area and can serve as a general template for those in the expansion area.

A type log from the Baltzell #N-23 well (Figure 72) in the SE quarter of the NW quarter of Section 30, T4N, R12W, shows several stacked sandstone lenses in the Cypress Sandstone in this instance the stacked intervals are A, B, C, D, and E. The Spontaneous Potential trace on the electric logs from the 1940-50s characteristically "amplify" the deflection between the cleaner reservoir sandstone lenses and the shaly sandstone breaks. Very characteristic within the Cypress and most other sandstone bodies within the Mississippian and Pennsylvanian section is a 10 foot genetic thickness tendency of units that is probably a function of accommodation space, and the rates of deposition versus. Subsidence was minimal under the conditions prevailing in the Illinois interior cratonic basin. The sandstone lenses commonly coalesce which may then show up as thicker units. The "10 foot rule" can be a very useful tool for correlating these thinly bedded units in cratonic settings. The individual Cypress sandstone intervals have a lenticular, tidal shoal geometry where each shoal defines discrete reservoir flow units.

Isopach maps of the 50 percent clean sandstone for the Cypress B, C, D, and E intervals were contoured by hand in Sections 19 and 30 T4N R12W in an earlier study. The D and C intervals are among the most laterally continuous of the Cypress sandstone lenses in Lawrence Field. Sandstones units with similar sedimentary features to those in the pilot area and directly correlative to the Cypress units in the Griggs lease area have been interpreted as linear tidal shoals from an earlier study in sections 19 and 30 of T4N R12W, the same township as the Griggs lease.

An example of one of these early hand contoured isopach maps in a portion of the expansion area is shown in (Figure 73). These maps all show a northeast – southwest orientation and are interpreted as stacked tidal ridges. These maps show stacked, compartmentalized sandstone lenses deposited by tidal processes in a coastal setting. Optimal petroleum recovery including

primary, secondary and tertiary requires knowledge of these reservoir compartments. Banked and by-passed oil may remain in compartments due to the drill pattern of production and injection wells. Enhanced oil recovery success requires that production and injection wells penetrate laterally continuous compartments. Correlation of individual compartments is critical.

A series of isopach maps of the five square mile area surrounding the initial Cypress sandstone ASP pilot in the Griggs lease in Section 32 T4N R12W were constructed using the 50 percent clean sandstone normalized Spontaneous Potential curves on geophysical logs for the entire Cypress interval including the B, C, D, and E intervals. An isopach map of the total middle Cypress, 50% clean normalized SP sandstone thickness map of the study area is shown in Figure 74. This map combines sandstones in the B, C, D, and E intervals and has a contour interval of five feet. These units are all interpreted to be tidal shoal deposits that are found in modern high tidal range settings. The elongated, shoal geometry are oriented in a northeast-southwest direction. The basal Cypress A interval appears to be a deltaic depositional facies which is less permeable and therefore is, more commonly, non-productive. Thickness maps of the Cypress B interval and D intervals are shown in Figures 75 and 76. These isopach maps were modeled using GeoGraphix mapping software and have a contour interval of three feet. These maps illustrate sandstone lense geometries and a consistent northeast-southwest orientation associated with tidally influenced shoal deposition. Correlation of individual intervals can be difficult as they rapidly pinch and swell within the Lawrence Field Cypress intervals. Multiple iterations are necessary in order to assure that cross-correlations are minimized. If interval geometries' are "amoebic" in geometry rather than characterizing geometries expected from a given environment of deposition, then correlations are likely incorrect. This can play a critical role in defining flow units in compartmentalized reservoirs and the implementation of any recovery program for an oil field, particularly secondary and tertiary programs. Individual flow units must have an injector(s) and producer(s) in order to recover oil after primary recovery.

Reservoir and non-reservoir facies observed and described in core in the pilot area are also observed in core in the expansion area. Figure 77 shows the location of a detailed cross section (Figure 78) in Section 30 T4N R12W indicating by color code the depths of various reservoir and non-reservoir facies. The reservoir facies observed in core in Section 30 T4N R12W are the same as those observed in the Griggs lease and the same lithofacies color coded system was used. The cross section also has core measured permeability plotted on a track to the right of the facies color code. The ripple bedded facies is the least porous and permeable of the three reservoir facies and is color coded green. It also exhibits a high degree of variability in porosity and permeability ranging from 18% to 5% porosity and 150md – 10md permeability. The rightmost track in Figure 78 contains a graph of core measured permeability in red, the colorcoded track corresponds to the three reservoir and two non-reservoir facies in the legend in Figure 71. The mottled/obscurely bedded facies indicated by a red bar possesses the best porosity and permeability values, the parallel/sub parallel bedded tidal rhythmites also possess very good porosity and permeability are indicated by yellow bars, the ripple bedded facies possessing good to poor porosity and permeability is indicated on the cross section and in core by green bars. The non-reservoir flaser/wavy/lenticular bedding facies is indicated by a purple bar and the nonreservoir calcite cemented sandstone facies is indicated by a light blue bar. A legend describing the color code scheme for the three reservoir facies and the two non-reservoir facies is illustrated in Figure 78. Most facies are observed in all cored intervals of the Cypress Sandstone. The cross section in Figure 78 shows lateral continuity in some of the calcite cemented intervals as well as

continuity in some of the reservoir facies. The mottled/obscurely bedded facies is the least common of the reservoir facies in this cross section. The same facies with the same diagnostic sedimentary structures are present is all core of the Cypress Sandstone in the study area of Lawrence Field.

Figure 79 is a regional cross section using cored wells to connect the pilot area in the Griggs lease in Sec 32 T4N R12W with the heavily cored area in Sec 30 T4N R12W. Core measured permeability is graphed in red on the right track of each log. The Barlow Limestone is the datum for the cross section. The Cypress A, B, C, D, and E intervals are correlated on the cross section and show a high degree of correlation with intervals identified in Sec 30 T4N R12W with those identified on the type Griggs 107 well log API 121013125200. Core measured permeability graphs show stacked sandstone lenses similar to those in the Griggs 107 well in Figure 63. The cross section also shows up to three intervals of calcite cemented sandstones within the Cypress Formation and that these intervals likely form permeability barriers in much of the expansion area. The thickest calcite cemented interval is 36 inches in the 121012760800 well shown in Figure 79. The sedimentary structures observed, described and documented in these core correspond to those described in core from the Griggs lease in the pilot area. Deposition by tidal processes in the accumulation of stacked sandstone lenses composed of fine grained to very fine grained sandstone lenses separated by flaser bedded intervals composed of interbedded shale and very fine grained sandstone or calcite cemented sandstone. The most commonly observed reservoir quality facies in the expansion area contains parallel laminated tidal rhythmites and ripple laminated facies.

### **Petrographic Analysis Cypress Sandstone Reservoirs**

X-ray diffraction analyzes of the bulk mineral and clay mineral fractions of 98 Cypress Sandstone samples from eleven cored wells were completed. Ouartz is the most common mineral found in Cypress reservoir sandstones and usually makes up more than 90 percent of samples. Calcite cemented intervals contain less than 90 percent quartz, pores in these samples are filled with 10 to 20 percent iron rich calcite. However, carbonates are usually a minor component of samples at less than 1 percent. Clay minerals range from 1 to 8 percent in most sandstone samples. Potassium and plagioclase feldspars are also minor components of reservoir sandstones usually making up 1 to 4 percent of most samples. Trace amounts of pyrite/marcasite were detected in some samples usually less than 1 percent. Siderite was only rarely detected and when present was 1 percent or less. The results of X-ray diffraction analyses and the abundance of detected minerals for samples from the Griggs 108 well are shown in Figure 80. Analyses for the clay mineral fraction for samples from the Griggs 108 well are shown in Figure 81. The clay mineral suite in these samples consists of Fe-rich chlorite, kaolinite, illite and minor amounts of mixed layered illite/smectite. Clay minerals in sandstone samples are diagenetic and formed as the result of dissolution of feldspar grains. Diagenetic clay minerals commonly occur in pores where they may react with reservoir fluids.

Petrographic examination of thin sections, SEM/EDX and X-ray diffraction analyses of Cypress samples from the ripple bedded reservoir sandstone facies shows that these sandstones are very fine-grained and are highly cemented by quartz overgrowths as shown by the thin sections in Figures 82 and 83 and the Scanning Electron Photomicrographs in Figure 84. Thin section point count analyses and XRD mineralogical analyses show that most Cypress Sandstone samples are composed of approximately 95 percent quartz, less than 1 percent K-feldspar, less than 3%

plagioclase feldspar, less than 2% clay minerals and less than 1% other minerals. The Cypress Sandstone samples in Figure 82 are from the Plains Illinois Griggs 107 well. A common feature of the ripple bedded facies is porous laminae alternating with finer-grained non porous laminae (Figure 82. Styolitic partings are common in this facies and separate non porous tightly cemented very fine grained sandstone from porous intervals. The most common diagenetic clay mineral in the ripple-bedded facies is Fe-rich chlorite as shown in Figures 84 and 85. Numerous sand grains in the Scanning electron photomicrographs are coated by chlorite. Several stages of Fe-rich chlorite precipitation are evident in this sample. The bottom left photomicrograph (Figure 84) shows quartz overgrowth precipitated over chlorite clay minerals. The bottom right photograph shows a grain completely coated by chlorite and an area occupied by a degraded feldspar grain with diagenetic chlorite and illite.

X-ray diffraction analysis shows that most Cypress reservoir samples with good core measured porosity and permeability values contain less than 2 percent clay minerals and less than 4 percent feldspars and have very high quartz content, thin section and Scanning electron microscopy analysis shows that many pores are partially lined with diagenetic clay minerals that are likely derived from degraded feldspar grains. This complicates the mineralogical associations within the sandstone and is a factor in the response of these sandstones to fluids introduced for reservoir treatments in conjunction with Enhanced Oil Recovery. The degradation and dissolution of feldspars has enhanced porosity and permeability but has also lined many pores with diagenetic clay minerals such as Fe-rich chlorite, kaolinite illite, and mixed layered illite-smectite.

X-ray diffraction and thin section analysis of the bioturbated reservoir facies shows amounts of quartz, feldspar, and clay minerals similar to those measured in samples from the ripple-bedded facies of 95% or greater quartz, 3 % or less feldspar and 2% or less clay minerals. Thin section examination shows (Figures 86 and 87) that samples from this facies are less tightly cemented by quartz overgrowths, are more porous, possess greater amounts of intergranular porosity and are more poorly sorted than samples from the ripple – bedded facies (Figures 86, 87, 88). The mineralogical difference between the two facies is in the clay mineral suite. The clay minerals in the bioturbated facies consists primarily of kaolinite, with lesser amounts of illite and Fechlorite. Some XRD analyses of bioturbated samples contained no mixed layered illite/smectite. The predominant clay mineral in this facies is kaolinite which can be an abundant pore filling and pore lining mineral (Figures 86, 87, 88, 89). PIMA and XRD analyses of Cypress Sandstone samples show that the kaolinite clay minerals are diagenetic, and well crystallized. The kaolinite in the Cypress Sandstone occurs as vermicular or book-like stacks of plates. SEM/EDX analyses confirm the vermicular and booklet morphology findings.

Calcite cemented intervals a few inches thick are found in some Cypress Sandstone lenses and can be useful marker horizons for correlating geophysical logs (Figures 70 and 71). XRD analysis of these intervals show that they contain 80 percent or less quartz and 17 to 20 percent calcite. Thin sections of calcite cemented sandstone intervals show that intergranular porosity of approximately 18 percent has been filled by iron rich carbonate cement (Figure 90). The photomicrograph in Figure 90 shows calcite cement stained dark navy blue indicating that the calcite is iron rich because the thin section was stained with a mixture of alizarine red containing potassium ferricyanide. These carbonate cemented intervals have little to no porosity and permeability and where they are laterally extensive can form permeability barriers.

### **Conclusions**

Three different reservoir facies were identified in Cypress Sandstone reservoirs in cores in the pilot area in Sec. 32-T4N-R12W in Lawrence Field as well as in examination of cores in an expansion area of five square miles. Interpretation of sedimentary structures in cores, analysis of porosity and permeability data and analysis of petrographic data including XRD analyses, thin section analyses, and SEM/EDX analyses show distinctive characteristics of three different reservoir facies with different flow unit characteristics within the Cypress Sandstone. The most common reservoir facies consists of ripple- bedded fine- grained to very fine- grained sandstone with occasional occurrences of herringbone cross bedding and tidal couplets. The ripple-bedded reservoir facies has core measured porosity values ranging from 16% to 19% and core measured permeability values most commonly in the 100 md. range. A second less common reservoir facies consists of obscurely bedded, bioturbated, poorly sorted, fine-grained sandstone. Core measured porosity commonly exceeds 20% and permeabilities are commonly greater than 200 md. in the bioturbated facies. This facies has the highest core measured porosity and permeability values observed in Cypress sandstone reservoirs in the study area. A tidally influenced depositional system has introduced a high level of reservoir compartmentalization in Cypress reservoirs. Petrographic examination also shows differences between these two reservoir facies that increase reservoir complexity and introduce production obstacles on a microscopic scale. Both reservoir facies contain clay mineral suites that can be highly reactive to fluids introduced for enhanced oil recovery treatments. Although the volume of clay minerals is relatively low they are most commonly located in pores where they are most likely to come in contact with fluids introduced for treatments. Because these reservoirs are located in close proximity to one another Fe-rich chlorite and to a lesser degree illite and mixed layered illite/smectite should be taken into consideration when developing formulations for ASP treatments.

While compartmentalization is evident in all the targeted sandstones, some sandstones exhibit a directional orientation that must be considered in reservoir development for the most effective recovery of petroleum. Effective implementation of flooding in pilot areas should take into account compartment orientation that is dictated by depositional trends and type and location of permeability barriers. The more promising and connected reservoirs in the pilot area appear to be in the Pennsylvanian age Bridgeport B and some of the Cypress intervals contain continuous sandstones. Remaining oil saturation is also a key factor in successful implementation of ASP flood technology. Areas swept by previous polymer and marafloods have expanded beyond those originally anticipated. As a result, oil saturation in pilot areas may be less than previously calculated. Knowledge and understanding of the impact of previous, waterfloods, marafloods and polymer floods is very important in determining the amount of recoverable oil in target reservoirs and will be strongly considered in determining areas for expansion of the ASP flood. Reservoir characterization of Cypress sandstone lenses show that these sandstones contain intervals of highly variable vertical permeability. Interpretation of the Cypress Sandstone interval in cross sections in Section 32-T4N-R12W suggest that permeability barriers are subtlety reflected on geophysical logs but, likely play a major role in compartmentalization of these reservoirs. Intervals with very high permeability may be susceptible to channeling The Mississippian Cypress Sandstone is more complexly compartmentalized than the Bridgeport Sandstone. Mineralogy of the pores is complex with diagenetic clay minerals including Fe-rich chlorite, illite, mixed-layered illite/smectite and kaolinite playing a major role in the response to

fluids introduced during drilling and treatment. Although, the major component is quartz as both a grain composition and cementing agent it is not the major component in pore mineralogy.

### **Geocellular Modeling**

Reservoirs within Lawrence Field are characterized as being highly compartmentalized resulting in multiple flow unit configurations. In order to help characterize such complex systems and visualize the complexities, a strategy has been developed to utilize a conceptual geologic model to guide the construction of a geocellular model of the reservoir architecture. The process combines traditional methods along with geostatistical methods. This combined process creates a beneficial check and balance loop where the geocellular and the geological models should complement each other. Cases where the resulting models show significant discrepancies must be resolved either by reinterpreting the geologic model or resolving input errors to the numerical model. The geostatistically generated geologic model (porosity, permeability, thickness, geometry, and depth) is also used as input to the reservoir simulation model. The more consistent the geostatistical model is to the actual geology, the more relevant the simulation model results will be and the greater the likelihood of success of an EOR project.

Prior to creating a geocellular model, a conceptual geologic model is generally completed to provide guidance for the geocellular model. The geological model defines a modeling datum, structure, reservoir and non-reservoir characteristics including facies interpretations (lithology, depositional environment) and thicknesses. Geometry, particularly of reservoir facies compartments is essential. Well files are examined for continuity and consistency of data for modeling which includes wireline logs (in digitized format) and core with core analyses, particularly porosity and permeability.

The geocellular model area at Lawrence Field is located in the north half of section 32 where the Rex Energy ASP EOR pilots are located (Figure 91). Two separate models were generated, one for the Cypress Sandstone and one for the Bridgeport B Sandstone. The workflow used for generating these models was developed during the course of preparing models for other EOR projects within the Illinois Basin and employed the geostatistical geologic modeling software Isatis® by Geovariance Corporation.

### **Data Selection and Normalization**

In mature basins like the Illinois Basin, a robust model of reservoir architecture requires a larger data distribution than that offered by the available core analysis data or porosity logs. As a result, the modeling methodology developed for past projects (MGSC, 2009; Frailey et al., 2012a; Frailey et al., 2012b) typically relies on the spontaneous potential (SP) log as an indicator of reservoir quality largely because of its availability, but also because of its relative correlation with permeability.

First, the SP logs were normalized in order to produce a curve or value that was an approximate indicator of the percentage of sandstone relative to shale (Figure 92). The normalization process reduces well-to-well SP variation that results from fluid chemistry (electrical activity) and other borehole conditions. At the conceptual level, normalizing an SP log is straightforward. A 10-20 foot thick, shale-free, brine-saturated sandstone represents the maximum SP (SPmax) while a pure shale interval represents the minimum SP (SPMin). These two values are then used with the following equation to normalize SP:

$$SP_{norm} = \frac{SP_{observed} - SP_{\min}}{SP_{\max} - SP_{\min}} \times -100$$

However, application is considerably more complex. It is rare to find a sandstone that is composed of pure sand everywhere in a field, especially for fields in the Illinois Basin. As a result, normalization frequently requires a modified approach. If a sandstone that is consistently free of shale is not available, then a sandstone that has a consistent SP log signature throughout the field can be used as long as some approximated percentage of sandstone to shale can be assigned to the formation. For this study, the Buchanan sandstone, usually directly above the Barlow limestone, was found to have the most consistent log signature in the field. After a statistical analysis comparing the Buchanan to several other formations present to determine its relative percentage of sandstone versus shale, the Buchanan was assigned a normalized SP value of 78.4%. This resulted in modifying the equation above like so:

$$SP_{norm} = \frac{SP_{observed} - SP_{\min}}{SP_{\max} - SP_{\min}} \times -78.4$$

The shale used was the Frailey shale located between the Barlow limestone and Buchanan sandstone. The important aspect to consider is that for the purpose of this study, the normalization does not necessarily represent an absolute ratio of the sandstone/shale composition of the formation but instead is designed to create a consistent scale for comparing the reservoir quality of the formations between wells. The actual values of the normalized SP are relative to the field.

For the Cypress Sandstone, geocellular models were generated using the SP logs from wells drilled mostly on ten acre spacing during the 1950s. These logs were used for modeling because of the consistency of logging parameters and drilling program, The normalized SP data values were generated from the SP traces and then converted into the desired petrophysical properties utilizing transform equations relating permeability and porosity values to the normalized SP values, which is described later. For the Bridgeport B sandstone, however, a different approach was taken after creating a model using the previous methods. As the study area had an abundance of modern logs compared to other fields in the Basin, there was a motivation to try to combine the data sets. A number of methods were employed to combine the data sets, including using collocated co-kriging to correlate normalized SP and cross plotted porosity from the modern logs. The best results were generated through simple regression of normalized SP and cross plotted porosity from adjacent wells to create a synthetic porosity curve for each well.

### **Grid and Discretization**

The grids for the two formations covered roughly the same area. Both grids centered on the northern half of section, 32 T 4N R 12W, in Lawrence county. The model boundaries were centered on the area of the ASP EOR pilots. The Cypress sandstone grid consisted of cells with  $50 \times 50$  foot horizontal spacing with 82 cells in the X direction and 62 cells in the Y direction, for total surface area coverage of  $12.71 \times 10^6$  square feet or 291.8 acres. The Bridgeport B sandstone grid was expanded slightly to better cover all areas possibly influenced by the ASP pilots as well as refined to better capture heterogeneity of the reservoir. The Bridgeport B sandstone grid consisted of cells with  $25 \times 25$  foot horizontal spacing with 188 cells in the X

direction and 123 cells in the Y direction, for total surface area coverage of  $14.45 \times 10^6$  square feet or 331.8 acres.

Prior to modeling, the structure of the formations was modeled and removed so that the data reverted as close to their original position during deposition as possible. This required selecting appropriate stratigraphic origins. For the Cypress sandstone, the Barlow limestone, which is usually 30-50 feet above the top of the Cypress sandstone, was used. For the Bridgeport B sandstone, a thin, unnamed coal directly above the sandstone was used. The effect of using a different stratigraphic origin on the geocellular model was investigated for the Bridgeport B sandstone, as shown in Figure 93. The stratigraphic origin also served as the origin of the grids that were used during the modeling process. Both grids enclosed a constant vertical thickness and used a constant thickness of 1 foot for each layer. The Cypress sandstone model used a thickness of 116 feet, resulting in a total volume of  $1474 \times 10^6$  cubic feet, while the Bridgeport B sandstone model used a thickness of 46 feet, resulting in a total volume of  $2659 \times 10^6$  cubic feet. It is important to note that it is not suggested that either formation had a constant thickness equal to that of the respective model as the models were designed so that the vertical boundary was equal in length to the thickest interval of each formation and thus both models enclosed the entire volume of the formation of interest within the study area.

### **Geostatistical Analysis and Simulation**

After the data set had been assembled and processed, geostatistical techniques were applied to quantify the geometry and distribution of petrophysical properties. This consisted of calculating semivariograms and semivariogram maps from the data set. The semivariogram map of the Cypress sandstone indicated a trend of northeast-southwest direction. The model fitted to the semivariogram had a range of 2700 feet in the N50° direction, 600 feet in the N140° direction, and 17 feet in the vertical direction. The Cypress model used a spherical structure and had a sill of 1. The semivariogram map of the Bridgeport B sandstone indicated a trend of northeast-southwest direction. The model fitted to the semivariogram had a range of 2400 feet in the N80° direction, 1200 feet in the N170° direction, and 38 feet in the vertical direction. The Bridgeport B model used an exponential structure and had a sill of 1. The semivariogram maps and semivariograms for the two formations are shown in Figure 94.

The semivariograms were used to simulate the desired properties through the turning band method (Matherhorn, 1973; Journel, 1974) to generate a large number of unique, equiprobable realizations. For both the Cypress and Bridgeport B sandstone models, 100 realizations using 1200 turning bands were generated. The realizations were then ordered from lowest to highest distribution of normalized SP or porosity with the median ( $P_{50}$ ) simulation serving as the most representative of the reservoir architecture. All images of the models shown in this report are taken from the  $P_{50}$  simulation.

### **Model Property Transformation**

After an acceptable geocellular model had been constructed, the models were populated with petrophysical properties using transform equations. For the Cypress sandstone model, the simulation-generated normalized SP values had to be converted into permeability and porosity for geological modeling and for use in reservoir simulation. This was accomplished using transform equations derived from regression analysis. Permeability and porosity measurements

from core analysis were plotted against normalized SP log data and a curve was fitted to the data. Figure 95 contains the plots and resulting transform equation for the Cypress sandstone model. A different approach was employed for the final geocellular model of the Bridgeport B sandstone for the reasons described earlier. For the Bridgeport B sandstone, the normalized SP log data was plotted against the cross plotted porosity log data from adjacent wells with modern logs. A curve was fitted to this data and the resulting equation of the curve was used to convert all normalized SP data into porosity data for use in simulation. Figure 96 contains the plots and resulting transformation for the Bridgeport B sandstone model. Once the geocellular model had been finalized, the cross plotted porosity curve data was plotted against measurements of porosity and permeability from core analysis and a curve fitted to the data much like the process for converting normalized SP into porosity and permeability. The effect of combining the newer data with the older data is demonstrated in Figure 97.

### **Validation and Post-Processing**

The average permeability and porosity of the Cypress sandstone model was 25 md and 17% respectively. When non-reservoir portions were filtered out, the average permeability and porosity rose to 51 md and 18%. The maximum and minimum of permeability and porosity was from 8 to 126 md and from 16% to 21% respectively. The average permeability and porosity of the Bridgeport B sandstone model was 30.7 md and 14% respectively. When non-reservoir portions were filtered out, the average permeability and porosity rose to 38 md and 15%. The maximum and minimum of permeability and porosity was from 7 to 390 md and from 11% to 24% respectively. The final Bridgeport B geocellular model was upscaled and exported for reservoir simulation purposes.

After validating the statistical model with the geological model and post processing, the finalized geocellular models were used to examine the reservoir architecture to better understand the implications for EOR activities such as ASP. As shown in Figures 98, 99, and 100, the Cypress sandstone model reveals that the reservoir is composed of thin, elongated pods of sandstone that coalesce and merge to form larger flow units within the field. The different pods may have thin shale units that act as baffles or barriers to flow. The figures illustrate how the complicated geometry of the Cypress sandstone can result in unexpected results during EOR activities. For example, an injector located at a given pod may not influence a producing well adjacent to it but actually a different well located further away. The reservoir portion of the Bridgeport B model shown in Figures 101, 102, 103, 104, and 105, is less continuous in the study area compared to the more widely distributed Cypress sandstone reservoir. However, the model reveals that within the main body of the sandstone, there is considerable variation of reservoir quality leading to internal compartmentalization. The modeling results underline the need to perform careful characterization of reservoir architecture for EOR projects in these types of reservoirs in order to increase the chance of success.

### **Bridgeport Channel Fill Reservoir Model**

In addition to the geocellular models of the Cypress and Bridgeport B in section 32 of T 4N R 12W, two dimensional models of the permeability and porosity of the Bridgeport channel-fill reservoir in Section 5 were also constructed, the location of which are shown in Figure 106. The reservoir architecture of the formation in this area has lower heterogeneity and complexity, a less rigorous approach was required. This consisted of using linear-interpolation methods to estimate

the permeability and porosity between wells using the abundant core analysis data available. The resulting cross sections, shown in Figures 107 and 108, demonstrate that the Bridgeport channel fill reservoir sandstone in this area has a much different architecture than the Griggs-Middagh area to the north in section 32, which is believe to be the result of different depositonal systems. The high permeabilities and porosities result in improved communication between wells in this area. However, the variation in the permeability and porosity distribution shown in the cross sections demonstrate there is still a degree of compartmentalization in these formations that could result in channelized flow which may leave zones of by passed oil. High permeability thief zones shown in this example must be considered and incorporated in the planning and development of EOR flood projects.

### **Reservoir Simulation Modeling**

Landmark's VIP was used to estimate the enhanced oil recovery of ASP on the geocellular model of the Bridgeport formation. The dimensioned number of model cells was 47 x 31 x 27. Each cell size was 100 ft x 100 ft x 2 ft. The northern and southern part and the upper and lower layers of the geocellular model were considered unproductive; a 15% porosity cutoff was used in VIP to remove this part of the model for reservoir simulation. Of the 33,511 total cells, 9,985 were active as a result of the porosity cutoff. No water-oil contact was placed in the model. The OOIP was 3,918 Mstb.

VIP does not offer ASP modeling capability, but does offer polymer EOR; however, the different types of data were not available to complete this type of modeling. Therefore an incremental EOR was used based on injected water with viscosity assigned at a value similar to polymer (10 cp). The ASP part of the EOR estimate was based on pilot performance at Rex Energy's Lawrence field tests.

#### **Relative Permeability**

The depth, net thickness, porosity, and permeability for each model were included in the geocellular model. Net thickness was assumed to be equal to gross thickness. Relative permeability was the only rock property added to the reservoir model; however, no relative permeability data specific to the Bridgeport in Lawrence field were available. The end points of the oil-water and gas-oil relative permeability curve were selected based on general Basin observations and published waterflooding information.

Irreducible water saturation of 35% was selected based on historical observations from Illinois State Geological Survey staff. Residual oil saturation to gas and water of 18 and 25%, respectively, was selected based on numerous relative permeability data sets from Honarpour et al. (1986). The residual or trapped gas saturation of 10% was based on Craig's (1993) data collection of minimum or trapped gas saturation in the presence of a waterflood. Craig's reported trapped gas saturation data ranged from about 2 to 20%.

The relative permeability to oil at irreducible water was selected as 0.8, and the relative permeability to water at residual oil was selected as 0.3. The gas relative permeability at the irreducible water saturation was 0.9. These relative permeability values use the absolute permeability as a base. A Corey exponent of 3.0 was used for each of the relative permeability data sets.

### Fluid Properties

Crude oil, associated (hydrocarbon) gas, CO2, and water properties were required. The water properties are constant. The water density, viscosity, and formation volume factors were 1.1 g/cm3 (69 lbm/ft3), 0.8 mPa  $\cdot$  s, and 1.01 rb/stb, respectively. Water and rock compressibility of  $2.1 \times 10$ –5 and  $3.4 \times 10$ –5 kPa ( $3 \times 10$ -6 and  $5 \times 10$ -6 psi-1), respectively, were used.

No specific PVT data were available for this study. Consequently, the hydrocarbon fluid properties were defined using a five-component Peng-Robinson equation of state (EOS) which has been previously used for Illinois Basin oilfield studies. Published data supported these fluid properties generated by this EOS (Sims, 1993). The Pederson oil viscosity correlation was used.

#### Well locations

The model's wells were completed in all layers. Historically, numerous wells were within the area defined by the geologic model. However, only those completed in the Bridgeport and were produced for a relatively significant period of time were included in the model.

### **Well Configuration**

Wells were simulated with a maximum rate. Production wells had a minimum bottom-hole flowing pressure constraint and injectors had a maximum bottom-hole injection pressure. As such wells attempted to produce or inject the specified constant rate while honoring the specified bottom-hole flowing pressure. For producing wells, if the bottom-hole flowing pressure equaled the minimum specified bottom-hole flowing pressure, the wells' production rate fell below the maximum specified production rate. For injection, if the bottom-hole injection pressure equaled the maximum specified bottom-hole injection pressure, the wells' injection rate fell below the maximum specified injection rate.

### **Simulation Settings**

The model was run with IMPES (implicit pressure, explicit saturation). A minimum time step of 0.01 days was allowed; maximum was 100 days. A maximum pressure change 2,068 kPa (300 psia) was used. Maximum saturation and composition changes of 0.1 were used.

### **Modeling Scenarios**

A rigorous history match of the historical production and injection data was not attempted. Primary production was simulated for 25 years at which time pressure and oil rate were relatively low. At this time 40 years of waterflooding started at which time water cut exceeded 99% and oil rate was low. An east-west cross-section of oil saturation is shown (Figure 109) through the center of the sand and the end of primary and waterflooding. Throughout primary production solution gas is liberated. By the end of primary, significant gas saturation is at the top of the formation and oil saturation is near the base. During the waterflood period, water more effectively displaces oil from the bottom of the formation and higher oil saturations are near the top of the formation (Figure 110).

Total oil recovery was 48.7% (Figure 111). The oil recovery during primary was 31.5% and during waterflooding was 17.2%. Total recovery is consistent with Mast and Howard (1991) estimate of 48%; however, they reported that primary was about 24% and waterflood was another 24%.

If ASP data and model were available, ASP scenarios would have been simulated starting at the end of combined 65 years of primary and waterflood production periods. To estimate the incremental oil recovery effect of polymer only, the primary and waterflood scenarios with water viscosity of the model increased to 10 cp. This assignment of water viscosity includes in situ reservoir water and water injection. During primary there is no mobile water, so this has no effect. The viscous "water" injection during the waterflood period was used to estimate the incremental oil production over the waterflood (with 0.8 cp water). This resulted in an additional 2% oil recovery over about 12 years (Figure 111).

This incremental oil production was combined with the peak oil production and cumulative production reported by Rex Energy to estimate the ASP EOR of 470 Mstb or 15.1% of OOIP (Figure 111). OOIP in the model is 3.12 mm STB.

# **Field Operations**

Rex Energy Corporation is reporting a positive response on its ASP Middagh pilot project in the Pennsylvanian Bridgeport B sandstone reservoir at Lawrence Field. Oil response in the 15 acre, 18 well flood has continued to show an increase in oil cut from 1% to 12%. Total pattern production increased from 16 BOPD and stabilized at a range of 65-75 BOPD in the last three months of 2011. Peak production rose to 100 + BOPD. Oil cut in the pilot increased for 1.0% to ~ 12.0% with an individual well showing oil cuts greater than 20%. A second, 58 acre pilot (Perkins-Smith) adjacent to and likely in communication with the Middagh pilot has been initiated. Preliminary brine injection has been implemented and ASP injection commenced in June 2012. Response is expected by mid-2013 with peak recovery expected by late 2013.

Rex Energy is projecting full scale expansion with the next step of development being a 351 acre project scheduled to begin in mid-2013. Preliminary development has been completed in the Delta Unit area located in the south half of section 32, T4N, R12W and ASP injection in this unit is scheduled to begin during the fourth quarter of 2013.

# Assessment of ASP EOR Potential in Sandstone Petroleum Reservoirs in the Illinois Basin

A series of maps with Pennsylvanian and Chesterian age producing well color coded according to producing horizon are included in Appendix A. These maps include the 25 fields in Illinois with the most production from these reservoirs and are the most likely locations for ASP flood candidates in the Illinois basin. These maps are arranged alphabetically by field name.

### **Assessment of Pennsylvanian Sandstone Reservoirs**

There are numerous opportunities for Alkaline Surfactant Polymer floods in both Pennsylvanian age reservoirs similar to those found in the Bridgeport sandstones as well as Chesterian age sandstone reservoirs similar to those found in the Cypress Sandstone in Lawrence Field. There are many shallow sandstone reservoirs with limited or depleted pressure in the Illinois Basin that are better suited for ASP than for CO<sub>2</sub> enhanced recovery techniques. Most oil fields in the Illinois basin are candidates for ASP flooding as a tertiary recovery technique.

Pennsylvanian age sandstone reservoirs are shown in Figure 112. Most Pennsylvanian sandstone production is located around the perimeter of the Illinois Basin and approximately 75 percent of Pennsylvanian production in the Illinois Basin is associated with the LaSalle Anticlinal trend, the same trend as Lawrence Field. Environments of deposition in most Pennsylvanian reservoirs can be attributed to channel fill or fluvial to deltaic deposition with characteristics similar to those found in the Bridgeport B in Lawrence Field. Tidally influenced deposition of Pennsylvanian aged siliciclastics including tidal couplets have been observed and described by Kvale 1991. Approximately 13 percent of the oil produced to date in the Illinois Basin is attributed to Pennsylvanian sandstone reservoirs (Howard, 1991). Pennsylvanian reservoirs are among the shallowest and youngest found in the Illinois Basin ranging in depth from 200 to approximately 1000 feet. Pennsylvanian oils are generally good quality with gravities of 34 API or higher. Many Pennsylvanian reservoirs have been successfully waterflooded including those along the LaSalle Anticlinal trend in Lawrence Field. This indicates that reservoir pressure has been maintained resulting in conditions that may be well suited for implementation of ASP technology. These reservoirs also have relatively high porosity and permeability usually over 18 percent porosity and permeability ranging from 100 to over 1,000 md equivalent to those found in the channel fill Bridgeport B found in Section 5 T3N R12W or the tidally influence deltaic sandstone deposits located in Section 32 T4N R12W.

Additionally, many Pennsylvanian sandstone reservoirs are well suited for application of ASP flood technology because their reservoir geometries can be reliably mapped using available geophysical logs of several different vintages. One of the most important factors in successful implementation of an ASP flood project is knowledge of the limits and boundaries of individual lenses of reservoir sandstones. This knowledge is needed to design effective well injection patterns that will allow accurate calculations of the volume of fluids needed for injection as well as the placement of injection wells needed for an efficient sweep of the remaining oil in place. Economic success of ASP flood technology requires detailed knowledge of reservoir geometry, location of reservoir boundaries, location of flow units and potential thief zones within the reservoir, oil saturation, oil composition, composition of reservoir fluids, and the mineralogy of the reservoir sandstone to determine if there will be adverse reactions to injected ASP fluids.

### **Assessment of Chesterian and Cypress Sandstone Reservoirs**

Most mature oil reservoirs in the Illinois Basin are found in sandstones in the Middle Mississippian Chesterian Series. The location of wells producing from Chesterian sandstone reservoirs is shown in Figure 113 where Chesterian wells are highlighted in blue. According to (Howard, 1991) 60 percent of the oil produced to date in the Illinois Basin is from sandstones in the ten cyclical siliciclastics alternating with widespread thin limestones that comprise the Chesterian Series. These sandstone reservoirs are relatively shallow, occurring at depths of 3,000 feet or less and usually have characteristics similar to those found in Cypress Sandstones in Lawrence Field. The Cypress Sandstone is the most widespread sandstone strata in the Chesterian Series as well as the most oil productive strata in the Illinois Basin with production exceeding a billion barrels of oil to date. Although the Cypress is a mature play, field studies indicate that underdeveloped petroleum reserves can be identified through application of detailed reservoir characterization. The widespread character of the sandstones and the maturity of the oilfields are elements that show excellent additional potential for tertiary oil recovery in particular that ASP technology can be broadly applied to Cypress Sandstone reservoirs as well as to most other sandstone reservoirs in the Chesterian Series.

The regional Cypress Sandstone architecture was established by constructing a Cypress net sandstone thickness map (Figure 114). This map shows significant sandstone depositional trends concentrated in and aligned with the present structural low of the Basin. The dominant trend occurs as a band of sandstone that is approximately 30 miles wide, has a net sandstone thickness that exceeds 150 feet and is aligned northeast-southwest through the southeastern part of Illinois. The thick sandstone packages in the Illinois Basin are relatively undercharged.

Cypress Sandstone reservoir architecture at many fields is characterized by multiple sandstone lenses that are vertically stacked or shingled. Each lense is commonly less than 10 feet thick, with the overall stacked thickness ranging from less than 10 feet to over 40 feet. These sandstones commonly form as linear ridges, oriented northeast-southwest and are compartmentalized. The linear sandstone ridges are analogous to modern-day tidal shoals. The more continuous, channel-like sandstones that exceed a thickness of 100 feet rarely produce petroleum. Successful exploration and development, and implementation of secondary and tertiary recovery programs in these compartmentalized reservoirs requires a thorough understanding of reservoir models.

The focus of the examples in this report in the Tamaroa and Richview Fields (Figure 115) is on the thin, stacked, tidally disbursed sands that form stacked sandstone reservoirs in the Cypress Sandstone and are similar to Cypress sandstone reservoirs found in Lawrence Field. Significant to an understanding of the Cypress depositional system, is a widespread interval that commonly contains thin red, green or variegated beds and a rare thin coal or pebble conglomerate. This interval occurs within the shale interval between the lower thick sandstone and the thin upper sandstone (Figure 60). It is apparent that sea level dropped at the point where the red beds are found and subaerial exposure of most, if not the entire Basin resulted. Erosion and valley incisement resulted from this event and as sea level rose, thick sand packages filled portions of these eroded valleys. These transgressive sands, located in the lower and middle Cypress, are juxtapose to the older and unrelated regressive Cypress sands.

A net sandstone thickness map of the Cypress Formation shows major fairways of thick sandstone in the central portion of the Illinois Basin (Figure 116). Several thick sandstone fairways can be identified on the map. The northeast - southwest sandstone belts, in general, are 6 to 15 miles wide and 50 to 150 miles long. The most common spontaneous potential (SP) electric log response in the thick Cypress Sandstone fairways is blocky and massive with a sharp base and top. Thickness of these sandstones can exceed 120 feet (Figure 116). Wells that offset these thick sandstones can thin gradually, change to multiple, thinner, stacked sandstones separated by shales or thin or even disappear abruptly along the edges of the sandstone belts.

Massive Cypress sandstones, including those within closed structures, are rarely productive, although thin upper Cypress sandstones that overlie the massive sandstone may be productive. Few reservoirs are located within the thick sandstone fairways.

#### Tamaroa Field

Tamaroa and Tamaroa South fields, discovered in 1942 and 1956 respectively, are located in northeastern Perry County, Illinois (Figure 115). The fields produce principally from lenticular sandstones located in the upper portion of the Chesterian Cypress Formation at a depth of approximately 1150 feet. These sandstone bodies, deposited as elongate bars, are typically less than 10 feet thick, 1/4 to 1/2 mile wide, and less than 2 miles long. Mapping of reservoir sandstone lenses at Tamaroa Field required the construction and interpretation of detailed cross sections. Examples of interpretation of individual sandstone lenses used for mapping are shown in Figures 117 and 118. The Cypress Formation was divided into lower, middle and upper intervals for local mapping purposes. The lenticular or ridge forming sandstones occur in the upper interval Grube 1992). Highlighted in color are the Y2 and Y3 lenticular sandstones which form the principal reservoirs in the Tamaroa area (Figures 117, 118). The Y2 and Y3 sandstones are commonly less than 10 feet thick and separated by shale as shown on Figure 117 but, in some cases, they coalesce, forming abnormally thick upper Cypress sandstone, shown in Figure 117. Compartments are maintained in these thicker sandstones because they are typically separated by shaly beds and shale rich impermeable zones less than 1 foot thick as observed in core and core analyses. Electric logs are unable to resolve the thin, impermeable zones that partition the thicker sandstones (Figure 119). The bars trend northeast-southwest in subparallel alignment and are vertically stacked (Figure 120 and 121). .The map (Figure 121) shows an outline of the Y2 and Y3 sandstones greater than 4 feet thick combined with the Barlow structure. This figure highlights the northeast-southwest trend and the subparallel alignment of these lenticular sandstone bodies. The trapping mechanism for the Tamaroa area fields is shown to be draping of the lenticular sandstones across the crest of structural folds. Spontaneous potential and gammaray log character, as well as core data, show that shales, ranging in thickness from 10 feet to less than 1 foot, separate the sandstones (Figure 119). The porous and permeable portions of closely spaced subparallel bars and vertically stacked, shale-separated bars create discrete reservoir compartments within these fields as the bars drape over the structural folds. Understanding and modeling compartmentalized reservoirs is essential for optimizing hydrocarbon recovery from fields such as those in the Tamaroa area (Figure 122). An understanding of the geometry and dimensions of these lenticular sandstone bodies is necessary to define each particular sandstone lens and to correctly correlate the horizon in which the lens was deposited. This is necessary to define compartments and determine communication potential (Grube 1992). Only then can each separate lens be efficiently drained. Figure 121 is a simplification of the bar configuration that occurs in the Tamaroa South portion of the field area (red arrow in figure with combined bars

and structure. Figure 122 shows that primary recovery will occur in all three lenses but only the lower blue, Y2 lense can be drained by secondary injection through the A or B well. The upper red, Y3 lenses cannot be waterflooded with this well configuration although miscorrelation of the lenses could lead to an interpretation that the B and C wells are in communication or that the A and C wells are in communication.

The range of recovery efficiencies for the various pools in the Tamaroa area appears to be related to the degree to which the geology of the reservoirs was understood and was employed in the design and implementation of drilling and development programs. Reservoir volumetric calculations indicate that recovery efficiencies among the pools range from 5% to 43%. Cumulative production of 768,000 barrels of oil from all the Tamaroa area Cypress reservoirs is equal to about 24% of the 3.2 million barrels of original oil in place (STOOIP). Recoverable reserves that may remain in the reservoirs, based on a recovery efficiency of 43%, are estimated to be approximately 608,000 barrels. Reservoirs such as those found in the Tamaroa Field are good candidates for ASP flooding because there is sufficient oil in place and reservoir geometries can be well defined.

#### **Richview Field**

Richview Field, discovered in 1946, is located in eastern Washington County, south-central Illinois. Petroleum is produced from northeast-southwest trending, vertically stacked, lenticular sandstone bodies in the upper part of the Mississippian Cypress Formation (Grube and Frankie 1999). The sandstone lenses that make up the primary reservoirs range from 1 to 2 miles in length, are up to 1/2 mile in width, and average 10 feet in thickness. Reservoir porosity averages 20% and permeability averages 175 millidarcies. The reservoirs extend over 640 acres at an average depth of 1,500 feet. Discrete reservoir compartments are created within the field by shale beds that separate the vertically stacked sandstone lenses. Combined stratigraphic/structural trapping occurs where stacked, compartmentalized sandstone lenses lap onto and drape over a structural saddle. Geometry and stratigraphic associations indicate that these sandstones were deposited in tidally influenced coastal, shallow marine environments (Figure 123).

Maintenance of reservoir pressure is a significant factor that has influenced the ultimate cumulative oil recovery. Initiation of waterflooding after as little as one year of primary production appears to have positively affected recovery efficiency at Richview Field. Of the estimated 7.3 million barrels of stock tank original oil in place (STOOIP), 3.3 million barrels have been produced, yielding a recovery efficiency of 45%.

The reservoir at Richview Field was characterized, in part, through lithofacies mapping and depositional facies interpretation. Four separate reservoir intervals were defined within the Cypress based on correlations of distinctive spontaneous potential (SP) and resistivity log signatures (Grube and Frankie 1999). Three correlation parameters were used to define the divisions; 1) similarity of log character, 2) stratigraphic position of sandstones in the Cypress Formation, and 3) stratigraphic position of shales in the Cypress Formation. Sandstones within these intervals have been designated in ascending order as the A, B, C, and D (Figure 124).

The B and C sandstones form the primary reservoirs in Richview Field (Figure 125 and 126). A shaly interval, ranging in thickness from less than 1 foot to 4 feet, commonly separates the B and C sandstones. This shaly interval decreases in thickness towards the middle of the field,

becoming imperceptible on some logs. A shale interval, commonly 10 feet thick but ranging from 0 to 30 feet thick, separates the A sandstone from the overlying B sandstone. Drill cuttings from representative wells across the field commonly contain red and green to variegated mudstone beds near the top of the shale between the A and B sandstones. Rare coal cuttings are also observed in this shale interval.

Drill cuttings and core plugs of reservoir rock from all intervals are lithologically similar and are composed of very light gray to white to light brown oil-stained, moderately well sorted, fine to very fine grained sandstone. The B and C reservoir sandstones appear to be very clean where the SP log shows at least a 75% clean deflection. Silica cement appears to be pervasive throughout the sandstones and it is the dominant cement in the reservoirs.

Core descriptions from core analysis reports and observations of core plugs from the Cecil Newcomb et al. No. 2 show that thin, wispy, wavy shale laminations are common in some parts of the reservoir sandstones. Thin sections show that these discontinuous laminations are paper thin and have a somewhat cyclical occurrence. Scattered flat clay clasts were also observed in some beds in the cores and core plugs. Calcareous beds, typically less than two feet thick, occur

in some cores at the base of the B and/or in the uppermost part of the C sandstones and may be distinguished on logs by high resistivity spikes with a correspondingly low SP. Fossil fragments are commonly observed in these beds. Some of the sandstones include thin limestone beds within the sandstones. These features corresponds with those observed in core from Cypress sandstone reservoirs in Lawrence Field.

Sedimentary features indicate that tidal processes more than storm processes controlled Cypress deposition. Thick beds of sandstone that contain wispy, wavy, discontinuous shale laminations or even grade to flaser type beds predominate over scattered, thin beds of sub-horizontal or cross-laminated sandstones. Sandstone bodies, particularly in the upper Cypress, are lenticular, a mile or two in length, and less than a half mile in width. The lenses commonly form a series of subparallel ridges that trend northeast-southwest. These ridges are made up of thin discrete bodies, generally three to ten feet thick, that stack and appear to coalesce on electric logs. Sedimentary features and sandstone body geometries are not those generally found in river dominated (lobate) or wave dominated (cuspate) deltaic depositional systems. The lenticular, stacked and aligned sandstone bodies of the Richview Field are most analogous to the linear tidal ridges that form in the high-tidal-range dominated environments of the Ord River Delta of northern Australia (Wright et al. 1975) or the Gulf of Korea portion of the Yellow Sea (Off 1963).

Retaining reservoir energy is crucial to maximizing recovery efficiency, particularly in a reservoir of limited extent with a correspondingly limited drive. Initiation of waterflood projects early in the life of production at Richview Field probably retained or at least reestablished reservoir energy. The high recovery factor (45.6%) calculated for Richview Field is likely to be, in part, the result of these pressure-maintenance, waterflood projects.

A potential problem with waterflooding and enhanced oil recovery techniques such as ASP flooding of Mississippian sandstone reservoirs such as those at Richview Field is that the stacking or shingling of reservoir sandstones creates discrete compartments that can be bypassed

by a waterflood (Figure 127). This situation can develop either where a compartment is not present in an injection well but is present in the offseting producer(s) or where the injector well (probably a converted producer) penetrates a compartment that is not in communication with a producer. Primary production is therefore drained from the separate compartment while the waterflood, in communication through another compartment or multiple compartments, bypasses the separate compartment. Stratigraphic correlations between vertically stacked or shingled, discontinuous reservoir compartments are not always obvious. A misunderstanding of these characteristics can lead to miscorrelations that consequently inhibit development and production. Within Richview Field, the thickening of the C sandstone from north to south is the result of shingling or stacking of additional sandstone lenses, some of which may contain bypassed oil as described above.

A similar waterflood or Enhanced Oil Recovery problem develops where multiple stacked reservoir sandstones are present in a waterflood unit, but permeability variations between compartments are great enough to cause channeling of the flood away from the lower permeability compartments. In this case, the less permeable compartments would contain bypassed, movable oil. Even compartments that show an increase in permeability away from the wellbore would contain bypassed oil. Because hydraulic fracturing was a common completion practice in many of the Mississippian stacked sandstone reservoirs in Illinois, including Richview, the capability to selectively flood a lower permeability compartment may be limited. The induced fractures are typically designed to propagate through all compartments within the oil column causing communication between all compartments. Therefore a particular compartment cannot be isolated for flooding. It is recommended that reservoir continuity and flow unit correlation be evaluated through use of field pressure analyses, including pulse, interference, build-up, draw-down and tracer tests (Lee, 1982). Pressure maintenance and other reservoir management requirements can also be evaluated through the use of field tests and accurate, per-well production histories that include water and, if possible, gas production.

It has been established that most Chesterian sandstone reservoirs in the Illinois basin bear some similarity with Cypress Sandstone reservoirs found in Lawrence Field, Richview Field, Tamaroa Field or in case studies of other fields in the basin. These examples all show a commonality of multiple, stacked, thin sandstone lenses that may be inadequately drained due to compartmentalization of reservoirs. Each reservoir must be mapped in detail to ensure that enhanced oil recovery programs such as ASP flooding are implemented in an efficient and economic manner.

# Assessment of ASP Technology for Petroleum Reservoirs in U. S.

The Illinois Basin is an interior cratonic Basin with the following factors influencing deposition of siliciclastics that may host petroleum reservoirs, gentle low gradient sea floor, low rate of subsidence relative to the rate of sedimentation and a thin vertical interval to accommodate influxes of sediment. These conditions are in large part responsible for the distribution, geometry, size, compartmentalization and complexity of petroleum reservoirs in the Illinois Basin. The other interior cratonic basins in the United States with significant oil production include the Williston, Michigan and Forest City basins. Most of the oil reservoirs in these basins are hosted in carbonates. This project did not assess the potential of ASP flood technology in carbonate reservoirs because the ASP pilots in Lawrence Field were conducted in sandstone reservoirs and there was no opportunity to include carbonate reservoirs in the project. Given the success of the ASP technology in sandstone reservoirs in Lawrence Field with reservoir characteristics such as good porosity, permeability, favorable response to waterflood technology, limited areal extent of reservoirs and complex reservoir heterogeneity it is likely that many carbonate reservoirs would respond favorably to ASP floods. This section will review sandstone reservoirs in interior cratonic basins first and then will review the potential of successful application of ASP technology in selected sandstone reservoirs with similar depositional environments and other characteristics in other types of basins in the U. S. Much of the information in this section is from the series on National assessment of United States oil and gas resources published in 1995 by the USGS (Gautier, D. L, G. L. Takahashi, and K. L. Varnes editors 1995). Each Basin/province in the United States was treated separately and published in a series for a national assessment of oil and gas resources in the United States. Tables at the end of this section were generated using data from the USDOE TORIS database.

The Michigan Basin, an interior cratonic basin, is largely confined to the state of Michigan (Dolton 1995). Although most oil reservoirs are in carbonate rocks some reservoirs are hosted in the Devonian age Berea Sandstone. Environments of deposition for Berea Sandstone reservoirs have been interpreted as elongate nearshore siliciclastics deposited in a delta complex. Oil is stratigraphically trapped at the updip portion of the elongate sandstone bodies on the eastern side of the Michigan basin. Producing elongate sandstone bodies typically trend northwest. Berea Sandstone reservoirs are typically composed of fine grained sandstone that may contain dolomitic cement, micaceous and pyritic intervals. Reservoir thicknesses in existing fields are commonly 10 to 20 feet thick, porosities range from 7 to 24 percent and average 12.5 percent. Oil is high quality, sweet and light with gravities ranging from 44 to 46 API. Reservoirs are generally located at depths of 1,500 to 2600 feet below the surface and are relatively small in size with less than 7 MMBO of production.

The Williston Basin is a large interior cratonic basin located primarily in North Dakota, South Dakota, and Montana (Peterson 1995). Over 1,260,516,337 barrels of oil have been produced in the North Dakota portion of the Williston Basin. Most of this production is from carbonate reservoirs. Sandstone production in the Williston Basin is from the Pennsylvanian age Tyler Formation. Siliciclastics in the upper unit of the Tyler Formation have been interpreted as being deposited as a barrier island complex in a prograding delta environment (Sturm, 1982). The Tyler Formation produces oil from barrier island as well as channel fill sandstones located in southwestern North Dakota. Approximately 73,473,133 barrels of oil have been produced from sandstone reservoirs in the Tyler Formation. Most of these sandstone reservoirs are located on

structural anticlines therefore the primary trapping mechanism is structural closure but there is also a strong stratigraphic component. There are also sandstone reservoirs where the only trapping mechanism is stratigraphic. Sandstone reservoirs in the Tyler Formation range in depth from 4,000 to 8,000 feet. There are approximately 20 fields in these sandstones, two are larger than 10 MMBO (Peterson 1995).

The Forest City Basin is an interior cratonic basin where sandstone reservoirs most resemble those found in the Illinois Basin. Most oil reservoirs in the Forest City Basin are located in northeastern Kansas with some located in Nebraska. The main sandstone reservoirs are fluvial-deltaic Pennsylvanian sandstones of Desmoinesian age with average net pay of 18 feet (Charpentier 1995). Approximately eighty percent of the oil production in the Forest City Basin is from Desmoinesian sandstone reservoirs. These reservoirs are combination structure-stratigraphic traps at depths from 150 - 1,500 feet. This is a very mature play where the Paola-Rantoul Field was the first significant field with more than 41 MMBOE was discovered in 1882 in Miami County Kansas.

Other sandstone plays in the Forest City Basin include Middle to Upper Ordovician Simpson Group sandstone reservoirs that have an average of 10 feet net pay at depths that range from 1,900 – 3,200 feet below the surface. These reservoirs are located in Kansas and Nebraska with the largest reservoir in the Falls City Field in Richardson County, Nebraska where more than 5 MMBO have been produced.

#### Sandstone Reservoirs in Non-Interior Cratonic Basins

There are numerous highly productive sandstone reservoirs deposited in fluvial/alluvial to submarine environments that are potential candidates for successful application of ASP flood technology in non-interior cratonic basins across the United States. Select sandstone reservoirs plays in some US basins and the possible application will be discussed in this section. In general ASP flood technology has the potential to be very broadly applied to many if not most oil reservoirs in the US. The main factors influencing successful, economic application of the technology is adapting specific formulations to the reservoir rocks, oils and other reservoir fluids, it is necessary to adapt to individual reservoirs. Detailed reservoir characterization and knowledge of individual reservoir geometries, boundaries, compartments, potential barriers to fluid flow, and flow units are all helpful in designing and implementing economically successful ASP floods.

The Bend Arch-Fort Worth Basin contains sandstone reservoirs in the Lower Pennsylvanian Bend sandstones and conglomerates as well as the Strawn Pennsylvanian Desmoinesian age quartz sandstones (Ball and Perry 1996). Reservoirs in these sandstones have produced 1.4 BBO. The largest and most productive Desmoinesian Pennsylvanian sandstone reservoir in the Bend Arch-Fort Worth Basin occurs in the KMA Field discovered in 1931 where it has produced 147 MMBO. These Pennsylvanian Desmoinesian age sandstone reservoirs were deposited in fluvial-deltaic environments and have complex geometries. Porosities range from 14 to 23 percent, permeabilities average more than 100 md, and oil columns range from 65 to 400 feet. Drilling depths range from 6,000 to 7,000 feet below the surface. Trapping mechanisms are stratigraphic, structural anticlines or combination structural-stratigraphic. The reservoir characteristics outlined above indicate that ASP technology could be successfully applied to Desmoinesian age sandstone reservoirs because the porosity and permeability values are similar

to those in Pennsylvanian age Bridgeport sandstones deposited in deltaic environments in Lawrence Field. The oil columns are much thicker in the Arch Bend Fort Worth Basin than those in the Illinois Basin indicating that there is a larger potential volume of recoverable in the Desmoinesian reservoirs than in the Bridgeport reservoirs in the Illinois Basin.

Pennsylvanian (Missourian-Virgilian) sandstones deposited in marine shelf sandstone environments are another sandstone reservoir play in the Bend Arch Fort Worth Basin. Permian (Wolfcampian) sandstones are also part of this play. Environments of depositions interpreted in Permian age sandstones include prodelta –front, bar and blanket sandstones, channel to mouthbars and distributary channel sandstones. There are also sandstones associated with marine slopes such as submarine channel fills and submarine fan lobes. This diverse range of environments of deposition ranges from fluvial deposits through deeper marine submarine fan lobe deposits. Porosity ranges from 14 - 25 percent in shelf sandstones and permeabilities range from 10 to 380 md and oil columns vary from 55 to 215 feet thick. Reservoir depths range from 500 to 7,000 feet below the surface. The post Desmoinesian play has produced 384 MMBO from sandstone reservoirs. The Fargo Field discovered in 1940 with 34 MMBO of production to date is the largest oil field in this play (Ball and Perry 1996). It is likely that many of the reservoirs in this play contain sufficient remaining oil saturation in large enough volumes that ASP technology could be applied as an economic tertiary oil recovery strategy. This is particularly appropriate for shallower reservoirs where pressures are two low for implementation of miscible CO<sub>2</sub> floods. As stated earlier each reservoir must be evaluated individually before the best type of EOR strategy can be selected.

The Denver Basin contains several mature sandstone reservoir plays that may respond to appropriately selected EOR strategies such as ASP flood technology. The Denver Basin is located in eastern Colorado, southeastern Wyoming, the southwestern corner of South Dakota, and the Nebraska Panhandle.

One sandstone play in the Denver Basin includes sandstone reservoirs the Upper Cretaceous Pierre Shale (Higley et al., 1995). These sandstones were deposited in an offshore marine ridge environment. These reservoirs produce from depths ranging from 4,000 to 5,000 feet below the surface. Oil reservoirs are located in elongate sand bodies made up of fine-grained sandstones in the Richards and other sandstone members of the Pierre Shale. These sandstone reservoirs range in thickness from 4 to 48 feet, with an average thickness of 20 feet. Average porosity is 14 percent, average permeability for two fields with data are 0.1 md and 8 md. Oil gravity ranges from 40 to 65 API. The Spindle Field is the largest oil field that produces from the Shannon and Sussex sandstones with 60.25 MMBO produced to date from depths from 4,700 to 5,100 feet below the surface.

The quality of these reservoirs is controlled in large part by environments of deposition, the primary reservoir facies are trough-crossbedded fine to medium grained sandstone that represent high depositional energy resulting in good porosity and permeability values. Although the environments of deposition of sandstones in the Pierre Shale are different from those found in the Mississippian Cypress Sandstone in Lawrence Field, there are important similarities that these two sandstone reservoir plays share such as the factors controlling reservoir heterogeneity cause highly complex, compartmentalized reservoirs. These factors include numerous permeability barriers located between thin-bedded reservoir sandstones caused by interbedding

of sandstones and other finer grained clastics such as mudstone deposited by alternating high and low energy regimes. Other factors include highly variable distribution of porosity and permeability resulting in differing flow units that impacts the sweep efficiency of secondary and tertiary recovery programs.

Approximately 90 percent of the 800 MMBO produced from the Denver Basin is from the J Sandstone with some production from the overly D. Sandstone (Higley et al., 1995). This play produces primarily oil from the J Sandstone of the Muddy Sandstone Formation of the Lower Cretaceous Dakota Group. Production from the J and D Sandstones occurs over most of the Denver Basin. The most common trapping mechanisms are stratigraphic and combination stratigraphic-structural. Reservoirs are located at depths ranging from 3,000 to 8,000 feet below the surface. The most productive facies are those associated with deltaic environments. These sandstones can attain thicknesses of 540 feet, however reservoir intervals are much thinner and average about 25 feet. Core measured porosity values vary with depth with the highest average porosities of 24 percent found at 4,000 feet and averages of 7 to 10 percent found at deeper depths of 9,000 feet. The Adena Field is the largest field producing from the J Sandstone with 59 MMBO of production to date. Average porosity for the J Sandstone in the Adena Field is 19.7 percent and the average permeability is 356 md.

Anadarko Basin covers the western part of Oklahoma, southwestern part of Kansas, the northwestern part of Texas Panhandle and the southwestern corner of Colorado Henry and Hester 1995). The Middle and Upper Devonian Misener Sandstone play ranges in depth from 4,000 to 13,000 feet. This sandstone is among the deepest oil plays in the Anadarko Basin. The formation reaches a maximum thickness of 160 feet, reservoirs are usually 30 feet thick of less in this play. Traps in this play are primarily stratigraphic. The largest oil reservoir in this play is the Sooner Trend where there is an estimated potential recovery of approximately 16 MMBO from the Misener Sandstone (Henry and Hester, 1995). Production in this play ranges in depth from 5,800 and 6,200 feet.

The Powder River Basin is located in northeastern Wyoming and a small portion of southeastern Montana. This basin is approximately 250 miles long and 100 miles wide and comprises a major portion of the Cretaceous age Western Interior Seaway (Dolton and Fox, 1996). There are several major sandstone plays in the basin's three major reservoir systems, the Pennsylvanian-Permian, the Lower Cretaceous, and the Upper Cretaceous.

The Pennsylvanian Upper Minnelusa Sandstone play are primarily stratigraphic traps in sandstones deposited as eolian dunes (Dolton and Fox 1996). There are also combination stratigraphic – structural stratigraphic traps in the Minnelusa Sandstone play. Sandstone reservoirs in the Upper Minnelusa are usually composed of very mature, fine to medium grained orthoquartz sandstone. Reservoir porosities commonly range from 12 to 24 percent in existing fields. Oil gravities generally are in the 18 to 40 API range, oil gravity generally increases with depth. Reservoirs are usually located at depths ranging from 5,000 to 15,000 feet below the surface. There are more than 160 fields with approximately 500 MMBO of known recoverable oil reserves.

The Lower Cretaceous Lakota Formation is the lowermost unit of the Inyan Kara Group that unconformably overlies the Jurassic Morrison Formation. Lakota sandstone reservoirs are

located in channel sandstones deposited in alluvial to deltaic environments of deposition. The trapping mechanism is usually stratigraphic where channel deposits are sealed by overlying fine grained alluvial deposits. Lakota reservoirs are composed of fine to coarse grained sandstone with occasional intervals of conglomerates and pebbles. Producing intervals generally range in thickness from 6 to 13 feet with porosities as high as 25 percent. Oil gravities range from 26 to 45 API. Reservoirs are located at depths ranging from 2,000 – 13,000 feet below the surface (Dolton and Fox, 1996).

The Fall River Sandstone play is also a unit in the Lower Cretaceous Inyan Kara Group. Sandstone reservoirs were deposited in distributary and estuarine channel environments. Reservoirs are commonly composed of point bar facies that are stratigraphically sealed updip by fine-grained abandoned channel deposits or low energy marine fine grained clastics (Dolton and Fox, 1996). Reservoir sandstones are fine- grained, mature quartz rich sandstones. Porosity of Fall River sandstones reservoirs ranges from 8 – 23 percent and is most commonly in the 13 to 18 percent range. Oil gravities range from 28 to 46 API. Drilling depths range from 4,000 to 14,500 feet below the surface. There are over 30 oil fields that combined have produced approximately 170 MMBO from reservoirs in the Fall River sandstone play.

Sandstone reservoirs in the Muddy Sandstone play are found in the Lower Cretaceous Muddy New castle Sandstone Formations. These sandstones form a complex that is composed of large volumes of siliciclastics transported into the Cretaceous Western Interior Seaway from the east. Reservoirs are located throughout the complex wedge of clastics deposited during this period in a large variety of environments depending in part on where the sand was being deposited relative to the location of the shoreline at the time of deposition (Dolton and Fox, 1996). Environments of deposition of reservoir sandstones includes marine bar, strandline, distributary channel, estuarine, alluvial and lower delta plain.

Reservoir quality varies greatly in the Muddy Sandstone Formation due to the large variety of facies associated with the broad spectrum of depositional environments. Channel fill deposits will likely have much different reservoir qualities than those found in a lower delta plain sandstone. Marine bars are a common reservoir facies that are usually elongate sandstone bodies that are generally oriented in a north-south direction (Dolton and Fox, 1996). Commonly a single field will have several traps and pools with varying environments of deposition with different reservoir qualities. In general Muddy sandstone reservoirs are composed of fine to very fine grained sandstone. Average reservoir porosities vary greatly and usually range between 9 and 22 percent and depend in large part on facies, the mean porosity for reservoirs is approximately 15 percent. Porosity generally decreases with depth. Average permeability ranges from 1 to more than 1,000 md. The reservoir intervals range from 10 to 25 feet. Oil gravities are generally high, ranging from 35 to 50 API. Reservoir depths range from 3,000 to 14,000 feet below the surface. Over 170 fields have been discovered in the Muddy Sandstone play with more than 550 MMBO of recoverable oil.

Sandstone reservoirs in the Upper Cretaceous Frontier Formation make up the Deep Frontier Sandstone play in the Powder River Basin (Dolton and Fox, 1996). Sandstone reservoirs in this play occur in stratigraphic traps in offshore marine shelf sandstone environments. The primary reservoir facies in this play are high energy marine bar complexes that are oriented in a northwest-southeast direction. Average porosities usually range from 10 to 15 percent and

reservoir thickness ranges from 4 to 130 feet. Oils have high gravities ranging from 34 to 47 API and are rich in dissolved gas There are currently over 20 individual reservoirs in the play with more than 40 MMBO.

The Turner Sandstone is a member of the Upper Cretaceous Carlile Shale. This play consists of marine sandstones that commonly have poor porosity and permeability. Reservoirs are composed of quartz grains, chert, lithic fragments and large amounts of clay (Dolton and Fox, 1996). Reservoir sandstones range in thickness from 5 to 35 feet. Oil gravities range from 39 to 43 API. Reservoirs are located from 500 to 8,000 feet below the surface. Approximately 20 MMBO of known recoverable reserves have been discovered in this play.

The Sussex and Shannon Sandstone members of the Upper Cretaceous Cody Shale make up the Sussex-Shannon sandstone play. These sandstones were deposited in a marine shelf environment where currents reworked sand sheets originally deposited on the shelf into broad, elongate offshore marine bars (Dolton and Fox, 1996). Mapping of select Sussex Sandstone reservoirs show twelve distinct, well-sorted, imbricated sandstone lenses oriented in a northwest direction. The areal extent of many of the mapped sandstones in this play show sandstone bodies 0.5 - 12 miles wide, 5 - 30 miles long, and up to 33 feet thick. Reservoirs in this play may be as much as 20 miles long, 3 miles wide and 30 feet thick. Thicknesses of reservoirs in the Sussex-Shannon play range from 5 to 32 feet. Porosity averages between 10 to 15 percent and permeability ranges from 1 to 20 md. Oil gravities range from 35 to 39 API. Drilling depths range from 7,000 to 11,000 feet below the surface. Approximately 180 MMBO has been discovered in this play, the largest producing Sussex field is the House Creek with about 24 MMBO known recoverable barrels of oil. The largest Shannon field is the Hartzog Draw with 120 MMBO.

The Mesaverde-Lewis Sandstone play consists of marine sandstone reservoirs in the Upper Cretaceous Mesaverde Formation and Lewis Shale Formation. Sandstone reservoirs in this play were deposited in a wave dominated deltaic environment where sand was reworked into offshore marine bars (Dolton and Fox 1996). Average reservoir thickness generally ranges from 10 to 150 feet. Porosity averages range from 12 to 18 percent and average permeability ranges from 2md to 34 md. Oil gravities range from 35 to 47 API. Reservoir depths generally range from 5,000 to 9,000 feet below the surface. The trapping mechanism usually consists of stratigraphic updip pinchouts of marine sandstones into much finer grained prodelta and shelf facies. These reservoirs can be complex with multiple oil-water contacts. Marine bar complexes in these reservoirs commonly are oriented in a northwest direction. Approximately 110 MMBO have been discovered in this play, about 15 of these fields are larger than 1MMBOE and 45 are smaller than 1MMBOE.

# **Compilation of United States Oil Producing Basins**

The tables presented below are the result of a set of queries to the TORIS database (circa 1985). The fields of interest to this project were those fields which produced oil from reservoirs similar to the target sandstone reservoirs of Lawrence Field. The criteria used to query the database were: reservoirs with a sandstone lithology; reservoirs that had a depth of 3000 ft. or shallower; and reservoirs that had a fluvial/near-shore depositional system similar to the target reservoirs. Upon completion of the database query the fields were sorted by state. Through the use of state

survey web sites, the National Atlas web site, and the USGS' National Oil and Gas Assessment web page it was determined to which basin each of the remaining fields belonged.

A value of -1 in the following tables refers to data that was unobtainable or not available from the entity responsible for supplying the data for the TORIS database.

Well Spacing (Acres). The result obtained when the proven acreage is divided by the actual number of wells in the reservoir. The TORIS value for Well Spacing for a reservoir may differ considerably from that obtained using the traditional concept of well spacing. For example, consider that it is planned to develop the XYZ Field's A Reservoir on a 40 acre spacing. But currently there are 10 injectors and 5 producers in the field and only 5 injectors and 2 producers are completed in the A reservoir. Given that there are 400 proven acres in this reservoir, this would yield a 57 acre spacing (400/7) and not the eventual planned 40 acre spacing.

# **Appalachian Basin**

Field	Reservoir	OOIP	Depth	Field	Proven	Well	Net Pay	Porosity	So	Sw	Temp	Pressure	Permeability	API	Viscosity	Salinity	Cum Oil	Year for
Name	Name	(BBL)	(Feet)	Acres	Acres	Spacing (Acres)	(Feet)	(%)	(%)	(%)	(°F)	(PSI)	(MD)	Gravity	(CP)	(PPM TDS)	Prod (BBL)	Cum Oil
MANNINGTON	BIG INJUN	210,000,000	2100	22000	22003	11	18	15	44	48	74	917.7	22	39	4.3	150000	32,017,000	1973
SALEM	GORDON	207,500,000	2800	41800	41800	14	8	12	64	20	86	1218.7	20	42	3.8	160000	41,162,000	1973
WALTON (JOHNSONS & ROCK CREEKS)	BIG INJUN	132,500,000	2050	8780	11000	11	21	22	35	52	75	896.2	20	43	3.11	160000	33,000,000	1982
JACKSONBURG-STRINGTOWN	GORDON	88,469,000	2850	15386	15386	12	10	12	57	26	82	100	30	42	4.2	170000	20,458,000	1973
CENTERPOINT	BIG INJUN	78,790,000	2000	12980	12980	11	10	17	45	47	76	874.7	20	45	2.8	150000	11,646,000	1973
WOLF SUMMIT-BIG ISAAC	FIFTH	68,916,000	2900	17229	17229	14	5	20	49	38	87	1261.7	20	42	4.2	160000	12,630,000	1973
SMITHFIELD	BIG INJUN	63,800,000	2200	13030	13030	11	10	12	49	40	77	960.7	27.9	42	4	150000	11,650,000	1973
BURNING SPRINGS	BURNING SPRINGS	26,316,000	700	-1	6579	-1	-1	0.2939	-1	-1	-1	-1	-1	-1	-1	-1	7,700,000	1973
CAMERON-GARNER	GORDON	22,500,000	2800	8340	8340	11	5	11	55	24	84	1218.7	20	45	3	170000	5,975,000	1973
YELLOW CREEK (BIG SPRINGS)	BEREA	21,654,000	2300	4812	4812	9	8	12	52	27	81	1003.7	10	42	4.1	160000	6,165,000	1973
PORTO RICO	GORDON	20,800,000	2600	5587	5587	12	6	12	53.6	20	84	1132.7	20	43	3.8	160000	6,791,000	1973
FINK CREEK (DRY FORK)	BEREA	20,784,000	1480	-1	5196	11	8	0.28387	-1	-1	-1	-1	-1	-1	-1	-1	7,132,000	1973

# Bend Arch – Fort Worth Basin

Field	Reservoir	OOIP	Depth	Field	Proven	Well	Net Pay	Porosity	So	Sw	Temp	Pressure	Permeability	API	Viscosity	Salinity	Cum Oil	Year for
Name	Name	(BBL)	(Feet)	Acres	Acres	Spacing (Acres)	(Feet)	(%)	(%)	(%)	(°F)	(PSI)	(MD)	Gravity	(CP)	(PPM TDS)	Prod (BBL)	Cum Oil
ARCHER COUNTY REGULAR		1,189,030,000	1350	-1	7000	-1	59	16	-1	-1	100	220	400	36	5	-1	244,601,000	1976
JACK COUNTY REGULAR		73,146,800	2500	-1	7500	6.52174	10	22	-1	-1	102.5	-1	106	38	1.53033	-1	41,080,000	1982
BAYLOR COUNTY REGULAR		63,837,200	1400	-1	3000	-1	20	24	-1	-1	83.8	-1	560	36	4.49257	-1	30,688,500	1976
SHACKELFORD COUNTY REGULAR	TANNEHILL SAND	49,043,800	450	-1	7400	2.17319	5	23	-1	-1	67.65	-1	160	40	9.38543	-1	8,864,400	1981
GATEWOOD		30,000,000	1600	-1	800	-1	20	23	-1	-1	87.2	-1	148	33	7.63267	-1	10,106,900	1977
VOSS	TANNEHILL	24,325,200	2000	-1	1090	20	22	22	-1	-1	94	-1	158	34	3.71122	-1	7,830,000	1982

# **Big Horn Basin**

Field	Reservoir	OOIP	Depth	Field	Proven	Well	Net Pay	Porosity	So	Sw	Temp	Pressure	Permeability	API	Viscosity	Salinity	Cum Oil	Year for
Name	Name	(BBL)	(Feet)	Acres	Acres	Spacing (Acres)	(Feet)	(%)	(%)	(%)	(°F)	(PSI)	(MD)	Gravity	(CP)	(PPM TDS)	Prod (BBL)	Cum Oil
GRASS CREEK	FRONTIER	84,200,000	750	1720	1750	5	76	22	58.5638	41.4362	70	200	35	44	2.80705	5000	40,784,000	1981
ELK BASIN	FRONTIER	78,000,000	1084	-1	1400	24.1379	40	26	71.8352	28.1648	77.344	-1	350	43	2.77261	4762	14,800,000	1981

# **Cherokee Platform**

Field	Reservoir	OOIP	Depth	Field	Proven	Well	Net Pay	Porosity	So	Sw	Temp	Pressure	Permeability	API	Viscosity	Salinity	Cum Oil	Year for
Name	Name	(BBL)	(Feet)	Acres	Acres	Spacing (Acres)	(Feet)	(%)	(%)	(%)	(°F)	(PSI)	(MD)	Gravity	(CP)	(PPM TDS)	Prod (BBL)	Cum Oil
CUSHING	ALL	1,064,000,000	2800	36420	24940	40	50	19	19	45	100	800	50	42	5	100000	481,000,000	1982
PERU-SEDAN	PERU	706,800,000	1200	-1	26500	10	25	20	-1	-1	81.6	-1	70	33	8.30674	-1	198,600,000	1980
WINTERSCHIED	BARTLESVILLE	226,500,000	1630	-1	14600	40	15	28	-1	-1	89.34	-1	358.122	39	2.43169	-1	99,954,000	1975
SEELEY-WICK	BARTLESVILLE	201,450,000	1950	-1	5840	20	45	17	-1	-1	95.1	-1	25	40	1.71479	-1	31,910,000	1980
CLEVELAND	BARTLESVILLE SAND	145,000,000	2800	560	-1	12.1697	70	12.5	-1	-1	107	-1	60	40	5	220000	55,000,000	1982
GLENNPOOL (BERRYHILL																		
GLENN SAND)	GLENN SAND	138,000,000	1500	1840	-1	3	71	20	-1	-1	95	660	270	38	3.3	45000	47,000,000	1981
MORAN	BARTLESVILLE	98,900,000	820	4520	4520	20	17	21	76	24	77	367.3	88	22	750	-1	35,420,000	1980
OWL CREEK	SQUIRREL	82,586,300	864	-1	1740	20	38	23	-1	-1	78	-1	170	24	60.4457	-1	11,500,000	1980
IOLA CONSOL	BARTLESVILLE & SQUIRREL	60,680,000	860	-1	1910	10	30	25	65	35	74	500	209.311	20	700	-1	4,160,000	1980
MUSKOGEE	ALL	54,000,000	1300	4600	-1	10	25	10	50.929	49.071	100	500	15	38	4	200000	27,000,000	1982
QUINCY	BARTLESVILLE	35,039,500	1500	-1	2080	20	20	19	-1	-1	87	-1	6	40	2.43844	-1	5,810,000	1980
NORFOLK, WEST	PRUE	22,110,300	2800	-1	1330	110.833	25	15	-1	-1	99.2	-1	10	38	1.47054	200371	-1	1975

# **Forest City Basin**

Field	Reservoir	OOIP	Depth	Field	Proven	Well	Net Pay	Porosity	So	Sw	Temp	Pressure	Permeability	API	Viscosity	Salinity	Cum Oil	Year for
Name	Name	(BBL)	(Feet)	Acres	Acres	Spacing (Acres)	(Feet)	(%)	(%)	(%)	(°F)	(PSI)	(MD)	Gravity	(CP)	(PPM TDS)	Prod (BBL)	Cum Oil
PAOLA-RANTOUL	BARTLESVILLE	399,763,000	700	-1	28180	30	16	20	-1	-1	72.6	-1	75	31	25.5009	-1	176,600,000	1980

# **Gulf Coast Basins**

Field	Reservoir	OOIP	Depth	Field	Proven	Well	Net Pay	Porosity	So	Sw	Temp	Pressure	Permeability	API	Viscosity	Salinity	Cum Oil	Year for
Name	Name	(BBL)	(Feet)	Acres	Acres	Spacing (Acres)	(Feet)	(%)	(%)	(%)	(°F)	(PSI)	(MD)	Gravity	(CP)	(PPM TDS)	Prod (BBL)	Cum Oil
SMA CKOV ER	NACATOCH	800,000,000	2000	21760	43970	10	22	32	35	65	110	874.7	5000	20	75	30000	350,000,000	1977
VAN		640,000,000	2700	-1	4520	7	114	29	-1	9	125	885	1000	35	4	70000	484,680,000	1982
VAN	DEXTER	634,000,000	2700	2360	-1	7	120	30	21.1445	78.8554	135	750	1000	35	1.6	53000	485,000,000	1982
SMACKOVER	GRAVES	500,000,000	2400	21700	43970	20	20	25	35	65	120	500	1000	20	56	43000	165,000,000	1977
EL DORADO, SOUTH	NACATOCH	283,304,000	2100	-1	10651	53.3684	20	25	58	42	110	-1	194.627	32	6.5	30000	102,000,000	1977
SACATOSA	SAN MIGUEL 1	210,700,000	1248	12264	500	10	23	25	39.088	60.912	71	1228	3.6	40	1.7	31.9	20,000,000	1982
SMA CKOV ER	BLOSSOM	210,000,000	2600	21760	43970	20	11	28	40	60	125	200	1500	20	71.2	45000	65,000,000	1977
LOMA NOVIA	LOMA NOVIA SAND	176,000,000	2750	-1	7400	10	16	29	42	58	114	1197.2	600	26	40	13000	47,800,000	1981
SANDY BEND	NACATOCH	155,000,000	2300	8200	-1	10	30	25	42	58	115	350	1800	19	12	35000	11,470,000	1981
GOVERNMENT WELLS NORTH	GOVERNMENT WELLS SAND	150,000,000	2200	-1	5611	10	25	32	-1	-1	114	100	800	21	2.32271	5680	77,580,000	1982
OAIBOURNE	NACATOCH	145,000,000	1250	1112	1345	40	90	30	37.194	62.806	100	100	140	37.1	3.06	25000	62,000,000	1982
STEPHENS	BUCKRANGE	126,000,000	2100	18000	5980	20.316	5.3	31	47	57	114	917.7	92	30	12	58800	21,400,000	1981
TAYLOR INA	NAVARRO RESERVOIR	123,400,000	900	-1	4700	7	20	32	52	48	80	401.7	85	16	390	-1	34,300,000	1982
SLOCUM	CARRIZO SAND	114,100,000	530	-1	2500	5	24	37	61	39	75	120	2655	19	1000	-1	45,000,000	1982
PIEDRE LUMBRE	GOVERNMENT WELLS SAND	95,000,000	1950	1135	1135	10	18	32.5	21	79	110	300	288	21.2	9.8	58300	20,830,000	1982
CORSICANA	SHALLOW	88,751,500	1125	-1	4000	10	14	39	-1	-1	79.125	-1	1700	36	9.91691	-1	39,077,200	1976
LUNDELL	COLE SAND	85,100,000	1550	-1	5000	89	12	32	51	49	111	300	2630	19.3	22.5	-1	9,870,000	1982
OHERN	PETTUS	83,000,000	2800	-1	2300	10	23	28	-1	-1	136	-1	286	29.4	2.19448	-1	29,000,000	1982
LOPEZ	MIRANDO SAND	75,000,000	2250	-1	3544	10	22	32	38	62	111	720	500	21	8.9	22700	30,540,000	1982
BELLEVUE	NACATOCH	68,200,000	900	720	900	15	40	37	39	61	75	401.7	1387.18	19.5	675	22700	12,500,000	1982
STEPHENS	SMART AREA (TOKIO)	67,067,900	2650	-1	5320	37.8788	14	25	46	54	115	-1	124.561	30	8	-1	19,900,000	1981
CHAMPAGNOLLE	OLD	66,275,000	2690	-1	4475	13.473	10	30	40	60	115	-1	506.25	22	35	-1	29,140,000	1981
KAYE	NAVARRO	65,520,900	2500	4760	4760	20	10	23	-1	-1	102.5	-1	256.295	36	2.69015	-1	3,340,000	1982
IRMA	OLD NACATOCH	62,200,000	1150	-1	2300	20	13	40	55	45	88	-1	1500	14	377.394	-1	10,646,700	1977
GOVERNMENT WELLS, SOUTH	GOVERNMENT WELLS	60,000,000	2200	6060	4500	28	10	30	30	70	105	100	300	21.4	15.9	10000	27,000,000	1982
SUMERSET	OLMOS B	59,000,000	1000	-1	-1	20	-1	0.28	-1	-1	92	-1	85	34	-1	-1	14,827,300	1977
WORTHAM		56,000,000	2900	-1	800	30	35	27	-1	-1	109.3	-1	1620	39	4.04654	-1	24,500,000	1982
HOFFMAN		48,350,000	2000	-1	4700	16	9	30	-1	-1	94	-1	750	23	27.2295	-1	18,000,000	1981
ESPERANCE POINT	VARIOUS	48,200,000	56.3	5181	-1	40	70	30	35	65	169	2667	287	45	0.6	50000	19,500,000	1981
MIRANDO CITY	MIRANDO SAND	46,000,000	1600	-1	500	-1	20	32	-1	-1	87.2	-1	1600	22	33.6272	-1	12,100,000	1981
LISBON	NACATOCH	45,173,000	2060	6800	-1	10	10	25	53	47	110	900.5	1500	34	7.6	30000	16,400,000	1982
COLE, WEST	MIRANDO SAND	42,700,000	2375	-1	2375	21	16	29	52	48	115	1035.95	850	22	8.3366	-1	3,190,620	1977
AVIATORS	MIRANDO SAND	40,700,000	1700	-1	1840	10	16	32	47	53	107	745.7	400	21	32	-1	9,750,000	1977
CEDRO HILL	COLE SAND	38,000,000	1440	-1	1800	34	12	35	54	46	105	633.9	800	19.2	29.895	-1	6,403,540	1977
RED RIVER BULL BAYOU	TUSC	37,617,000	2350	7151	6500	63.2549	8	20	27	73	138	500	350	42	0.9	50000	19,208,000	1982

# Illinois Basin

Field Name	Reservoir Name	OOIP (BBL)	Depth (Feet)	Field Acres	Proven Acres	Well Spacing (Acres)	Net Pay (Feet)	Porosity (%)	So (%)	Sw (%)	Temp (°F)	Pressure (PSI)	Permeability (MD)	API Gravity	Viscosity (CP)	Salinity (PPM TDS)	Cum Oil Prod (BBL)	Year for Cum Oil
POOLE CONSOLIDA\ED	TAR SPRINGS	102,530,000	1946	7080	7080	13.055	14	28	62.3794	37.6206	87.244	-1	358.122	34	4.04451	-1	32,046,600	1975
HITESVILLE CONSOLIDATED	PENNSYLVANIAN	53,060,000	1016	2850	-1	14.1042	18	28.9834	-1	-1	74.224	-1	440.537	38	5.93062	-1	14,854,500	1975
CABORN CONSOLIDATED	MANSFIELD	49,073,800	659	1930	1930	10	27	19	41	59	63	300	183	34	7	25000	9,086,000	1980
TAFFY	TAR SPRINGS	45,989,400	400	2640	2600	7	19	21	-1	-1	85	-1	95	34	8	-1	14,407,800	1975
UNIONTOWN CONSOLIDATED	PENNSYLVANIAN	45,300,000	765	2920	2920	13.5526	15	29	-1	-1	70.71	-1	442.051	36	11.163	-1	25,391,900	1975
HEUSLER CONSOLIDATED	MANSFIELD	34,855,100	1470	2340	2340	10	21	16	42	58	72	300	180	37	24	33000	9,399,940	1977
SMITH MILLS CONSOLIDATED	PENNSYLVANIAN	26,060,000	1507	2290	-1	17.2653	11	28	-1	-1	81.098	-1	358.122	34	6.06303	-1	13,671,500	1975

# **Laramie Basin**

Field	Reservoir	OOIP	Depth	Field	Proven	Well	Net Pay	Porosity	So	Sw	Temp	Pressure	Permeability	API	Viscosity	Salinity	Cum Oil	Year for
Name	Name	(BBL)	(Feet)	Acres	Acres	Spacing (Acres)	(Feet)	(%)	(%)	(%)	(°F)	(PSI)	(MD)	Gravity	(CP)	(PPM TDS)	Prod (BBL)	Cum Oil
ROCK RIVER	CRETACEOUS	60,770,000	2750	1235	-1	12	69	17	-1	-1	104	400	20	36	1	6720	38,020,000	1981

# Los Angeles Basin

Field	Reservoir	OOIP	Depth	Field	Proven	Well	Net Pay	Porosity	So	Sw	Temp	Pressure	Permeability	API	Viscosity	Salinity	Cum Oil	Year for
Name	Name	(BBL)	(Feet)	Acres	Acres	Spacing (Acres)	(Feet)	(%)	(%)	(%)	(°F)	(PSI)	(MD)	Gravity	(CP)	(PPM TDS)	Prod (BBL)	Cum Oil
YORBA LINDA	SHALLOW	357,000,000	650	-1	-1	0.780856	400	30	-1	-1	85	-1	371.939	12.7	1154.67	-1	51,800,000	1980

# **Marathon Thrust Belt**

Field	Reservoir	OOIP	Depth	Field	Proven	Well	Net Pay	Porosity	So	Sw	Temp	Pressure	Permeability	API	Viscosity	Salinity	Cum Oil	Year for
Name	Name	(BBL)	(Feet)	Acres	Acres	Spacing (Acres)	(Feet)	(%)	(%)	(%)	(°F)	(PSI)	(MD)	Gravity	(CP)	(PPM TDS)	Prod (BBL)	Cum Oil
TOBORG	TORBORG SAND	204,200,000	500	-1	5000	5	27	30	53	47	73	100	86	21	371	25000	116,000,000	1982

# Nemaha Uplift

Field	Reservoir	OOIP	Depth	Field	Proven	Well	Net Pay	Porosity	So	Sw	Temp	Pressure	Permeability	API	Viscosity	Salinity	Cum Oil	Year for
Name	Name	(BBL)	(Feet)	Acres	Acres	Spacing (Acres)	(Feet)	(%)	(%)	(%)	(°F)	(PSI)	(MD)	Gravity	(CP)	(PPM TDS)	Prod (BBL)	Cum Oil
SHANNON	LAYTON	53,463,700	2314	2080	1340	20	50	18	-1	-1	101.652	-1	55	42	1.13791	-1	6,030,000	1980
ROCK	BARTLESVILLE	44,760,000	2765	-1	760	40	30	18	-1	-1	109.77	-1	15	38	1.27802	-1	10,888,500	1975

# **North-Central Montana Basin**

Field	Reservoir	OOIP	Depth	Field	Proven	Well	Net Pay	Porosity	So	Sw	Temp	Pressure	Permeability	API	Viscosity	Salinity	Cum Oil	Year for
Name	Name	(BBL)	(Feet)	Acres	Acres	Spacing	(Feet)	(%)	(%)	(%)	(°F)	(PSI)	(MD)	Gravity	(CP)	(PPM TDS)	Prod (BBL)	Cum Oil
						(Acres)												
CUT BANK	CUT BANK SAND	730,000,000	2950	65000	-1	160	19	13	40	60	85	1500	57	37	2.6	8000	126,000,000	1982
CAT CREEK	CAT CREEK SANDS	30,000,000	1100	-1	-1	6.08334	30	21.5	36.4813	63.5187	77.6	-1	139.982	52	1.14702	1690	22,112,000	1982
WHITLASH	SWIFT-SUNBURST	25,700,000	2600	1920	1950	20	15	16	75.1147	24.8852	101.6	-1	26.2144	38	1.50428	-1	4,900,000	1982
FRED & GEORGE CREEK	SUNBURST	21,629,000	2600	1040	-1	40	16	28	41	59	80	2000	1270	41	1.4	7100	9,802,000	1982

# **Powder River Basin**

Field	Reservoir	OOIP	Depth	Field	Proven	Well	Net Pay	Porosity	So	Sw	Temp	Pressure	Permeability	API	Viscosity	Salinity	Cum Oil	Year for
Name	Name	(BBL)	(Feet)	Acres	Acres	Spacing (Acres)	(Feet)	(%)	(%)	(%)	(°F)	(PSI)	(MD)	Gravity	(CP)	PPM TDS	Prod (BBL)	Cum Oil
SALT CREEK	2ND WALL CREEK AMOCO OPERATED	786,000,000	1950	12770	24509	10	71	19	59.8145	40.1855	100	650	52	37	3.1	-1	340,400,000	1982
SALT CREEK	FIRST WALL CREEK-MAIN RSVR ONLY	288,000,000	1200	-1	-1	10	71.4	17.8	28	72	85	550	12.4	40	1.443	-1	105,450,000	1982

# San Joaquin Basin

Field	Reservoir	OOIP	Depth	Field	Proven	Well	Net Pay	Porosity	So	Sw	Temp	Pressure	Permeability	API	Viscosity	Salinity	Cum Oil	Year for
Name	Name	(BBL)	(Feet)	Acres	Acres	Spacing (Acres)	(Feet)	(%)	(%)	(%)	(°F)	(PSI)	(MD)	Gravity	(CP)	(PPM TDS)	Prod (BBL)	Cum Oil
COALINGA	TEMBLOR	3,210,000,000	2800	19200	10560	6	165	26.9	52	48	100	700	683	22.8	50	5000	682,000,000	1982
BUENA VISTA	FRONT - HILLS - UPPER	1,450,000,000	2500	2357	-1	6.35593	80	30	48	52	140	-1	500	26.5	4.27402	-1	455,200,000	1982
ROUND MOUNTAIN	ROUND MTN JEWETT & PYRAMID HILL	280,000,000	1791	2500	620	9	72	35	40	60	111	250	170	21.3	100	1000	89,200,000	1972
MOUNT POSO	UPPER VEDDER	273,500,000	1800	3645	-1	5	59	33	58	42	110	100	2200	16	277	1225	123,800,000	1983
ROUND MOUNTAIN	VEDDER	176,000,000	2300	1415	990	9	67	35	43	57	110	250	6000	15	300	2300	59,600,000	1972
BELRIDGE NORTH	TULARE	136,000,000	900	2100	-1	-1	40	33	69	31	95	100	2000	13	1875	14000	8,000,000	1980
KERN BLUFF	MIOCENE	61,300,000	1082	670	610	7	70	29	48	52	97	479.96	5000	15	1500	90	10,686,000	1982
TEJON GRAPEVINE	WESTERN AREA S	56,100,000	2649	880	540	6	55	29	42	58	127	940	2000	15.8	167	1100	16,100,000	1980
ROUND MOUNTAIN	COFFEE CANYON-VEDDER & PYRAMID HILL	53,200,000	1500	435	435	9	82	32	36	64	105	250	1500	16.9	300	1000	18,500,000	1972
ANT HILL	OLCESE	48,000,000	2286	295	285	10	100	34	57	43	122	-1	350	13.5	3000	1500	5,851,480	1977
WHITE WOLF	REEF RIDGE	30,000,000	2500	200	-1	20	100	30.8	62.5933	35	105	610	393	14.4	2000	16000	8,000,000	1983
ANTELOPE HILLS	WILLIAMS AREA EAST BLOCK AGUA	28,000,000	2300	535	145	10	80	33	54	46	123	-1	698.242	18.9	11.6708	2600	6,600,000	1980
WHEELER RIDGE	CENTRAL AREA COAL OIL CANYONMAIN	24,800,000	2350	1200	170	10	100	29	58	42	121	-1	363.051	22.3	6.90489	6000	9,300,000	1980
CYMRIC	SHEEP SPRINGS ETCHEGOIN	21,800,000	2450	4500	170	5	40	35	54	46	123	500	750	17	30	15000	3,807,300	1982
JASMIN	CANTLEBERRY VEDDER (2 AREAS)	20,700,000	2800	460	410	7	26	35	40	59	125	900	1055.02	13	300	170	2,450,000	1980

# San Juan Basin

Field	Reservoir	OOIP	Depth	Field	Proven	Well	Net Pay	Porosity	So	Sw	Temp	Pressure	Permeability	API	Viscosity	Salinity	Cum Oil	Year for
Name	Name	(BBL)	(Feet)	Acres	Acres	Spacing (Acres)	(Feet)	(%)	(%)	(%)	(°F)	(PSI)	(MD)	Gravity	(CP)	(PPM TDS)	Prod (BBL)	Cum Oil
HORSESHOE	GALLUP	97,400,000	1500	7490	-1	40	18	15.5	46	54	87	-1	14	42	1.63	19000	36,700,000	1981

# Southern Oklahoma Basin

Field	Reservoir	OOIP	Depth	Field	Proven	Well	Net Pay	Porosity	So	Sw	Temp	Pressure	Permeability	API	Viscosity	Salinity	Cum Oil	Year for
Name	Name	(BBL)	(Feet)	Acres	Acres	Spacing	(Feet)	(%)	(%)	(%)	(°F)	(PSI)	(MD)	Gravity	(CP)	(PPM TDS)	Prod (BBL)	Cum Oil
						(Acres)												
HEARLDTON	PENNSYLVANIAN	940,000,000	1700	-1	1500	2.25226	104	24	-1	-1	80	300	386	30	13	86452	310,760,000	1981
HEWITT	PENNSYLVANIAN	591,000,000	900	2610	2600	20	90	21	47.7942	52.2058	96	-1	184	35	8.7	118900	257,352,000	1982
EOLA ROBBERSON	BROMIDE	330,000,000	1300	1960	648	81.8095	148	10	81.4232	18.5767	92	-1	196	39	3.8	208458	125,190,000	1981
LOCO	LOCO DEEP - HOXBAR SAND	71,640,000	1200	-1	-1	10	27	21	-1	-1	185	-1	180	24	263	-1	8,180,000	1981

# Ventura Basin

Field	Reservoir	OOIP	Depth	Field	Proven	Well	Net Pay	Porosity	So	Sw	Temp	Pressure	Permeability	API	Viscosity	Salinity	Cum Oil	Year for
Name	Name	(BBL)	(Feet)	Acres	Acres	Spacing (Acres)	(Feet)	(%)	(%)	(%)	(°F)	(PSI)	(MD)	Gravity	(CP)	(PPM TDS)	Prod (BBL)	Cum Oil
PLACERITA	ALL AREAS	314,000,000	1527	715	700	3	300	33	50	50	100	100	2500	15.9	1440	2200	43,600,000	1982
SHIELLS CANYON	SESPE	81,000,000	1000	965	-1	6.43333	59	29	-1	-1	70	-1	436.711	32	18.9898	35910	23,200,000	1980
OAKRIDGE	MIOCENE	45,500,000	2450	425	425	14	90	30	37	63	119	-1	135	20.4	16.6	342	13,000,000	1982
CAPITAN	VAQUEROS	38,000,000	1400	270	260	5	150	21	54	46	100	100	2500	22	20	1400	12,700,000	1983
OAK PARK	SESPE UPPER	26,600,000	1420	150	100	3	400	20	44	56	97	-1	235	23	19.4493	7150	6,273,550	1977

# **Technology Transfer**

### **Publication**

Jikich, S., J. Grube, B. Seyler, N. Webb, and J. Damico, 2012 Reservoir Characterization Aids Implementation of Alkaline-Surfactant-Polymer in Illinois Basin, American Oil Reporter, June, 2012

### **Abstracts for Poster Presentations**

Beverly Seyler, John Grube, Bryan G. Huff, Curt S. Blakley, and Philip Johanek, 2009, Reservoir Characterization of the Mississippian Cypress Sandstone at Lawrence Field, Illinois, Program with abstracts 2009 Eastern Section American Association of Petroleum Geologists p. 50

John P. Grube, James Damico and Beverly Seyler, 2009, Enhanced Oil Recovery and CO<sub>2</sub> Sequestration Potential of Chesterian (Mississippian) Sandstones in the Illinois Basin in Program with abstracts 2009 Eastern Section American Association of Petroleum Geologists p. 38

Curt S. Blakley, John P. Grube, Philip Johanek, Vineeth Madhavan, Nathan Webb and Beverly Seyler, 2010, Characterization of Pennsylvanian Bridgeport Sandstones in the Illinois Basin, Proceedings from Annual Meeting of Eastern Section of American Association of Petroleum Geologists, Program with Abstracts, Kalamazoo, MI, September 25-29, 2010, pg. 41.

Grube, J.., Damico, J.R., B. Seyler and S. M. Frailey, 2010, Characterization of Compartmentalized Reservoirs for EOR Pilots within the Illinois Basin, Proceedings from Annual Meeting of Eastern Section of American Association of Petroleum Geologists, Program with Abstracts, Kalamazoo, MI, September 25-29, 2010, pg. 41.

Beverly Seyler, John Grube, Bryan G. Huff, Curt S. Blakley, James Damico, Philip Johanek, Vineeth Madhavan, and Nathan Webb, 2010, Reservoir Characterization for Enhanced Oil Recovery in Middle Mississippian Cypress Sandstones at Lawrence Field, Illinois, AAPG abstract volume 2010 Annual Conference.

Vineeth Madhavan, Nathan D. Webb, John P. Grube, Curt S. Blakley, Beverly Seyler, Philip Johanek, 2011, Reservoir Characterization for the Application of ASP Flood Technology in the Bridgeport Sandstone in Lawrence Field, Illinois, AAPG National Meeting Houston, Texas, April 12, 2011

John P. Grube, Curt S. Blakley, James R. Damico, Philip Johanek, Vineeth Madhavan, Roland Okwen, Beverly Seyler, and Nathan D. Webb, 2012, Alkaline-Surfactant-Polymer Flood Application for Enhanced Oil Recovery Has Potential for Significant Recovery of Remaining Reserves in the Mature Lawrence Field, Illinois, National AAPG meeting, Long Beach, California April, 2012.

Nathan D. Webb, John Grube, Curt S. Blakley, Beverly Seyler, Vineeth Madhavan, 2012, Reservoir Characterization of Lower Pennsylvanian Sandstones for the Application of ASP Flood

Technology in Lawrence Field, Illinois

### **Presentations**

Two poster presentations were given at the Eastern Section American Association of Petroleum Geologist Meeting in Kalamazoo, Michigan on September 27, 2010 and have been posted on the Illinois State Geological Survey website at <a href="http://www.isgs.uiuc.edu/sections/oil-gas/pdf-files/lawrence-field.pdf">http://www.isgs.uiuc.edu/sections/oil-gas/pdf-files/lawrence-field.pdf</a>.

Presentations pertinent to the project were made at a PTTC Workshop on Enhanced Oil Recovery held in Evansville, Indiana, on March 2, 2011 in conjunction with the annual Illinois Oil and Gas Association Meeting.

A poster session entitled Reservoir Characterization for the Application of ASP Flood Technology in the Bridgeport Sandstone in Lawrence Field, Illinois was presented by Vineeth Madhavan in Houston, TX on September 8 and 9, 2011. This presentation was given in conjunction with a training course in modern fluvial and coastal environments that are modern analogs to the environments of deposition in the Pennsylvanian formations and the Mississippian Cypress Formation in Lawrence Field

Scott Frailey gave a presentation at the SPE Forum in Dallas, Texas on December 13, 2011 that highlighted the Lawrence Field ASP EOR project. The presentation was made at the 2011 Dallas E&P Forum sponsored by SPE Dallas and SIPES entitled, "Raising the Dead: New Techniques and Technologies for Bringing Old Oil Fields Back to Life."

Damico, J.R., 2012, *ASP Flooding in the Illinois Basin*, An oral presentation at the PTTC sponsored Enhanced Oil Recovery Workshop held in conjunction with the Annual Eastern Section of the American Association of Petroleum Geologists meeting in Cleveland, Ohio, on September 22, 2012.

### Summary

Reservoir characterization under this DOE grant supported research for implementation of Alkaline- Surfactant-Polymer Floods in two distinct sandstone reservoirs in Lawrence Field, Lawrence County, Illinois. ASP flooding was an untested technology in the Illinois Basin and this project presented an exceptional opportunity to conduct reservoir characterization in support of this unconventional recovery technique on two of Illinois's most prolific reservoirs.

Most of the unrecovered oil in Lawrence Field is contained in Pennsylvanian age Bridgeport sandstones and Mississippian age Cypress sandstones. These reservoirs are highly complex and compartmentalized. Detailed reservoir characterization including the development of 3-D geologic and geocellular models of target areas in the field were completed to identify areas with the best potential to recover remaining reserves including unswept and by-passed oil.

This four year project was designed to compile, interpret, and analyze the data required to conduct reservoir characterization for the Bridgeport and Cypress sandstones in pilot areas and expansion areas in preparation for full scale commercial implementation of ASP flooding in Lawrence Field. Geologic and geocelluar modeling needed for reservoir characterization and reservoir simulation were completed for the purpose of designing effective ASP flood patterns for individual reservoir compartments. Characterizing the complex reservoir geology that identifies the geologic conditions that will optimize oil recoveries for expansion of the ASP flood from small, limited pilots in the Bridgeport and Cypress sandstones to a larger area of Lawrence Field was the primary objective of this project. The success of the ASP test pilot in the Middagh lease in increasing production from 1% to 12% oil cut suggests that these reservoirs likely possess reservoir qualities suited for successful implementation of this EOR technique on a commercial scale. Additional objectives of this project included assessing the applicability of ASP flood technology to similar reservoirs in the Illinois Basin and other U.S. reservoirs.

Reservoir characterization has a critical role in the development of a complex chemical EOR process such as ASP, especially in highly compartmentalized reservoirs that extend laterally from several acres to tens of acres in size. A synergistic approach between reservoir characterization and formation evaluation coupled with reservoir modeling and simulation, reservoir management, well management and corresponding surface facilities is the best approach to assure success in chemical flooding involving a high degree of technology such as ASP.

Two distinctive types of reservoir sandstones were identified in the Pennsylvanian Bridgeport B interval in Lawrence Field. These two reservoir types were deposited at different times and under different environmental settings resulting in large variations of reservoir qualities. The thickest reservoir sandstone identified in the Bridgeport B interval consisted of relatively thick, 100 feet or more medium grained channel fill sandstones located and mapped in Section 5 T3N R12W of Lawrence County. The channel fill sandstones are highly porous and permeable with average porosity of 20 percent or greater and average permeability greater than 300 md. The channel fill sandstones were deposited in channels incised into the original Bridgeport B siliciclastics and are younger than the fine grained elongate east west oriented, thinner sandstone deposited in Section 32 R4N T12W of Lawrence County. The sequence stratigraphic framework developed during this study show that depositional environments of the Pennsylvanian

Bridgeport sandstone reservoirs are complex and are characterized by sea level drop resulting in regressive incisement, followed by transgressive infill packages that commonly show tidal influence in the upper sediments of the cycle.

The potential for channelized flow in more permeable portions of the channel fill facies in Section 5 versus reservoir sandstone lenses with lower permeability found in the thinner fine-grained elongate Bridgeport B sandstone facies in Section 32 has added to the difficulty of implementing EOR techniques in these reservoirs. The more permeable intervals likely have less residual oil as primary production and secondary waterflooding have selectively recovered more oil from these intervals while leaving more recoverable oil in the less porous and permeable intervals. Thus, techniques to reduce channelized flow must be designed and implemented. Compartments can be most effectively drained where they are geologically well defined and reservoir management practices are coordinated through unified, compartment-wide, development programs

The overprint of diagenetic alteration has added to the high degree of variability in these reservoirs taking place over a geologic time frame resulting in reservoir areas of both enhanced and diminished porosity and permeability. Compaction of grains, particularly in some ripple-bedded intervals has greatly reduced porosity and permeability, diminishing reservoir quality. Other facies, such as the cross bedded facies in channel fill sandstones have increased porosity and permeability due to the lack of compaction. Large amounts of intregranular porosity were preserved in channel fill sandstones resulting in excellent porosity and permeability. Thin section and X-ray diffraction analysis show that the identified clay mineral suites in reservoir intervals should be considered because they are primarily located in pores where interaction with existing or injected fluids is likely. The bulk mineralogy of these sandstones consists of primarily quartz, siderite, clay minerals, carbonates and plagioclase and potassium feldspar. The clay mineral suite in most Bridgeport B interval sandstones consists primarily of kaolinite, illite, Mg rich chlorite. These data are important for determining the suitability of various EOR techniques.

Three different reservoir facies were identified in Cypress Sandstone reservoirs in cores in the pilot area in Sec. 32-T4N-R12W in Lawrence Field as well as in examination of cores in an expansion area of five square miles. Interpretation of sedimentary structures in cores, analysis of porosity and permeability data and analysis of petrographic data including XRD analyses, thin section analyses, and SEM/EDX analyses show distinctive characteristics of three different reservoir facies with different flow unit characteristics within the Cypress Sandstone. The most common reservoir facies consists of ripple- bedded fine- grained to very fine- grained sandstone with occasional occurrences of herringbone cross bedding and tidal couplets. The ripple-bedded reservoir facies has core measured porosity values ranging from 16% to 19% and core measured permeability values most commonly in the 100 md. range. A second less common reservoir facies consists of obscurely bedded, bioturbated, poorly sorted, fine-grained sandstone. Core measured porosity commonly exceeds 20% and permeabilities are commonly greater than 200 md. in this facies. The obscurely bedded facies has the highest core measured porosity and permeability values observed in Cypress sandstone reservoirs in the study area. It is interpreted that a tidally dominated depositional system has introduced a high level of reservoir compartmentalization in Cypress reservoirs. Petrographic examination also shows differences between these two reservoir facies that increase reservoir complexity and introduce production obstacles on a microscopic scale. Both reservoir facies contain clay mineral suites that may be

reactive to fluids introduced for enhanced oil recovery treatments. Although the volume of clay minerals is relatively low they are most commonly located in pores where they are most likely to come in contact with fluids introduced for treatments. Because these reservoirs are located in close proximity to one another Fe-rich chlorite and to a lesser degree illite and mixed layered illite/smectite should be taken into consideration when developing formulations for ASP treatments.

Aseries of isopach maps of the five square mile area surrounding the initial Cypress sandstone ASP pilot in the Griggs lease in Section 32 T4N R12W were constructed using the 50 percent clean sandstone normalized Spontaneous Potential curves on geophysical logs for each of the Cypress intervals including the B, C, D, and E intervals. These intervals are interpreted to be tidal shoal deposits similar to those found in modern high tidal range settings. The elongated, shoal geometries are oriented in a northeast-southwest direction. These maps illustrate sandstone lense geometries that individually are up to ten feet thick and average a few to many tens of acres in size. Correlation of individual intervals can be difficult as they rapidly pinch and swell within the Lawrence Field Cypress intervals.

While compartmentalization is evident in all the targeted sandstones, some sandstones exhibit a directional orientation that must be considered in reservoir development for the most effective recovery of petroleum. Effective implementation of flooding in pilot areas should take into account compartment orientation that is dictated by depositional trends and type and location of permeability barriers. The more promising and connected reservoirs in the pilot area appear to be in the Pennsylvanian age Bridgeport B and some of the Cypress intervals contain more continuous and better developed reservoir sandstones. Reservoir characterization of Cypress sandstone lenses show that these sandstones contain intervals of highly variable vertical permeability. Interpretation of the Cypress Sandstone interval in cross sections in Section 32-T4N-R12W suggest that permeability barriers are subtlety reflected on geophysical logs but, likely play a major role in compartmentalization of these reservoirs. Intervals with very high permeability may be susceptible to channeling. It is more difficult to define separate reservoir compartments in the Mississippian Cypress Sandstone than in the Bridgeport Sandstone.

Assessment of several Chesterian age Cypress sandstone reservoirs in different fields in the Illinois Basin confirms the widespread nature of tidally deposited elongate sandstone lenses orientated in a northeast-southwest direction. The Cypress sandstone reservoirs in the Richview and Tamaroa Fields in Illinois exhibit similarities to those found in Cypress Sandstone reservoirs in Lawrence Field. These reservoirs are composed of thin, stacked, elongate, compartmentalized sandstone lenses. Knowledge of reservoir sandstone geometries and the ability to map their boundaries plays an important role in successful implementation of ASP flood technology. The theme of tidally influenced deposition in most Chesterian age strata aids in accurately mapping reservoir sandstone geometries and offers insights to mapping and correctly orienting reservoir flow units and identifying potential permeability barriers.

### **Conclusions**

The focus of this study was on reservoir characterization in support of an ASP pilot project in Lawrence Field Illinois. The targeted EOR reservoirs are in shallow Pennsylvanian age Bridgeport and Mississippian Chesterian age sandstones that were nearing depletion after decades of primary and waterflood production starting as early as 1906. An ASP flood was successfully implemented in a pilot area in the Middagh lease in Section 32 T4N R12W in Lawrence Field in eastern Illinois. The pilot was completed in a Pennsylvanian age Bridgeport B sandstone reservoir that detailed mapping showed consisted of an east west trending elongate sandstone body bounded on the north and south by impermeable shale. The success of increasing the oil cut from 1% to 12% in the 15 acre 18 well ASP pilot suggests that detailed reservoir characterization of individual reservoirs can be utilized as a tool to successfully apply ASP flood technology more broadly in Lawrence Field as well as in other mature oil fields in the Illinois Basin and mature oil provinces across the United States. The substantial increase in production following the ASP flood in the Middagh pilot suggests that there is likely sufficient remaining unswept petroleum to warrant expansion to larger areas of Lawrence Field. The low oil cut at Lawrence Field is representative of most mature fields in the Illinois Basin and highlights the potential for additional petroleum recovery in reservoirs similar to those in Lawrence Field. Rex Energy Corporation has identified a large 351 acre expansion area located to the south of the Middagh lease. Detailed characterization of the geologic parameters of individual reservoirs in Lawrence Field illustrated large variations in reservoir qualities such as reservoir thickness, porosity, permeability, mineralogy, geometry, flow units, depositional facies, location of permeability barriers and diagenetic alteration over short distances. These factors in large part control reservoir quality and impact the location of reservoir fluid and may aid in identifying the location of unswept oil. Mapping the location, thickness, depth and lateral extent of individual reservoir compartments are needed for successful, commercially viable injection of ASP fluids to most effectively recover unswept oil. Accurately delineating reservoir compartments is essential in preventing loss of injection fluids off pattern and detailed definition of reservoir compartments is needed to strategically locate injection wells.

Assessment of similar reservoirs in the Illinois Basin suggests that there are numerous opportunities in mature reservoirs in Pennsylvanian and Middle Mississippian Chesterian age sandstones for much broader application of ASP flood technology. Most sandstone reservoirs in the Illinois basin are compartmentalized, shallow, fine-grained and possess reservoir qualities that are similar to those described in this study with porosity ranging from 16 to 20 percent and permeability ranging from 75md to 1000md. A major finding of this study is that each potential EOR reservoir must be evaluated separately. It is particularly important to define reservoir geometries and to establish the location of reservoir boundaries to ensure economic strategies for injecting fluids. Other findings for this study include general geologic considerations that may be used to more broadly apply ASP flood technology to the Illinois Basin and other basins with sandstone reservoirs in the US.

Reservoirs within Lawrence Field are characterized as being highly compartmentalized resulting in multiple flow unit configurations. In order to help characterize such complex systems and visualize the complexities, a strategy was developed to utilize a conceptual geologic model to guide the construction of geocellular models of the reservoir architecture. The process combines traditional methods along with geostatistical methods. This combined process creates a beneficial check and balance loop where the geocellular and the geological models should complement

each other. Cases where the resulting models show significant discrepancies must be resolved either by reinterpreting the geologic model or resolving input errors to the numerical model. The geostatistically generated geologic model (porosity, permeability, thickness, geometry, and depth) is also used as input to the reservoir simulation model. The more consistent the geostatistical model is to the actual geology, the more relevant the simulation model results will be and greater the likelihood of the success of an EOR project. In the case of the Bridgeport B sandstone reservoir modeled in Section 32 T4N R12W, there was excellent agreement between the independently created geologic and geocellular models. The agreement between the two models increased the likelihood of reservoir simulation accurately predicting reservoir behavior during the ASP pilot flood.

Compartmentalization of reservoir sandstones is controlled in part by the prevailing conditions and environments during deposition. Interior cratonic seas with low subsidence rates gave rise to widespread, complex and discontinuous reservoir sandstone lenses in Pennsylvanian and Middle Mississippian strata. Confined basin configuration with shallow water depths stimulated tidal currents that spread, reworked, and stacked siliciclastic sediments. Post-Pennsylvanian deformation formed structures that trap petroleum where stratigraphically complex sandstones form along or near the structural crest of the LaSalle Anticlinal Belt. Sedimentary structures observed in numerous core of the reservoir interval are diagnostic of deposition by tidal processes. Cypress reservoirs contain lateral and vertical permeability barriers forming compartments that vary substantially in size and geometry. Permeability barriers can be difficult to distinguish on logs and can cause correlation problems. Generally, individual compartments tend to be 10 feet or less in thickness, sandstones greater than 10 feet thick are commonly stacked or shingled sandstones. Individual compartments should display geometries indicative of their environment of deposition. Compartments can be most effectively drained where they are geologically well defined and reservoir management practices are coordinated through unified, compartment-wide, development programs.

Reservoir characterization is important for implementation of Enhanced Oil Recovery programs because the economic success of an EOR project is dependent on the design and implementation of the project being aligned with the unique geologic characteristics of each reservoir. The potential for channelized flow in the more permeable portions of the Pennsylvanian channel fill facies in Section 5 and the cross-bedded facies in the lower portion of the Bridgeport B sandstone reservoir in Section 32 versus intervals with low permeability has added to the difficulty of implementing EOR techniques in these reservoirs. The more permeable intervals have less residual oil as primary production and secondary waterflooding have selectively recovered more oil from these intervals while leaving more recoverable oil in the less porous and permeable intervals. Thus, techniques to reduce channelized flow must be designed and implemented.

Compartments can be most effectively drained where they are geologically well defined and reservoir management practices are coordinated through unified, compartment-wide, development programs. The overprint of diagenetic alteration has added to the high degree of variability in these reservoirs taking place over a geologic time frame resulting in areas of both enhanced and diminished porosity and permeability. Compaction of grains, particularly in some fine to very fine-grained ripple-bedded intervals has greatly reduced porosity and permeability, diminishing reservoir quality. Other facies, such as the cross bedded facies have increased

porosity and permeability due to the lack of compaction in channel fill deposits. Thin section and X-ray diffraction analysis shows that the identified clay mineral suite in reservoir intervals should be considered because they are primarily located in pores where interaction with existing or injected fluids is likely. These data are important for determining the suitability of various EOR formulations and techniques.

Depositional environments of the Pennsylvanian Bridgeport sandstone reservoirs are complex and are characterized by sea level drop regressive incisement, followed by transgressive infill packages that commonly show tidal influence in the upper sediments of the cycle. Understanding the depositional setting is necessary to unravel the complexity of the reservoir facies and their individual characteristics that are fundamental components for the design and implementation of successful ASP-EOR projects

The Bridgeport B sandstones in Section 32 may be a better area to test the ASP flood technology than the channel fill facies reservoirs in Section 5. The Bridgeport B reservoirs in this area have not been as effectively produced as the channel facies reservoirs in Section 5 because of their more compartmentalized characteristics. Yet, because these target reservoirs are more confined, flow units and their geometries tend to be more mappable and therefore the chemical flood can be designed and implemented for the greatest recovery potential. A better understanding of reservoir characteristics allows for better cost control which increases the economic feasibility of EOR projects. The thick sandstones in eastern Section 5 are along the flank of the structure with a portion of the sandstone dropping below the original oil-water contact. Loss of expensive EOR chemicals into the water zone becomes a factor. Oil saturations have been lowered due to primary and secondary production and particularly where the Maraflood Project was implemented. While highly porous and permeable reservoirs are generally very good targets for EOR application, there is less remaining oil to recover using ASP technology in the Maraflood pilot area which successfully recovered 34% of the residual oil in the channel fill sandstone in Section 5 T3N R12W. It is difficult to correlate preferential flow units within the channel facies reservoirs with standard mapping techniques using the older style SP- electric logs that are principally available throughout Lawrence Field. Recent porosity logs and core information have greatly enhanced the ability to delineate reservoir characteristics that are necessary for constructing accurate geologic and geocellular models.

The potential for channelized flow in highly permeable intervals versus intervals with low permeability has added to the difficulty of implementing EOR techniques in these reservoirs. The highly permeable intervals have likely been depleted by successful waterflooding operations leaving more recoverable oil in the less porous and permeable intervals.

Flow units are commonly related to facies. The best reservoir qualities in the study area are associated with channel fill sandstone deposits in the Pennsylvanian post Bridgeport B strata. Fluvial deposits with tabular cross bedding that fill the lower portions of incised valleys contain some of the highest porosity and permeability values measured in petroleum reservoirs in the Illinois Basin.

Petrographic examination of thin sections from Pennsylvanian Bridgeport B interval and Mississippian Cypress sandstones show that diagenetic alteration has resulted in additional compartmentalization. Cementation of reservoir quality sandstone intervals by ferroan calcite has

caused major permeability barriers/obstacles in many cored wells. Compaction of ductile grains particularly in some ripple-bedded intervals has greatly reduced porosity and permeability diminishing reservoir quality. Other facies, such as the mottled sandstone/obscurely bedded facies have increased porosity and permeability due to dissolution of feldspar grains. The overprint of diagenetic alteration has added to the high degree of variability in these reservoirs.

X-ray diffraction and thin section analysis has shown that the identified clay mineral suite in reservoir intervals should be considered because they are primarily located in pores where interaction with existing or injected fluids is likely. These data are important for determining the suitability of various EOR techniques.

Implementation of enhanced oil recovery program in mature Pennsylvanian and Chesterian sandstones has broad application in numerous shallow and older fields in the Illinois Basin and other basins in the United States. This study shows that detailed reservoir characterization is necessary for the successful application of ASP flood technology. There are many mature sandstone reservoirs found in other basins across the United States that should be good candidates for ASP flooding provided reservoir characterization drives the project.

## Acknowledgments

This project was funded in large part by U.S. Department of Energy Contract DE-NT0005664

Rex Energy Corporation is acknowledged for their cooperation and sharing of pertinent data. Their geologic staff in particular Steve Whitaker and Bruce Schonert were very helpful.

We acknowledge Landmark Graphics as part of the University Grants Program. Geographix Software was used for mapping and cross sections.

### References

- Abrams, A., 1988, The Influence of Fluid Viscosity, Interfacial Tension and Fluid Viscosity on Residual Oil Saturation Left by Waterflood, SPE Reprint Series No. 24, Surfactant/Polymer Chemical Flooding -1, SPE, Richardson, Tx, pages52-62.
- Abreu, V.; Neal, J. E.; Bohacs, K. M. & Kalbas, J. L., 2010, Sequence Stratigraphy of Siliciclastic Systems: the ExxonMobil Methodology; Atlas of Exercises, SEPM.
- Armstong, M., Gali, A. G., Le Loc'h, G., Francois, G., Eschard, R., 2003, Plurigaussian Simulations in Geosciences. Berlin, Germeany: Springer-Verlag.
- Ball, J.T. and Pitts, M.J., 1984, Effect of Varying Polyacrylamide Molecular Weight on Tertiary Oil Recovery from Porous Media of Varying Permeability, SPE/DOE 12650.
- Ball, M. M., and Perry, W.J., Jr., 1996, Bend Arch-Fort Worth Basin Province (045), in Gautier,
  D. L., Dolton, G.L., Takahashi, K.I., and Varnes, K.L., ed., 1995 National assessment of
  United States oil and gas resources; results methodology, and supporting data: U.S.
  Geological Survey Digital Data Series DDS-30, Release 2.
- Blatchley, R. S., 1913, The Oil Fields of Crawford and Lawrence Counties, Vol. 22, Illinois State Geological Survey.
- Bohacs, K. & Suter, J., 1997, Sequence Stratigraphic Distribution of Coaly Rocks: Fundamental Controls and Paralic Examples, AAPG Bulletin 81(10), 1612--1639.
- Boyd, R.; Dalrymple, R. & Zaitlin, B. A., 1992, Classification of clastic coastal depositional environments, Sedimentary Geology 80, 139-150.
- Bristol, H. M., and R. H. Howard, 1971, Paleogeologic map of the sub-Pennsylvanian Chesterian (Upper Mississippian) surface in the Illinois Basin: Illinois State Geological Survey Circular 458, in cooperation with Indiana Geological Survey and Kentucky Geological Survey, 14 p.
- Burdyn, R.F., Chang, H.L. and Foster, W.R., 1975, Alkaline Waterflooding Process," United States Patent 3,927,716.
- Burk, J.H., 1987, Comparison of Sodium Carbonate, Sodium Hydroxide, and Sodium Ortho Silicate for EOR, SPE Reservoir Engineering, pages 9-16.
- Catuneanu, O.; Abreu, V.; Bhattacharya, J. P.; Blum, M. D.; Dalrymple, R. W.; Eriksson, P. G.; Fielding, C. R.; Fisher, W. L.; Galloway, W. E.; Gibling, M. R.; Giles, K. A.; Holbrook, J.; Jordan, R.; Kendall, C. G. S.; Macurda, B.; Martinsen, O. J.; Miall, A. D.; Neal, J. E.; Nummedal, D.; Pomar, L.; Posamentier, H. W.; Pratt, B. R.; Sarg, J. F.; Shanley, K. W.; Steel, R. J.; Strasser, A.; Tucker, M. E. & Winker, C., 2009, 'Towards the Standardization of Sequence Stratigraphy', Earth-Science Reviews 92(1-2), 1--33.

- Charpentier, R. R., 1995, Forest City Basin Province (056), in Gautier, D. L., Dolton, G.L., Takahashi, K.I., and Varnes, K.L., ed., 1995 National assessment of United States oil and gas resources-Results, methodology, and supporting data: U.S. Geological Survey Digital Data Series DDS-30, Release 2, one CD-ROM.
- Clark, S.R., Pitts, M.J., and Smith, S.M., 1993, Design and Application of an Alkaline-Surfactant-Polymer Recovery System to the West Kiehl Field, SPE Advanced Technology Series, Vol. 1, pages 172-179.
- Clegg, K. E., 1959, Subsurface geology and coal resources of the Pennsylvanian System in Douglas, Coles, and Cumberland Counties, Illinois, Illinois State Geological Survey, pp. 16.
- Clifton, H. E., 1982, M 31: Sandstone Depositional Environments, American Association of Petroleum Geologists, chapter Estuarine Deposits, pp. 179--189.
- Craig, Jr., F.F., 1993, The Reservoir Aspects of Waterflooding. SPE Monograph Series, vol. 3, 4th edition.
- Dalrymple, R. W. & Choi, K., 2007, Morphologic and facies trends through the fluvial–marine transition in tide-dominated depositional systems: A schematic framework for environmental and sequence-stratigraphic interpretation, Earth-Science Reviews 81, 135--174.
- Delshad, M., Asakawa, K., Pope, G. A., Sepehrnoori, K., 2002, Simulations of Chemical and Microbial Enhanced Oil Recovery Methods," SPE 75237.
- Dolton, G. L., 1995, Michigan Basin Province (063), in Gautier, D. L., Dolton, G.L., Takahashi, K.I., and Varnes, K.L., ed., 1995 National assessment of United States oil and gas resources-Results, methodology, and supporting data: U.S. Geological Survey Digital Data Series DDS-30, Release 2, one CD-ROM.
- Droste, J. B. & Keller, S. J., 1989, Development of the Mississippian-Pennsylvanian Unconformity in Indiana.
- Dwarakanath, V., Chaturvedi, T., Jackson, A.C., Malik, T., Siregar, A., and Zhao, P., 2008, Using Co-Solvents to Provide Gradients and Improve Oil Recovery During Chemical Flooding in a Light Oil Reservoir, SPE 113965.
- Edinga, K.J., McCaffery, F.G. and Wytrychowski, I.M., 1980, Cessford Basal Colorado A Reservoir Caustic Flood Evaluation," J. Pet. Tech., volume 32, pages 2103-2110.
- Elbe, C. F.; Greb, S. F. & Williams, D. A., 2001, The geology and palynology of Lower and Middle Pennsylvanian strata in the Western Kentucky Coal Field, International Journal of Coal Geology 47, 189--206.

- Etheredge, F. D., 1953, Electric Log Study of the Basal Pennsylvanian Sandstone, Louden Pool, Fayette County, Illinois, Master's thesis, University of Illinois.
- Flaaten, A. K., Nguyen, Q. P., Pope, G. A., Zhang, J., 2008, A Systematic Laboratory Approach to Low-Cost, High-Performance Chemical Flooding, SPE 113469.
- Frailey, S.M., I.G. Krapac, J.R. Damico, R.T. Okwen, and R.W. McKaskle, 2012a, CO2 Storage and Enhanced Oil Recovery: Bald Unit Test Site, Mumford Hills Oil Field, Posey County, Indiana. J.H. Goodwin and C.C. Monson (eds.): Illinois State Geological Survey, Open File Series 2012-5, 172 pp.
- Frailey, S.M., T.M. Parris, J.R. Damico, R.T. Okwen, and R.W. McKaskle, 2012b, CO2 Storage and Enhanced Oil Recovery: Sugar Creek Oil Field Test Site, Hopkins County, Kentucky. C.C. Monson and J. H. Goodwin (eds.): Illinois State Geological Survey, Open File Series 2012-4, 234 pp.
- French, T.R., Peru, D.A., and Thorton, S.D., 1989, Low pH Alkaline Chemical Formulations, Department of Energy Report, Nipper-375, page 19.
- French, T.R., Zheng. C., and Bryant, R., 1998, Design and Operation of the Sho-Vel-Tum Alkali-Surfactant-Polymer Project," Hart's Petroleum Engineer International, pages 35-42.
- Gao, S., Li, H., and Yang, Z., Pitts, M.J., Surkalo, H. and Wyatt, K., 1996, Alkaline/Surfactant /Polymer Pilot Performance of the West Central Saertu, Daqing Oil Field," SPE Reservoir Engineering, pages 181 to 188.
- Gao, Shutang, Li, Huabin, and Li, Hongfu, 1995, Laboratory Investigation of Alkaline-Surfactant-Polymer Technology for Daqing Enhanced Oil Recovery, SPE Res. Eng., pages 194-197.
- Grube, J. P., 1992, Reservoir Characterization and Improved Oil Recovery from Multiple Bar Sandstones, Cypress Formation, Tamaroa and Tamaroa South Fields, Perry County, Illinois, Illinois State Geological Survey, Illinois Petroleum 138, 49 p.
- Grube, J. P. and W. T. Frankie, 1999, Reservoir Characterization and Its Application to Improve Oil Recovery from Cypress Formation (Mississippian) at Richview Field, Washington County, Illinois, Illinois State Geological Survey, Illinois Petroleum 155, 39 p.
- Gu, H., Yang, R., Guo, S., Guan, W., Yue, X., and Pan, Q., 1998, Study on Reservoir Engineering: ASP Flooding Pilot Test in Karamay Oil Field, SPE 50918, presented at the SPE International Conference and Exhibition in China, Beijing.
- Gupta, R., and Mohanty, K.K., 2008, Wettability Alteration of Fractured Carbonate Reservoirs, SPE 113407.

- Hawkins, B., Taylor, K. and Nasr-El-Din, H., 1991, Mechanisms of Surfactant and Polymer Enhanced Alkaline Flooding: Application to David Lloydminster and Wainwright Sparky Fields, CIM/AOSTRA 91-28, Proceedings of the 1991 CIM Annual Technical Conference.
- Henry, M. E., and Hester, T.C., 1995, Anadarko Basin Province (058), in Gautier, D. L., Dolton, G.L., Takahashi, K.I., and Varnes, K.L., ed., 1995 National assessment of United States oil and gas resources--Results, methodology, and supporting data: U.S. Geological Survey Digital Data Series DDS-30, Release 2, one CD-ROM.
- Hernandez, C., Chacon, L.J., Anselmi, L., Baldonedo, A., Qi, J., Dowling, P.C., Pitts, M.J., 2003, ASP System Design for an Offshore Application in the La Salina Field, Lake Maracaibo, SPE 84775.
- Higley, D. K., Pollastro, R.M., and Clayton, J.L., 1995, Denver Basin Province (039), in Gautier,
  D. L., Dolton, G.L., Takahashi, K.I., and Varnes, K.L., ed., 1995 National Assessment of
  United States oil and gas resources; Results, methodology, and supporting data: U.S.
  Geological Survey Digital Data Series DDS-30, Release 2, one CD-ROM.
- Honarpour, M., Koederitz, L.F., and Harvey, A.H., 1986, Relative Permeability of Petroleum Reservoirs, CRC Press.
- Howard, R. H. & Whitaker, S. T., 1988, Hydrocarbon accumulation in a paleovalley at Mississippian-Pennsylvanian unconformity near Hardinville, Crawford County, Illinois: a model paleogeomorphic trap, Illinois State Geological Survey.
- Howard, R. H., 1979, The Mississippian-Pennsylvanian unconformity in the Illinois Basin-oil and new thinking, in J. E. Palmer and R. R. Dutcher (eds.), Depositional and structural history of the Pennsylvanian System of the Illinois Basin, Guidebook for field trip 9, Part 2, Ninth International Congress on Carboniferous Stratigraphy and Geology: Illinois State Geological Survey, p. 34-43
- Howard, R. H., 1991 Hydrocarbon Reservoir Distribution in the Illinois Basin, in M. W. Leighton, D. R. Kolata, D. F. Oltz and J. J. Eidel (eds.), Interior Cratonic Basins, American Association of Petroleum Geologists Memoir 51, 819 p.
- Howard, R. H., and S. T. Whitaker, 1988, Hydrocarbon accumulation in a paleovalley at Mississippian-Pennsylvanian unconformity near Hardinville, Crawford County, Illinois: a model paleogeomorphic trap: Illinois State Geological Survey, Illinois Petroleum 129
- Hughes RE, Demaris PJ, White WA. 1992. Underclays and related paleosols associated with coals. In: Martini IE Chesworth W, editors. Weathering, soils and paleosols. Amsterdam: Elsevier. p 501-523. Inoue A, Utada M, Wakita K. 1992.

- Hughes, R. E., D. M. Moore, and C. Reynolds, Jr., 1993, The Nature, Detection, Occurrence, and Origin of Kaolinite/Smectite, in Kaolin Genesis and Utilization, edited by H. H. Murray, W. M. Bundy, and C. C. Harvey, pp. 291-323, The Clay Minerals Society, Special Publication 1, Boulder Colorado
- Jacobson, R.J., (2000), Depositional History of the Pennsylvanian Rocks in Illinois, Geonote 2, ISGS
- Journel, A.G., 1974, Geostatistics for conditional simulation of ore bodies. Economic Geology, vol. 69, no. 5, pp. 673–687.
- Krumrine, P.H. and Falcone, J.S., 1983, Surfactant, Polymer and Alkali Interactions in Chemical Flooding Processes, SPE 11778.
- Krumrine, P.H., Falcone, J.S. Jr., and Campbell, T.C., 1982, Surfactant Flooding 1: The Effect of Alkaline Additive on IFT, Surfactant Adsorption and Recovery Efficiency, Soc. Pet. Eng. J., Vol 22, pages 503-513.
- Kumar, K., Dao, E.K., Mohanty, K.K., 2008, Atomic Force Microscopy Study of Wettability Alteration, SPE 93009.
- Kvale and Archer, 1991, E.P. Kvale, A.W. Archer, Characteristics of two Pennsylvanian-age semidiurnal tidal deposits in the Illinois Basin, U.S.A, ,in: D.G. Smith, G.E. Reinson, B.A. Zaitlin, R.A. Rahmani (Eds.), Clastic Tidal Sedimentology, Can. Soc. Pet. Geol. Mem., 16 (1991), pp. 179–188
- Lowenstam, H., 1951, Subsurface Geology of Clay County, Illinois State Geological Survey, reports of Investigations 148, pp. 27-50.
- Lumm, D. K. (1998), 'Subsurface Geometry and Petrography of Rock Units Between the Beech Creek ("Barlow") Limestone (Pope Group) and the Springfield Coal (Carbondale Formation) Across Part of the LaSalle Anticlinorium, Lawrence County, Illinois Vol. 1', PhD thesis, University of Kentucky.
- Manji, K.H. and Stasiuk, B.W., 1988, Design Considerations for Dome's David Alkali/Polymer Flood, Can. J. Pet. Tech., vol 27, pages 49-54.
- Martin, F.D. and Oxley, J.C., 1985, Effect of Various Alkaline Chemicals on Phase Behavior of Surfactant/Brine/Oil Mixtures, SPE 13575.
- Martin, F.D., Oxley, J.C. and Lim, H., 1995, Enhanced Recovery of a "J" Sand Crude Oil with a Combinations of Surfactant and Alkaline Chemicals, SPE 14293.

- Mast, R.F., and Howard, R.H., 1991, Oil and Gas Production Recovery Estimates in the Illinois Basin, in M.W. Leighton, D.R. Kolata, D.F. Oltz, and J.J. Eidel, eds., Interior Cratonic Basins. American Association of Petroleum Geologists, Memoir 51, pp. 295–298.
- Matheron, G. 1973. The intrinsic random functions and their applications. Advances in Applied Probability, vol. 5, no. 3, pp. 439–468.
- Meyers, J., Pitts, M.J. and Wyatt, K., 1992, Alkaline-Surfactant-Polymer Flood of the West Kiehl Unit, SPE 24144, presented at the 8th SPE/DOE Symposium on EOR, Tulsa, OK, April 1992.
- Midwest Geological Sequestration Consortium, 2009, Enhanced Oil Recovery I: Loudon Single-Well Huff 'n' Puff. DOE Contract DE-FC26-03NT41994 (Issued December 31, 2009).
- Mihcakan, I.M. and Van Kirk, C.W., 1986, Blending Alkaline and Polymer Solutions Together into a Single Slug Improves EOR, SPE 15158.
- Miller, Bernie J., Pitts, M.J., Dowling, P., Wilson, D., 2004, Single Well Alkaline-Surfactant Injectivity Improvement Test in the Big Sinking Field, SPE 89384.
- Mohammadi, H., Delshad, M., and Pope, G.A., 2008, Mechanistic Modeling of Alkaline/Surfractant/Polymer Floods," SPE 110212.
- Najafabadi, N.F., Delshad, M., Sepehrnoori, K., Nguyen, Q.P., and Zhang, J., 2008, Chemical Flooding of Fractured Carbonates Using Wettability Modifiers, SPE 113369.
- Nelson, R.C., Lawson, J.B., Thigpen, D.R., and Stegemeier, S.D., 1984, Cosurfactant Enhanced Alkaline Flooding, SPE/DOE 12672.
- Nelson, W. J.; Devera, J. A.; Jacobson, R. J.; Lumm, D. K.; Peppers, R. A.; Trask, B.; Weibel, C. P.; Follmer, L. R.; Riggs, M. H.; Esling, S. P.; Henderson, E. D. & Lannon, M. S., 1991, Geology of the Eddyville, Stonefort, and Creal Springs quadrangles, Southern Illinois, Illinois State Geological Survey.
- Nelson, W. J.; Smith, L. B.; Treworgy, J. D.; Furer, L. C. & Keith, B. D., 2002. Sequence Stratigraphy of the Lower Chesterian (Missippian) Strata of the Illinois Basin. Illinois State Geological Survey, Bulletin 107, 70 p.
- Off, T., 1963, Rhythmic linear sand bodies caused by tidal currents: AAPG Bulletin, v. 47, p. 324-341.
- Olsen, P.K., Hicks, M.D., Hurd, B.F., Sinnorkt, A.A. and Sweigart, C.N., 1990, Design of a Novel Flooding System for an Oil-Wet Central Texas Carbonate Reservoir, SPE/DOE 20224.

- Oltz, D. F., 1994, Improved and enhanced oil recovery in Illinois through reservoir characterization, U. S. Department of Energy.
- Palmer, D., 1984, Geologic Evaluation of Bridgeport Main Sand, Robins 102-B Project, Lawrence County, Illinois, Technical report, Marathon Oil Company, Denver Research Center.
- Peppers, R. A., 1996, Palynological correlation of major Pennsylvanian (Middle and Upper Carboniferous) chronostratigraphic boundaries in the Illinois and other coal basins, Geological Society of America Memoirs 188, 1-112.
- Peterson, J. A., 1995, Williston Basin Province (031), in Gautier, D. L., Dolton, G.L., Takahashi, K.I., and Varnes, K.L., ed., 1995 National assessment of United States oil and gas resources-Results, methodology, and supporting data: U.S. Geological Survey Digital Data Series DDS-30, Release 2, one CD-ROM.
- Pitts, M., 1995, Investigation of Oil Recovery Improvement by Coupling an Interfacial Tension Agent and a Mobility Control Agent in Light Oil Reservoirs, Final Report, Bartlesville Project Office, U.S. Department of Energy, DOE/BC/14886-14.
- Pitts, M.J. and Surkalo, H., 1995, Detailed Evaluation of the West Kiehl Alkaline-Surfactant-Polymer Field Project and Its Application to Mature Minnelusa Waterfloods, Department of Energy Report, Final Report, DOE/BC/14860-9.
- Pitts, M.J., Campbell, T.A., Surkalo, H., and Wyatt, K., 1995, Polymer Flood of the Rapdan Pool, SPE Reservoir Engineering, pages 183-186.
- Pitts, M.J., Surkalo, H., and Mundorf, W.R., 1994, Detailed Evaluation of the West Kiehl Alkaline-Surfactant-Polymer Field Project and Its Application to Mature Minnelusa Waterfloods, Department of Energy Report, Annual Report for the Period January to December 1993, DOE/BC/14860-5.
- Pitts, M.J., Wyatt, K., Surkalo, H., 2004, Alkaline-Polymer Flooding of the David Pool. Lloydminster Alberta, SPE 89386.
- Plains Illinois, 2002, Reservoir Characterization for Pilot ASP Flood Project in Lawrence Field, Presentation
- Poettmann, F.H., 1983, Microemulsion Flooding, Improved Oil Recovery, Inter-State Oil Compact Commission, Oklahoma City, Ok, pages 173-250.
- Posamentier, H. W. & Allen, G. P., 1999, Facies and Log Expression of Systems Tracts Siliciclastic Sequence Stratigraphy, SEPM (Society for Sedimentary Geology), pp. 103-173.

- Potter, P. E. & Desborough, G. A., 1965, Pre-Pennsylvanian Evansville Valley and Caseyville (Pennsylvanian) Sedimentation in the Illinois Basin, Illinois State Geological Survey.
- Potter, P. E. & Glass, H. D., 1958, Petrology and Sedimentation of the Pennsylvanian Sediments in Southern Illinois: A Veritcal Profile, Illinois State Geological Survey.
- Qu, Zhijan, Zhang, Yigen, Zhang, Xiansong, and Dai, Jialin, 1998, A Successful ASP flooding Pilot in Gudong Oil Field, SPE 39613, presented at the SPE/DOE Improved Oil Recovery Symposium held in Tulsa, Oklahoma, April 19-22, 1998.
- Saleem, S.M. and Herandex, A., 1989, Enhanced Oil Recovery of Acidic Crudes by Caustic Cosurfactant-Polymer Flooding, J. Surf. Sci. Tech., volume 3, pages 1-10.
- Seethepalli, A., Adibhatla, B., Mohanty, K.K., 2004, Wettability Alteration During Surfactant Flooding of Carbonate Reservoirs, SPE 89423.
- Sharma, A., A. Aziz-Yarand, B. Clayton, G. Baker, P. McKinney, C. Britton, M. Delshad, G. Pope, 2012, The Design and Execution of an Alkaline-Surfactant-Polymer Pilot Test, SPE 154318
- Siever, R., 1951, The Mississippian-Pennsylvanian Unconformity in Southern Illinois, AAPG Bulletin 35(3), 542-581.
- Sims, S.K., 1993, Pressure-Volume-Temperature Correlations for Crude Oils from the Illinois Basin. Illinois State Geological Survey, Illinois Petroleum 140.
- Sloss, L. L., 1963, Sequences in the Cratonic Interior of North America, The Geological Society of America Bulletin 74, 93-114.
- Swann, D. H., 1963, Classification of Genevievian and Chesterian (late Mississippian) rocks of Illinois: Illinois State Geological Survey Report of Investigations 216, 91 p.
- Tabor, J.J., 1988, Dynamic and Static Forces Required to Remove a Discontinuous Oil Phase from Porous Media Containing both Oil and Water, SPE Reprint series No. 24, Surfactant/Polymer Chemical Flooding 1, SPE, Richardson, Tx, pages 42-51.
- Udden, J.A., 1912, Geology and Mineral Resources of the Peoria Quadrangle, Illinois: U.S. Geol. Survey, Bulletin 506, p. 47-50
- Udegbunam, E. O., and J. P. Grube, 1993, Reservoir characterization and evaluation of oil productivity of Mississippian Cypress reservoirs of Lawrence Field, presented at Fourth Annual Archie Conference, November 1-4, 1993, Houston, Texas, paper in proceedings (also ISGS reprint series 1993-O).

- Van Wagoner L., Posamentier H., Mitchum R., Vail P., Sarg J., Loutit T., Hardenbol J., 1988, An overview of the fundamentals of sequence stratigraphy and key definitions. in: Wilgus C., Hastings B., Ross C., Posamentier H., Van Wagoner J., Kendall C. (eds) Sea-Level Changes: An Integrated Approach. Society of Economic Paleontologists and Mineralogists Special Publication, 42, 39–45.
- Van Wagoner, J. C., Mitchum, R. M.; Campion, K. M. & Rahmanian, V. D., 1990, Siliciclastic sequence stratigraphy in well logs, cores, and outcrops, American association of Petroleum Geologists.
- Vargo, J., Turner, J., Vergnani, B, Pitts, M.J., Wyatt, K, Surkalo, H., and Paterson, D., 1999, Alkaline-Surfactant-Polymer Flooding of the Cambridge Minnelusa Field, SPE 55633, presented at the Rocky Mountain Regional Meeting in Gillette, Wyoming, May 15-18, 1999.
- Vargo, J., Turner, J., Vergnani, B., Pitts, M.J., Wyatt, J., Wyatt, K., Surkalo, H., Patterson, D., 2000, Alkaline-Surfactant-Polymer Flooding of the Cambridge Minnelusa Field, SPE 68285.
- Walker, R. G. & Cant, D. J.Walker, R., ed., 1984, Facies Models, Geoscience Canada Reprint Series 1, chapter Sandy fluvial systems, pp. 71-89.
- Wang, C., Wang, B., Cao, X., and Li, H., 1997, Application and Design of Alkaline-Surfactant-Polymer System to Close Well Spacing Pilot Gudong Oilfield," SPE 38321, Presented at the SPE Western Regional Meeting, Long Beach, Ca, June 25-27, 1997.
- Wang, D., Cheng, J., Wu, J., Wang, F., Li, H., and Gong, X., 1998, An Alkaline/Surfactant/ Polymer Field Test in a Reservoir with a Long-Term 100% Water Cut, SPE 49018, Presented at the Annual Technical Meeting and Exhibition in New Orleans, October 1998.
- Wang, D., Zhang, Z., Cheng, J., Yang, J., Gao, S., and Li, L., 1997, Pilot Test of Alkaline-Surfactant-Polymer Flooding in Daqing Oil Field, SPE Reservoir Engineering, November 1997, pages 229-233.
- Wanless, H. R. & Weller, J. M., 1932, Correlation and extent of Pennsylvanian cyclothems, Geological Society of America Bulletin 43(4), 1003-1016.
- Wanless, H. R., 1955, Pennsylvanian rocks of Eastern Interior Basin, AAPG Bulletin 39(9), 1753-1820.
- Weibel, C. P., 1996, Applications of sequence stratigraphy to Pennsylvanian strata in the Illinois basin, in Witzke, G. J., Ludvigson, G. A., and Day, J., eds., Paleozoic sequence stratigraphy: Views from the North American craton: Geological Society of America Special Paper 306, p. 331–339
- Weller, J. M., 1930, Cyclical Sedimentation of the Pennsylvanian Period and Its Significance, The Journal of Geology 38(2), 97-135.

- Willman, H. B.; Atherton, E.; Buschbach, T. C.; Collinson, C.; Frye, J. C.; Hopkins, M. E.; Lineback, J. A. & Simon, J. A., 1975, Handbook of Illinois Stratigraphy, Illinois State Geological Survey, Bulletin 95.
- Wright, L. D., J. M. Coleman, and B. G. Thom, 1975, Sediment Transport and Deposition in a Macrotidal River Channel, Ord River, Western Australia, in L. E. Cronin, ed., Estuarine Research, Vol. II: Academic Press, New York, p. 309-322.
- Wu, X., Zong, L., Chen, J., Wang, H., Yang, Y., Shan, C., and Geng, J., 2008, Application of Surfactants With Narrow Equivalent Weight Distribution and Desirable Structure to Daqing ASP Flooding, SPE 114345.
- Wyatt, K., Pitts, M.J., and Surkalo, H., 2004, Field Chemical Flood Performance Comparison with Laboratory Displacement in Reservoir Core, SPE 89385.
- Wyatt, K., Pitts, M.J., and Surkalo, H., 2008, Economics of Field Proven Chemical Flooding Technologies, SPE 113126.
- Wyatt, K., Pitts, M.J., Surkalo, H., 2002, Mature Waterfloods Renew Oil Production by Alkaline-Surfactant-Polymer Flooding, SPE 78711.
- Zhang, D.L., Liu, S., Yan, W., Puerto, M., Hirasaki, G.J., and Miller, C. A., 2006, Favorable Attributes of Alkali-Surfactant-Polymer Flooding, SPE 99744, presented at SPE/DOE Symposium on Improved Oil Recovery, 22-26 April 2006, Tulsa, Oklahoma.
- Zhang, J., Nguyen, Q.P., Flaaten, A.K., and Pope, G.A., 2008, Mechanisms of Enhanced Natural Imbibition With Novel Chemicals, SPE 113453.
- Zhao, P., Jackson, A.C., Britton, C., Kim, D. H., Britton, L.N., Levitt, D.B., and Pope, G. A., 2008, Development of High-Performance Surfactants for Difficult Oils, SPE 113432.

# **Figures**

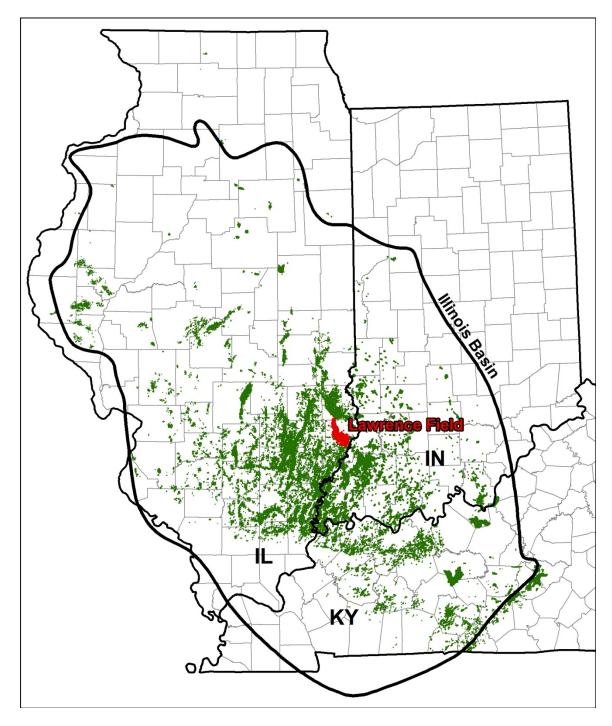
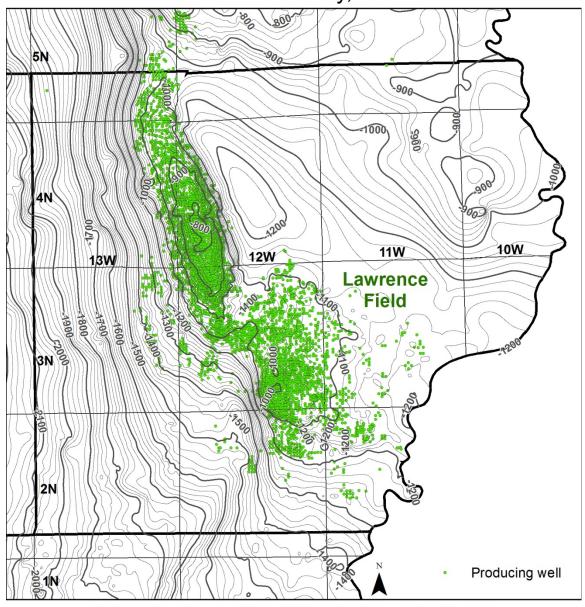


**Figure 1.** Outline of Illinois Basin with the location of Lawrence Field in southeastern Illinois highlighted in red. Oil fields are shown in green.

# Structure on Base of Barlow Limestone Lawrence County, Illinois



Contour interval equals 20 feet. Contours labeled and displayed with thicker line on 100 foot interval.

**Figure 2.** Lawrence Field in Lawrence County Illinois with oil wells shown in green. Structure on the base of the Barlow Limestone, a regional Mississippian marker bed. The two structures that make up Lawrence Field and the saddle that separates them are clearly shown; the Bridgeport Anticline to the north and the Lawrenceville Dome to the south.

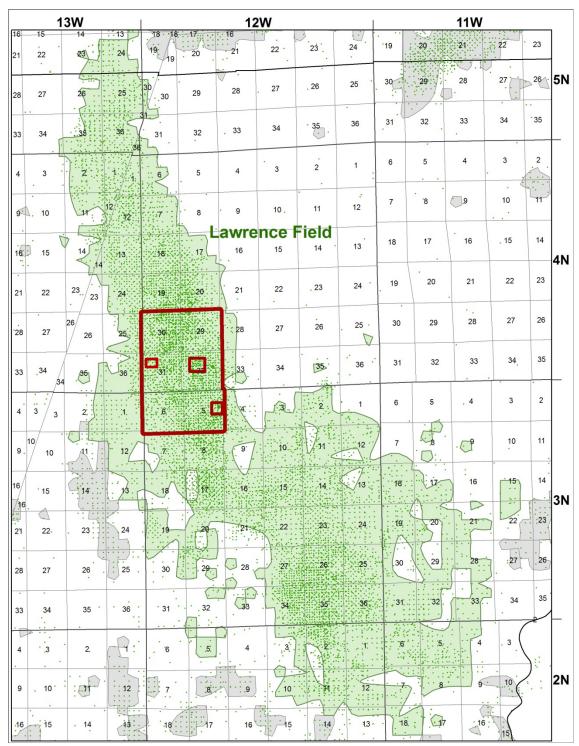


**Figure 3.** Lawrence Field, shaded green, with the main area of ISGS ASP research outlined with large red box. The small red box in the northeast half of Section 32 T4N R12W is the current Middagh ASP pilot area. The Griggs lease is located east and adjacent to the Middagh Pilot. The small red box approximately 1 mile west of the Middagh pilot in Section 31 T4N R12W is the Kimmel Maraflood pilot from the 1970s. The small red box in Section 5 T3N R12W is the 1980s Robins lease Maraflood surfactant-polymer pilot project location.

## ROBINS 102-B MARAFLOOD, LAWRENCE FIELD, IL BRIDGEPORT SAND, 25 Acre Pilot



**Figure 4.** Graph showing increased production from the Robins 102-B Maraflood surfactant flood starting in 1982. The 25 acre Bridgeport B channel sandstone pilot project in the SE quarter of Section 5, T3N R12W achieved 34% SOR recovery (15% PV), 450 mbo. The flood was a scientific success but was not expanded. An oil price drop at this time apparently did not offset the cost of polymer and surfactant.

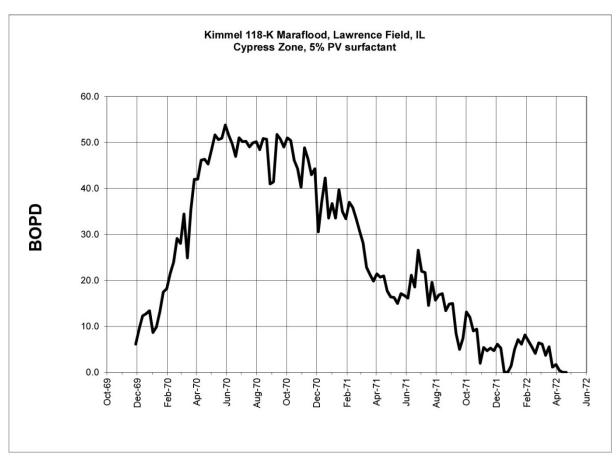


**Figure 5.** The Kimmel Maraflood project was a 2.5 acre Cypress sandstone reservoir pilot project that achieved 30% SOR recovery (10% PV).

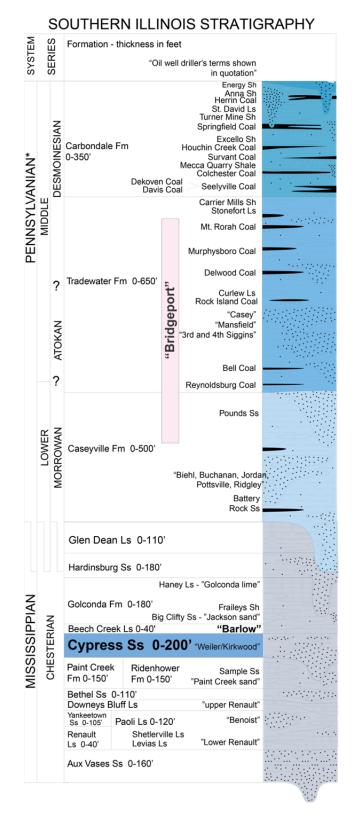


**Figure 6.** Stratigraphic column showing the Pennsylvanian "Bridgeport" and the Mississippian Cypress main pay intervals at Lawrence Field and the associated nomenclature.

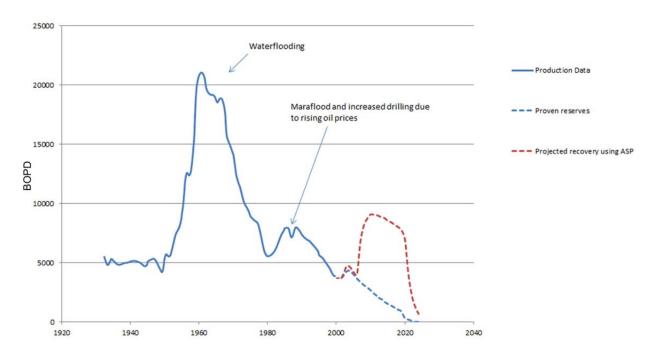


**Figure 7.** Graph shows projected field wide recovery potential with the application of ASP. Plains Illinois Corporation, operators in 2002, projected positive economics on 10% incremental recovery of produced oil, approximately 42 million barrels of oil at \$30. Rex Energy Corp., present operator, projects similar incremental potential recovery from 13,000 net acres (20 miles).

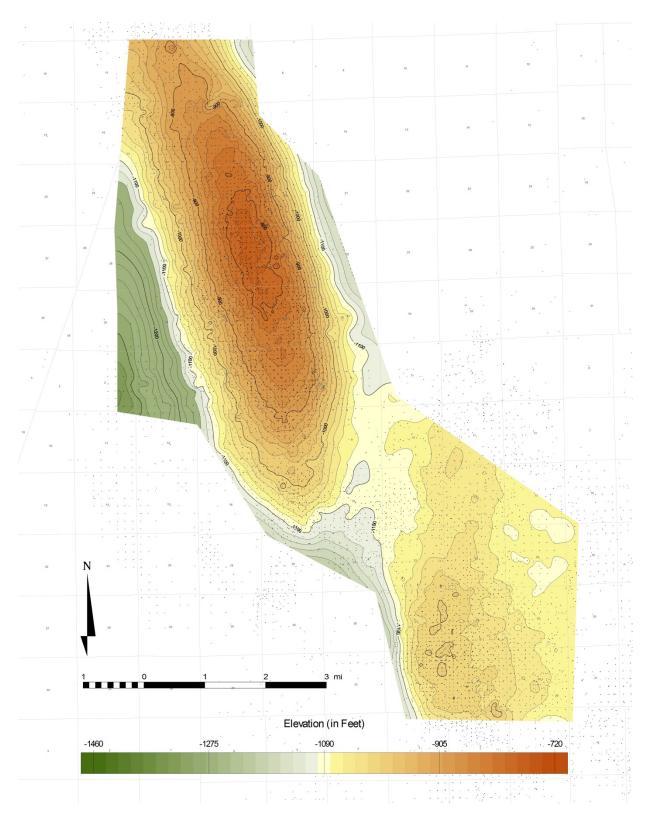


**Figure 8**. Contoured structure map on the base of the Mississippian Barlow Limestone, a regionally extensive Chesterian age thin limestone marker bed above which the Pennsylvanian Bridgeport sandstone reservoirs are found in Lawrence Field. Contour interval is 20'.

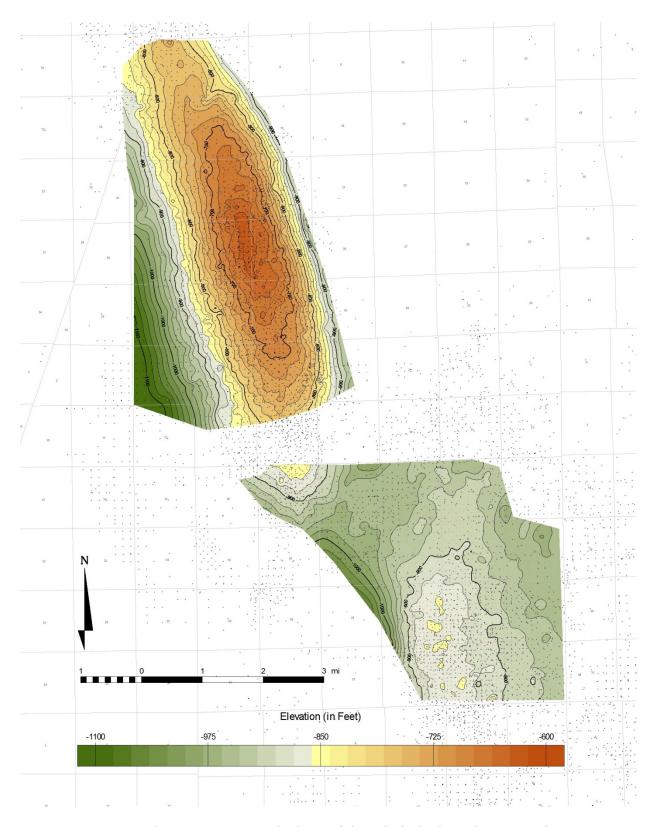


**Figure 9**. Contoured structure map on the base of the Mississippian Glen Dean Limestone. CI = 20 ft. The gap separating the northern and southern parts of the field is an area where the Glen Dean Limestone has been eroded.

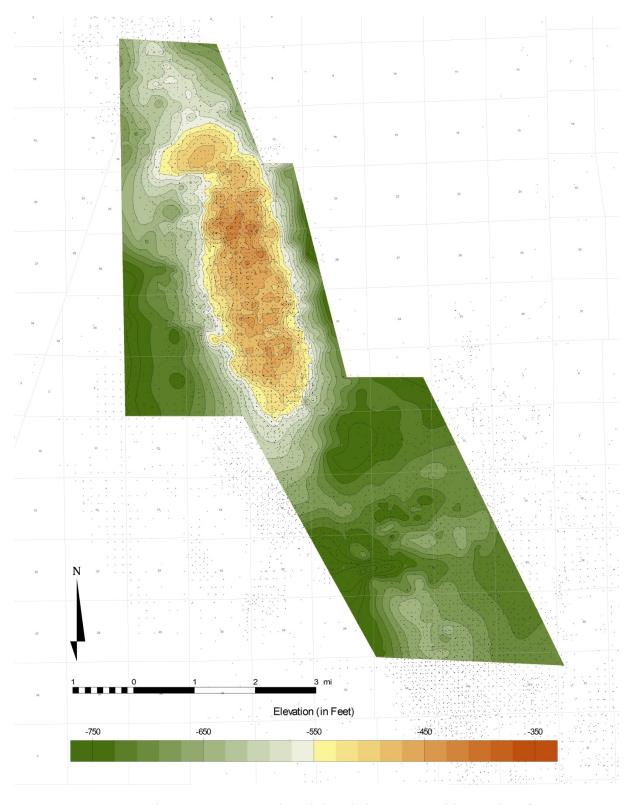
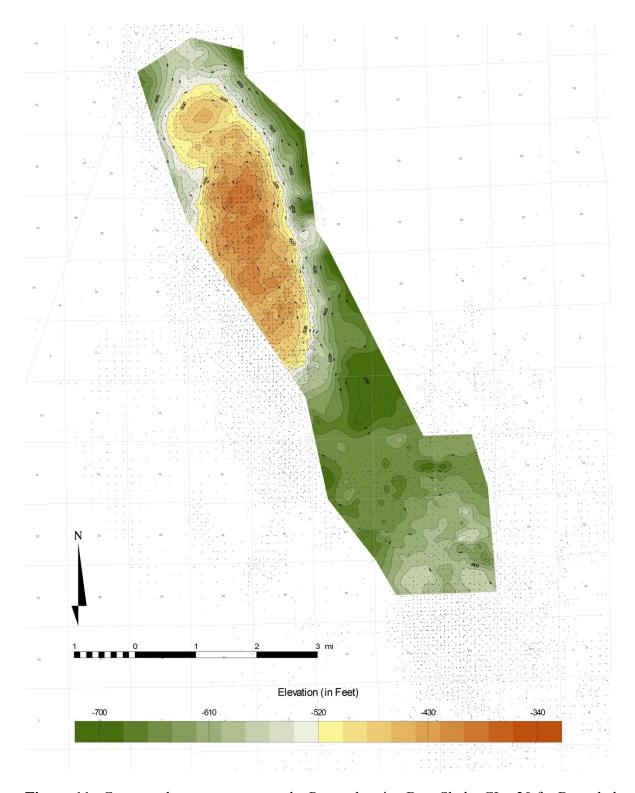
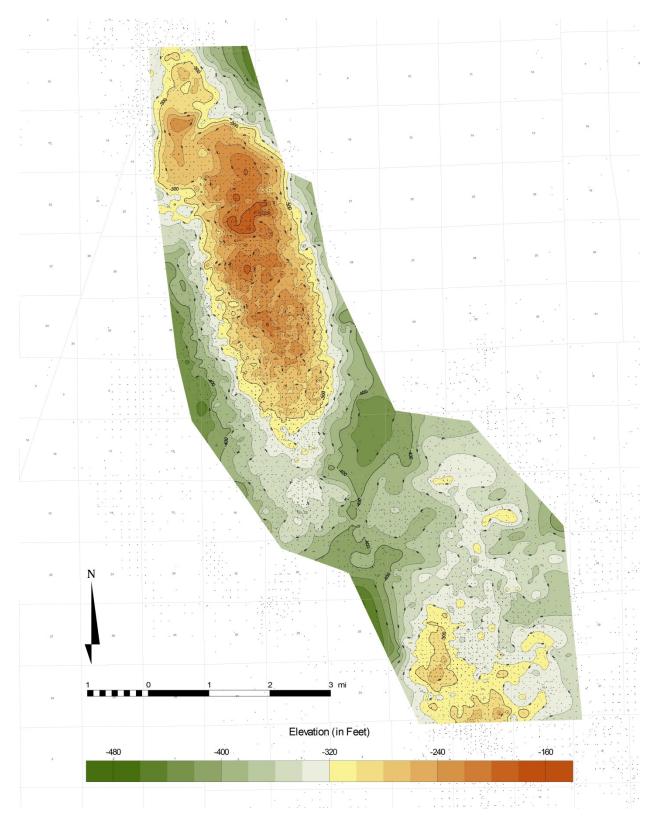


Figure 10. Contoured structure map on the Alpha Shale, contoured interval 20 ft.



**Figure 11**. Contoured structure map on the Pennsylvanian Beta Shale. CI = 20 ft. Beta shale has been eroded by younger channel sandstones along the southwestern portion of the Bridgeport Anticline.



**Figure 12**. Contoured structure map on the Pennsylvanian Carrier Mills Shale. CI = 20 ft

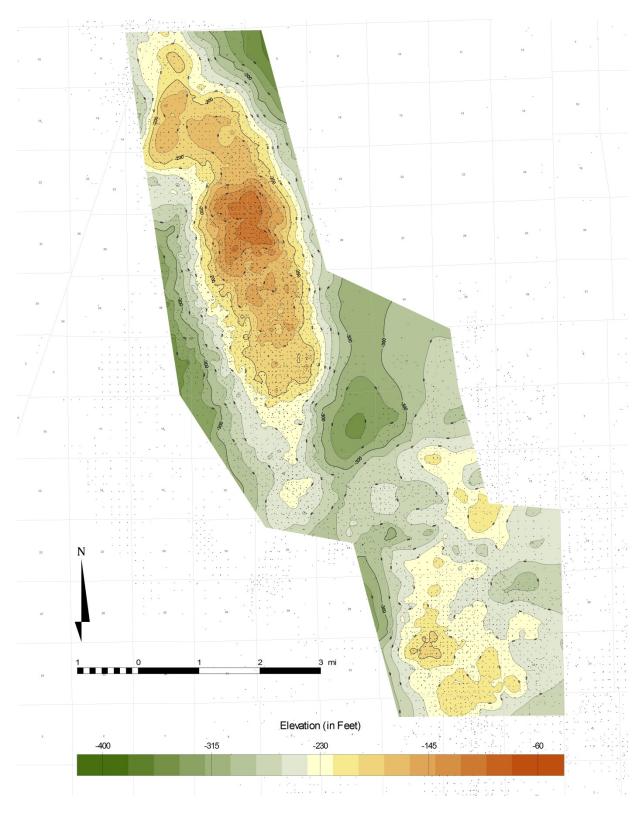


**Figure 13**. Contoured structure map on the Pennsylvanian Colchester coal. CI = 20 ft

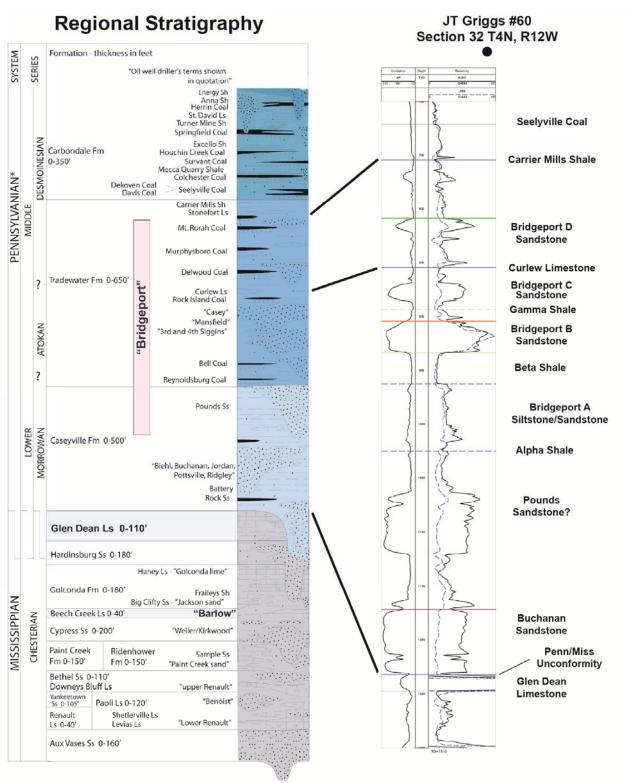


**Figure 14.** Regional Pennsylvanian stratigraphy, Bridgeport is an informal driller's term. Type log shows typical succession of Pennsylvanian rocks in Lawrence Field.

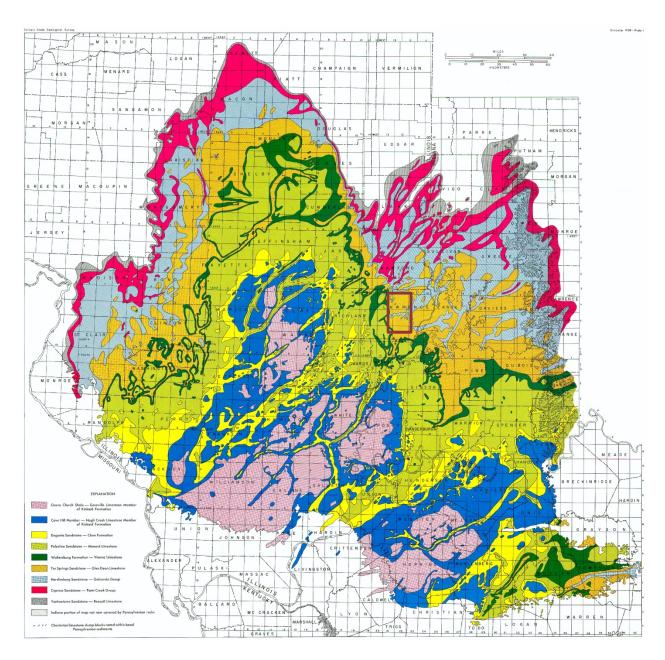


**Figure 15.** Subcrop map of paleochannels eroded into Mississippian strata. Early Pennsylvanian erosion removed older strata as river systems scoured deep channels into the bedrock, creating a high-relief surface that affected early Pennsylvanian sedimentation and complex sequence stratigraphic overprint. The Lawrence Field area is outlined in red. From Bristol and Howard, 1971

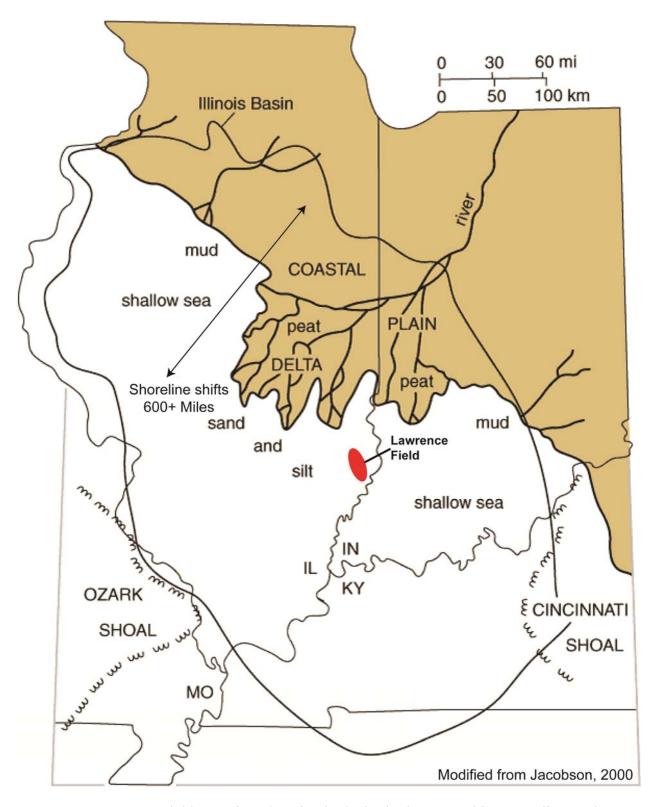


**Figure 16.** Lawrence Field occupies a location in the basin that was subject to sedimentation along a shifting shoreline, causing depositional conditions to alternate between marine and non-marine.



**Figure 17.** Core example of the Bridgeport A channel characteristics from the Griggs #106 well in the Se Ne of section 32. Medium to high angle tabular cross-bedded sandstones with pyrite cement is very common in the Bridgeport A sandstones particularly in the basal cross-beds, and occurs as banding and nodules in these beds. This channel scoured into a peat bog at its base. The banded oil staining in the core shows the influence of the cyclical cementation and reduction in reservoir quality.

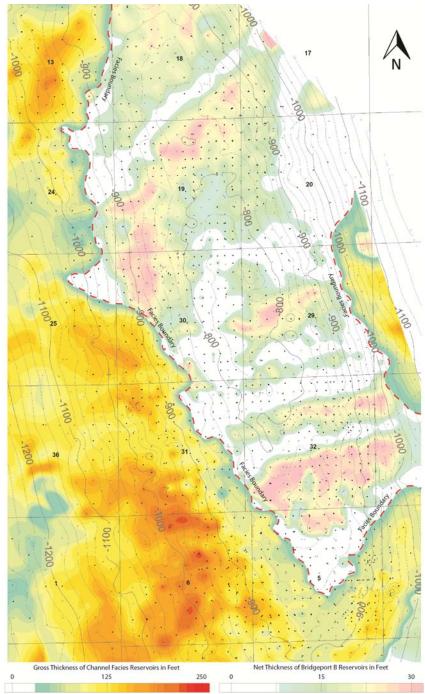


**Figure 18.** Isopach map of the Bridgeport B and stratigraphically correlative beds is a composite of two depositional facies. Bridgeport channel fill sandstone in bright colors and non-channel Bridgeport B in paler colors are mapped using normalized spontaneous potential (SP) 50% clean data. Structure with 25 foot contour interval is on the base of the Mississippian Barlow Limestone. In Section 32, Bridgeport B sandstones average  $\sim$ 25 feet thick and trend more or less east-west over the anticline. Two stratigraphically correlative sandstone intervals up to  $\sim$  200 feet thick enter Section 5, one from the northeast and one from the northwest, straddling the anticline and converging toward the south.

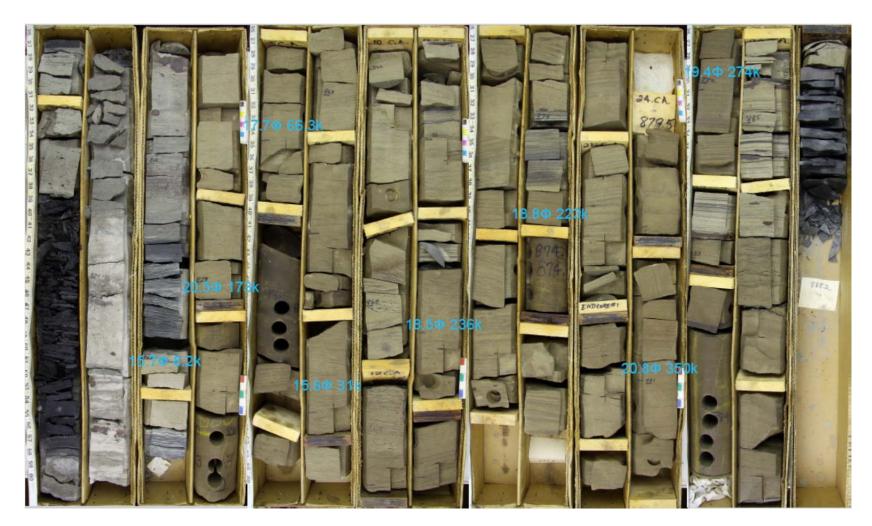


**Figure 19.** Core from the Johnson #32 well showing typical succession and arrangement of facies of the Bridgeport B in Section 32. The Bridgeport B is underlain by the widespread marine Beta Shale. The basal contact of the Bridgeport B sandstone and the Beta Shale is erosional and constitutes a sequence boundary. The Bridgeport B sandstone averages roughly 30' thick, is medium to fine grained and fines upward. Tabular crossbedded to planar bedded sandstone ( $\sim$ 20 $\Phi$  280k) generally makes up the lower portion of the Bridgeport B. The upper portion of the sandstone changes facies to wavy and ripple bedded ( $\sim$ 17 $\Phi$  125k). A sharp contact at 857.5' marks another facies change into lenticular bedded sediments that cap the succession as they transition into rooted sediments that supported the overlying coal. A few inches of dark grey shale on top of the coal indicates the next phase of transgression.

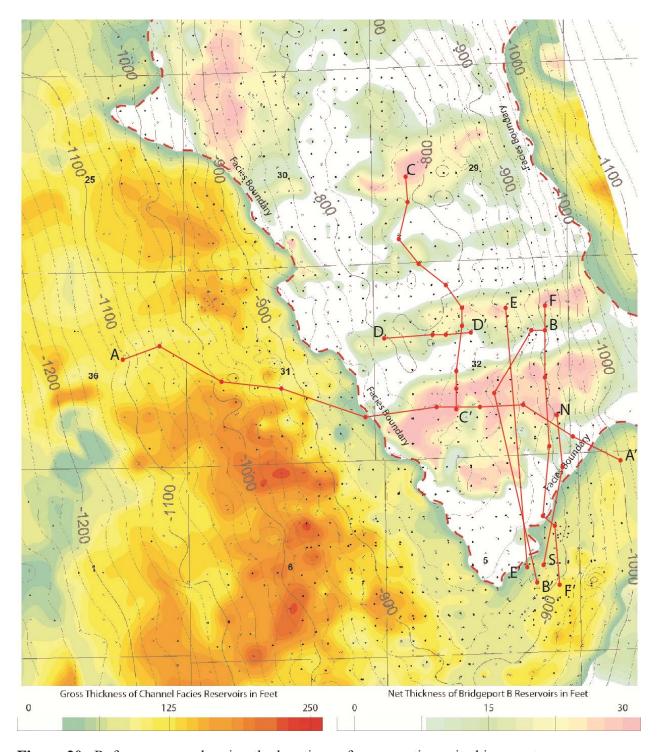
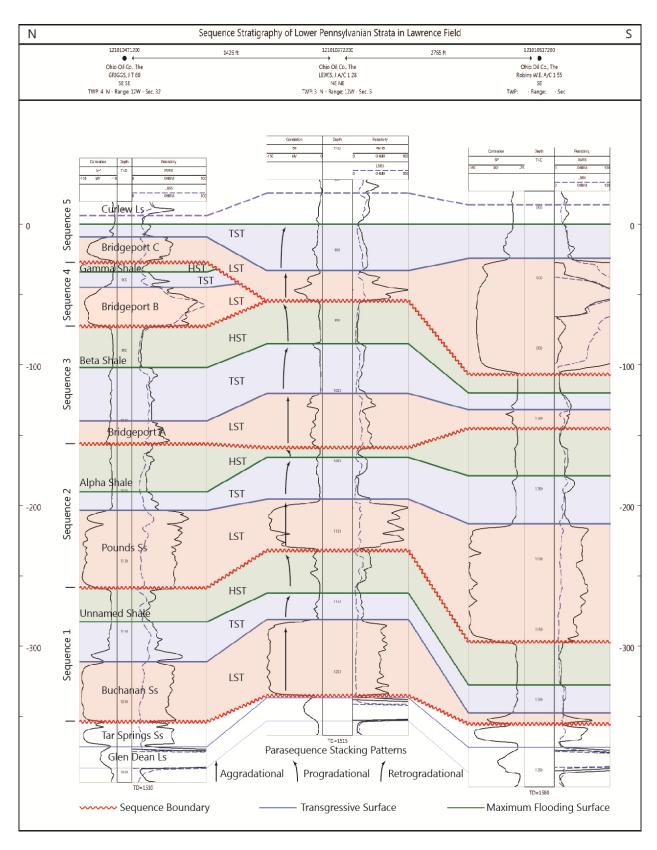
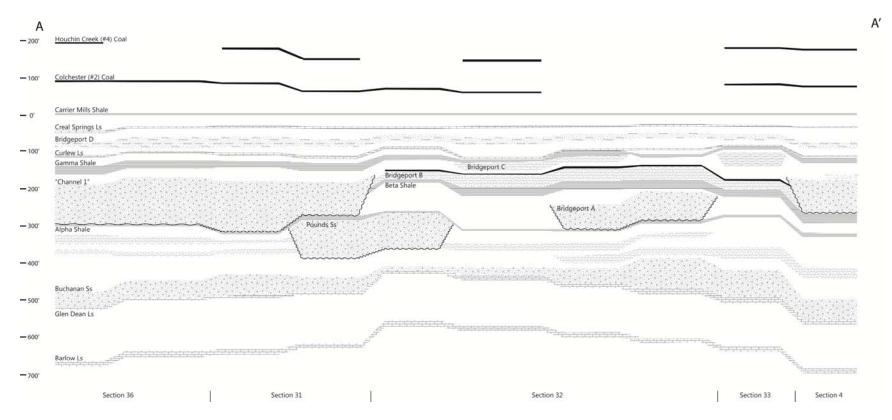


Figure 20. Reference map showing the locations of cross sections cited in report.



**Figure 21.** Sequence stratigraphic framework for the Lower Pennsylvanian strata of Lawrence Field. Location of three well cross section can be seen in Figure 20.



**Figure 22.** East-West cross section A-A' across the Bridgeport Anticline (see Figure 20) in the Northern part of Lawrence Field showing the stratal arrangement of lower Pennsylvanian sediments. The Carrier Mills Shale is the datum. Here, the discontinuous nature of the Bridgeport A, B, and C can be seen. The Bridgeport B is widely traceable in part because of the consistent underlying Beta Shale and overlying coal. The Bridgeport B is truncated to both the East and the West by younger Pennsylvanian channel fill deposits, making its lateral correlation outside of the field tenuous.

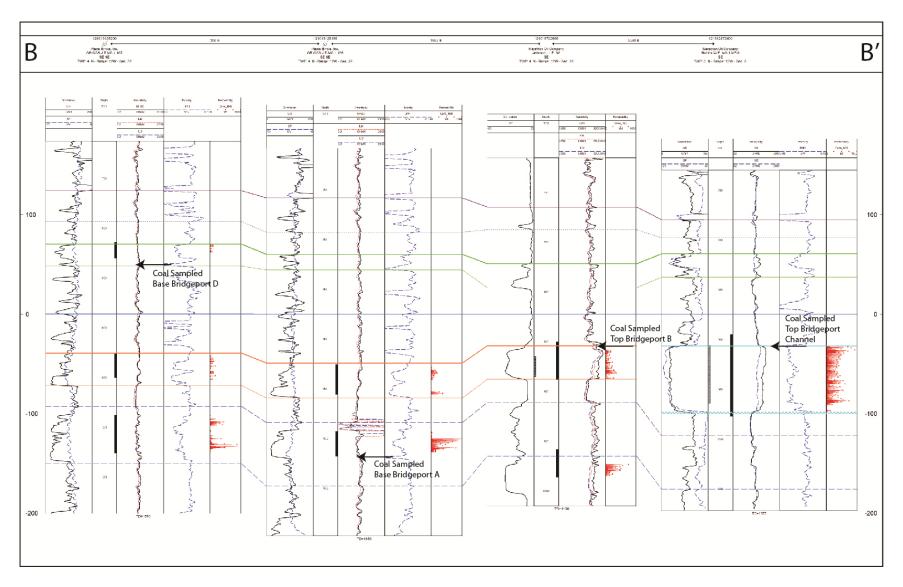


**Figure 23.** Cross section B-B' showing four wells where coals were sampled for palynological study (See Figure 20). The Curlew Limestone is used as the datum. The difficulty of correctly correlating the Bridgeport B reservoir when channel fill sandstones occupy the same stratigraphic position is apparent. Core measured permeability is plotted in red on the right side of each log with a scale of 0-1000 md.

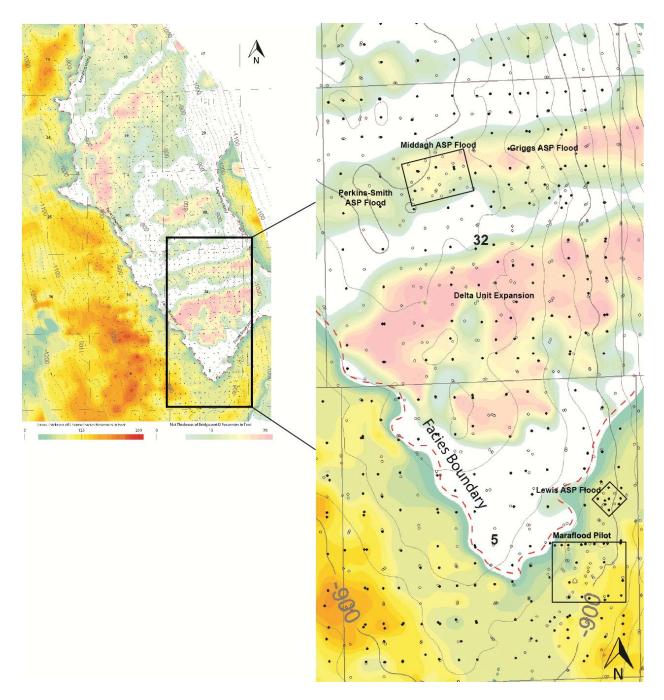


**Figure 24.** Isopach map showing the Bridgeport B sandstone on top of the Bridgeport Anticline. Thick channel fill deposits truncate the Bridgeport B to the west and southeast. Structure contours are on the Barlow Limestone. The Bridgeport B is compartmentalized into discreet sandstone bodies that are separated from one another by fairways of non-reservoir rock. Also shown are the present and expansion ASP flood areas. The 15 acre Middagh flood was reaching peak production at the end of 2011. Pre-flood production was 16 BOPD; peak ASP flood production was 100+ BOPD. The Perkins-Smith 58 acre flood was initiated in late 2011. No results have been reported to date. The Delta unit 350 acre expansion is under development with flood initiation expected in mid-2013.

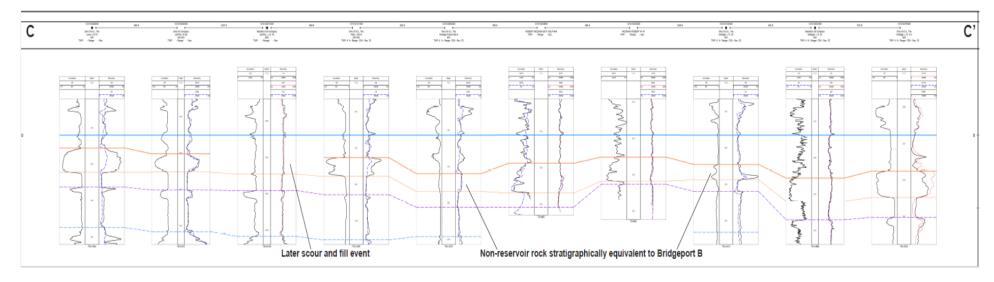


**Figure 25.** North-South cross section C-C' (see Figure 20) showing small scale compartmentalization of the Bridgeport B reservoir. East-west trending sandstone bodies are bounded by non-reservoir siltstones.

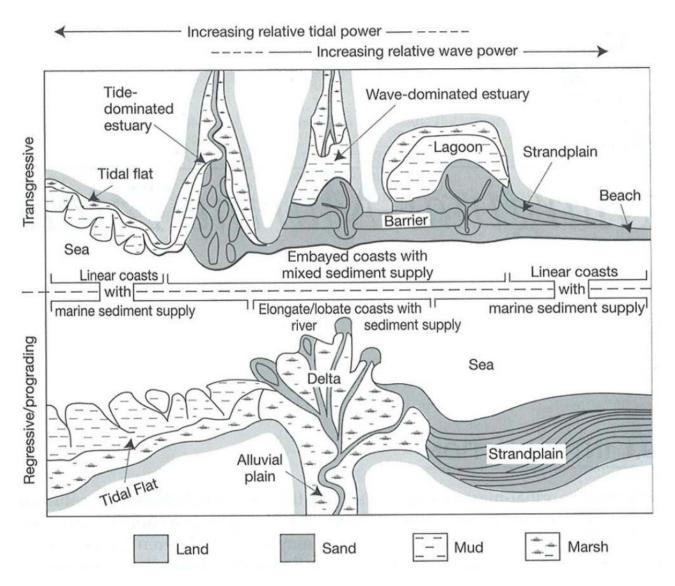


**Figure 26.** Depositional model of the principal coastal environments of the marginal marine setting (after Boyd et al, 1992). The Bridgeport B sandstone could have formed as tidally-influenced deltaic deposits in an estuarine setting (upper left in figure).

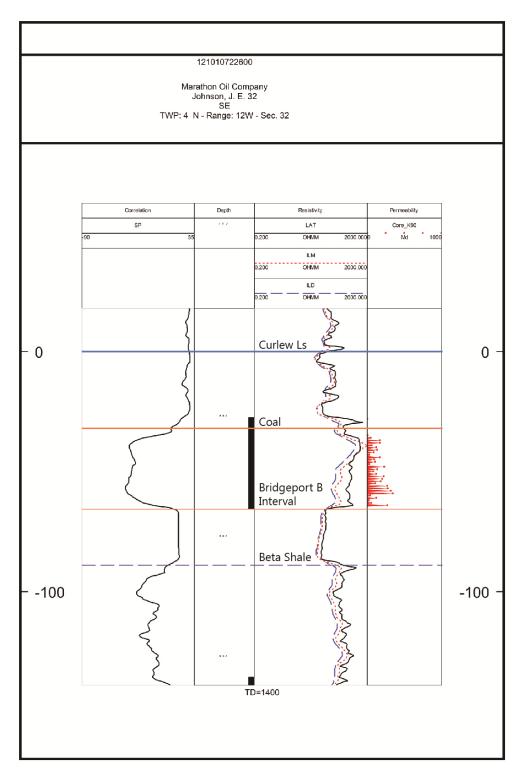


**Figure 27.** Johnson #32 well (See Figure 20) electric log indicating cored interval through a section of the better quality Bridgeport B reservoir that is scheduled for ASP development in 2013 (Figure 24).

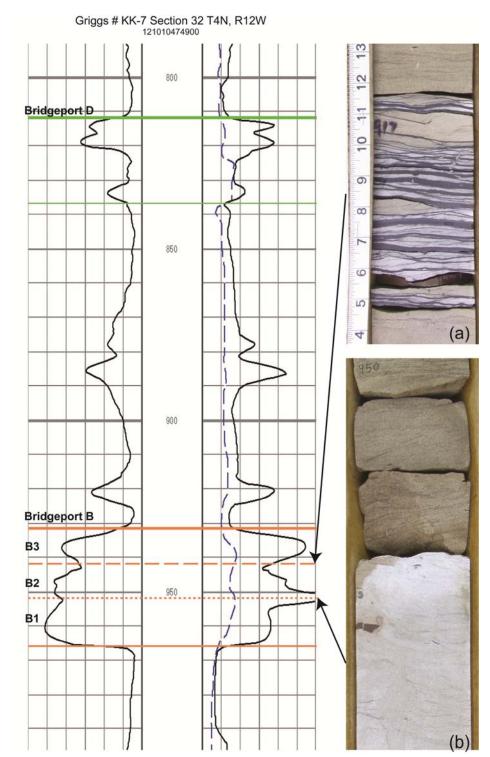


**Figure 28.** Typical log from Section 32 shows the Bridgeport D with the underlying Bridgeport B reservoir sandstone. Three stacked subunits, the B1, B2, and B3 are separated by baffles that are typically thin (usually 6"-1" thick) shaly intervals (a) or calcite cemented sandstone (b) that act to compartmentalize the reservoir. Tracing these features through the reservoir allows for the generation of flow unit maps.

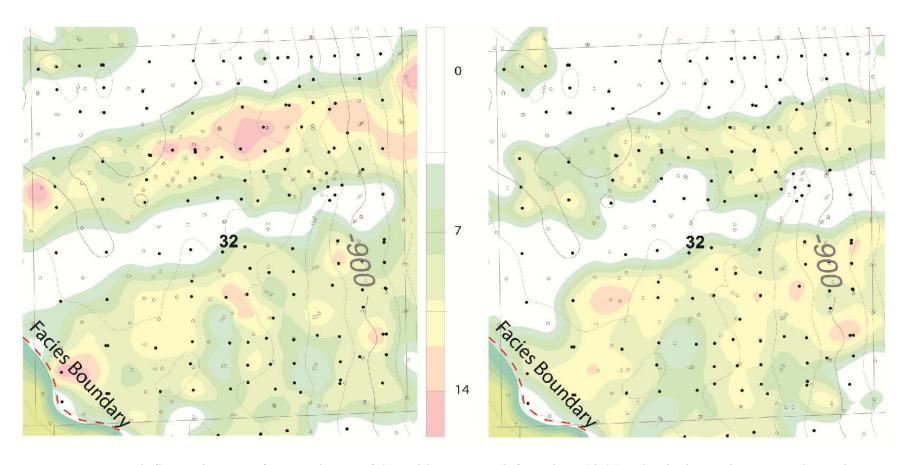


**Figure 29.** Isopach flow unit maps of net sandstone of the Bridgeport B1 (left) and B2 (right) subunits in Section 32 Sandstone is mapped with a 2' contour interval with the warmer colors representing thicker sandstone Reservoir sandstone in the northern half of Section 32 trends east-west whereas in the southern half of the section, the sandstone takes on a triangular shape and occupies the region between the two thick channel fill sandstone bodies that trend into Section 5 from the northeast and northwest. Bridgeport B1 and B2 sandstones develop predominantly in the same area. The B1 is thicker and better developed than the B2. Bridgeport B3 sandstone (not shown) is the thinnest and most poorly developed sandstone.

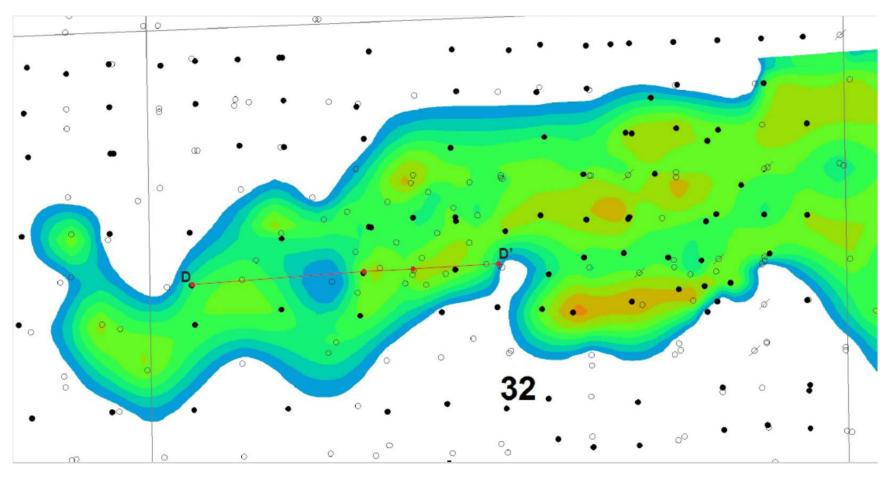


**Figure 30.** Isopach map showing the gross thickness of the cross bedded sandstone facies within the NE-SW trending Bridgeport B reservoir in the northern portion of Section 32.

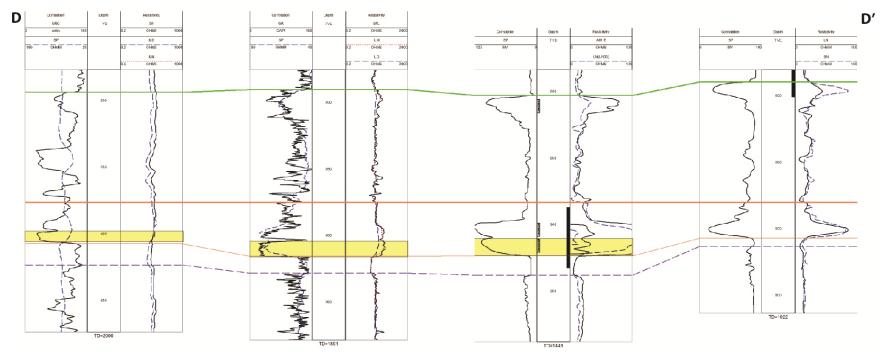


**Figure 31.** Cross section D-D' (See Figure 20 & 30) showing correlation of the cross bedded facies. The Bridgeport B is subdivided into facies to better understand and to more easily trace flow units within the reservoir. This cross section is an example where the cross bedded facies has been identified in the lower part of the Bridgeport B. Cross bedded facies sandstones are identified in cores by their fine-medium grained texture, presence of rip up clasts, and cross to subhorizontal bedding. This facies tends to manifest itself on logs by having a more blocky appearance.

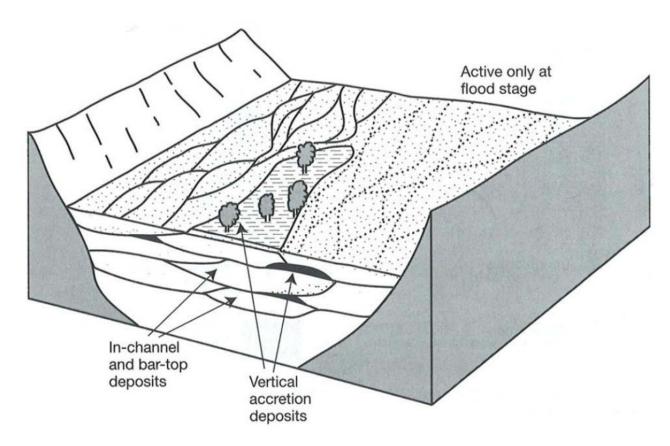


**Figure 32.** Depositional model of fluvial-deltaic architecture of braided stream deposits (after Walker and Cant, 1984). The thick and sometimes stacked and amalgamated sandstones of the Bridgeport channel facies could have formed in such an environment.

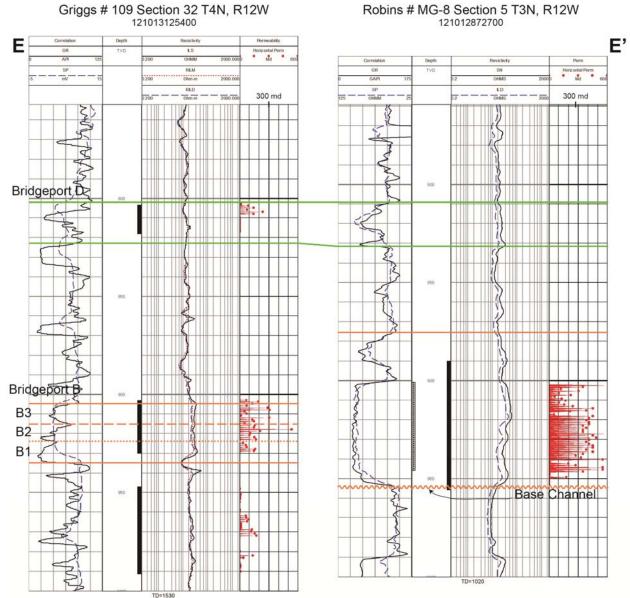


**Figure 33.** Cross section E-E' (See Figure 21) shows the two entirely different depositional settings between Section 32 and Section 5. The Griggs #109 well in Section 32 on the left shows the typical stacked Bridgeport B intervals while the Robins #MG-8 well in Section 5 on the right has 50 feet of characteristically thick and blocky sandstone. Core permeability is plotted in red on the right side of each log. Average permeability in Section 5 sandstone is 2.8 times greater (314 md) compared to 113 md in Section 32. These wells are separated by about 1.25 miles, but this rapid change commonly occurs over just a few hundred feet

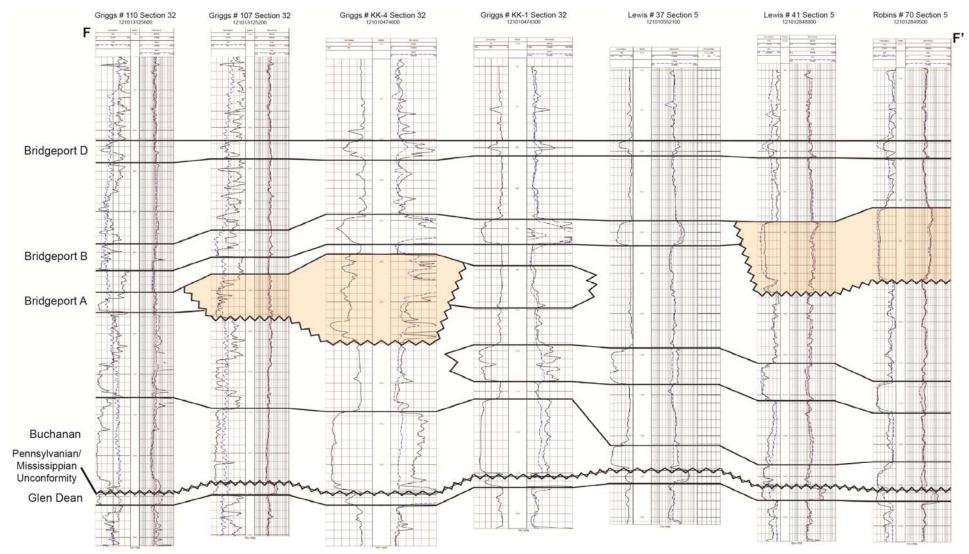


**Figure 34.** Cross section F-F' (See Figure 21) illustrates the complex stratigraphic relationships in the lower Pennsylvanian between Sections 32 and 5. This is characteristic throughout the much of the Illinois Basin. Channel fill sandstones change abruptly to non-channel fill tidal sandstone deposits in both the Bridgeport A and Bridgeport B intervals in this cross section. Sequence boundaries abound throughout this interval



**Figure 35.** Core example of channel fill Bridgeport B stratigraphic equivalent from the Robbins MG #8 well near the Maraflood pilot in section 5. Sharp scour contact with course rip-up and conglomeratic basal channel lag (approx. 950- 958 feet) transitions into very clean tabular cross bedded sandstone throughout most of the channel facies. Some core shows possible marine indicators in the upper feet of the core (tidal couplets and trace fossils).

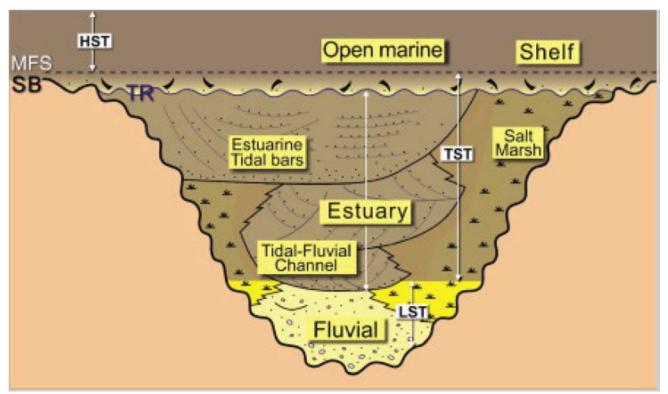


**Figure 36.** Schematic illustrating a tide dominated estuary within an incised valley. The entire system is transgressive in character with basal fluvial deposits overlain by estuarine deposits and capped by marine deposits of the succeeding cyclical estuarine fill complex deposited under continuously rising sea level (From Clifton, 1982). This incised valley fill model is analogous to the sedimentary structures observed in core in Section 5 T3N R12W. From Dalrymple and Choi, 2007.

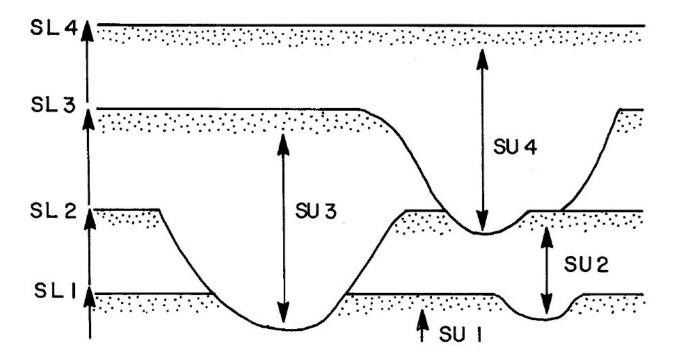


**Figure 37**. Schematic illustrating cyclical deposition under conditions where sea level drops and incisement occurs followed by sea level rise with periods of stillstand (SL). Stillstand units are transgressive in character and are relatively tabular or flat-lying. They can begin from channels incised into the previous unit. Basal deposition within the incised channels can be fluvial with associated sediments overlain by intertidal to supratidal units. The sedimentary structures observed in core and depositional characteristics in Section 5 are, in general, analogous to the incised valley models shown in figures 13 and 14. (From Clifton, 1982, also Dalrymple and Choi, 2007). This model displays the cyclical characteristics and complexity of the Pennsylvanian Bridgeport Formation at Lawrence Field.

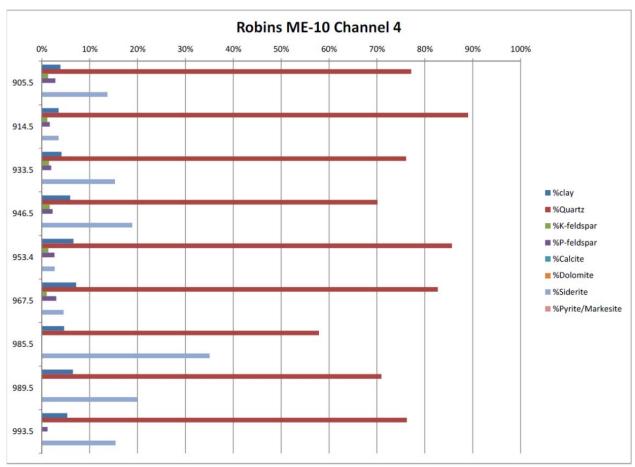


**Figure 38.** Graph shows that quartz sand is the major component of all analyzed core samples ranging from 58-88%. Siderite is the next most abundant mineral ranging from 2-35%, diagenetic clay minerals range from 3-7%, potassium and plagioclase feldspar are minor components. The average porosity and permeability of samples is much higher at 21% and 400 md respectively in these thick channel fill reservoirs than in the tidally influenced coastal reservoirs in the Griggs 109 and Johnson 32 wells.

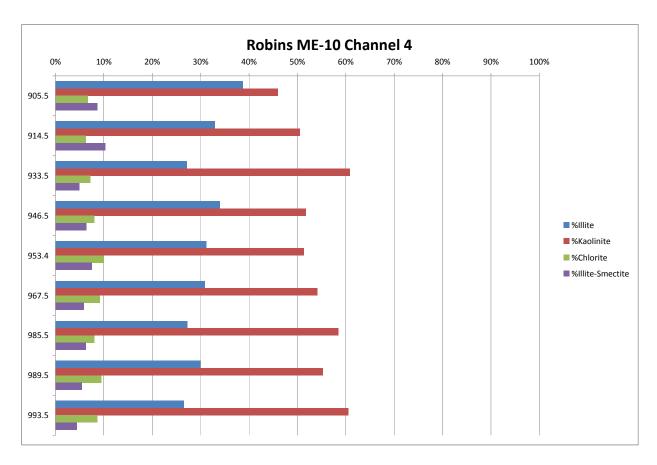


**Figure 39.** Bar graph chart showing relative abundance of types of clay minerals in the clay mineral fraction of core samples. The percent of clay minerals in the samples is shown in the previous chart. This chart shows that kaolinite is consistently the most abundant clay mineral.

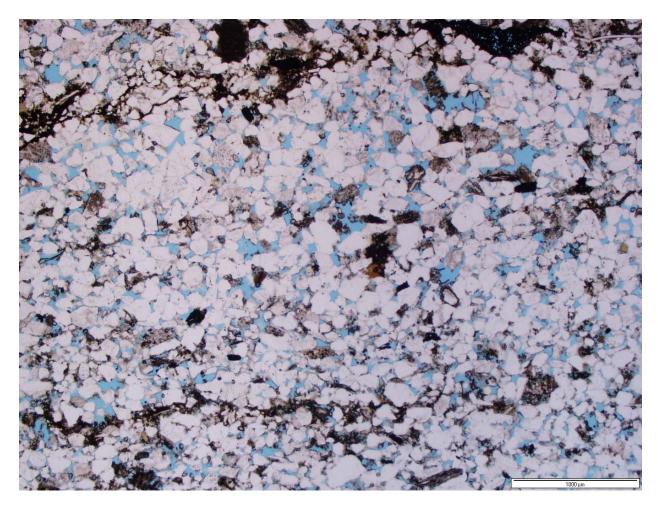


**Figure 40.** Thin section from 121012871800 Robins ME-10 well depth 905.5 ft., 2.5X white transmitted light, horizontal permeability is 221md, vertical permeability is 37.6md and porosity is 20.6%.

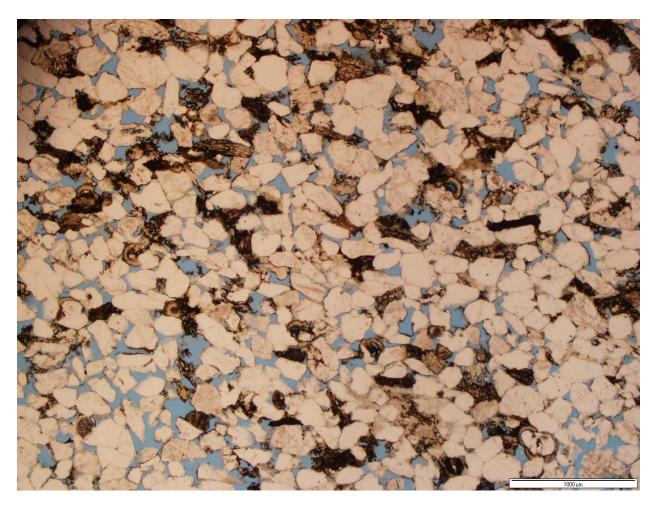


**Figure 41.** Thin section from 121012871800 Robins ME-10 well depth 914.5 ft., 2.5X white transmitted light, horizontal permeability is 1050md, vertical permeability is 820md, and porosity is 23%.

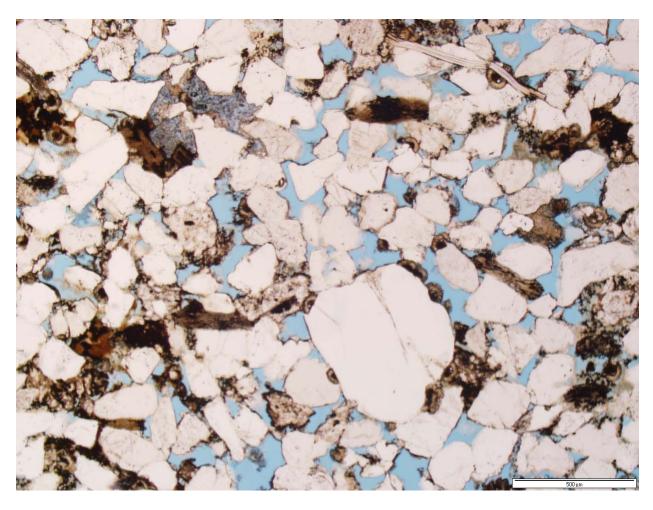


**Figure 42.** Thin section from 121012871800 Robins ME-10 well depth 923.5 ft., 5X white transmitted light, horizontal permeability is 710md, vertical permeability is 584md and porosity is 22.5%.

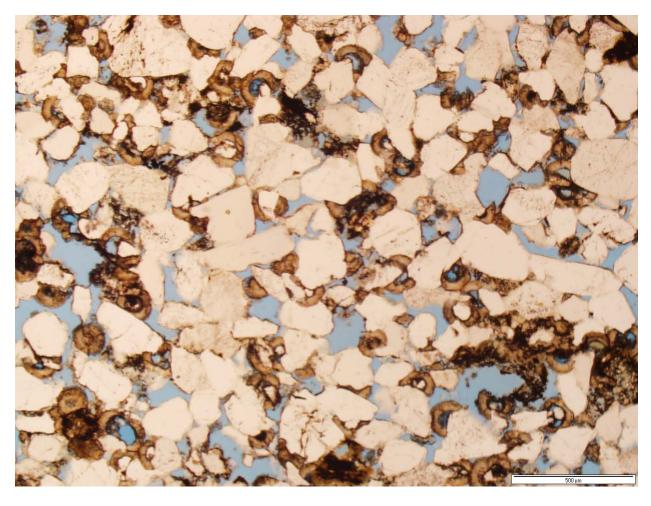


**Figure 43.** Thin section from 121012871800 Robins ME-10 well depth 933.5 ft., 5X white transmitted light, horizontal permeability is 385md, vertical permeability is 292md and porosity is 20.5%.

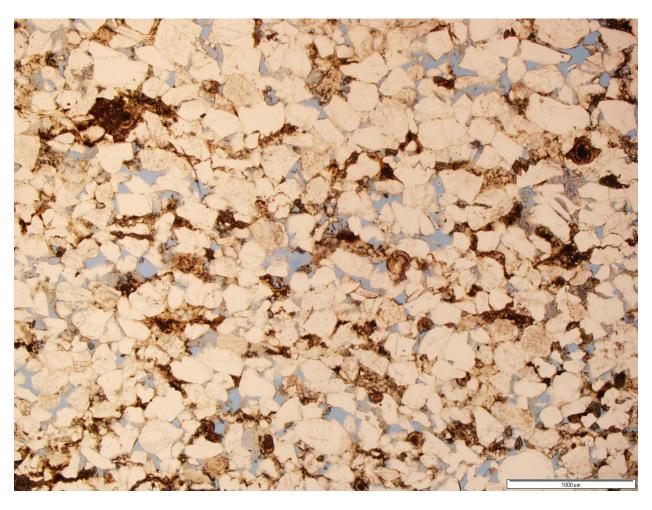


**Figure 44.** Thin section from 121012871800 Robins ME-10 well depth 946.5 ft., 2.5X white transmitted light, horizontal permeability is 80.3md, vertical permeability is 34md and porosity is 17.5%.

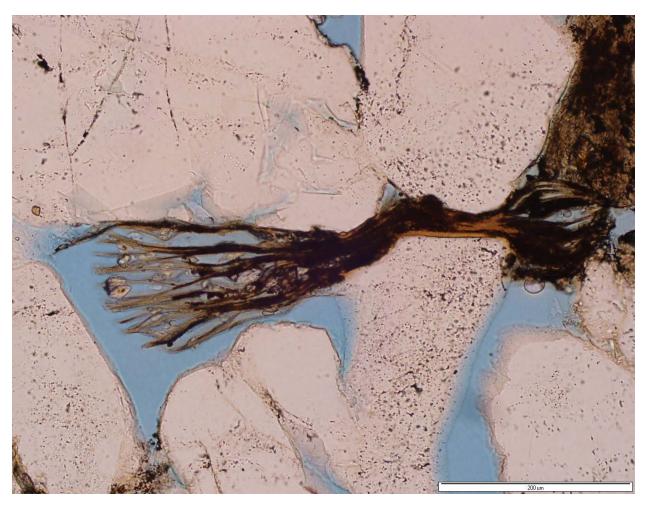


**Figure 45.** Thin section from 121012871800 Robins ME-10 well depth 953.4 ft., 20X white transmitted light, horizontal permeability is 557md, vertical permeability is 178md, and porosity is 22.3%.

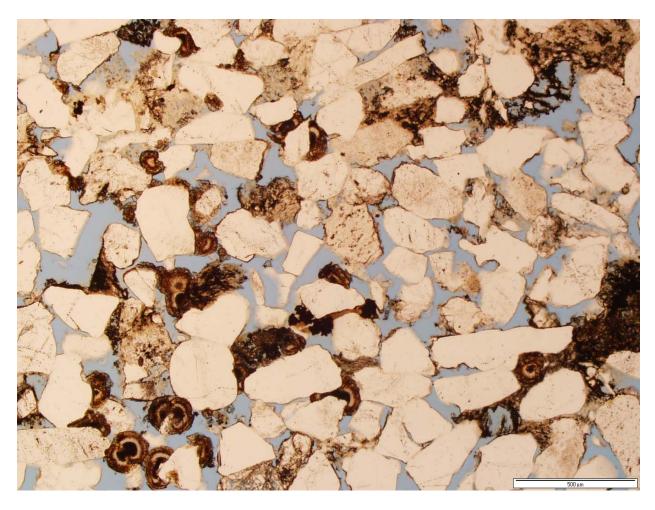


**Figure 46.** Thin section from 121012871800 Robins ME-10 well depth 967.5 ft., 5X white transmitted light, horizontal permeability is 455md, vertical permeability is 455md and porosity is 23.5%.

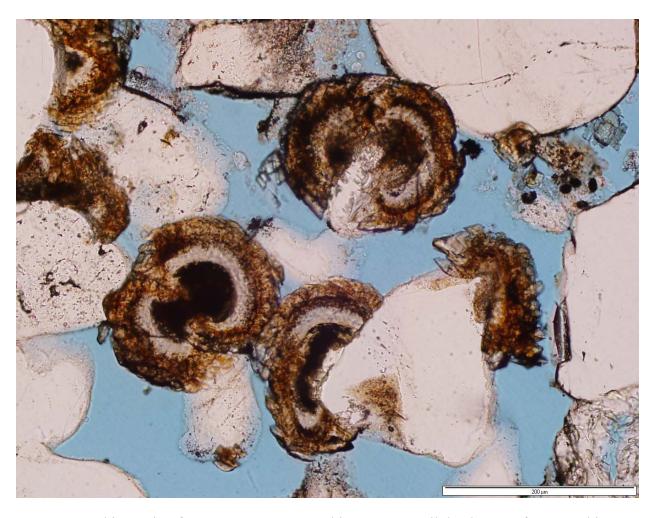


**Figure 47.** Thin section from 121012871800 Robins ME-10 well depth 967.5 ft., 20X white transmitted light, horizontal permeability is 455md, vertical permeability is 455md and porosity is 23.5%.

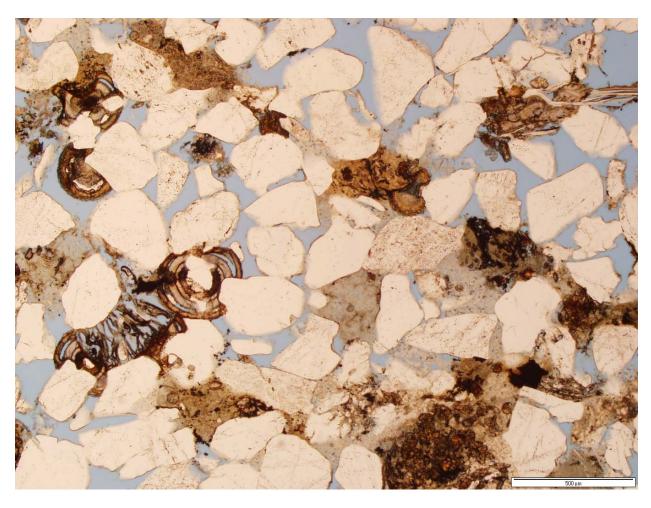


**Figure 48.** Thin section from 121012871800 Robins ME-10 well depth 993.5 ft., 20X white transmitted light, horizontal permeability is 415md, vertical permeability is 152md and porosity is 25.5%.

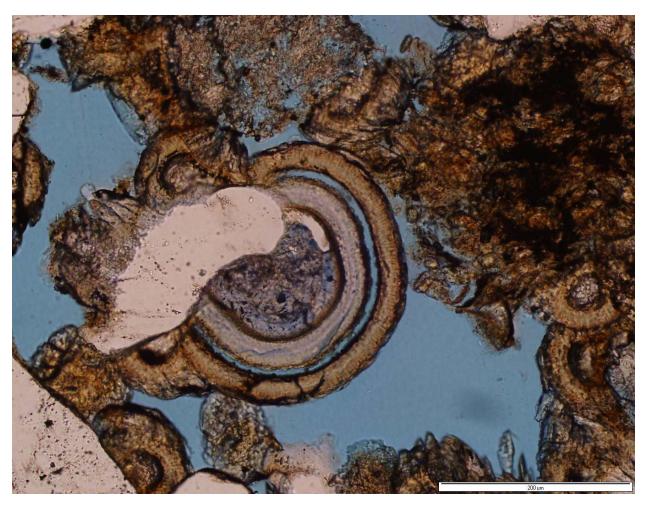


**Figure 49.** Thin section from 121012871800 Robins ME-10 well depth 985.5 ft., 20X white transmitted light, horizontal permeability is 38.8md, vertical permeability is 56md and porosity is 19.3%.

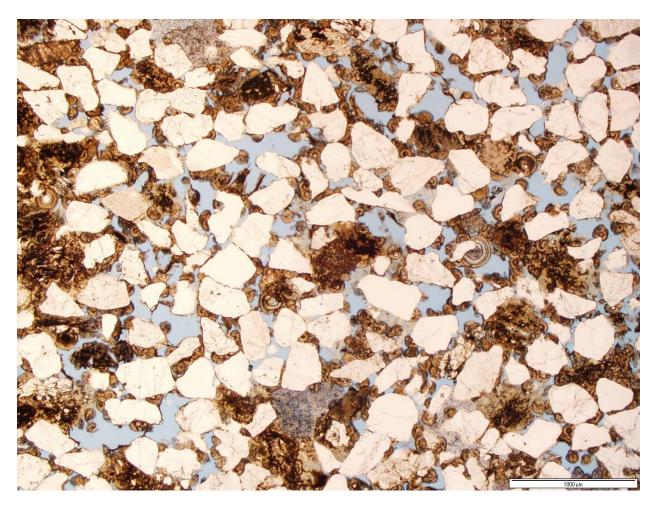


**Figure 50.** Thin section from 121012871800 Robins ME-10 well depth 985.5 ft., 2.5X white transmitted light, horizontal permeability is 38.8md, vertical permeability is 56md and porosity is 19.3%.

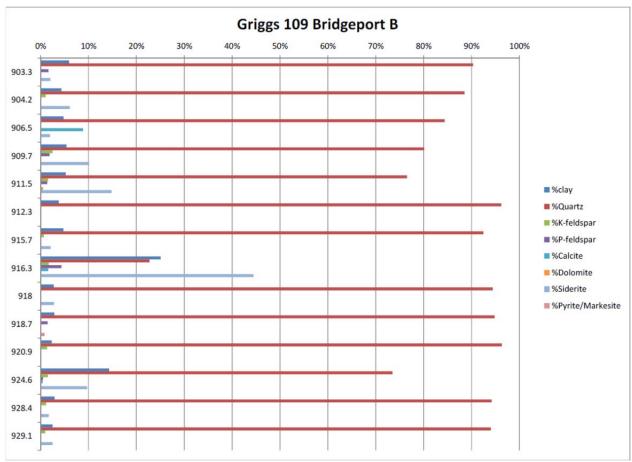


**Figure 51.** X-ray diffraction analyses of the bulk mineralogy of core samples from the Bridgeport B reservoir. The sandstone is fine to very fine grained has been interpreted as deltaic. The average porosity and permeability of the Bridgeport B in this well are 19% and ~150 md respectively. Quartz is the most abundant mineral and ranges between 75-95% in sandstone reservoir samples. Siderite and diagenetic clay minerals are the next most abundant minerals, siderite ranges between 2-15%, clay minerals range between 3-15%. Potassium and plagioclase feldspars are minor components in all samples. One sample at 906.5ft. has 8% calcite.

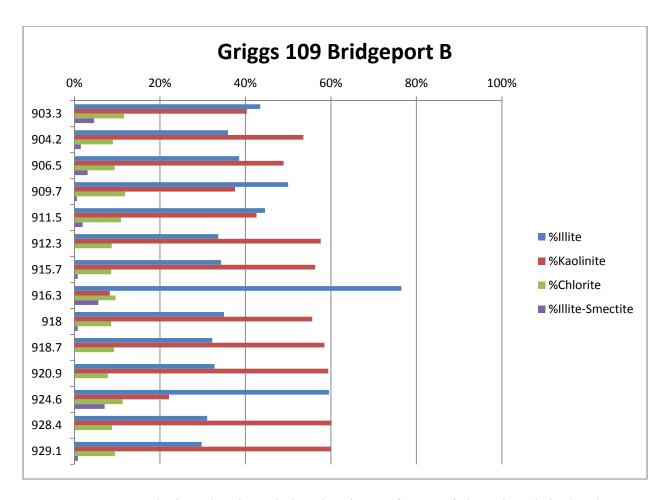


**Figure 52.** Bar graph chart showing relative abundance of types of clay minerals in the clay mineral fraction of core samples in the Bridgeport B sandstone in the Griggs 109 well in Section 32 T4N R12W. The percent of clay minerals in the samples is shown in the previous chart. This chart shows that kaolinite usually the most abundant clay mineral. There are a few examples in shale rich samples where illite is the most abundant clay mineral. Chlorite and mixed layered illite/smectite are the least common clay minerals

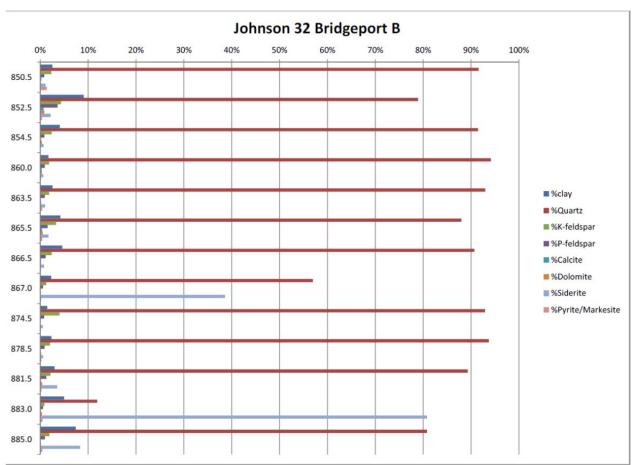


**Figure 53.** X-ray diffraction analyses of bulk mineralogy from core samples show that quartz is the most abundant mineral comprising between 78-93% of most reservoir samples. Two samples at 867 ft. and 883 ft. contain very large amount of siderite. Siderite (FeCO3) is a minor component in all other samples. Diagenetic clay minerals comprise 2-8% of samples. Although clay minerals are a minor component they play a major role in preserving porosity by coating many quartz grains, thereby limiting the development of quartz overgrowths. Potassium and plagioclase feldspar are minor components. The average porosity and permeability of these samples is also 19% and ~150 md respectively.

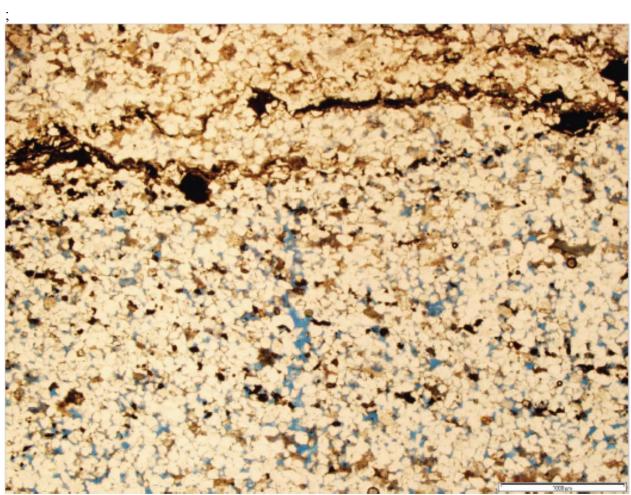


**Figure 54**. Thin section from Griggs 107 well Bridgeport B3 Fine grained sandstone at 929.5 ft,. 19.1Φ, 66k. Fracturing of the sandstone is apparent. Much porosity is occluded by compaction.

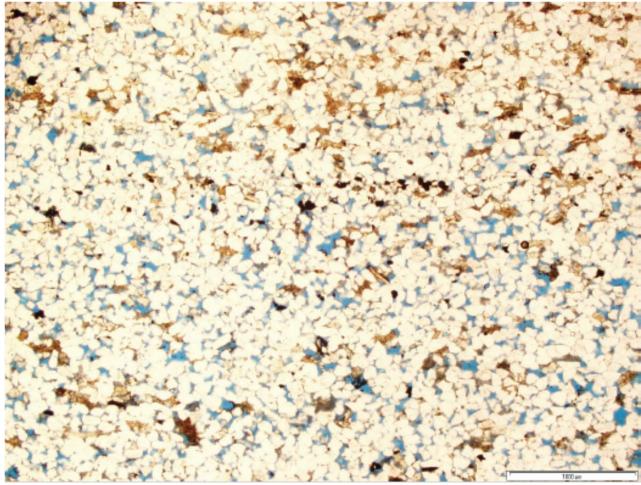


**Figure 55**. Thin section from Griggs 107 well. Fine grained sandstone. 20.3Φ, 171k. Moderate compaction & quartz cementation. Feldspar dissolution has enlarged some pores.

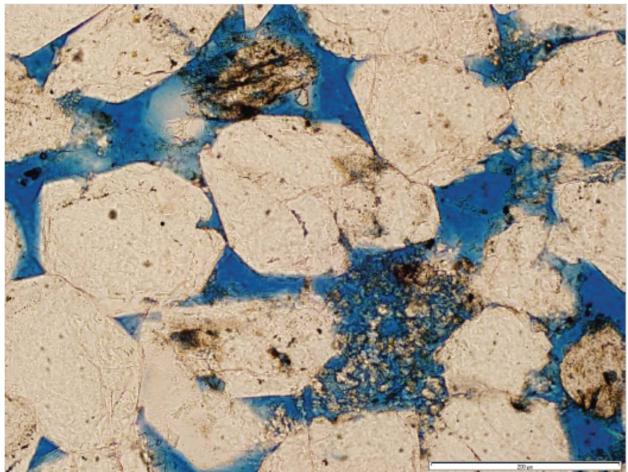


**Figure 56**. Thin Section from Griggs 107 well Bridgeport B2. Fine grained sandstone at 942.8 ft. with. 20.1Φ, 206k. Close-up showing quartz overgrowths cementing grains. Degraded feldspar grains have been replaced with kaolinite.

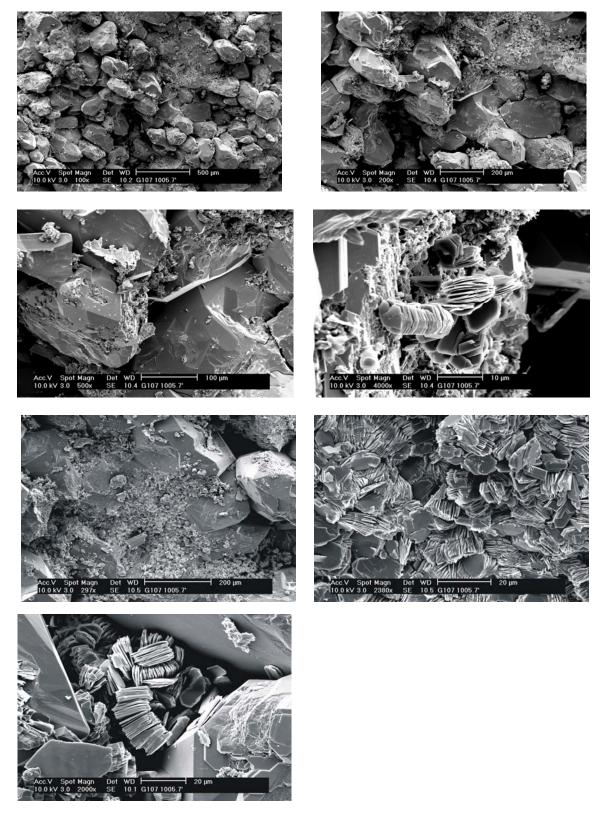


**Figure 57.** Griggs 107 Bridgeport A Pennsylvanian Sandstone. Sand grains in this sample are most commonly fine-to-medium grained. Quartz overgrowths are the main cementing agent. Large crystals of vermiform kaolinite are common.

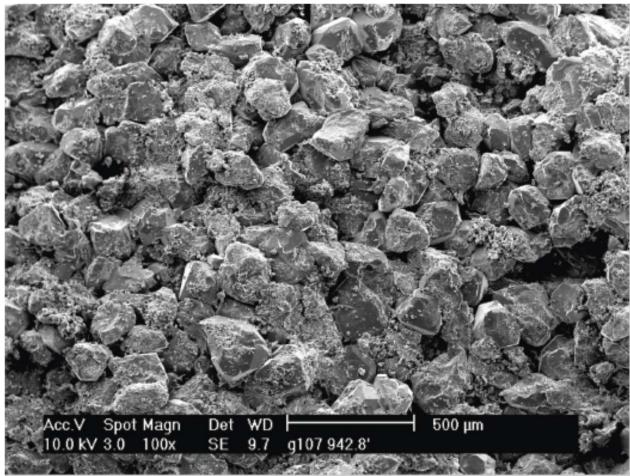


**Figure 58**. Griggs 107 well Bridgeport B2 at 942.8 ft. SEM micrograph shows quartz overgrowths, enlarged pores due to the dissolution of feldspar grains, and pore filling and bridging diagenetic clay minerals.

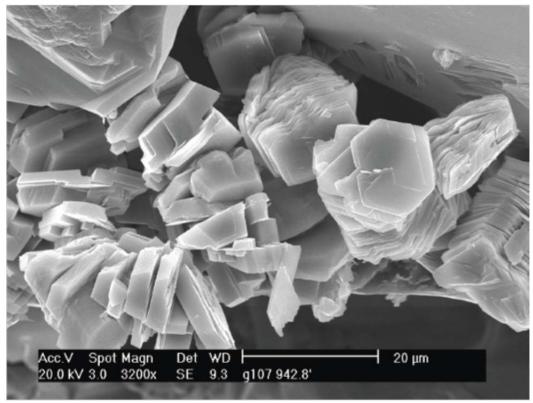


**Figure 59**. SEM micrograph shows close up booklets of the diagenetic clay mineral kaolinite from Griggs 107 at 942.8 ft in previous sample.

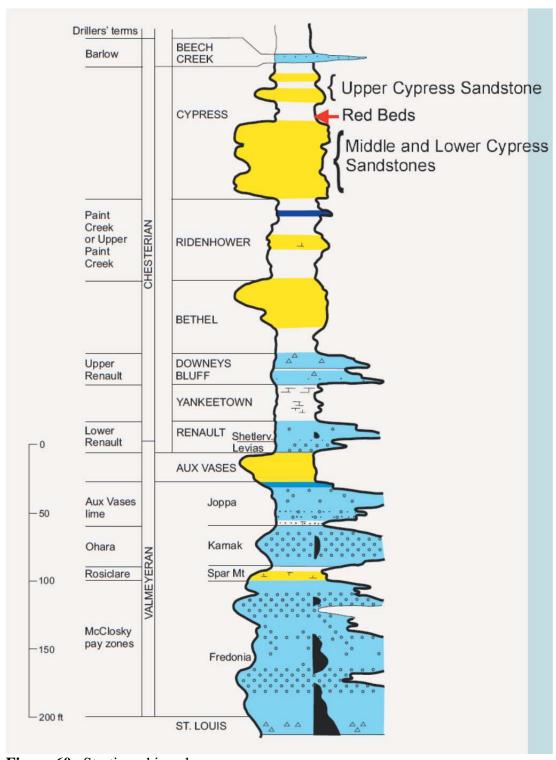
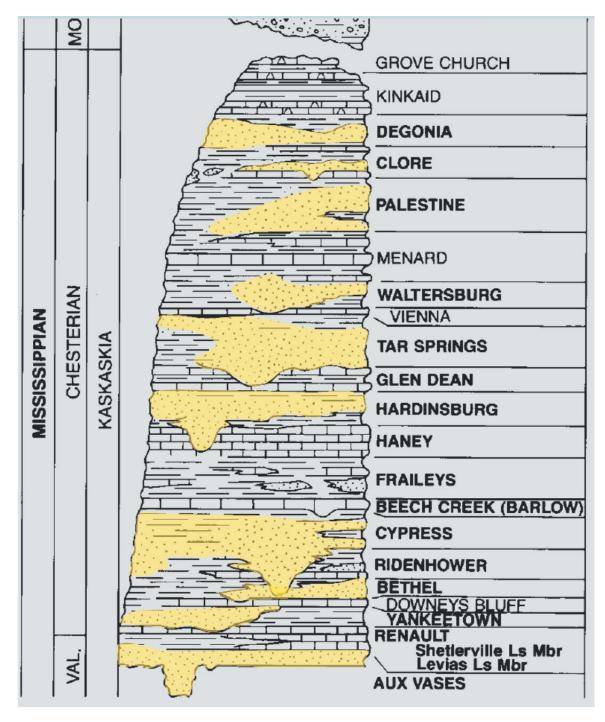
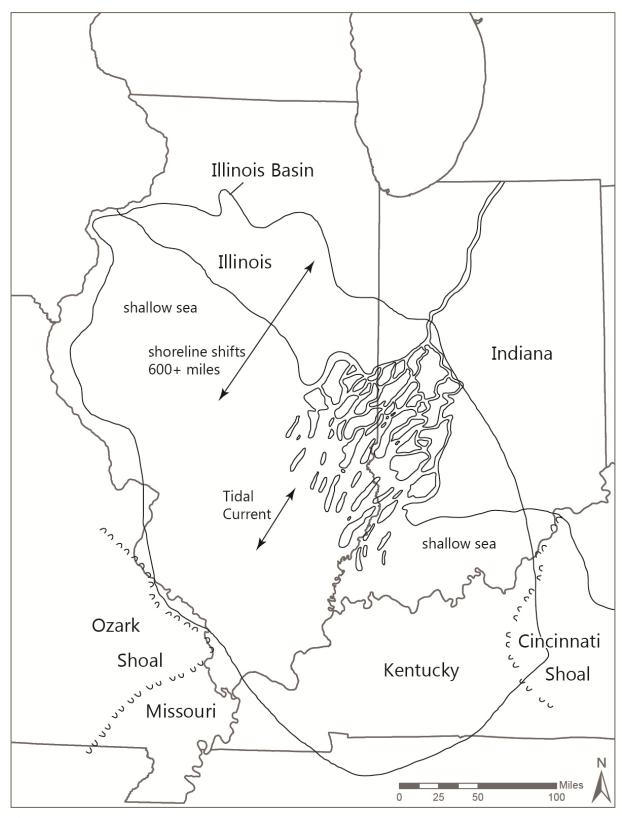


Figure 60. Stratigraphic column



**Figure 61**. Regional stratigraphic column of Middle Mississippian Chesterian strata. Illustrates 10 cycles of siliciclastics alternating with thin limestones.



**Figure 62**. Paleogeographic Map illustrating tidally dominated deposition of siliciclastics and shifting shoreline in response to changes in sea level.

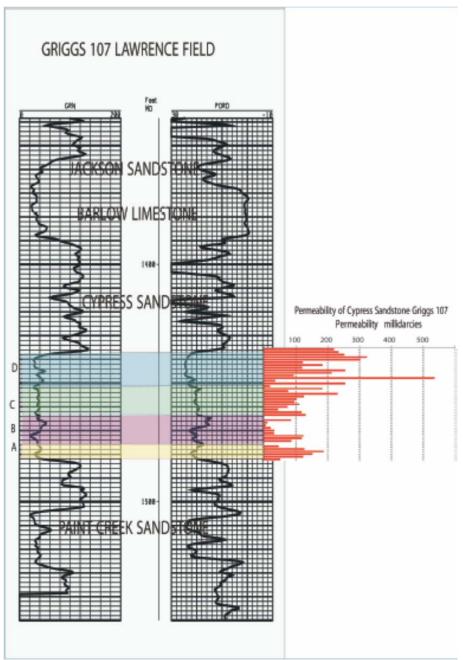


**Figure 63.** Type log from the 2001 drilled Griggs #107 well, SE NE of Section 32, T4N, R12W. The Cypress sandstone has been divided into five separate zones based on correlative units that commonly show lower energy shaly/sandstone breaks between genetic units both in core and on logs. These units, in ascending order, are informally titled the A,B,C,D, and E and are illustrated on the this log (E unit not present in this well). Core permeability values are plotted by the log. Note the very low values (or no values from lack of plugs) in the shale-to shaly-sandstone zones that bound the Cypress reservoir intervals. The thin, low permeability intervals form boundaries and baffles that effectively compartmentalize the Cypress Sandstone reservoir units.

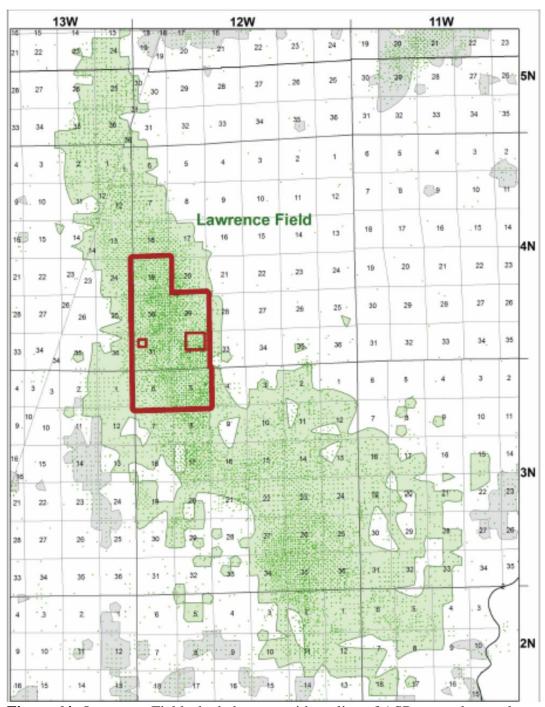


**Figure 64.** Lawrence Field, shaded green, with outline of ASP research area, large red box, and geocellular model area, small red box in the northeast quarter of section 32Map of Lawrence Field Griggs lease



**Figure 65**. Cypress D interval in the Griggs 107 well in the pilot area. This homogeneous, slightly mottled, fine-grained, clean sandstone is a less common facies within the Cypress intervals yet it displays the best porosity, 21 % and permeability, 320 millidarcies. The typical wispy shale laminations were likely destroyed by burrowers. Thin, ripple laminated sandstone beds with flat rip-up clasts at 1438 and 1441 feet are probably the result of changes in depositional energy or sediment supply and, if extensive, can compartmentalize this interval.



**Figure 66.** 121012892800 1301'-1307'. Very fine grained sandstone, tidal deposits. Escape burrow through several alternating fine and very fine grained episodes of sedimentation at 3002'. Tidal laminations and rhythmites can be viewed at 1307.



**Figure 67**. 121012892800 1307'-1313.5' Parallel tidal rhythmites and tidal couplets. Calcite cemented sandstone interval are present in the continuation of cored Cypress Sandstone interval from previous figure



**Figure 68**. Griggs 106 well. .Left example from the Cypress E Interval of herringbone and reverse bedded, ripple cross-laminated reservoir sandstone. Dark wispy, wavy clay laminations are ubiquitous within this facies. This is the predominant reservoir facies within all the Cypress intervals in this and nearby areas of study. Slight variations of this facies include subparallel-to horizontal laminated sandstone with a decrease in the pencilthin, dark gray clay laminations. Herringbone bedding is indicative of tidal current influence on these sediments which are tentatively interpreted as tidal shoal or bar deposits.

## Cypress A Interval Griggs 112 Example on Right side

Griggs 112. Example of fine-grained, subparallel laminated-to reverse and herringbone ripple cross-laminated sandstone, common throughout the Cypress reservoirs in this area. Note the increase of the wispy shale laminations from the planar laminated beds to the ripple laminated beds. The abundance of shale laminations and ripple bedding indicate that current velocities were probably low during most of Cypress deposition.



**Figure 69**. Core from Plains Illinois Griggs 107 well Sec. 32-T4N-R12W. Contact between oil stained reservoir quality sandstone with high core measured porosity and permeability values and interbedded, flaser bedded siltstone and shale permeability barrier.



**Figure 70.** Calcite cemented sandstone indicated at red arrow, limited to a few inches to a foot thick, compartmentalizes the sandstones and is observed in all Cypress core from the pilot area.



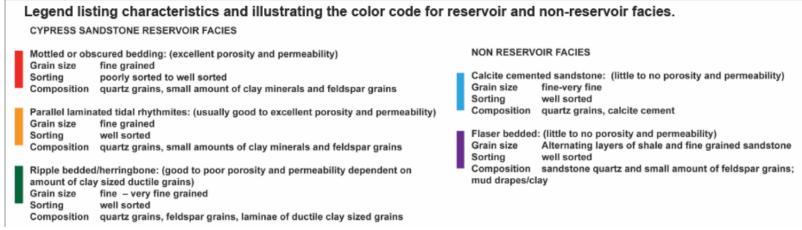


**Figure 71**. Core of entire middle Cypress with lithofacies description from the Griggs #107 well in the SE NE of Section 32. Cypress A interval is included below shale. Core is dominantly wavy laminated, ripple bedded sandstone with ubiquitous wispy shale lamina. Tidal couplets and tidal generated herringbone ripple beds are common sedimentary features. The uppermost 8 feet, the D interval is a mottled, poorly sorted facies lacking bedding features and has the best reservoir porosity and permeability. This appears to be a totally bioturbated facies. A common lithology noted is a calcite cemented sandstone that is generally less than a foot thick. These beds likely act as baffles or boundaries to fluid flow. Meteoric water percolation that leaches and re-precipitates lime during subaerial exposure of shoals is suggested as the source of these baffling beds.

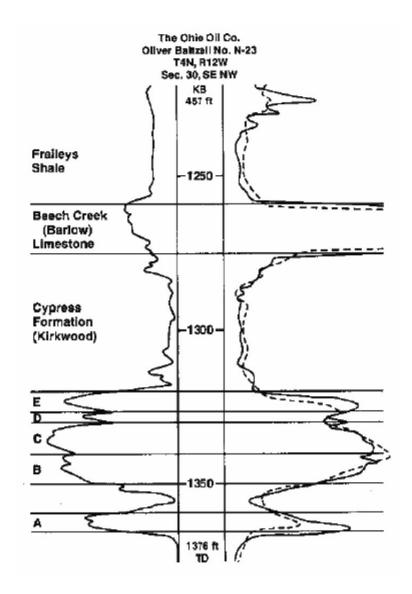


**Figure 72.** Type log from the Baltzell #N-23 well in the SeNw of section 30 showing the Cypress Sandstone stacked intervals "A" through "E". The SP trace on the logs from the 1940-50s characteristically "amplify" the deflection between the cleaner reservoir sandstone and the shaly sandstone breaks. Very characteristic within the Cypress and most other sandstone bodies within the Mississippian and Pennsylvanian section is a 10 foot genetic thickness tendency of units that is probably a function of accommodation space, and the rates of deposition vs. subsidence in cratonic basins. These intervals commonly coalesce which may then show up as thicker units. The "10 foot rule" can be very useful tool for correlating these thinly bedded units in cratonic settings.

The individual Cypress sandstone intervals have lenticular, tidal shoal geometry where each shoal defines discreet reservoir flow units. The following isopach maps (three of which were generated by computer with GeoGraphix software) display the shoal geometry.

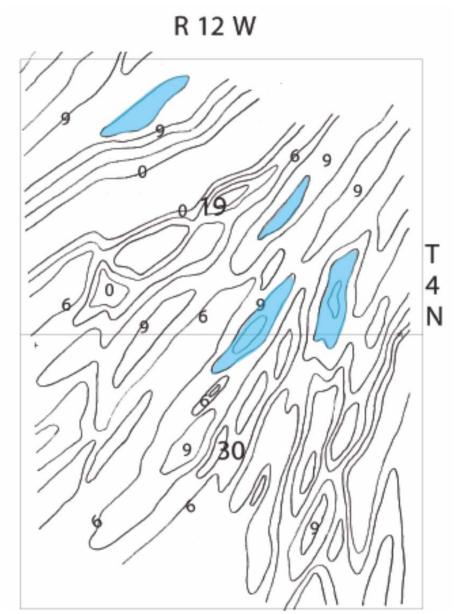


**Figure 73.** Comparison of an early version of Cypress D thickness map from sections 19 and 30 that was hand contoured. Note the geometry and trend that are common with the computer generated maps. (C.I. 3 feet)

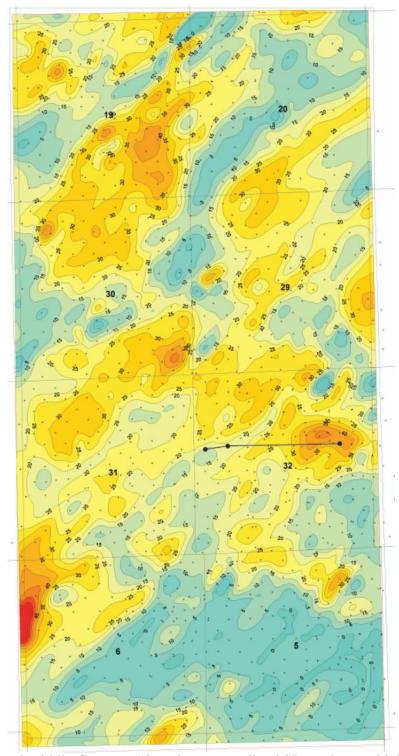


**Figure 74.** Total middle Cypress, 50% clean normalized SP sandstone thickness map of the study area. This interval includes the B,C,D,E intervals. These units are all interpreted to be tidal shoal deposits that are found in modern high tidal range settings. Note the elongated, shoal geometry trending northeast-southwest. The basal Cypress A interval appears to be a deltaic depositional facies which is less permeable and therefor is, more commonly, non-productive. (C.I. 5 feet).

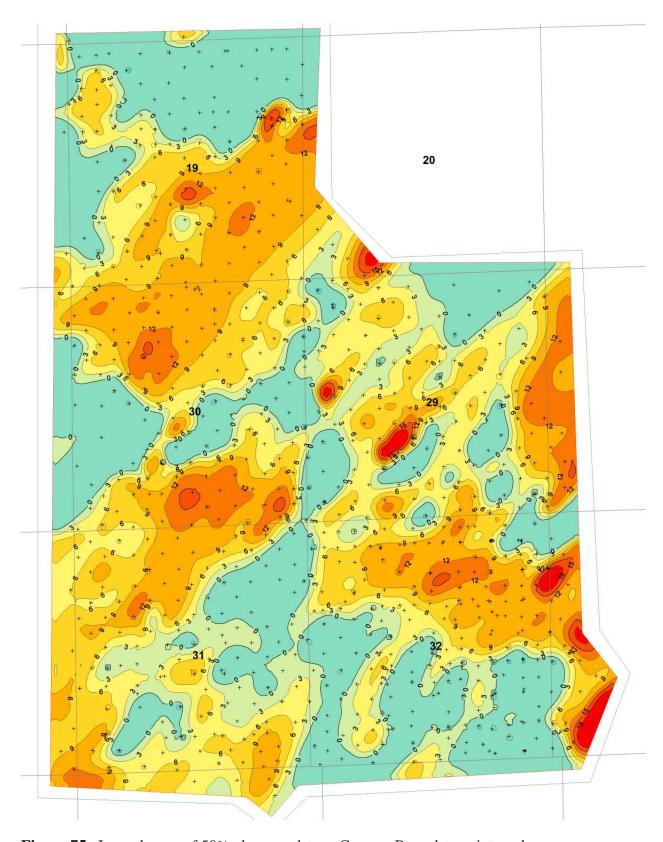


**Figure 75.** Isopach map of 50% clean sandstone Cypress B sandstone interval.

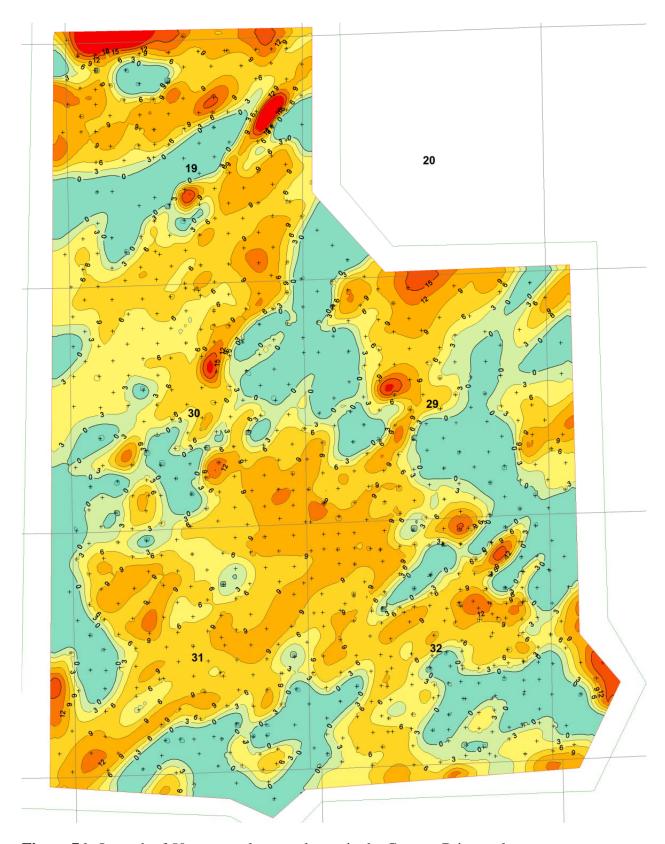
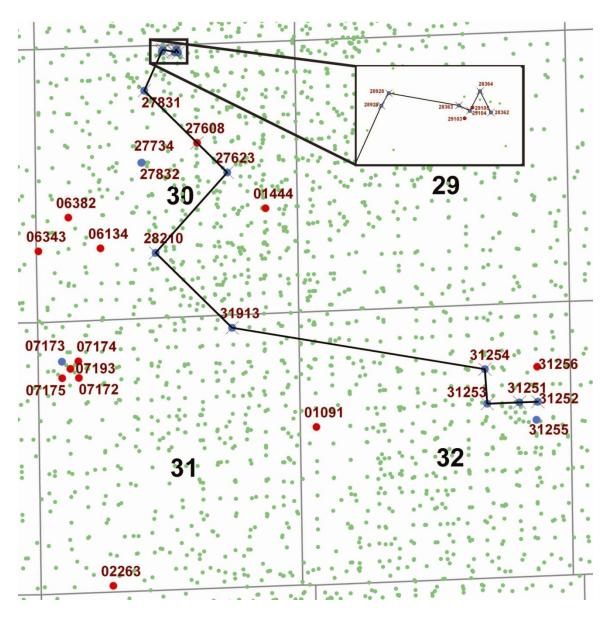
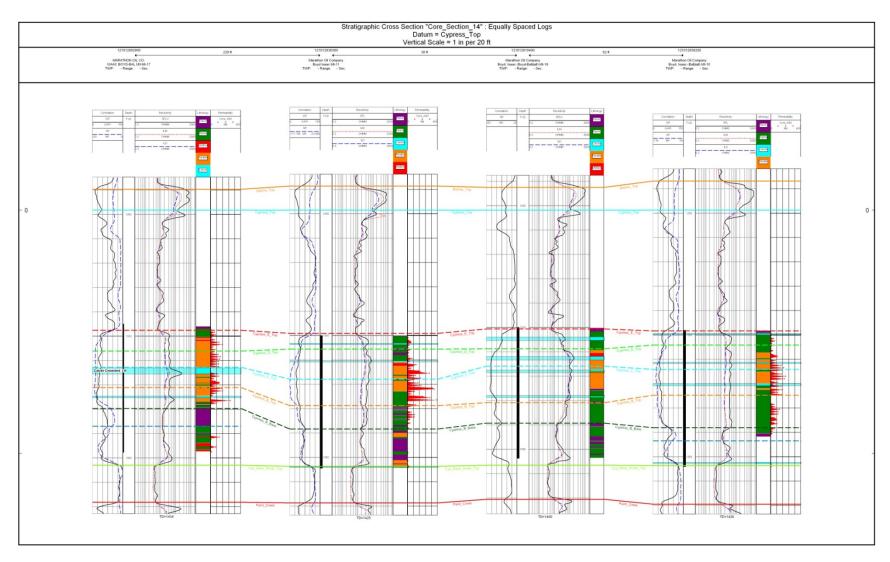


Figure 76. Isopach of 50 percent clean sandstone in the Cypress D interval



**Figure 77**. Location map for detailed cross section of cored wells in Sec 30 T4N R12W (see inset) and regional cross section of cored wells connecting pilot area in Sec 32 T4N R12W with Sec 30 T4N R12W.



**Figure 78**. Detailed core cross section in Sec 30 T4N R12W. The rightmost track for each well graphs core measured permeability in red, the color-coded track corresponds to the three reservoir and 2 non reservoir facies in the legend in figure 71. The mottled/obscurely bedded facies indicated by a red bar possesses the best porosity and permeability values, the parallel/sub parallel bedded tidal rhythmites also possess very good porosity and permeability are indicated by orange bars, the ripple bedded facies possesses good to poor porosity and permeability is indicated on the cross section and in core by green bars. The non-reservoir flaser/wavy/lenticular bedding facies is indicated by a purple bar and the non-reservoir calcite cemented sandstone facies is indicated by a light blue bar.

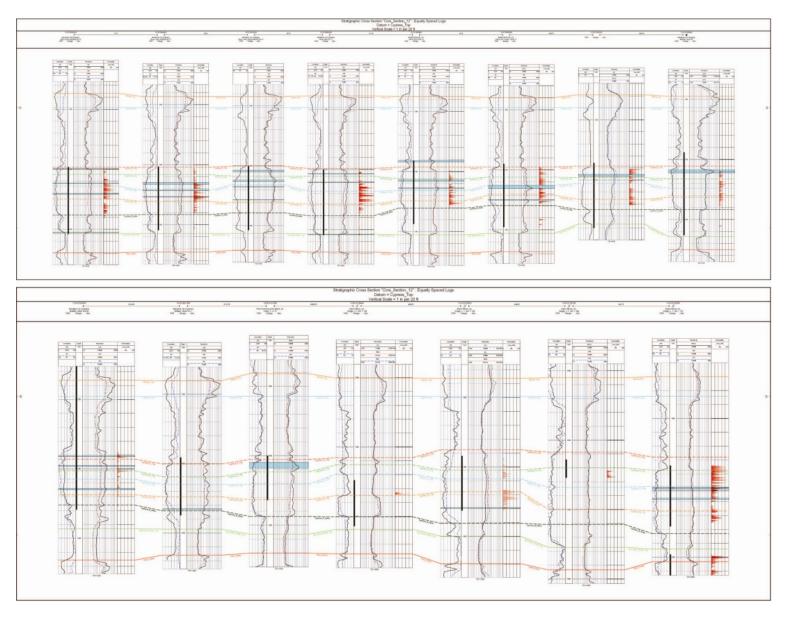


**Figure 79**. Cross section of cored wells connecting the Griggs lease in the pilot area through Sec. 30 T4N R12W in the expansion area. Datum is the Barlow Limestone. Core measured permeability is graphed in red to the right of geophysical logs. Calcite cemented sandstone intervals are shown in

blue. Location map is in figure 17. This cross section shows excellent correlation of the A, B, C, D, and E intervals in the Cypress Sandstone from pilot area in the Griggs lease to the heavily cored area in Sec 30 T4N R12W.

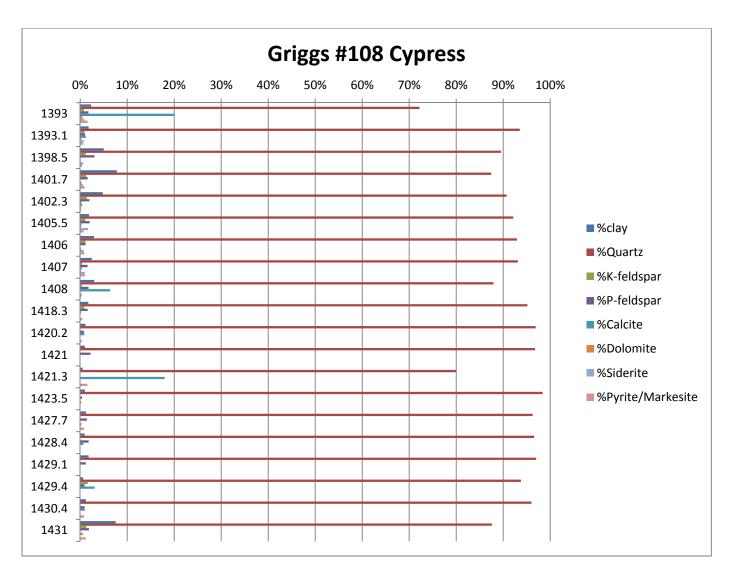


Figure 80. X-ray diffraction analyses of bulk mineralogy of samples from Griggs 108 well.

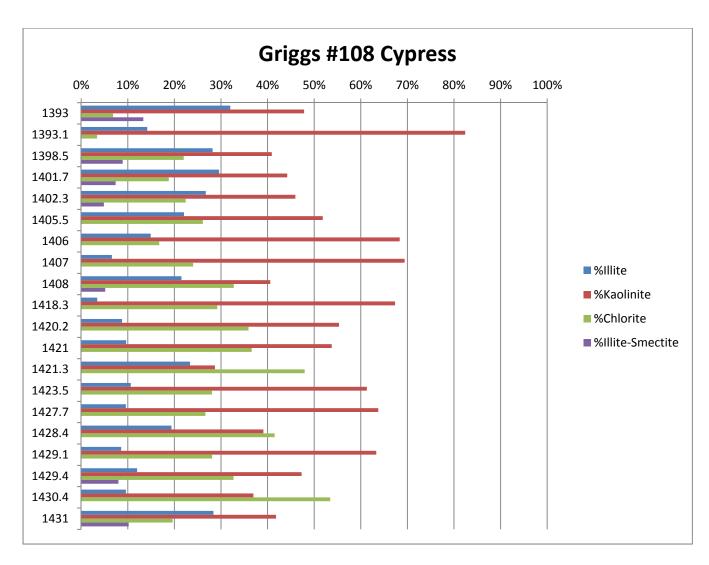
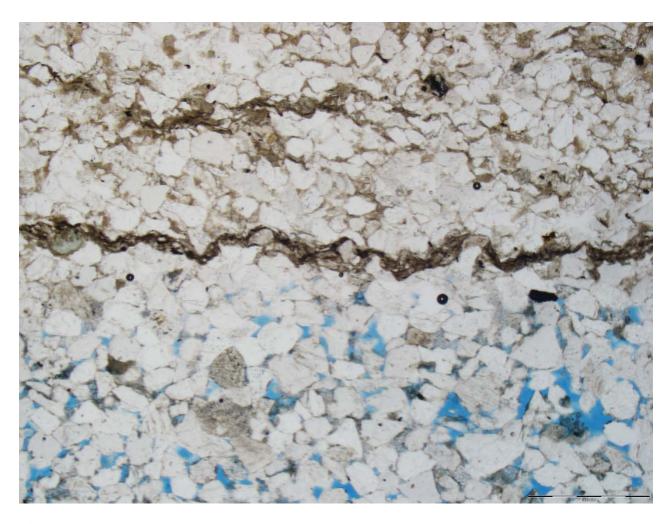
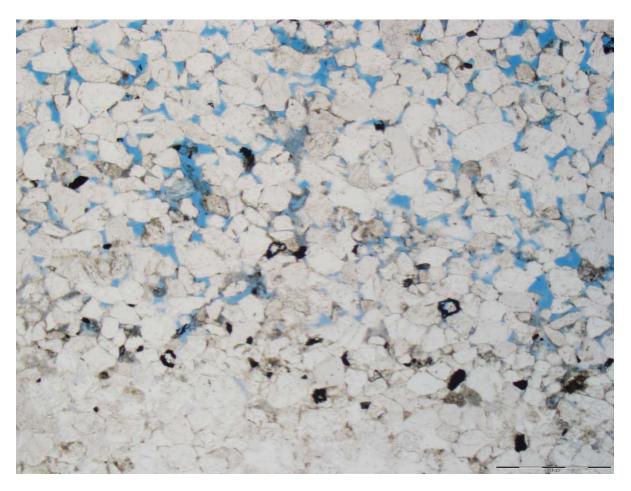


Figure 81. X-ray diffraction analyses of clay sized fraction of samples from Griggs 108 well.



**Figure 82**. Example from the Griggs 107 at 1453.4' shows porous laminae alternating with non-porous laminae. Porosity is highlighted by medium blue stained epoxy. A styolitic parting separates the nonporous tightly cemented fine-grained sandstone from the porous sandstone.



**Figure 83**. Thin section from the ripple bedded facies. The lower portion of the thin section shows sand grains tightly cemented by quartz overgrowths. There is a heavy mineral lag composed primarily of zircons that separates the tightly cemented non-porous sandstone from the porous upper portion of the thin section. Griggs 107 1450.3'.

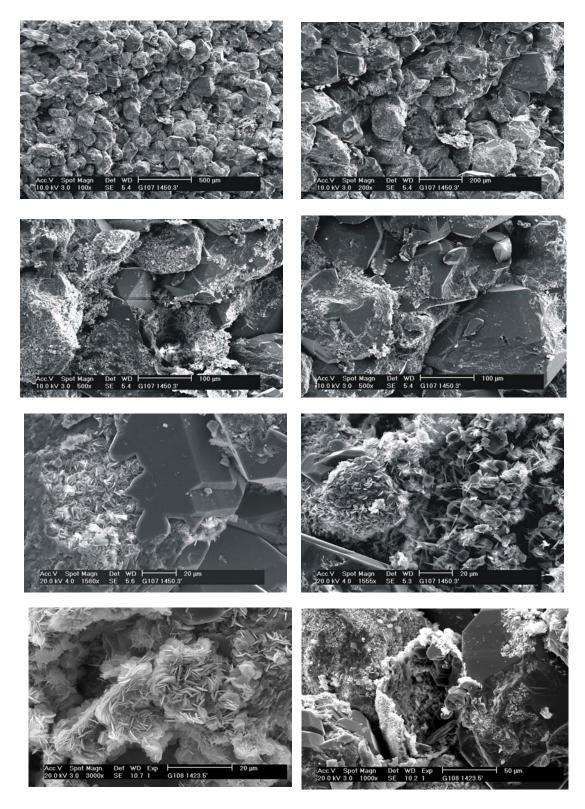


**Figure 84**. Cypress Sandstone sample from the Griggs 107 well. Cypress Sandstone is fine-grained and cemented by quartz overgrowths. The most common diagenetic clay mineral in the Cypress Sandstone is Ferich chlorite. Numerous sand grains in the photographs are coated by chlorite. Several stages of Ferich chlorite precipitation are evident in this sample. The bottom left photograph shows quartz overgrowth precipitated over

chlorite clay minerals. The bottom right photograph shows a grain completely coated by chlorite and an area occupied by a degraded feldspar grain with diagenetic chlorite and illite.

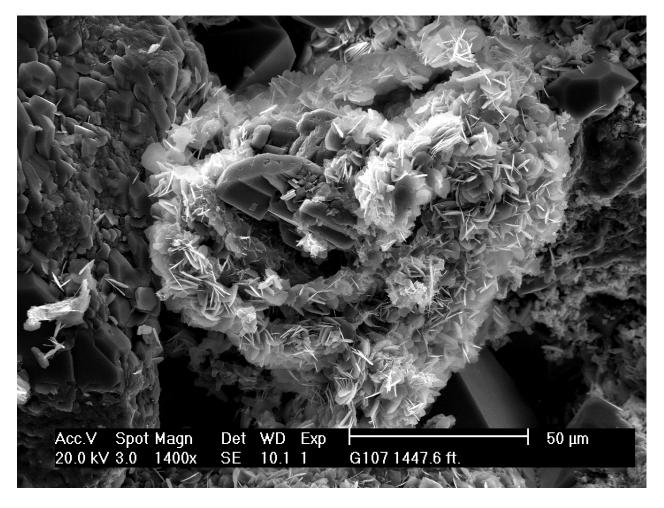


**Figure 85**. Scanning electron photomicrograph of grain coated with Fe-rich chlorite, the most common clay mineral in the ripple-bedded reservoir facies.

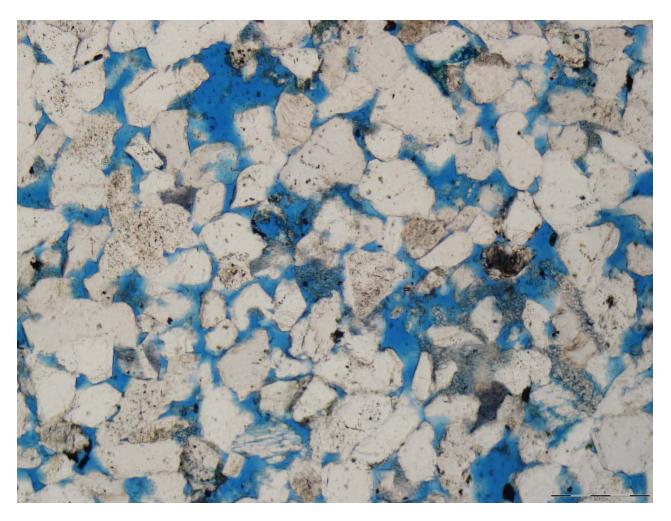


**Figure 86**. Griggs 107 well 1434.4' 219 perm 19.8% porosity. Thin section photomicrograph of sample from bioturbated facies. Large amount of intregranular porosity shown by blue stained epoxy. Euhedral quartz overgrowths shown in some grains. Degraded plagioclase feldspar grains as well as nearly completely degraded feldspar grains shown in sample.

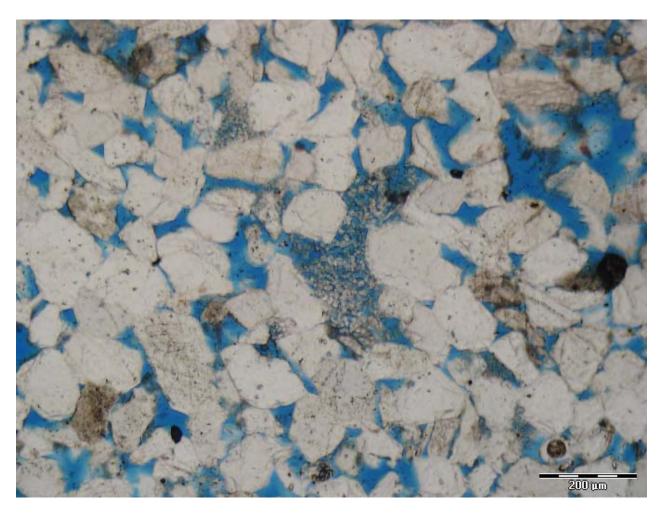


**Figure 87**. Griggs 107 well 1434' Bioturbated Cypress Sandstone Facies Interval (D). Most porous and permeable unit in Cypress 300md 20% porosity. Poorly sorted thin section with large amount of intergranular porosity. Some sand grains show euhedral quartz overgrowths. Large feldspar grain degraded to kaolinite in center of photomicrograph.

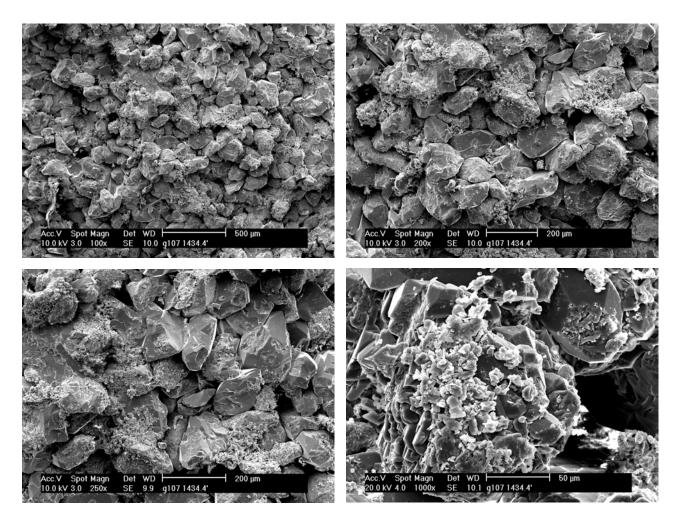


**Figure 88**. SEM photomicrographs from bioturbated facies in Griggs 107. Shows poorly sorted, fine-grained sandstone. Good intergranular porosity. Cemented by quartz overgrowths with large amounts of intergranular porosity. Some secondary porosity caused by dissolution and degradation of feldspar grains. Some feldspar grains degraded to kaolinite clay minerals.

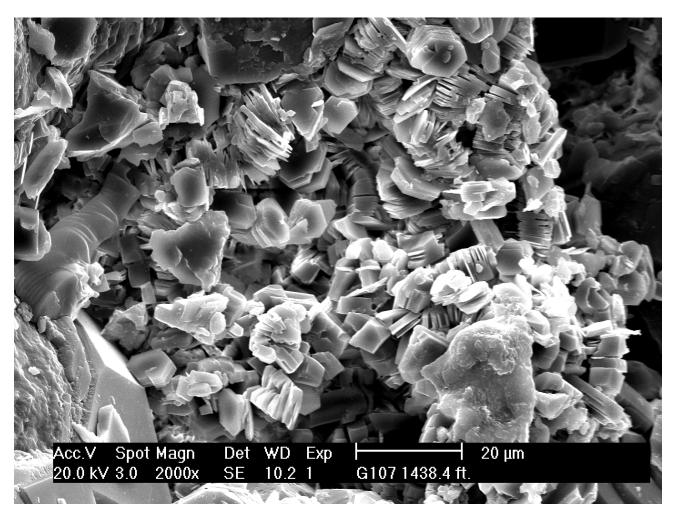


**Figure 89**. Close-up from sample of bioturbated facies in the Griggs 107 well at 1438.4'. This SEM close-up shows kaolinite clay mineral booklets likely derived from degradation of feldspar grains.



**Figure 90**. Griggs 107 1458' depth at red arrow in figure 12. This thin section is from 1458' depth indicated by red arrow in figure 70. This photomicrograph shows calcite cement stained dark navy blue indicating that the calcite is iron rich because the thin section was stained with a mixture of alizarine red containing potassium ferricyanide. The grains are fine-grained and angular. Porosity and permeability are minimal in intervals cemented by ferroan calcite.

Porosity = 2.2%

Perm. = 0.0006 md

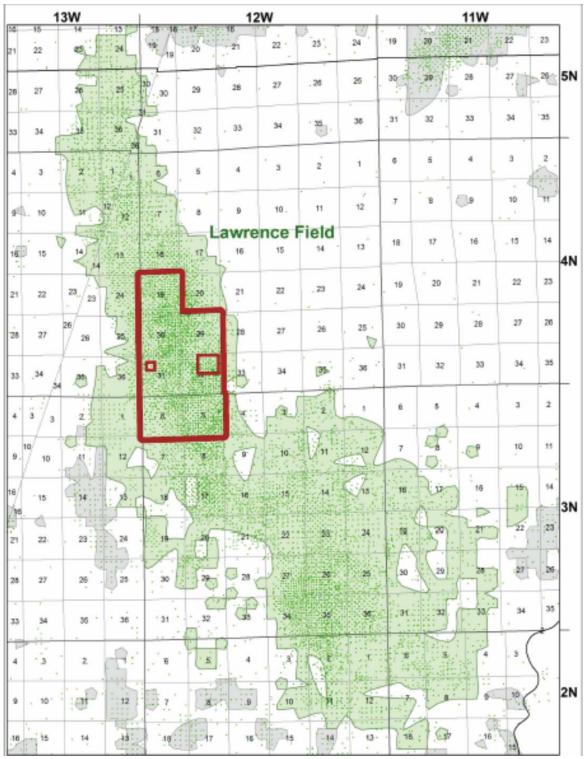


**Figure 91.** Lawrence Field, shaded green, with outline of ASP research area, large red box, and geocellular model area, small red box in the northeast quarter of section 32Map of Lawrence Field Griggs lease

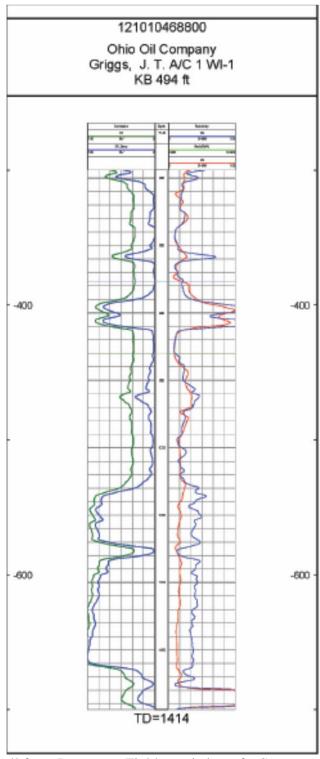


**Figure 92.** A typical well from Lawrence Field consisting of a Spontaneous Potential (SP) curve, in blue on the left, and two normal resistivity curves on the right. The SP curve was chosen as an analog for petrophysical properties for the geocellular modeling. The SP was first normalized (green curve) to remove well-to-well variation.

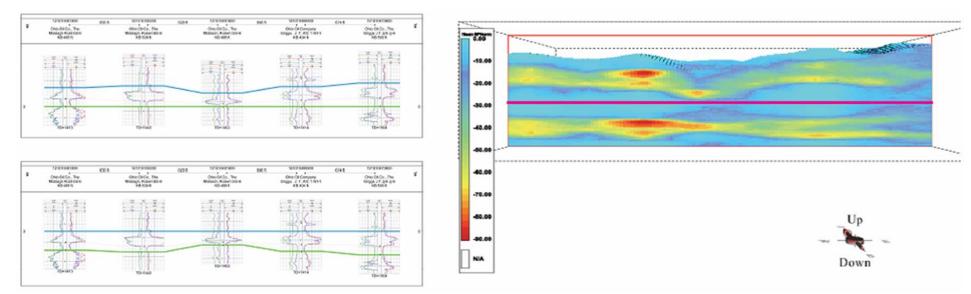
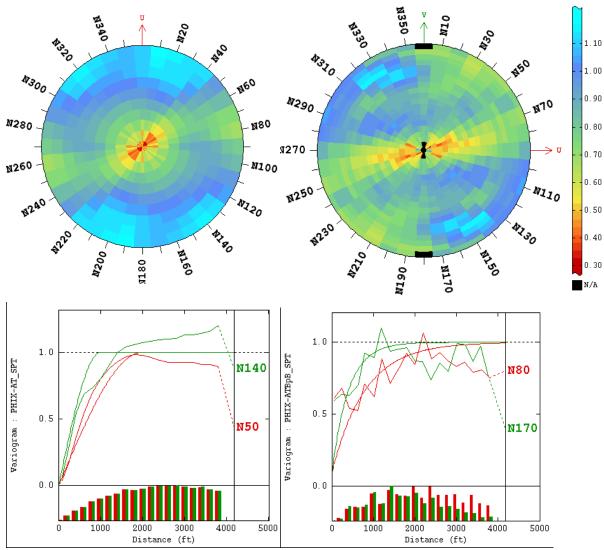
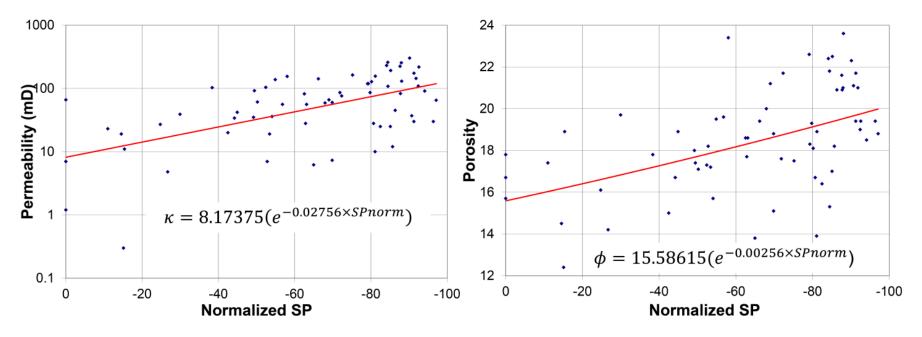


Figure 93. The effect of picking different stratigraphic datums on the modeling was examined during the course of the study. In the two cross sections on the left, two different origins were picked. In the top, the base of the shale (green line) occurring immediately below the Bridgeport B Sandstone was chosen as the datum while in the bottom cross section, the base of a coal marker (blue line) occurring above the Bridgeport B, was chosen. The effect of different stratigraphic datums on the modeling is shown in the image to the right. The two different models are stacked one on top of the other with the pink line separating the two. The top model uses the shale as the datum while the bottom model uses the marker bed. The nature of the two datums has dramatic effect on the continuity of the Bridgeport B sandstone. Because the marker bed tends to have a consistent stratigraphic position relative to the Bridgeport B, the Bridgeport B has a much more continuous nature. In the shale datum model, the shale has been eroded away in several places. As a result the Bridgeport B appears to be more discontinuous and compartmentalized. Using the marker bed as the stratigraphic datum more closely matches the geologic conceptual model.



**Figure 94.** The results of the semivariogram analysis of the Bridgeport B and Cypress sandstones. The results of the analysis of Cypress sandstone are shown on the left while the results of the analysis of the Bridgeport B sandstone are shown on right. The top images are semivariogram maps while the bottom two images show the semivariograms and the models fitted to them. The histogram at the base is the number of data points.

The semivariogram map of the Cypress shows a strong anisotropy in the N50° direction while the Bridgeport B has a strong anisotropy in the N80° direction. The resulting semivariograms and associated models demonstrate the magnitude of the anisotropy.



**Figure 95.** Plots of normalized SP from the log data versus permeability and porosity measurements from core data for the Cypress sandstone. The curve fitted to the data is shown in red and the resulting equation for each curve is shown on the plot. The equations were used to transform the model generated populations of normalized SP into the desired petrophysical properties. Due to the scatter of the data, the geologist's experience was relied on to select a suitable curve.

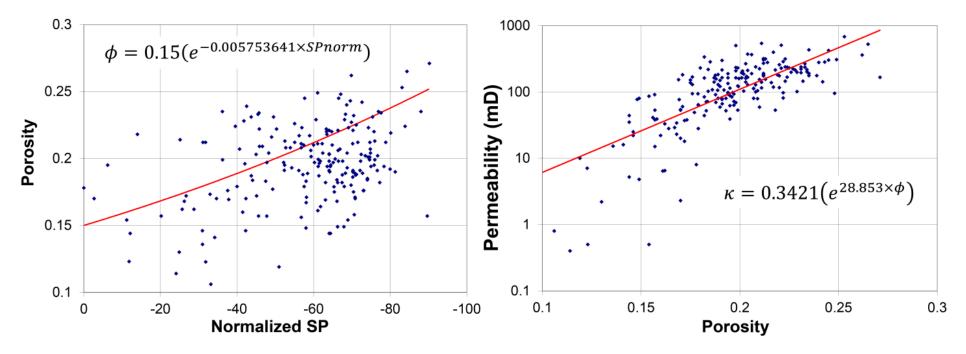


**Figure 96.** Plots of normalized SP versus cross plotted porosity and porosity versus permeability for the Bridgeport B sandstone. Curves are fitted to both sets of data and the resulting equation shown at the bottom. For the Bridgeport B model, the SP curves from the older geophysical logs were first converted into cross-plotted porosity using the equation on the left. The geocellular models were then built using the resulting porosity-curve data set. Once the geocellular model was complete, the simulated values of porosity were converted into permeability using the equation on the right.

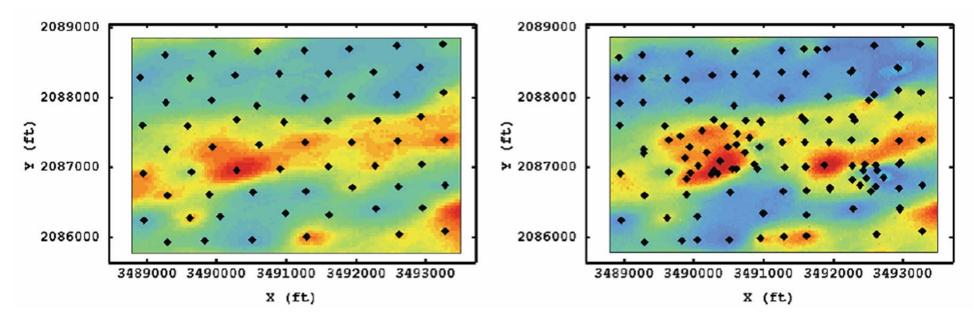


**Figure 97.** Two planar slices through the Bridgeport B geocellular model of porosity showing the effect of combining newer log data. Initially, the model was constructed using data derived from SP logs, as seen in the figure on the left. However, the area had a significant number of neutron-density porosity log data. A method to combine the two data sets was undertaken. The geostatistical method of Cokriging with collocated drift was attempted but a simple linear regression method produced the best correlation. The effect of the additional, newer data on the model is shown in the image on the right. While there are some significant differences, the overall outline of the field is similar, especially when a porosity cutoff is considered. The black diamonds in both images represents well locations.

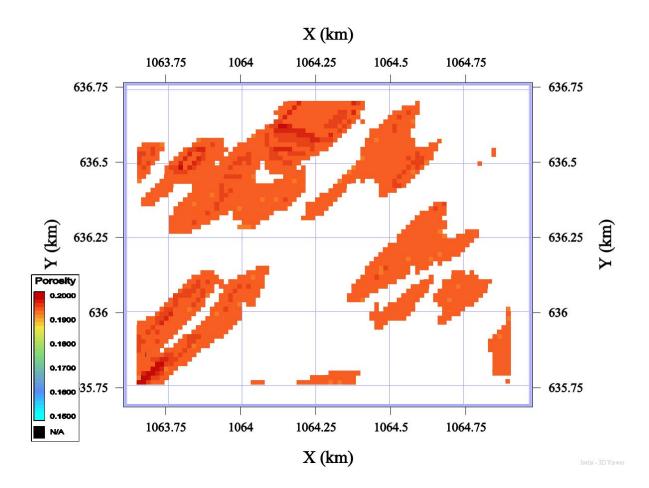


**Figure 98.** Planar view of the Cypress Sandstone geocellular model. A 19% cutoff has been applied to show the trend of the flow units in the field. The model shows good agreement with the isopachs of the Cypress D in Section 32.

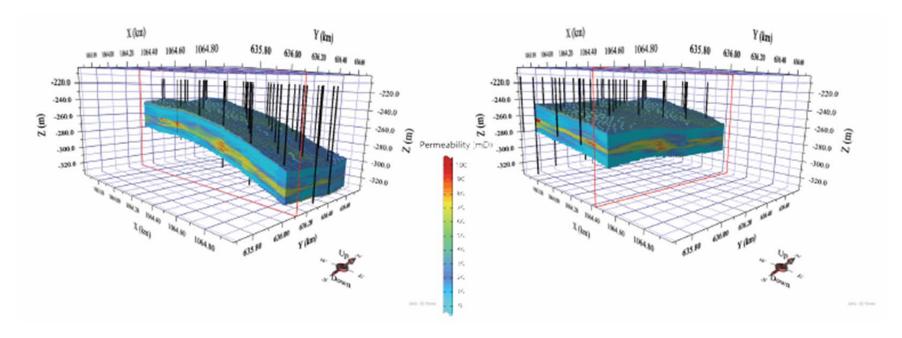


**Figure 99.** The geocellular model showing the reservoir architecture of the Cypress Sandstone. The upper two images show the permeability distribution within the model in structural space with the wells represented as thick, black lines. The image on the left shows a north to south cross section while the image on the right is a west to east cross section. Note the compartmentalization and the multiple, stacked units reflected in the model.

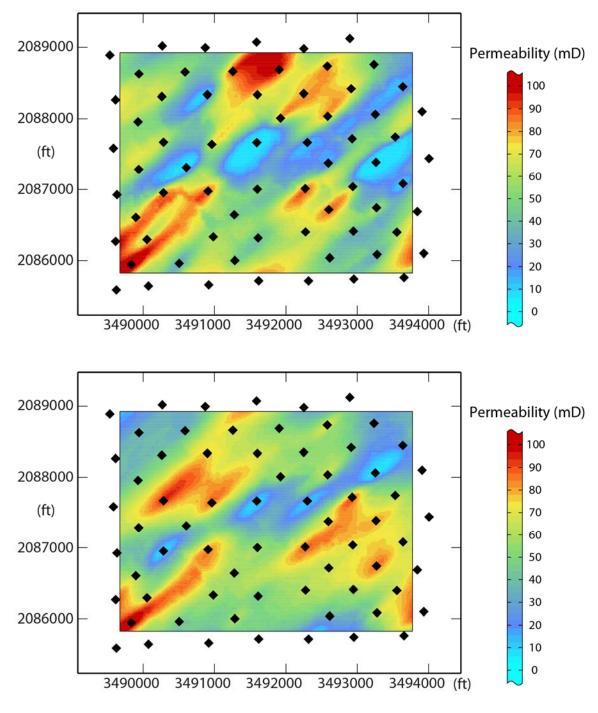


**Figure 100** Planar slices through the geocellular model of the Cypress sandstone showing the distribution of permeability. The upper figure is taken 60 feet below the Barlow limestone while the lower figure is taken 70 feet below the Barlow limestone. The model is in stratigraphic projection. The black diagrams represent wells with geophysical logs used to construct the model. The figures demonstrate the degree of compartmentalization in the reservoir and the inherent problems determining which wells are in communication.

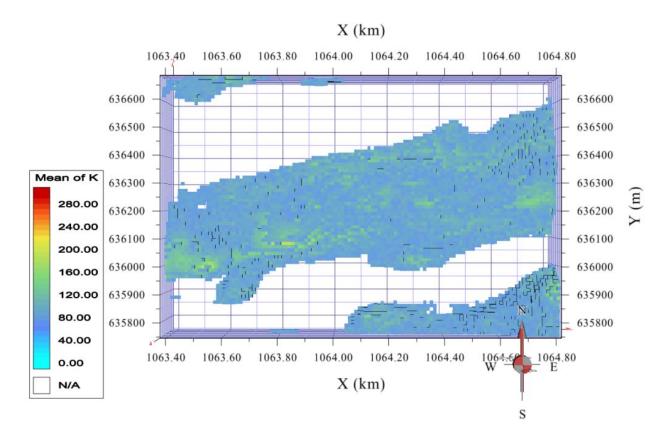


**Figure 101** Planar view of the Bridgeport B sandstone geocellular model. A 17% cutoff has been applied to show the geometry of the reservoir. The model shows good agreement with the isopach of the Bridgeport B in Section 32.

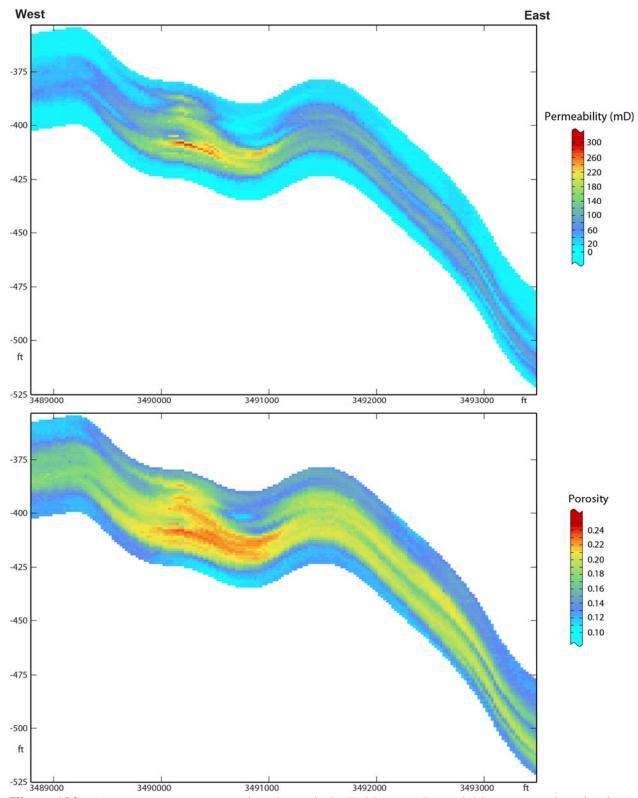


**Figure 102.** A west to east cross section through the Bridgeport B model in structural projection. The top figure shows the distribution of permeability while the lower one shows porosity. The trace of the cross section is shown in Figure X-X.

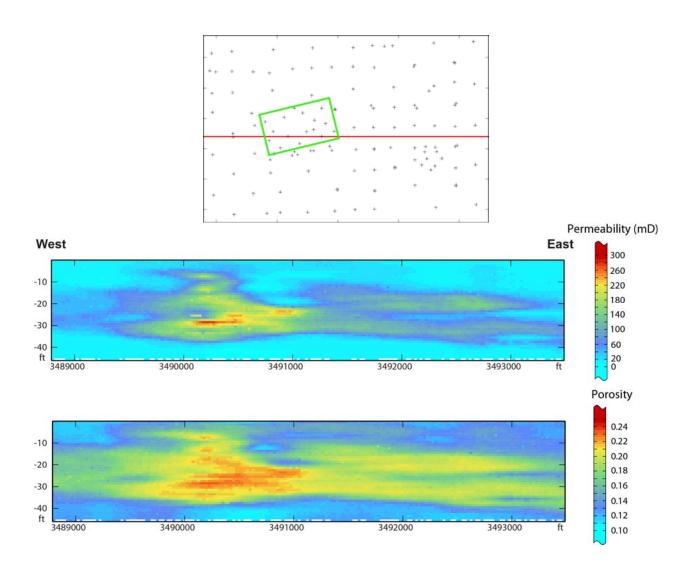


**Figure 103** A west to east cross section through the Bridgeport B model in stratigraphic projection. The top figure shows the distribution of permeability while the lower one shows porosity. On the plane view map of the model area at right, the trace of the cross section is a red line while the approximate location of the ASP pilot is shown as a green box.

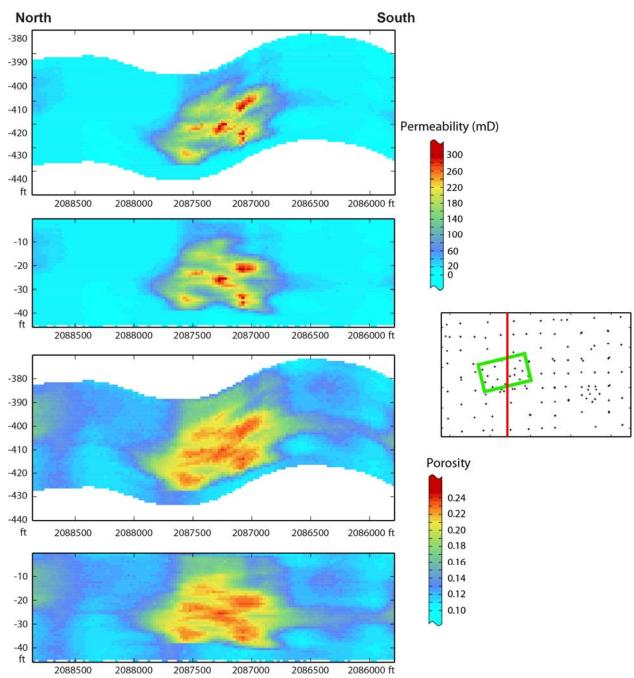


**Figure 104.** Cross section through the Bridgeport B model from north to south. The top two figures show the distribution of permeability while the lower two show porosity. Starting at the top, the first and third figures are projected structurally while the second and forth are projected stratigraphically. On the plane view map of the model area on the right, the trace of the cross section is a red line while the approximate location of the ASP pilot is shown as a green box.

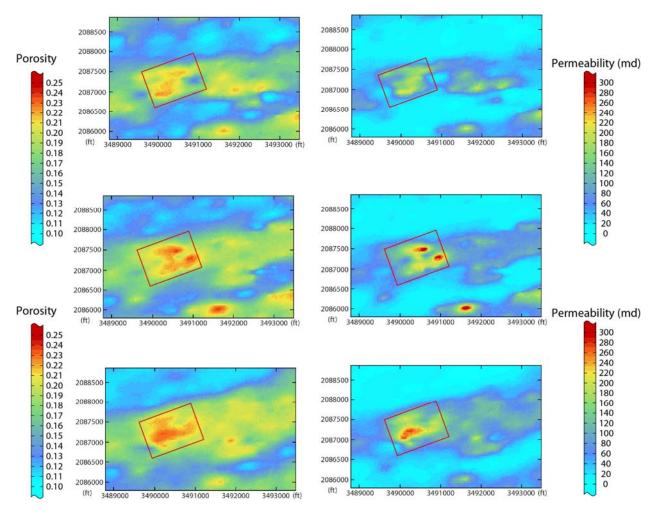


**Figure 105.** The geocellular model showing the reservoir architecture of the Bridgeport B Sandstone. The images show planar sections through the model in stratigraphic projection. The top-most images are taken at 17 ft. below the datum, the middle are taken at 23 ft. below, while the lowest images are taken at 28 ft. below the datum. Images on the left display porosity while images on the right display permeability. The red square is the approximate boundaries of the ASP pilot.

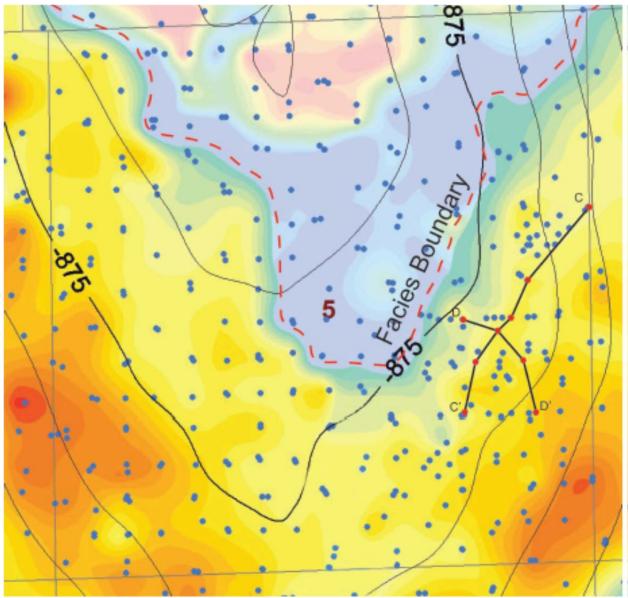


**Figure 106.** Permeability and porosity cross sections generated by Landmark GeoGraphix software package. The map shows the cross section grid in the eastern part of Section 5 through wells with core measured porosity and permeability values. The porosity and permeability values are from thick channel fill sandstone. This is the same area as the 1980s Maraflood pilot and the recently completed ASP pilot. Cross sections to the right show porosity and permeability values interpolated between the wells. The cross sections indicate the presence of flow units in the sandstones which have higher permeability and porosity.

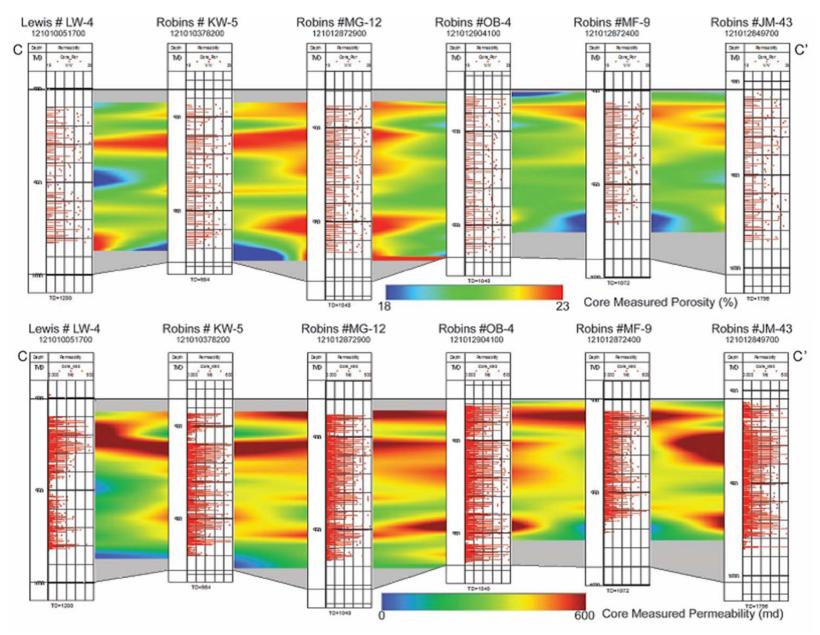


**Figure 107.** Cross section C-C' showing core porosity (top) and permeability (bottom). Warmer colors are areas of higher porosity and permeability (600 md) and cool colors are areas of lower porosity and permeability.

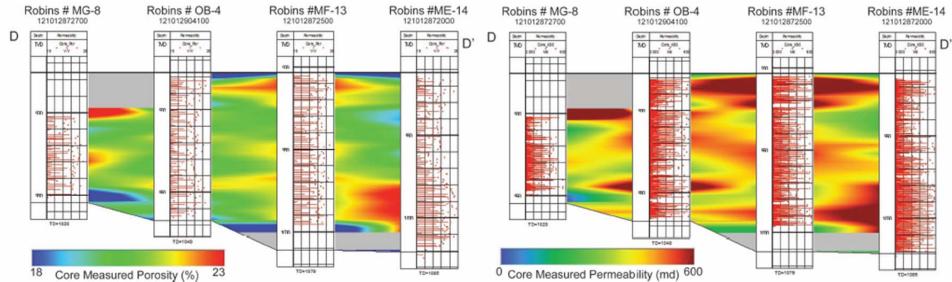


**Figure 108.** Cross section D-D' showing core porosity (left) and permeability (right). Warmer colors in the left section are areas of higher porosity (23%) and cool colors are areas of lower porosity (18%). Warmer colors in the right section are areas of higher permeability (600 md) and cool colors are areas of lower permeability.

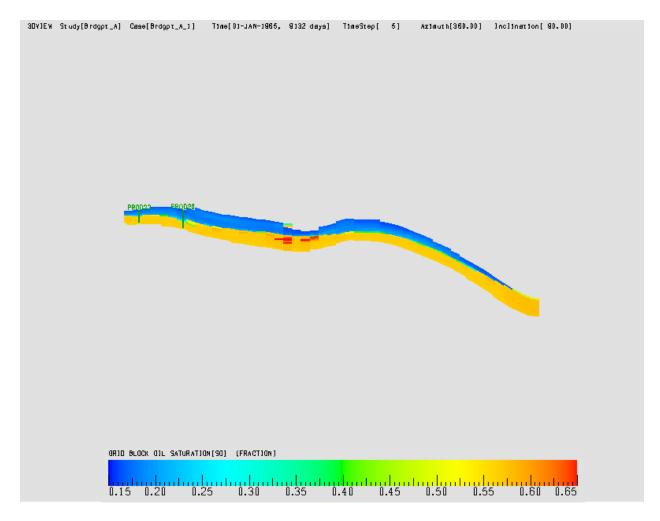


**Figure 109.** East-West Cross section showing oil saturation at the end of primary production, blue color is low oil saturation due to high gas saturation at top of formation.

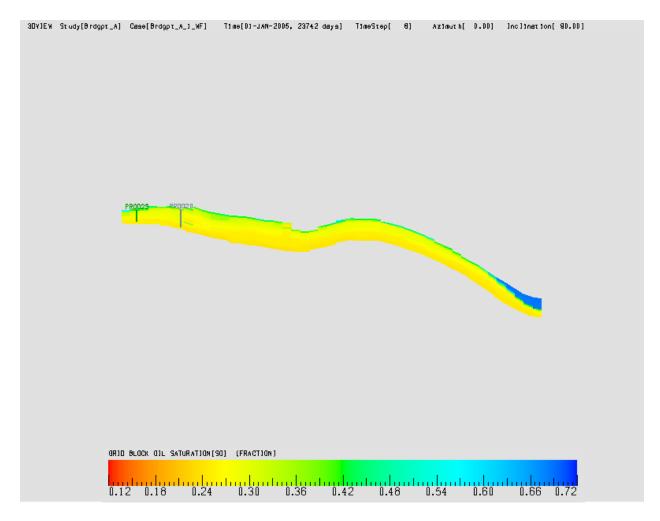


**Figure 110.** East-West Cross section showing oil saturation at the end of waterflood, blue color is low oil saturation due to high gas saturation at top of formation.

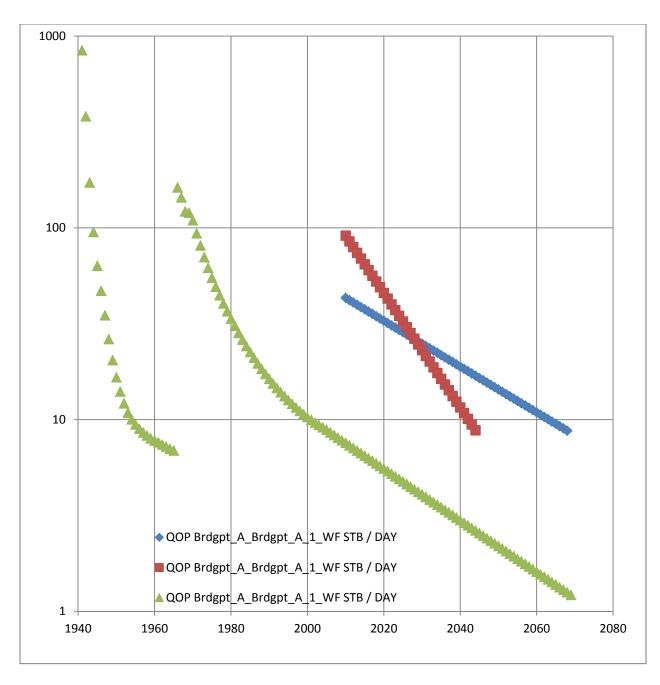


**Figure 111.** VIP projection of oil production with ASP adaptation based on Rex Energy reported oil production response at 15 acre, six-five spot pilot area.

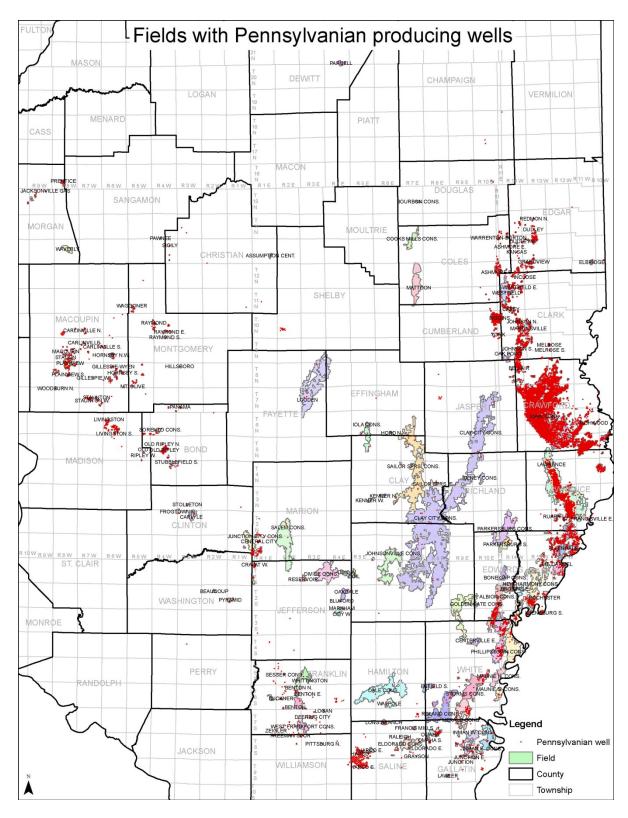


**Figure 112.** Map shows location of wells producing from Pennsylvanian reservoirs in red. Oil fields in pastel colors.

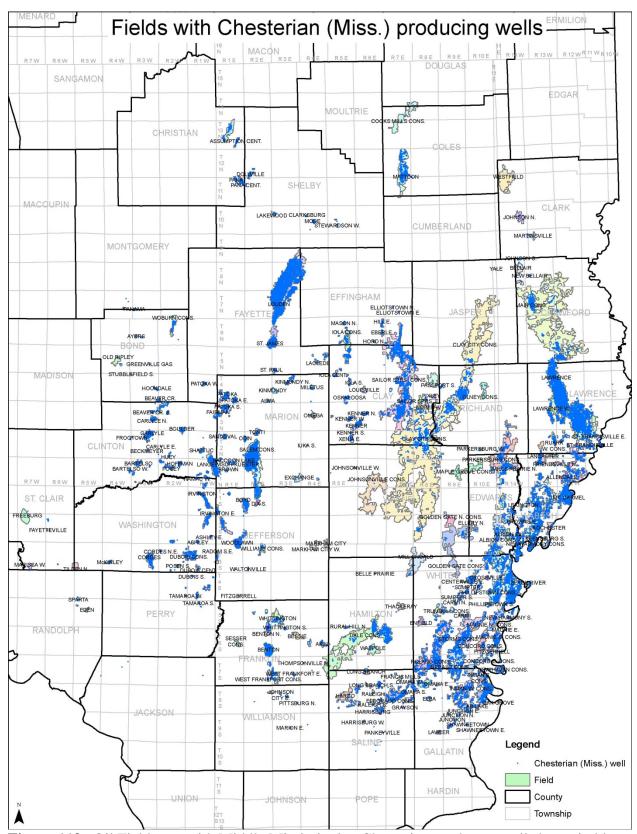
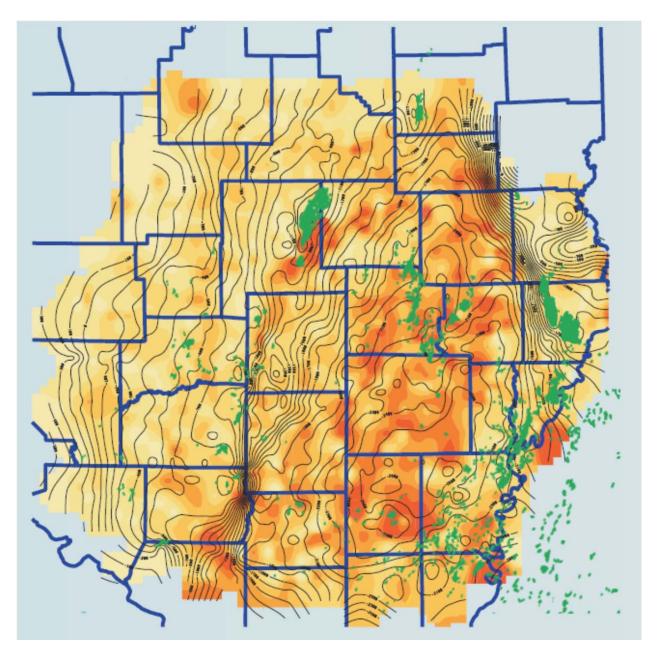
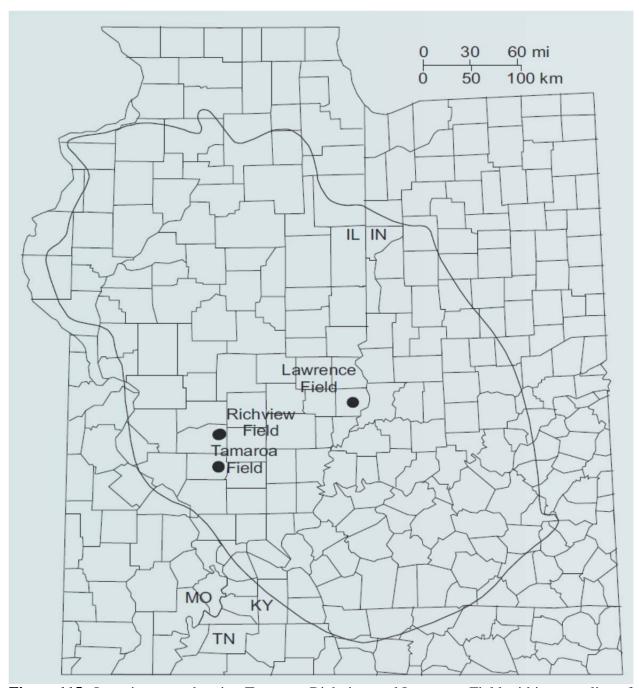


Figure 113. Oil Field map with Middle Mississippian Chesterian sandstone well shown in blue.



**Figure 114.** Net sandstone thickness map of the Cypress Formation that shows major fairways of thick sandstone in the central portion of the Illinois Basin.



**Figure 115.** Location map showing Tamaroa, Richview and Lawrence Field within an outline of the Illinois Basin.

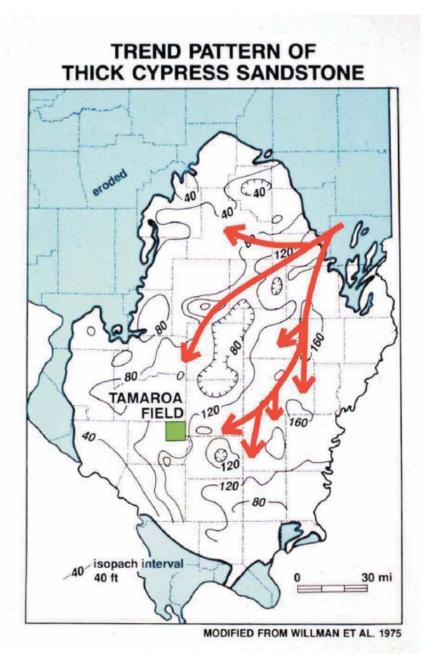


**Figure 116.** Thickness map of the Cypress sandstone and a projection of possible trends of prograding deltas, as determined from the trend of thick sandstones. Along the central, active portions of prograding deltas, thick estuarine and probably tidal bayhead deltas to fluvial sands were deposited. These deltas prograded from the northeast and down-dip to the southwest and south. Swann identified this fluvial-deltaic system and in 1963 titled it the Michigan River. Unlike the classic Mississippi River birdfoot type constructive delta, the Cypress deltas were likely influenced by destructive, sediment spreading, tidal currents. Thick, discontinuous sandbodies are common in the upper estuarine to fluvial portions of tidally dominate deltas (Modified from Willman et al., 1975).

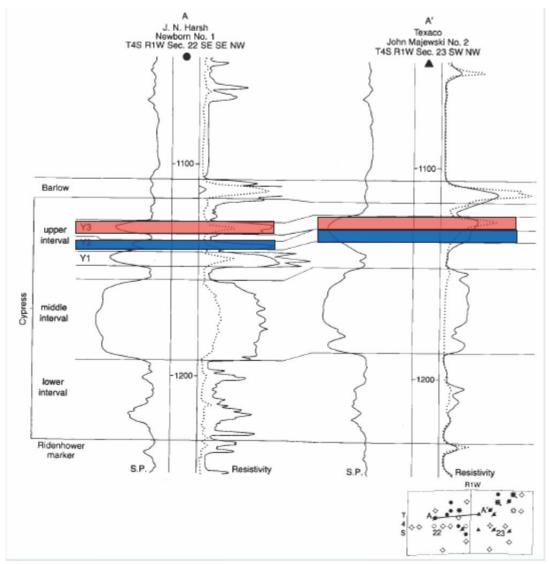


**Figure 117.** Cross section on the left shows the Cypress Formation divided into lower, middle and upper intervals used for local mapping purposes. The lenticular or ridge forming sandstones occur in the upper interval. Highlighted in color are the Y2 and Y3 lenticular sandstones which form the principal reservoirs in the Tamaroa area. The Y2 and Y3 sandstones are commonly less than 10 feet thick and separated by shale as shown on the left but in some cases, they coalesce, forming an abnormally thick upper Cypress sandstone, shown on right. Compartments are maintained in these thicker sandstones because they are typically separated by shaly beds and shale rich impermeable zones less than 1 foot thick as observed in core and core analyses. Electric logs are unable to resolve the thin, impermeable zones that partition the thicker sandstones.

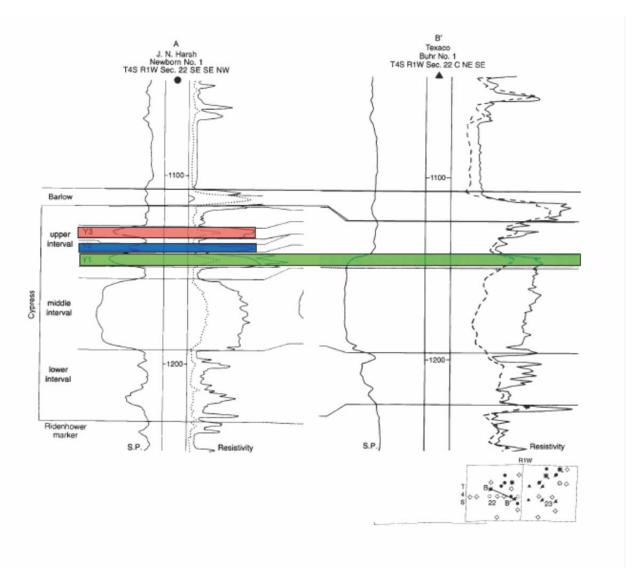


**Figure 118.** Cross section on the right shows the Y2 and Y3 sandstones changing facies to shale. The Y1 and middle Cypress sandstones coalesce.

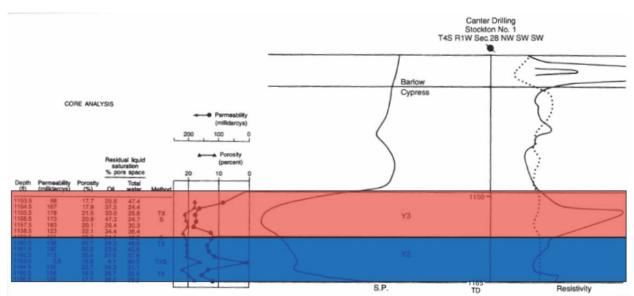


**Figure 119.** Comparison of the SP curve with the plotted permeability data from the Stockton #1 Cypress core analysis showing similar character. Multiple shingling events during deposition of the Y2 and Y3 sandstones have created permeability barriers at 1163.5 feet and possibly 1159 feet.

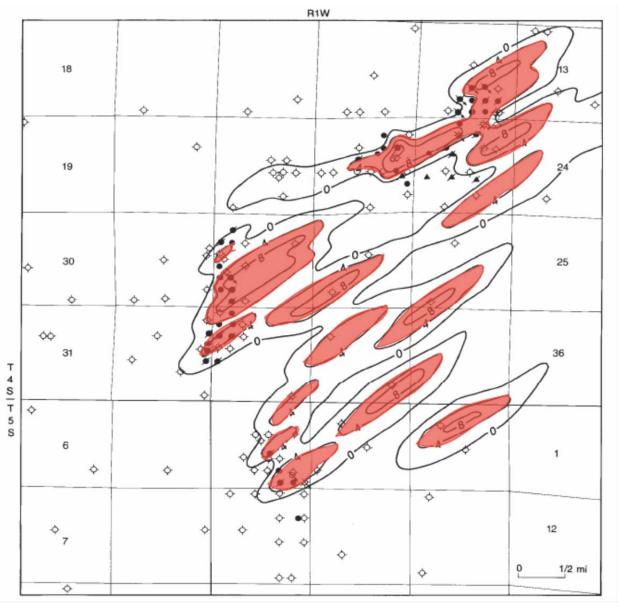


**Figure 120.** Thickness map of the Y3 Cypress sandstone showing the northeast-southwest trend and the subparallel alignment of these lenticular sandstones. Contour interval is 4 feet.

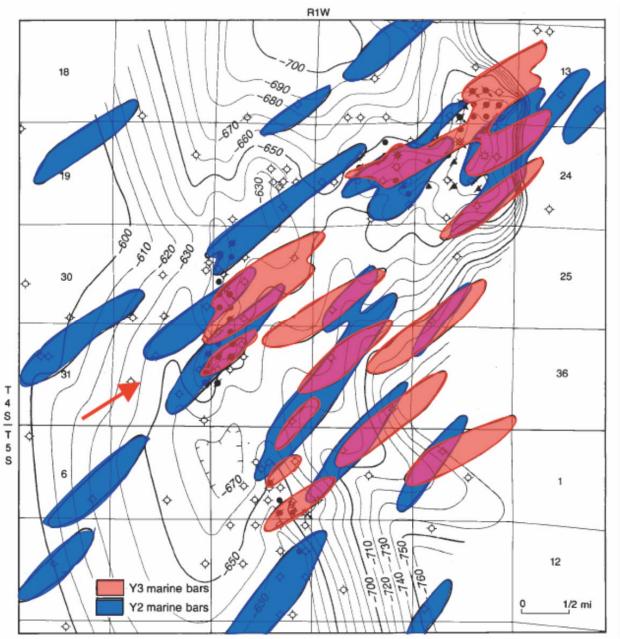


**Figure 121.** Map showing an outline of the Y2 and Y3 sandstones greater than 4 feet thick combined with the Barlow structure. Note the northeast-southwest trend and the subparallel alignment of these lenticular sandstone bodies. The trapping mechanism for the Tamaroa area fields is shown to be draping of the lenticular sandstones across the crest of structural folds.

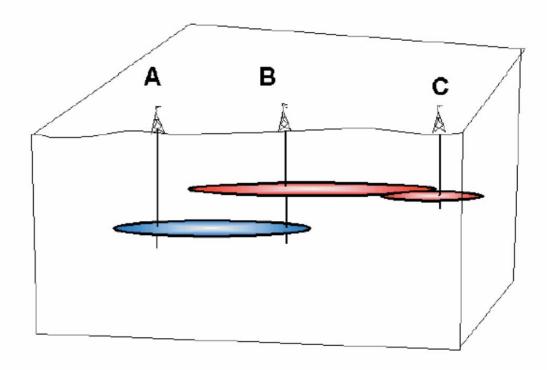


**Figure 122.** An understanding of the geometry and dimensions of these lenticular sandstone bodies is necessary to define each particular sandstone lens and to correctly correlate the horizon in which the lens was deposited. This is necessary to define compartments and determine communication potential. Only then can each separate lens be efficiently drained. This figure is a simplification of the bar configuration that occurs in the Tamaroa South portion of the field area (red arrow in figure with combined bars and structure). The figure shows that primary recovery will occur in all three lenses but only the lower blue, Y2 lense can be drained by secondary injection through the A or B well. The upper red, Y3 lenses cannot be waterflooded with this well configuration although miscorrelation of the lenses could lead to an interpretation that the B and C wells are in communication or that the A and C wells are in communication.

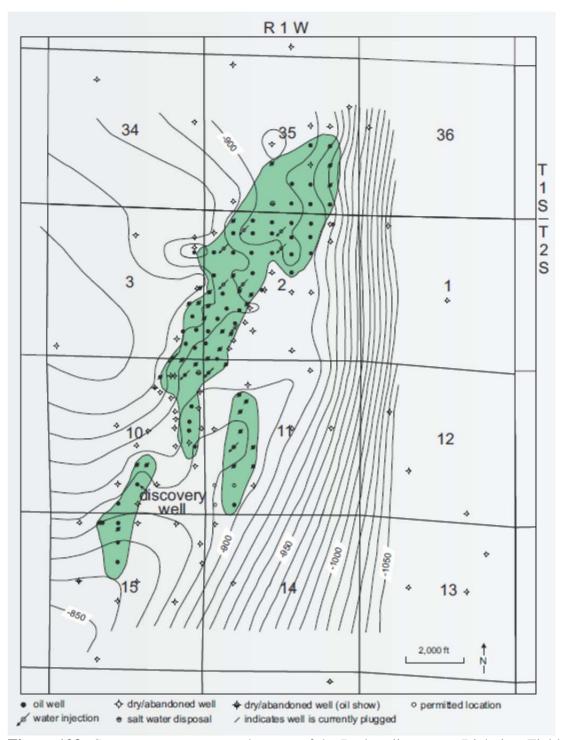


**Figure 123.** Structure map contoured on top of the Barlow limestone. Richview Field produces from a principal pool and two subsidiary pools offset to the southeast and southwest of the main pool. Contour interval is 10 feet.

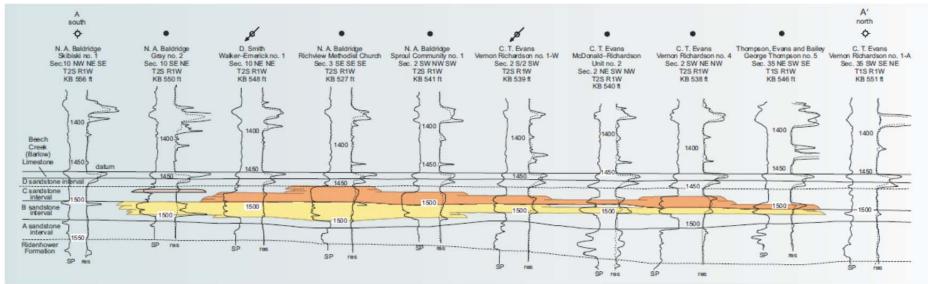


**Figure 124.** Stratigraphic cross section, A-A', showing the widespread shaly interval that separates the B and C sandstones. The C sandstone increases in thickness by the addition of stacked pods or lenses of sandstone. The B sandstone shows similar characteristics. Stacked lenses appear to form vertically continuous sandstones more than 20 feet thick but an examination of the SP traces show subtle to obvious positive deflections at the boundaries of the lenses. The SP deflections indicate that the lenses are commonly separated by very thin impermeable beds that compartmentalize and reduce the fluid flow capability of the B and C sandstones. Line of this cross section is shown on the thickness map of the B sandstone.

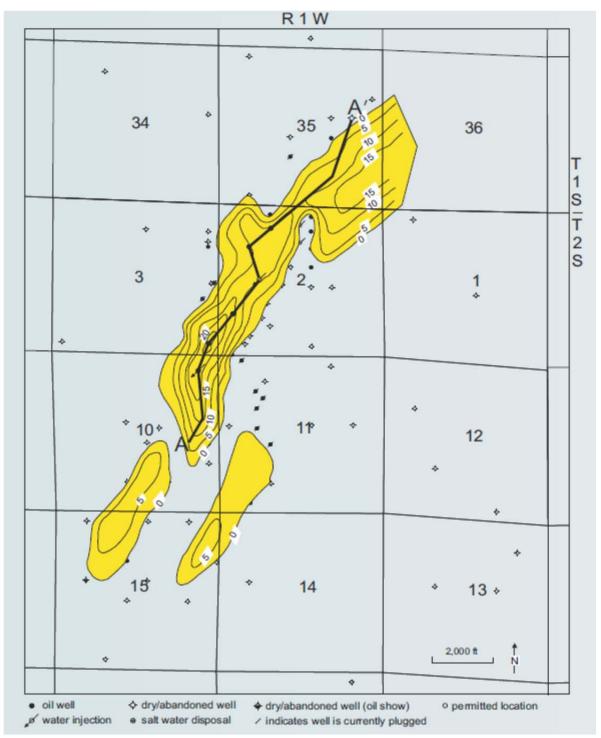


**Figure 125.** Net thickness map of the Cypress "B" interval shows a principal sandstone body with two southern offset lenses. These sandstone bodies trend northeast-southwest and measure over three miles in length and 1/3 to 1/2 mile in width. The B sandstone attains a thickness of approximately 25 feet along the south central portion of the main pool and is less than 10 feet thick in the two southern offsets. Contour interval is 5 feet. Location of cross section A-A' is shown.

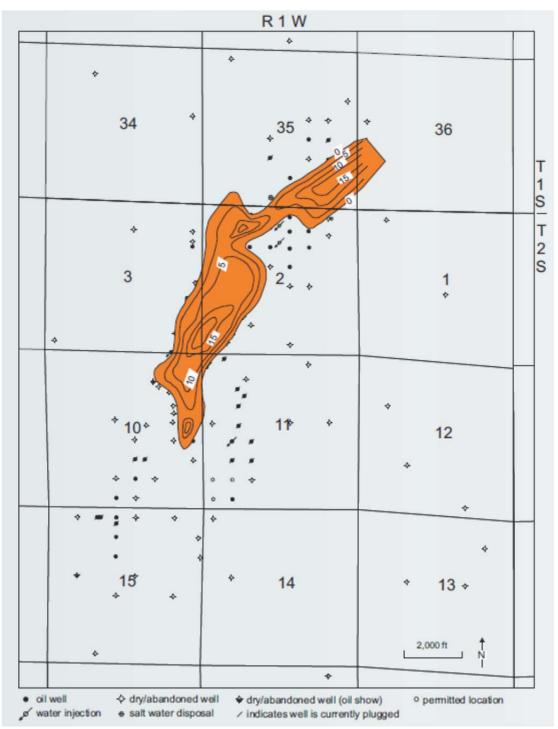


**Figure 126.** Net thickness map of the Cypress C interval shows this sandstone to be geographically coincident with the underlying B sandstone. Unlike the B sandstone, the C sandstone has no offset lenses. Thickness of this sandstone is greatest along the central part, reaching a maximum thickness of 20 feet. The C sandstone appears to increase in thickness from north to south by the addition of discrete, stacked or shingled pods of sandstone. This stacking characteristic shows an aspect of migration or aggradation during deposition from the north. This figure is a simplification of the stacked bar to south. Contour interval is 5 feet.

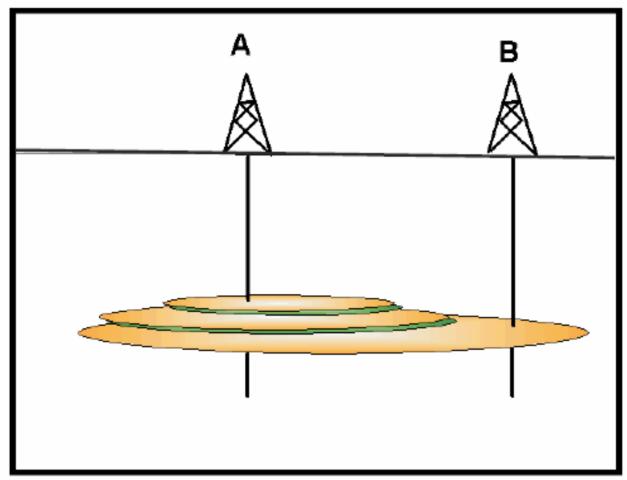


**Figure 127.** This figure is a simplification of the stacked bar to south. Contour interval is 5 feet. Configuration that occurs at Richview Field and is similar to the configuration at Lawrence Field and many other multiple layered reservoirs with permeability barriers separating the layers. The figure shows that primary recovery will occur in all three lenses but only the lower lense can be drained by secondary injection through the A or B well. The upper two lenses penetrated by well A will contain bypassed or banked oil which can be recovered by waterflooding with the addition of infill wells that penetrate the upper lenses.

## Appendix A

